



Programme Area: Carbon Capture and Storage

Project: Hydrogen Turbines Follow On

Title: Salt Cavern Appraisal for Hydrogen and Gas Storage

Abstract:

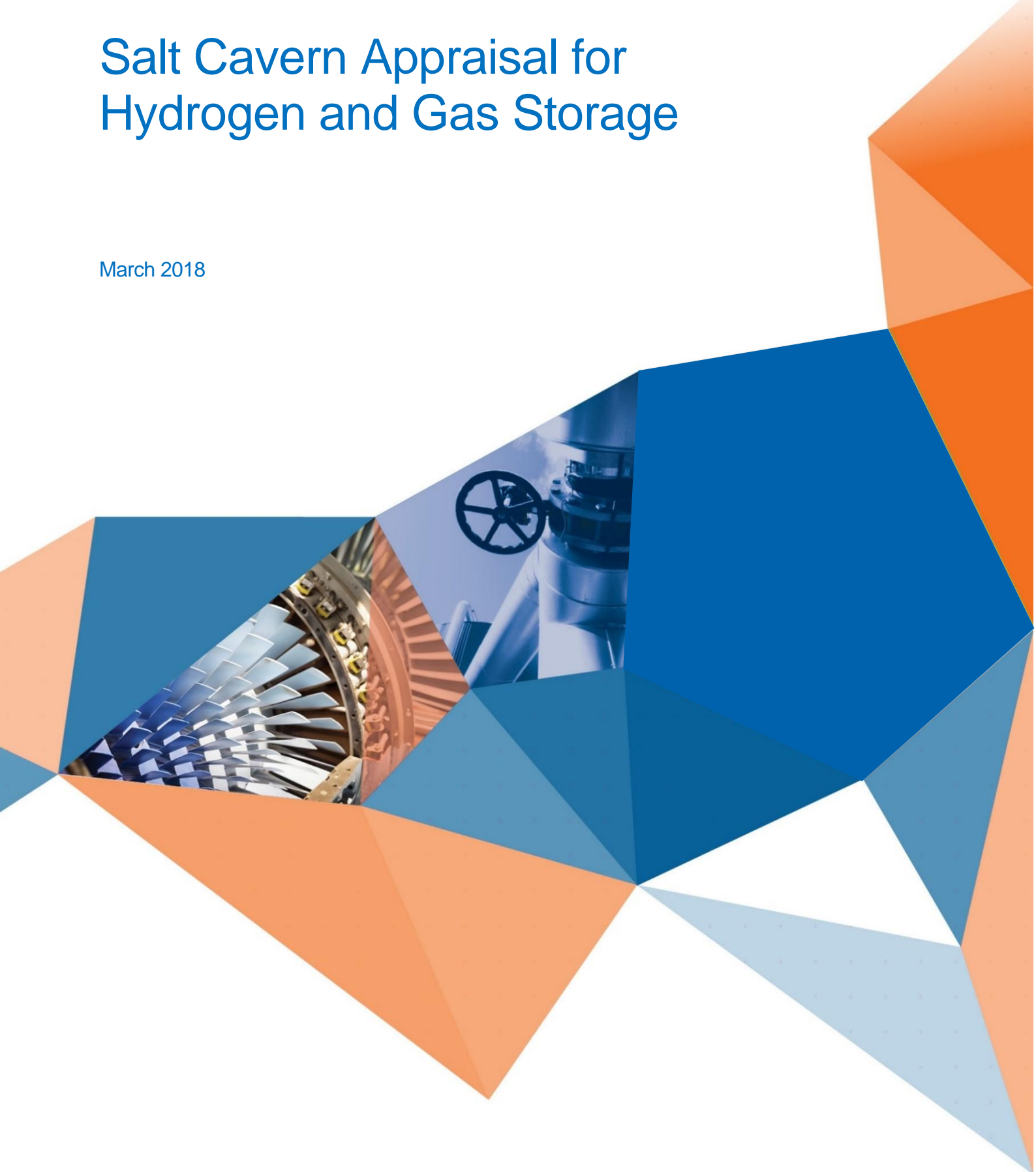
With the growth of renewables a clean, dispatchable power source will be required in the 2030s. One scheme for providing this involves storing large quantities of H₂ in salt caverns, and to use the inventory to produce power or heat during peak hours. Although H₂ is stored already in caverns in the UK, there has been little work on the effect of rapid repetitive cycling on cavern integrity. The suitability of UK salt caverns for use in storing H₂ in rapid cycle mode is examined, based on detailed geotechnical analysis of saltfields in Yorkshire, Teesside and Cheshire. A detailed analysis is carried out by Atkins on a Cheshire cavern, using a combination of superimposed seasonal and daily demand patterns. The limitations of today's market offering for firing H₂ in gas turbines is described. Outline costing for schemes taking H₂ from salt caverns and producing power are presented.

Context:

This knowledge gathering project collated data on the performance of gas turbines (conventional and novel cycles) operating on methane, hydrogen and mixtures of the two. It carried out plant and whole system modelling with the aim of understanding how much and in what circumstances gas (with and without CCS) is investable and fits and where it is unlikely to fit easily in the developing energy system from 2020-2050, to meet the increasing requirements for flexibility against an increasingly carbon-constrained system. The gas turbine generation work, was targeted at identifying improved configurations that could be taken to concept stage. At a wider level, the work provided greater understanding of factors affecting the deployment of methane and hydrogen turbines in the UK market and provided better, more accurate performance data for key configurations for future system modelling.

Salt Cavern Appraisal for Hydrogen and Gas Storage

March 2018



Notice

This document and its contents have been prepared and are intended solely for Energy Technology Institutes (ETI) information and use in relation to the Salt Cavern Appraisal for Hydrogen and Gas Storage Project.

Atkins Ltd assumes no responsibility to any other party in respect of or arising out of or in connection with this document and/or its contents.

Document history

Salt Cavern Appraisal for Hydrogen and Gas Storage			Document ref: 5149533-MD-REP-005			
Revision	Purpose description	Originated	Checked	Reviewed	Authorised	Date
Rev P1	Draft for ETI review	Ewan Murray Yulia Kopan Georgios Yfantis David McInroy	Evan Passaris Peter Tanner	Christopher McMichael Tom Sklaschus	Marco Clemente	02/06/17
Rev P2	Final report	Ewan Murray Georgios Yfantis	Evan Passaris Peter Tanner	Christopher McMichael Tom Sklaschus	Marco Clemente	31/08/17
Rev P3	Final report including client updates and low carbon case	Ewan Murray Georgios Yfantis	Evan Passaris Peter Tanner	Christopher McMichael Tom Sklaschus	Marco Clemente	20/12/17
Rev A1	Final report	Ewan Murray, Georgios Yfantis	Evan Passaris Peter Tanner	Christopher McMichael Tom Sklaschus	Marco Clemente	16/02/18
Rev A2	Final report, following client review	Nathan Leister	Ewan Murray	Tom Sklaschus	Christopher McMichael	07/03/18

Acknowledgements

The Atkins project team wish to acknowledge and thank the UK's leading cavern storage operators, including Storengy, SSE Gas Storage, Inovyn and SABIC, who have provided their operational data and technical expertise to assist Atkins in the development of the hydrogen storage model for each region. Their contribution has been critical to the development of this project on behalf of the ETI.

In addition the project team wish to thank the gas turbine (GT) Original Equipment Manufacturers (OEM), including Siemens and General Electric, who have provided invaluable insight into the current and future capability of H₂ capable machines.

Table of contents

Chapter	Pages
CHAPTER 1: INTRODUCTION	1-18
1. INTRODUCTION	1-19
1.1. <i>Background</i>	1-19
1.2. <i>Objectives</i>	1-20
1.3. <i>Study constraints</i>	1-20
1.4. <i>Methodology</i>	1-25
CHAPTER 2: INTEGRATING HYDROGEN INTO POWER GENERATION	1-26
2. POWER GENERATION	2-27
2.1. <i>Performance limits and NO_x emissions control</i>	2-28
2.2. <i>Ramp rate / flexibility</i>	2-33
2.3. <i>GT selection</i>	2-37
2.4. <i>CCGT arrangement</i>	2-40
2.5. <i>Power plant fuel requirement</i>	2-45
2.6. <i>Proposed plant solution</i>	2-48
CHAPTER 3: SUPPLY OF HYDROGEN TO POWER PLANT	2-49
3. SUPPLY OF HYDROGEN TO POWER PLANT	3-50
3.1. <i>Plant summary under daily cycle</i>	3-51
3.2. <i>Well design</i>	3-54
3.3. <i>Flowrates for cavern modelling</i>	3-63
3.4. <i>Surface processing plant</i>	3-65
3.5. <i>Proposed hydrogen supply arrangement</i>	3-66
CHAPTER 4: STORING HYDROGEN IN SALT CAVERNS	3-69
4. CAVERN STORAGE	4-70
4.1. <i>Introduction</i>	4-70
4.2. <i>Thermodynamic analysis for East Yorkshire and the Cheshire representative caverns</i>	4-71
4.3. <i>Coupled thermo-geomechanical analysis for East Yorkshire & Cheshire representative caverns</i>	4-77
4.4. <i>Geomechanical analysis of Teesside representative cavern</i>	4-89
4.5. <i>Conclusions</i>	4-93
CHAPTER 5: ECONOMIC VIABILITY	4-95
5. ECONOMIC VIABILITY	5-96
5.1. <i>Caverns and wells</i>	5-97
5.2. <i>Surface processing plant</i>	5-99
5.3. <i>Gas Turbine</i>	5-101
5.4. <i>Overall project costs</i>	5-106
5.5. <i>Permitting and legislation</i>	5-110
5.6. <i>Conservative estimate of the total storage resource in the three areas under consideration</i>	5-115
CHAPTER 6: LOW CARBON CASE	5-121
6. DEFINING THE SCENARIO TO ACHIEVE, LOW CARBON, HIGH HYDROGEN COMBUSTION	6-122
6.1. <i>Outlining the baseline case for a high hydrogen CCGT</i>	6-122
6.2. <i>Technical challenges to achieve high hydrogen</i>	6-125
6.3. <i>Technologies with potential for high H₂ combustion.</i>	6-128
6.4. <i>Fuel requirement of high H₂ case,</i>	6-131
6.5. <i>Impact on plant costs for high H₂ case</i>	6-132
6.6. <i>Conclusions and next steps in development</i>	6-135
CHAPTER 7: LIMITATIONS OF CAVERN PERFORMANCE, CHESHIRE CASE STUDY	6-136

7.	LIMITS OF CAVERN PERFORMANCE; CHESHIRE CASE STUDY	7-137
7.1.	<i>Introduction</i>	7-137
7.2.	<i>Acceptable limiting condition for thermal-loading of storage caverns</i>	7-137
7.3.	<i>Stress the Cheshire representative cavern to theoretical limits.</i>	7-138
7.4.	<i>Seasonal profile; analysis of seasonal plus diurnal loading cycles.</i>	7-152
7.5.	<i>Conclusions/ Discussion</i>	7-157
CHAPTER 8: STUDY CONCLUSIONS		7-158
8.	STUDY CONCLUSIONS	8-159
8.1.	<i>Current capability</i>	8-160
8.2.	<i>Future low carbon case</i>	8-160
8.3.	<i>Theoretical cavern limits</i>	8-161
8.4.	<i>Future areas of study</i>	8-162
CHAPTER 9: REFERENCES		8-165
9.	REFERENCES	9-166
APPENDICES		167

Tables

Table 1-1:	Power plant generating scenario load factor	1-22
Table 1-2:	Characteristics of representative caverns at each location to be considered.	1-24
Table 2-1:	Definition of starts and associated times (ETI, 2016)	2-34
Table 2-2:	CCGT plant performance (from GT PRO results), with ACC at ISO conditions & full load	2-35
Table 2-3:	Nominal H ₂ firing capability	2-39
Table 2-4:	SGT-800 performance at various fractions of H ₂ (Siemens)	2-41
Table 2-5:	SGT5-2000E performance with fuel gas stream 1 at various fractions of H ₂	2-41
Table 2-6:	SGT5-2000E performance with fuel gas stream 2 at various fractions of H ₂	2-42
Table 2-7:	Summary of strengths / weaknesses of selected GTs	2-42
Table 2-8:	CCGT performance on natural gas [Ambient conditions - ISO 15°C & 60% relative humidity (RH) @ full load]	2-43
Table 2-9:	CCGT block flexibility and response	2-44
Table 2-10:	Gas composition in the GT combustion chamber for fuel mixes (to OEM recommendations)	2-46
Table 2-11:	Summary of the power plant fuel requirement	2-47
Table 3-1:	Summary of the power plant fuel requirement of fuel gas streams	3-51
Table 3-2:	Scenario 3 parameters**	3-54
Table 3-3:	New versus old caverns and wells	3-55
Table 3-4:	9 7/8" Tubing grade selection for East Yorkshire	3-58
Table 3-5:	9 7/8" Tubing grade design life check for East Yorkshire	3-58
Table 3-6:	Tubing and casing grade selection for Teesside	3-60
Table 3-7:	10 3/4" casing and 7 7/8" tubing grade design life checks for Teesside	3-60
Table 3-8:	9 7/8" Tubing grade selection for Cheshire	3-61
Table 3-9:	9 7/8" Tubing grade design life check for Cheshire	3-62
Table 3-10:	Flow rates for power generation Scenario 3	3-63
Table 3-11:	Maximum achievable flowrates from a single well	3-64
Table 3-12:	Required flowrates for load profiles	3-64
Table 3-13:	Required flowrates based on initial modelling	3-64
Table 4-1:	Cyclic operations flowrates, corresponding to power generation Scenario 3, for the East Yorkshire and Cheshire caverns (expressed in Nm ³ /d).	4-71
Table 5-1:	Cost estimate for East Yorkshire site for fuel gas streams 1 or 2	5-98
Table 5-2:	Cost estimate for Cheshire site for fuel gas streams 1 or 2	5-98
Table 5-3:	Cost estimate for fuel gas stream 1 at Teesside	5-99
Table 5-4:	Cost estimate for fuel gas stream 2 at Teesside	5-99

Table 5-5: Surface plant cost estimates for East Yorkshire, Cheshire and Teesside	5-100
Table 5-6: Surface plant cost estimates for East Yorkshire, Cheshire and Teesside	5-101
Table 5-7: GT plant Cost estimate for fuel stream 2 (excludes 10% increase due to high H ₂)	5-103
Table 5-8: Cost estimate, sector package details	5-104
Table 5-9: Permitting and Legislation Issues	5-112
Table 5-10: Permitting and Legislation Issues	5-113
Table 5-11: Permitting and Legislation Issues	5-114
Table 5-12: Estimated new cavern potential in East Yorkshire	5-117
Table 5-13: Estimated new cavern potential in Cheshire	5-119
Table 5-14: Estimated new cavern potential in Teesside	5-120
Table 6-1: Indicative baseline assumptions	6-123
Table 6-2: Research papers supporting high H ₂ combustion	6-124
Table 6-3: Technical Challenges and possible mitigations	6-129
Table 6-4: Novel combustor technology summary	6-129
Table 6-5: High H ₂ case fuel requirement example	6-131
Table 6-6: Cost factors for high H ₂ case	6-133
Table 6-7: Cost factors for high H ₂ case	6-134
Table 7-1: Initial cyclic loading conditions, Run 1	7-139
Table 7-2: Trial and error analyses, Runs 1, & 2a-2d	7-141
Table 7-3: Further trial and error analyses, Runs 2e & 2f	7-142
Table 7-4: Seasonal modelling runs maintaining Scenario 3 daily	7-155

Figures

Figure 1-1: High level process block diagram, operating principles	1-19
Figure 1-2: Key Study Constraints	1-20
Figure 1-3: H ₂ fuel gas streams (mol%)	1-21
Figure 1-4: Power plant generation scenarios	1-22
Figure 1-5: Distribution of the main halite bearing basins in Britain and the location of operational and proposed underground gas storage sites (Evans, 2008)	1-23
Figure 2-1: Power generation block diagram / section map	2-27
Figure 2-2: Siemens DLE combustor estimated performance	2-29
Figure 2-3: Impact of N ₂ dilution effect on GT performance	2-31
Figure 2-4: Impact of steam dilution effect on GT performance	2-33
Figure 2-5: Relationship between the GT load and plant net efficiency	2-36
Figure 2-6: Typical part load efficiency CCGT power plant based on 6+1 'Econoflex 6' arrangement of SGT-800 (Siemens, 2014)	2-37
Figure 2-7: CCGT configuration for selected options	2-44
Figure 2-8: GT inlet fuel / diluent selection summary	2-45
Figure 2-9: Small frame GT power plant arrangement at full load	2-48
Figure 2-10: "E" class GT power plant arrangement at full load	2-48
Figure 3-1: H ₂ supply block diagram	3-50
Figure 3-2: Operating scenario considerations and interfaces	3-51
Figure 3-3: Scenario 1 daily profile	3-52
Figure 3-4: Scenario 2 daily profile	3-52
Figure 3-5: Scenario 3 daily profile	3-53
Figure 3-6: East Yorkshire conceptual well design	3-57
Figure 3-7: Teesside conceptual well design	3-59
Figure 3-8: Cheshire conceptual well design	3-61
Figure 3-9: Block Flow Diagram: Surface Processing Plant	3-65
Figure 3-10: Block flow diagram East Yorkshire and Cheshire arrangements (Scenario 3)	3-67
Figure 3-11: Teesside mass flow rate block diagram (Scenario 3)	3-68
Figure 4-1: Comparison of the effect of fuel gas stream 1 and fuel gas stream 2 on the resulting cavern temperature history	4-73
Figure 4-2: Cavern temperature history for the East Yorkshire cavern	4-74

Figure 4-3: Cavern pressure history for the East Yorkshire cavern	4-74
Figure 4-4: Cavern temperature history for the Cheshire representative cavern	4-76
Figure 4-5: Cavern pressure history for the Cheshire cavern	4-76
Figure 4-6: Finite difference grid used in the modelling of the East Yorkshire cavern	4-78
Figure 4-7: Details of the finite difference grid used in the modelling of the East Yorkshire cavern	4-78
Figure 4-8: Shear strength envelope for Fordon Evaporites Salt, expressed in terms of σ_1 and σ_3 .	4-81
Figure 4-9: Shear strength envelope for Fordon Evaporites Salt, expressed in terms of $\sqrt{J_2}$ and I_1 ,	4-82
Figure 4-10: Finite difference grid used in the modelling of the Cheshire cavern	4-83
Figure 4-11: Details of the finite difference grid used in the modelling of the Cheshire cavern	4-84
Figure 4-12: Shear strength envelope for Northwich Halite, expressed in terms of σ_1 and σ_3 .	4-86
Figure 4-13: Shear strength envelope for Northwich Halite, expressed in terms of $\sqrt{J_2}$ and I_1 .	4-87
Figure 4-14: Comparison between the Stublach and Holford caverns	4-88
Figure 4-15: Comparison the temperature distribution around the Stublach and Holford caverns	4-88
Figure 4-16: Comparison the $(\sigma_1 - \sigma_3)$ distribution around the Stublach and Holford caverns	4-89
Figure 4-17: Finite element mesh used in the modelling of the Teesside representative cavern	4-90
Figure 4-18: Details of the finite element mesh used in the modelling of the Teesside cavern	4-91
Figure 5-1: Annual Opex cost through GT Plant Design Life	5-105
Figure 5-2: CAPEX for SGT-2000E, fuel gas stream 2	5-107
Figure 5-3: CAPEX for SGT-800, fuel gas stream 1	5-107
Figure 5-4: CAPEX for SGT-2000E (fuel gas stream 2) in £/kW	5-108
Figure 5-5: CAPEX for SGT-800, (fuel gas stream 1) in £/kW	5-108
Figure 5-6: Annualised OPEX estimates for each site (AmecFw, 2012)	5-109
Figure 5-7: East Yorkshire and Teesside salt coverage and estimated heat map of usable salt area (map excerpt from BGS GeoIndex Onshore)	5-116
Figure 5-8: Cheshire salt coverage and estimated heat map of usable salt area (map excerpt from BGS GeoIndex Onshore)	5-116
Figure 6-1: Chapter Roadmap	6-123
Figure 6-2: Technical challenges	6-125
Figure 6-3: Technical challenges in fuel source	6-125
Figure 6-4: Molecular (mol%) and mass fraction (wt%) differences, fuel gas stream 1	6-126
Figure 6-5: Technical challenges in combustion	6-126
Figure 6-6: Technical challenges in GT type / configuration	6-127
Figure 6-7: Fuel requirement high H ₂ case	6-132
Figure 6-8: Fuel requirement high H ₂ case	6-134
Figure 7-1: Trial and error analyses averaged flowrates, Run 1	7-139
Figure 7-2: Trial and error analyses averaged flowrates, Runs 1, & 2a-2d	7-140
Figure 7-3: Modelling runs (Run 1, & 2a-d) against P _{max} and P _{min} limits	7-141
Figure 7-4: Additional trial and error analyses averaged flowrates, Runs 2e & 2f	7-142
Figure 7-5: Modelling runs (2e & 2f) against P _{max} and P _{min} limits	7-143
Figure 7-6: Cavern temperature cycles resulting from the execution of Run 2f	7-143
Figure 7-7: Development of temp. & pressure as a function of net H ₂ flow rate per day for 50 days	7-144
Figure 7-8: Development of temp. & pressure as a function of net H ₂ flow rate per day for 80 days	7-144
Figure 7-9: Development of temp. & pressure as a function of net H ₂ flow rate per day for 100 days	7-145
Figure 7-10: Cavern pressure that satisfies the temp. limit as a function of the applied flow rate	7-146
Figure 7-11: Results of the thermodynamic analysis when employing cyclic loading that incorporates 50 days steps	7-146
Figure 7-12: Results of the thermodynamic analysis when employing cyclic loading that incorporates 80 days steps	7-147
Figure 7-13: Temperature distribution results when employing 50 days steps cyclic loading	7-147
Figure 7-14: Minimum principal stress distribution results when employing 50 days steps cyclic loading	7-148
Figure 7-15: Single daily cycle, cavern pressure for a range of flow rates	7-148
Figure 7-16: Single daily cycle, cavern temperature for a range of flow rates	7-149
Figure 7-17: Development of cavern pressure between 62 barg and 83 barg	7-150
Figure 7-18: Cavern temperature history when pressure cycles between 62 barg and 83 barg	7-150

Figure 7-19: Min. principal stress distribution (in MPa) for daily cyclic loading between 62 barg and 83 barg	7-151
Figure 7-20: National Grid 2016 gas demand UK	7-152
Figure 7-21: Initial cavern seasonal cycle	7-153
Figure 7-22: Interpreted cavern demand from national profile	7-154
Figure 7-23: Pressure profile of individual cavern, Run 4	7-156
Figure 7-24: Temperature profile of individual cavern, Run 4	7-156
Figure 8-1: Fuel requirement high H ₂ case	8-161
Figure 8-2: East Yorkshire & Cheshire summary, current capability	8-163
Figure 8-3: Teesside Summary, current capability	8-164

Executive summary

The UK energy market is going through a period of transformation, as the country adopts widespread electrification to meet the challenging greenhouse gas reduction target of 34% by 2020 set out in the 2008 Climate Change Act. To help meet these targets, widespread renewables have been adopted across the UK which introduces additional challenges due to their inherently intermittent supply. Furthermore, due to factors such as the increased adoption of electrical cars there is a forecasted increase of peak electrical demand from its current level of ~60 GW to 85 GW in 2050 (National Grid, 2017).

To help meet these targets and provide a flexible, reliable and cost-effective energy source it is anticipated that gas will play an increasingly important role. Peak electrical demands in the future could be met through clean, hydrogen (H₂) fuelled, combined cycle gas turbines (CCGT), where large scale H₂ storage would be required to balance the demand cycle. The emergence of H₂ as a clean, flexible energy source offers additional benefits in the decarbonisation of the heat market by displacing natural gas. However, the conversion of existing methane storage assets or the creation of new storage assets to support H₂ energy storage has not been developed on this scale previously and so the technical capability and cost to achieve this needs to be fully understood.

The focus of this report was to establish the capability of salt caverns to store a H₂ rich fuel source under a challenging fast 'churn' generation cycle. Specifically, the objectives were defined as follows:

- Consolidate the ETI understanding of cavern flexibility, to support ETI system level modelling activities, for up to 100% H₂ and H₂ / methane mixtures, with a focus on flexibility and cost.
- Characterise the key constraints and their causes when operating fast churn storage at selected sites, including those caused by the integration of the H₂ supply and the gas turbines (GT).
- Identify a range of GT / CCGT offerings which match cavern capability or market needs.
- Provide insight on cavern capability and limitations on duty.
- To provide high level estimates for a complete plant solution, with greater capital expenditure (CAPEX) and operating expenditure (OPEX) certainty, in line with AACE5 level (-50% +100%).

To meet these objectives this study has reviewed the potential for H₂ storage to be developed at three different salt cavern fields across the UK (East Yorkshire, Cheshire & Teesside) to deliver 1 GWe under a 'fast churn' peak demand matching arrangement.

The study was undertaken in a collaborative manner with gas storage operators from the three regions providing key input and operational data. Thermo-mechanical modelling using industry leading software, including SCTS and FLAC, was used to better understand cavern behaviour and leading GT original equipment manufacturers (OEM) were consulted to better understand the current and potential future H₂ capabilities of GT technology. This was supported through technical review and feasibility assessment of aspects such as the well design and surface infrastructure to deliver the fuel stream at the required flowrate, for 1 GWe. Based on these activities the technical feasibility of developing a H₂ storage facility at each of the three sites has been evaluated and associated CAPEX and OPEX estimates developed.

Consideration has also been given to a low carbon case, where current technological limitations have been identified and future developments recommended to support a high H₂ capability presented.

Finally, based on the insights that these works have provided, a case study was developed where a series of sensitivity studies were undertaken to provide further understanding on the theoretical limits of the cavern (under a 'fast churn' cycle). In addition, the seasonal impact of the heat network and therefore current operating cycle of the cavern was overlaid with a 'fast cycle' daily 1 GWe electrical demand requirement to determine the cavern limits under a high H₂ case.

From the works undertaken, several key findings were found, which can be summarised as follows:

1. Consolidate the ETI understanding of cavern flexibility, to support ETI system level modelling activities, for up to 100% H₂ and H₂ / methane mixtures, with a focus on flexibility and cost.

At each of the selected salt fields, outline requirements for a flexible H₂ storage facility were identified, where two potential H₂ fuel gas streams were considered; fuel gas stream 1 with 89 mol% H₂ and fuel gas stream 2 with 53 mol% H₂ (typical of the outputs from a biomass/ coal gasifier and Auto Thermal Reformer for natural gas respectively)¹.

Salt caverns modelled at each of the three sites can safely provide the required storage to deliver 1 GWe, without an integrity issue. This is based on a balanced daily extraction / injection cycle of the fuel streams (with a net zero volume change over 24 hours). The site specific solutions are given below:

- At the East Yorkshire and Cheshire sites it has been shown that a single cavern (with two wells) can achieve the project requirements for both fuel gas stream 1 or 2 (based on E-class machines and 25 vol% H₂ capability).
- At the Teesside site it has been shown that 3 caverns would be required to meet the project requirements for fuel gas stream 1 and 2 caverns for fuel gas stream 2 (based on E-class machines and 25 vol% H₂ capability).

It was found that for this case, the daily extraction / injection cycle modelled meets the 1 GWe requirement without significantly stretching the performance of the cavern.

2. Characterise key constraints and their causes when operating fast churn storage at selected sites, included those caused by integration with the H₂ supply and the GTs.

Based on current technology, existing GTs have limited capability in firing high H₂ fuel gas streams.

- Small framed (50 MW) GTs can fire up to 60 vol% H₂ (Dry Low Emission, DLE type)
- Larger "E" class GTs (150 MW) can fire up to 25 vol% H₂ (diffusion burner type)

Some operational case studies exist that achieve higher H₂ combustion ratios in the GTs, often through steam/water dilution and at a potential emissions and performance penalty. However, a project in the European Union (EU) would need to meet current EU directive emission limits (60 ppm NO_x) and so NO_x emissions becomes a key design constraint for a new high H₂ plant.

It is not recommended to repurpose existing gas storage assets for H₂ storage. Any new facility should either consider the reuse of existing caverns by the drilling of new wells or the development of new caverns and therefore new wells. In each case it is recommended that a maximum of two wells per cavern are installed, where this design will ensure the high extraction / injection rates demanded by the 'fast churn' peak demand matching can be achieved and limits any temperature induced stresses on the cavern.

¹ These conclusions were made based on hydrogen / methane fuel mixes compatible with current GT capabilities

3. Identify a range of GT / CCGT offerings which match cavern capability or market needs.

A review of available GT / CCGT machines was undertaken, where a structured down selection process was used, based on specific criteria. These included: OEM advised maximum allowable H₂, history of H₂ rich application, NO_x emissions, GT flexibility.

From this an optimum arrangement to deliver the peak demand, 1 GWe, requirement for each fuel stream was identified:

- Fuel gas stream 1 – Small frame GT in a 2 x (6+1) configuration
- Fuel gas stream 2 – “E” class GT in a 2 x (2+1) configuration

It was found that the technical challenges to high H₂ combustion in GTs can be grouped into three areas, as follows:

- H₂ fuel impurities – characterised by the challenges to deliver low lower heating value (LHV), removal of impurities such as CO and CO₂ content and the cost of producing high volumetric flowrates of the final product.
- Combustion challenges in the GT – characterised by the challenges associated with stable combustion of the volatile H₂ and high temperature combustion.
- GT type / configuration – characterised by generation flexibility, availability of high H₂ GT and emissions control in line with EU limits.

Due to these challenges, 100% H₂ peak demand supply would be extremely challenging by 2030. However, 100% H₂ in the longer term, towards 2040, is increasingly seen as a possibility. It is possible that a future high H₂ case would involve bespoke H₂ ready GT designs to mitigate many of the technical barriers to the current capability of DLE and diffusion GTs alike.

4. Provide insight on cavern capability and limitations on duty.

The behaviour of caverns subject to H₂ cycles is a complex issue, with multiple interlinked variables, however fundamentally caverns should be operated within specific pressure (P_{max} , P_{min} & ΔP) and temperature (T_{min}) envelopes. Several analyses have been undertaken to better understand the behaviour of the cavern when subject to peak daily demand and seasonal cycles where it has been concluded that:

- The minimum average temperature in the cavern should not be lower than 14°C below the average geothermal gradient (Pellizzaro et al, 2011). This equates to T_{min} of 11.2°C at the Cheshire caverns.
 - This is assumed for a salt cavern which is subjected to a demanding pressure loading history, that cycles between P_{max} and P_{min} ,
 - Tensile stresses are expected to develop at the walls of the cavern, if the temperature in the cavern drops below T_{min} where slow extraction/injection cycles have taken place.
 - For fast loading cycles, even if temperature in the cavern is lowered below T_{min} , no tensile stresses develop at the walls of the cavern (with caution due to software limitations).
- Seasonal cycles may require the cavern to be operated in one mode (e.g. injection or extraction) over prolonged periods of time. In contrast, daily profiles may require multi-mode use throughout 24 hours and result in either a net decrease or increase of cavern H₂ volume.
 - A diurnal cycle with a net volume change of zero over a 24 hour period (i.e. extraction equates to injection) has limited impact on cavern integrity.
 - For seasonal cycles, net changes to cavern volume can adversely impact cavern integrity if these occur over prolonged periods of time.
 - Where, T_{min} is typically exceeded during intense extraction operations (e.g. several days continual extraction at max flowrate).

- Based on the Cheshire assessment, the acceptable H₂ flow rate into and out of the cavern is in the order of 1.6 million Nm³/day
 - Assumes nominal cavern temp of ~25.2°C pre-debrining due to the geothermal gradient).
 - Assumes cavern is emptied under continual extraction to P_{min} (80 days) then filled back to P_{max} (80 days),
- Cavern behaviour is inherently linked to the loading history that has taken place in the past. As such, it is not possible to prescribe stand-alone specific operations that will result in specific pressure and temperature conditions. Every imposed loading condition is radically affected to what has happened to the cavern before, so results from this work should be considered indicative only.

5. To provide high level estimates for a complete plant solution, with greater CAPEX and OPEX certainty, in line with AACE5 level (-50% +100%).

For a circa 1 GWe plant the CAPEX required (for the CCGT plant only) is approx. £644M for the “E” class GT in a 2 x (2+1) configuration (25 vol% H₂) and £768M for the small frame GT in a 2 x (6+1) configuration (60 vol% H₂). As informed by discussions with OEMs, a 10% CAPEX increase has been included in these CAPEX figures for GT plant modifications associated when combusting high H₂ ratios.

The plant total CAPEX costs across the three sites is broadly similar (average. £855M for fuel gas stream 2, SGT-2000E GTs), but dominated by the GT plant cost. The annual OPEX cost is dominated by the high service, insurance and grid connection charges associated with the GT plant. These costs would benefit from more detailed cost modelling around the available revenue streams for such a low carbon, peak demand matching plant.

Chapter Roadmap

This study has been structured into the Chapters outlined in Figure 0-1 below:

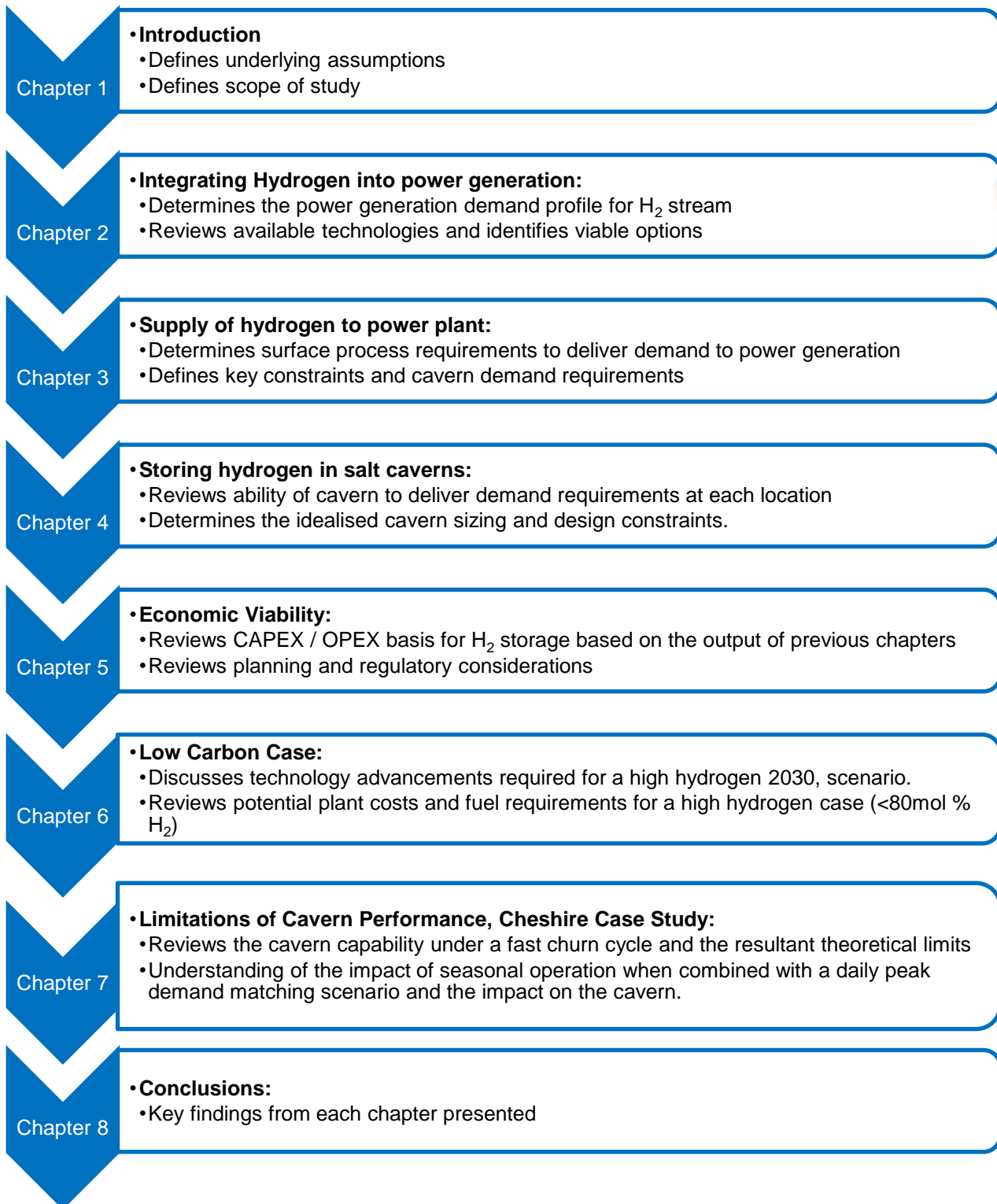


Figure 0-1: Study methodology and document structure

As shown in Figure 0-1, Chapters 2, 3 & 4 present the fundamental features and constraints of the power generation, H₂ transfer and cavern storage elements of a H₂ storage facility. Chapter 5 then presents the economic considerations of such a facility.

The project work presented in Chapters 2 to 5 was developed on the basis of current market expectations and technology, and caverns were selected based on existing caverns in the selected regions. When results were pulled together, two limitations were highlighted:

- I. Firstly, based on guidance provided by GT OEMs, a conservative approach was taken to the proportion of hydrogen that could be safely and effectively burned in the GTs, with significant amounts of natural gas added. This resulted in a significant carbon intensity of the power generated which negates the primary driver of such a system. Given that this is a market which is in an early phase of development and innovation, such conservatism may be misplaced. Chapter 6 therefore explores potential market developments which could better achieve high (preferably 100%) hydrogen combustion and therefore the underlying aims of this study (i.e. low carbon generation).
- II. Secondly (for East Cheshire and East Yorkshire), the size of the single cavern was such that a 1 GWe daily cycle (at least for the hydrogen / methane mixtures covered in Chapters 2 – 5) did not provide a significant challenge to cavern integrity. Chapter 7 provides the results from further analysis undertaken to identify the boundaries of cavern performance for both long and short emptying / filling cycles. In addition, Chapter 7 provides analysis of a cavern operating with daily cycles imposed on a longer, deeper seasonal cycle. This additional investigation work has been based on the Cheshire cavern.

Glossary

A annulus	Annulus immediately outside of the gas carrying completion tubing
ACC	Air Cooled Condenser
ALARP	As Low As Reasonably Practicable
ATR	Auto Thermal Reforming
bgl	Below Ground Level
BGS	British Geological Survey
Brine	The fluid resulting from the dissolution of salt formations with fresh water during salt solution mining, which is said to be saturated when the maximum salt per unit weight has been dissolved corresponding to approximately 26% by weight at 20°C.
Cavern	Developed volume in a salt formation by drilling and leaching, including the cavern sump.
CCGT	Combined Cycle Gas Turbine
COMAH	Control of Major Accident Hazards
Completion	Technical equipment inside the last cemented casing of a well (typically consisting of production tubing and associated components such as nipples and SSSV)
Containment	Capability of a salt cavern and its storage well to resist potential leakage or migration of the gas contained therein.
Convergence	Time-dependent decrease of salt cavern volume due to creep, also dependent upon the minimum operating pressure.
Creep	Geological process that causes salt and other evaporates to flow into subsurface voids that are operated at a significantly lower pressure than the pressure originally exerted on the walls of the salt cavern by the formation.
Cushion gas volume	Gas volume required in a cavern for stability reasons and to maintain an adequate minimum storage pressure for meeting working gas volume delivery with a required withdrawal profile.
DCR	Design and Construction Regulations
Deviatoric stress	Is a stress component which consists of unequal principal-stresses. There are three deviatoric stresses, obtained by subtracting the mean from each principal stress. Deviatoric stresses control the degree of the distortion of geological materials.
DLE	Dry Low Emissions (can be referred to as DLN or premix)
ETI	Energy Technologies Institute
EU	European Union
Formation	Body of rock mass characterised by a degree of homogeneous lithology which forms an identifiable geologic unit.
GE	General Electric
Geostatic stress	The primitive, otherwise known as undisturbed, stress naturally existing in

the underground geological formations before the caverns were developed. The geostatic state of stress within an undisturbed and continuous geological formation is expected to depend on the pressure exerted by the weight of overburden and the potential existence of tectonic forces.

GT	Gas Turbine
GTPro	Thermoflow software; GT combined cycle design program to create cycle heat balance and physical equipment needed to realise it.
GWe	Giga Watt electrical
Halmostatic pressure	The pressure in a cavern when the cavern's well is filled with saturated brine up to ground level, where it is opened to atmosphere.
HP	High Pressure
HRSG	Heat Recovery Steam Generator
IGCC	Integrated Gasification Combined Cycle
In situ	Latin term, refers to site conditions in the original place
ISO	International Organization for Standardization
LCCS	Last Cemented Casing Shoe, bottom end of a casing providing both an anchor and pressure containment barrier.
LHV	Low Heating Value
Lithology	Characteristics of rock formations based on description of colour, rock fabrics, mineral composition, grain characteristics, and crystallisation.
Load	The percentage of rated power output the GT is running at.
Load Factor	The average percentage operating hours running per year.
Log	Graphic representation of a subsurface feature obtained through any of several logging techniques such as gamma-ray absorption, echometric etc.
Logging	Measurement of physical parameters versus depth in a well, such as density logging for locating cavern tops or casing setting depths, echometric logging for internal cavern configurations etc.
MIT	Mechanical Integrity Test, testing procedure that verifies that a salt cavern is capable of storing gas within design limitations with no significant loss from the cavern or cavern well.
MPa g	Mega pascal gauge
mol%	Mole fraction is the amount of a constituent part (expressed in moles) against total amount, and is dimensionless
NG	Natural Gas
NORSOK	The NORSOK standards are developed by the Norwegian petroleum industry to ensure adequate safety, value adding and cost effectiveness for petroleum industry developments and operations.
OCGT	Open Cycle Gas Turbine
OEM	Original Equipment Manufacturer
Overburden	All sediments or rock that overlie a geological formation.
ppg	Pounds per gallon

ppmvd	Parts Per Million, Volumetric Dry
RH	Relative Humidity
Solution mining	Controlled leaching of the salt cavern to its desired shape and size.
Sump	Bottom part of the cavern filled with sedimented, mostly insoluble materials and residual brine.
TIT	Turbine Inlet Temperature
UK	United Kingdom
UKCS	United Kingdom Continental Shelf
USA	United States of America
vol%	Volumetric fraction is the volume of constituent part against total volume, and is dimensionless
Well	Cased borehole and its technical equipment, including the wellhead, that provides access to an underground salt cavern.
Wobbe Index	An indicator of the interchangeability of fuel gases
Wt%	Mass fraction is the mass of constituent part against total mass, and is dimensionless
Working gas volume	Volume of gas in the storage cavern above the designed level of cushion gas volume, which can be withdrawn/injected with installed subsurface and surface facilities (wells, flow lines, etc.) subject to legal and technical limitations (pressures, gas velocities, flowrates, etc.).
Zechstein	Zechstein (ZG), a unit of sedimentary rock layers of Middle to Late Permian age located in the European Permian Basin which stretches from the east coast of England to Northern Poland.

Chapter 1: Introduction

1. Introduction

Atkins has been appointed by the Energy Technologies Institute (ETI) to provide the ‘Salt Cavern Appraisal for Hydrogen and Gas Storage’ project to investigate H₂ storage in different salt cavern fields and H₂ combustion to meet the typical UK power demand.

The ETI aims to consolidate its understanding of what flexibility of supply salt caverns may offer the power (and potentially the heat, transport and industrial) market. This report presents a detailed investigation of the UK salt cavern resource and capability.

1.1. Background

In 2012 a study was commissioned by the ETI which considered the techno-economic potential of combining H₂ storage in salt caverns with GTs to provide a low carbon, dispatchable power supply to meet typical power demand cycles (AmecFw, 2012). The study demonstrated the significant potential that salt caverns could bring in acting as a buffer between a constant H₂ supply and a variable power demand.

In the study, the H₂ generation plants were fitted with Carbon Capture and Storage (CCS), which ran continuously at full load, filling the salt caverns during periods of low power demand. During periods of peak power demand the stored H₂ could be combusted through a GT to generate electricity.

Figure 1-1 presents a simple diagram of the underlying principle considered in the study. During power generation the power plant is fed by both the salt caverns and the H₂ production plant in parallel. The H₂ production source is considered as a continuous supply, and so, conversely when the cavern is filling there is no power generated.

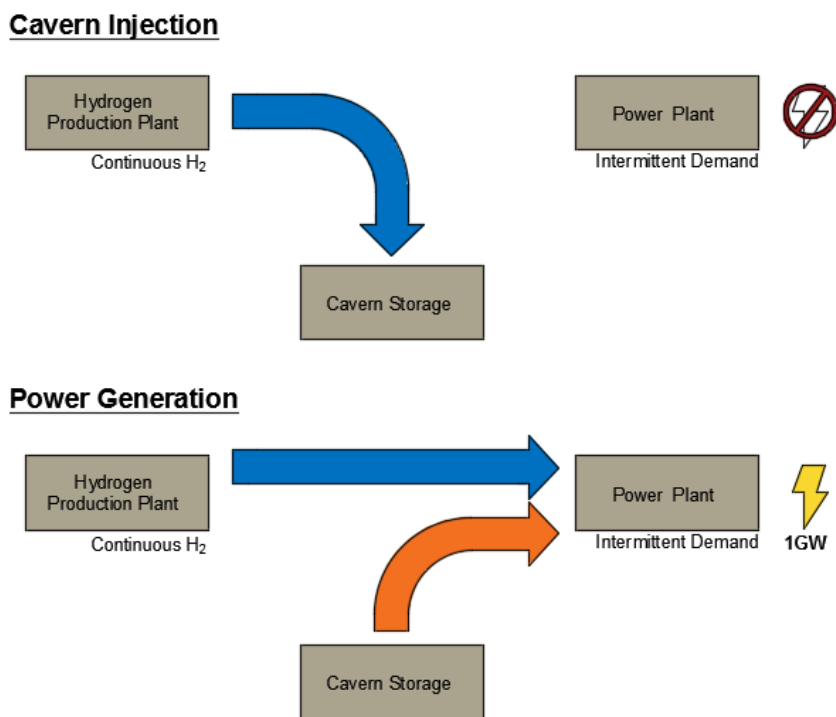


Figure 1-1: High level process block diagram, operating principles

For clarity, the preceding work by Amec Foster Wheeler incorporated the following assumptions, which have helped inform this study (AmecFw, 2012):

- The H₂ production source is continuous and can be sized to a specified production rate. The operation principle is set out in Figure 1-1.
- It is assumed that the H₂ would be supplied at 30-40 barg from the production source.
- The study produced approx. 1.3 GW peak for 12 hours per day. The average load factor was 36%.
- The modelling was based on General Electric (GE) frame 9F syngas variant, with efficiency of 34.4% with N₂ as the diluent. “E” class machines were not reviewed in any detail.
- Plant thermal efficiency may be 0.5% higher with N₂ dilution and comparable with steam dilution (though at a penalty of increased water consumption, and possible increased visible exhaust plume is expected).
- The work included high level power recovery figures from the pressure let down equipment as the cavern extracts the available gas. For the Cheshire and Yorkshire sites, this was assumed to be ~30 MW.
- The CAPEX and OPEX figures presented for the syngas production area, topside facility and power island area have been reviewed and used to inform these elements within Chapter 5 of this study.

1.2. Objectives

The objectives of this study are defined as follows:

1. Consolidate the ETI understanding of cavern flexibility, to support ETI system level modelling activities, for up to 100% H₂ and H₂ / methane mixtures, with a focus on flexibility and cost.
2. Characterise key constraints and their causes when operating fast churn storage at selected sites, including those caused by integration with the H₂ supply and the GTs.
3. Identify a range of GT / CCGT offerings which match cavern capability or market needs.
4. Provide insight on cavern capability and limitations on duty.
5. To provide high level estimates for a complete plant solution, with greater CAPEX and OPEX certainty, in line with AACE5 level (-50% +100%).

1.3. Study constraints

To ensure the objectives outlined in Section 1.2 are achievable, several key study constraints have been identified. These are presented in Figure 1-2, where the constraint inter-dependencies are shown in the central oval.

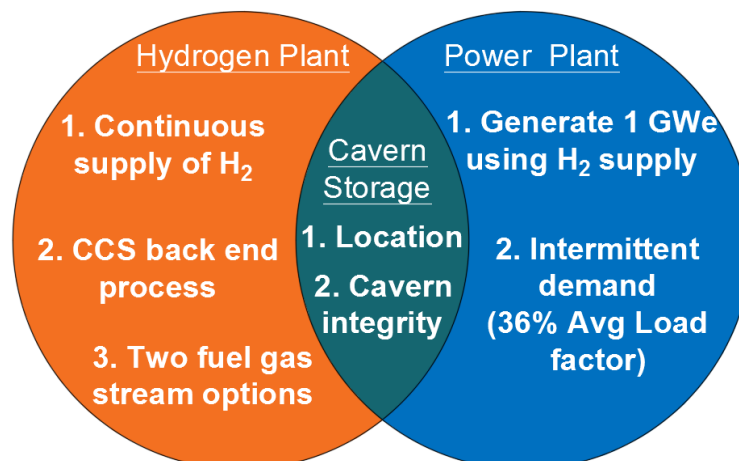


Figure 1-2: Key Study Constraints

Hydrogen production plant

The source of the clean, low carbon H₂ fuel is a fundamental driver for this project. As outlined in Section 1.1 it is assumed that the H₂ plant will provide a continuous supply of H₂. The original Amec Foster Wheeler 2012 report (AmecFw, 2012) considered several different technologies for providing a H₂ rich fuel from gas, coal or biomass. Each case utilised carbon capture to remove CO₂. This study has not considered the H₂ production process, but has assumed the following two H₂ fuel gas streams:

- Fuel gas stream 1: 89 mol%² H₂ fuel gas stream, as would be produced by gasification of biomass or coal.
- Fuel gas stream 2: Fuel gas stream of 53% mol% H₂ and 44 mol% N₂, as would be produced by Auto Thermal Reforming (ATR) of natural gas.

The H₂ fuel gas streams are summarised in Figure 1-3 and presented in detail in Appendix A.1.

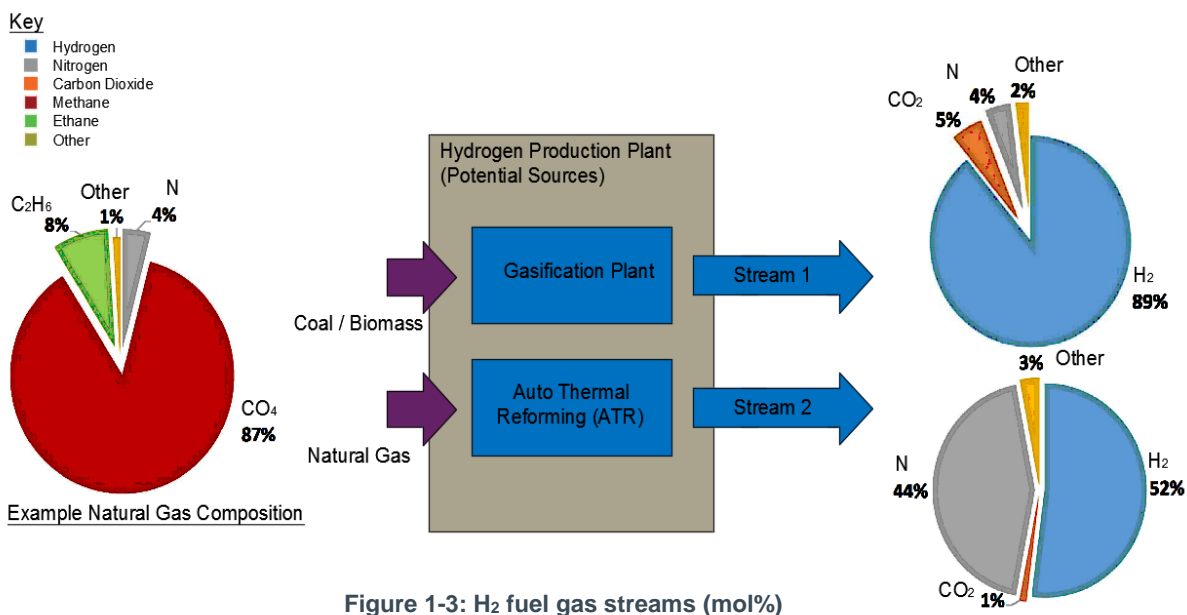


Figure 1-3: H₂ fuel gas streams (mol%)

Fuel gas stream 2 has a relatively low lower heating value (LHV) than compared to that of natural gas; ~9128 kJ/kg versus ~46,260 kJ/kg. Fuel gas stream 1 is a purer H₂ fuel gas stream with a higher LHV than fuel gas stream 2. As stated in Section 1.1, the H₂ rich fuel gas stream delivered from the H₂ production facility will be either wholly routed to the power plant or diverted to the underground storage cavern(s) depending on power generation load and fuel demand requirements. However, with the power plant off-load all H₂ rich fuel will be diverted directly to the storage cavern(s).

Power plant

It is anticipated that a H₂ storage based source of power generation would be ideally placed to address the UK's increasing requirement for a low carbon 'on demand' power supply (ETI, Dennis Gammer, 2015). This would support the UK as it drives to meet its 2020 and 2050 climate change targets by offsetting the intermittency of renewable power supplies (e.g. wind / solar) and improving the efficiency of next generation fossil fuel power stations complete with CCS.

² Note that for an ideal gas, mol% fraction can be assumed equal to vol% fraction. However, in this report mol% has been typically used to describe the fuel gas stream and vol% as the H₂ GT capability.

To understand how this could be accomplished it is first necessary to define the anticipated power demand and therefore the operating regime that a H₂ storage based source of power generation would need to meet. As an initial target, it is assumed that a capacity of 1 GWe power output would be required. This is considered credible based on a review of the forecast for CCGT and OCGT generation required for the year 2030 and beyond.

Furthermore, this study assumes an average target load factor of 36%. This is representative of a station running during the working day, but offline at night and weekends (AmecFw, 2012). Or in the case of this study, to meet the peak electricity demand in the morning and evening every day of the week. Three power generation scenarios (Figure 1-4) which closely meet the 36% load factor, for a fleet producing at circa 1 GWe power output, have been considered by this study. These are outlined below (and presented in Figure 1-4 and Table 1-1):

- Scenario 1: operating from 7am to 7pm at 70% average load.
- Scenario 2: operating for morning peak between 6:30am and 10am at 90% average load then idling at 40% average load throughout day and meeting the evening peak between 5:30pm and 9pm.
- Scenario 3: operating for morning peak between 5am and 10am at 90% average load and restarting for the evening peak between 5pm and 10pm.

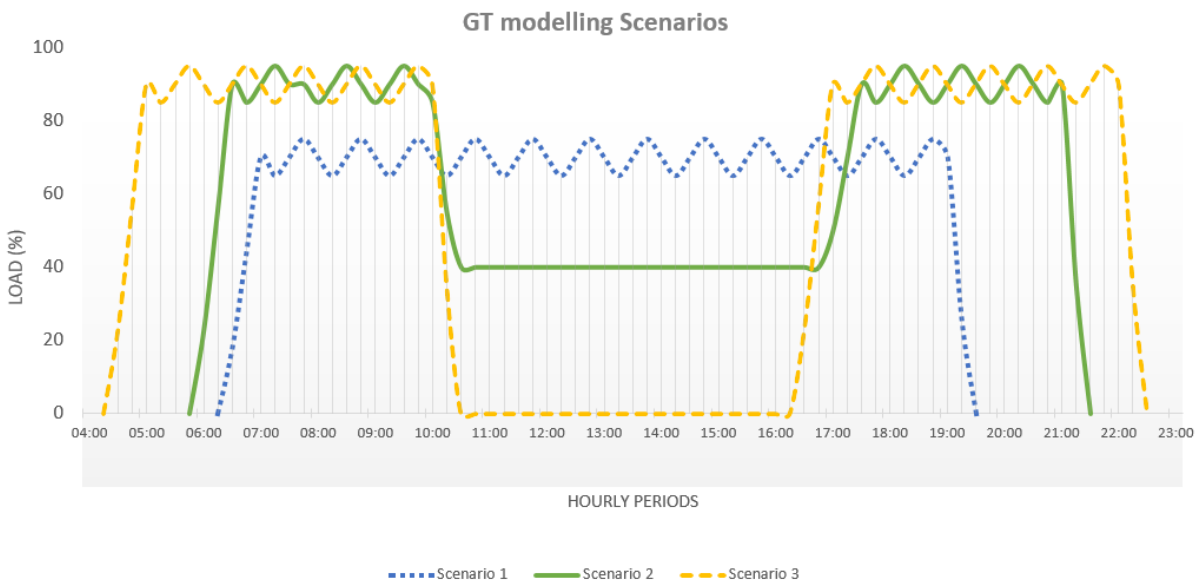


Figure 1-4: Power plant generation scenarios

Table 1-1: Power plant generating scenario load factor

	Scenario 1	Scenario 2			Scenario 3	
	7:00am-7:00pm	6:30-10:00am	10:00-5:30pm	5:30-9:00pm	5:00-10:00am	5:00-10:00pm
Operation (hr)	12	3.5	7.5	3.5	5	5
GT average load (%)	70%	90%	40%	90%	90%	90%
Avg. load factor (%)	35%	38%			38%	

The three operating scenarios for the power plant all show power generation to meet the peak daily

demand with one or two power plant starts per day. The power plant is assumed to operate in the peak demand matching regime throughout the year, with the exception of outages for GT inspection and maintenance.

Cavern storage

As outlined in the 2012 Amec Foster Wheeler report (AmecFw, 2012), there are geological limitations which restrict the locations in the UK which can be used for salt cavern storage. Specifically, the salt formations in which caverns can be constructed are limited to the areas shown in Figure 1-5.

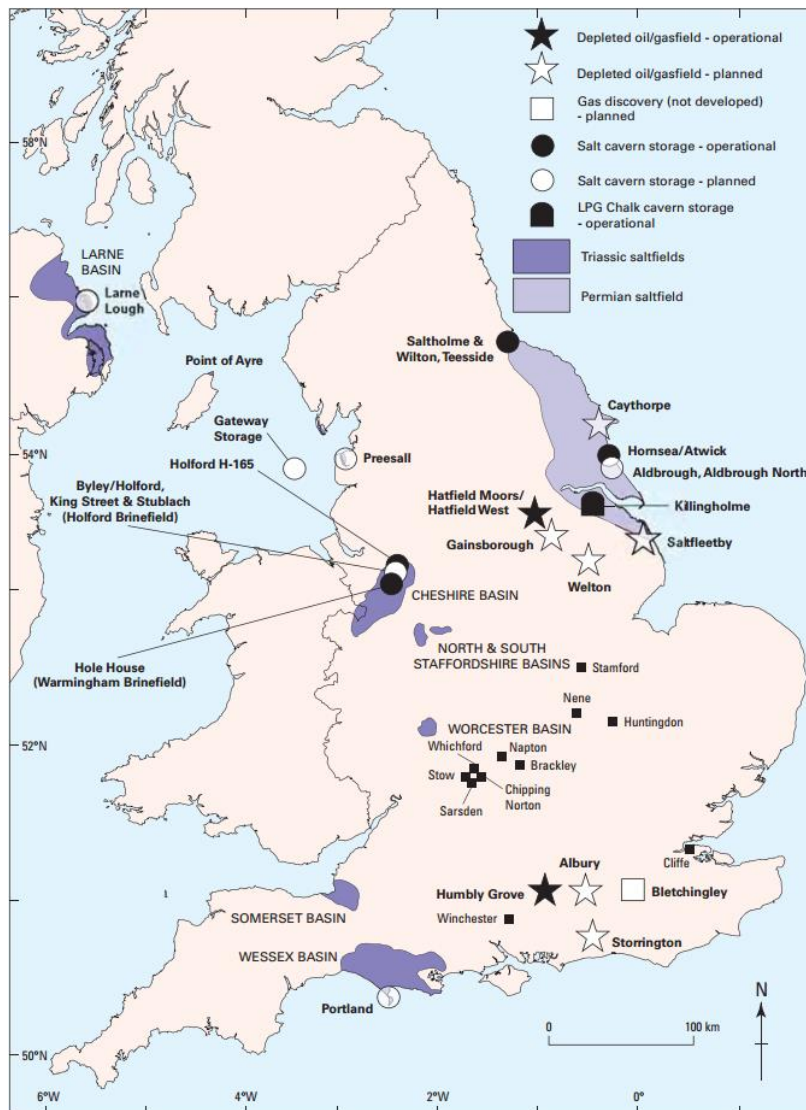


Figure 1-5: Distribution of the main halite bearing basins in Britain and the location of operational and proposed underground gas storage sites (Evans, 2008)

As shown in Figure 1-5, there are many existing salt caverns which are typically located within the East Yorkshire, Teesside and Cheshire regions. Of these, three caverns are currently being used for H₂ storage, where all three are located in 'Brinefield no.4' at North Tees, Teesside; although this does not preclude the other regions as potential storage locations.

The depth and size of the salt formations at each of these locations vary, as does the local geology and the method of storage (i.e. wet storage, where gas is displaced with water or dry storage, where gas pressure is adjusted only), therefore it is important to understand how these differences impact the

potential for H₂ storage. Appendix A.2 provides a detailed discussion of the geology and stratigraphy found at each of the areas identified.

This study considers the potential for introducing H₂ storage at each of the locations (East Yorkshire, Teesside and Cheshire) developing an understanding of the potential to re-purpose existing caverns (typically used for natural gas storage or chemical storage) or to develop new ones. To achieve this a representative cavern geometry has been defined for each location, this is presented in detail in Appendix A.3 and summarised in Table 1-2 below. The representative caverns have been derived through review of the existing cavern fields at each location.

Table 1-2: Characteristics of representative caverns at each location to be considered.

	East Yorkshire	Teesside	Cheshire
Geological formation	Permian, Zechstein II	Permian, Zechstein III	Triassic, Mercia Mudstone Group
Cavern roof depth [m]	1,720	647	545
Cavern bottom depth [m]	1,830	670	620
Cavern volume [m ³]	275,700	51,100	304,400
Depth of last cemented casing shoe [m]	1,710	645	535
Nominal gas storage operating range P_{max}/P_{min} [barg]	271 / 120	halmostatic	95 / 30
Type of storage operation	dry	wet	dry
Operator & source of data	SSE	SABIC	Storengy / Inovyn

The differences in geology at each location impact the operating characteristics of the cavern where it is critical to understand the stability of the salt caverns and the mechanical behaviour of the surrounding rock material. Effectively the salt cavern acts as a subsurface pressure vessel which is exposed to pressure and temperature fluctuations during periods of gas import and export (where it is also constantly exposed to an external pressure due to the formation). During these periods the cavern walls will be subject to increased stresses therefore, like any pressure vessel, limitations are placed on the maximum / minimum pressure and flow rate that the cavern can be exposed to. However, unlike pressure vessels the derivation of these are based on the material properties of the surrounding geology and the typically compressive forces that these exert on the cavern. The assumed operating ranges for the representative caverns are presented in Table 1-2.

One of the fundamental reasons that salt formations are used, and will continue to be used, as gas storage vessels is the ability of the salt formation to 'heal' itself. Salt is an elasto-visco-plastic material, meaning caverns will be subject to creep over time (i.e. the salt formation will try to close the void). This gradual closure of the storage caverns is closely dependent on the creep characteristics of the site-specific salt and the operating pattern of the caverns. If cavern convergence is left uncontrolled it will result in loss of storage volume and can lead to substantial flexure and high strains in the overburden strata, which in turn may substantially increase their permeability.

The rate of creep is dependent on several factors including the pressure cycles the cavern is subject to, therefore it is also important to understand how the operating regime of H₂ storage will impact the cavern integrity over its predicted life. This study therefore assesses the behaviour of caverns at each location against a defined operating regime to determine the overall impact to the cavern. Appendix A.4 provides a summary of the theory used to assess cavern behaviour.

1.4. Methodology

As discussed in the preceding sections, the development of a dispatchable H₂ storage based power source is a wide and complex topic, with many variables, therefore it is essential that its assessment is undertaken in a structured, methodological manner. The project in its simplest form can be summarised in three key aspects:

- I. H₂ production
- II. Cavern storage
- III. Power generation

Although each of these areas are intrinsically linked with each other, for ease of discussion, it is considered sensible to present each area independently, where the H₂ production plant has already been discussed in detail in (AmecFw, 2012) and is therefore out with the scope of this study. Albeit details from the original study will be called out (as presented in Section 1.3).

One of the key objectives of this study is to develop an understanding of cavern capability to support the power generation process. To achieve this it is first necessary to define the power generation regime that the cavern must support. Although this may appear counter intuitive, where the power generation regime requirements are used to define cavern limitations rather than cavern limitations used to define power regime, the main reason for this is the complexity of assessing cavern behaviour. By defining the power regime first, the number of cavern operating permutations to be considered can be limited. Chapter 2 discusses the power generation regime in detail.

It is noted that simply defining a power regime, and therefore the H₂ storage requirements placed on the caverns, does not provide the full picture required to assess cavern behaviour. Therefore, it is essential to understand the process by which the H₂ will be transferred between source, cavern and power generation assets. Chapter 3 discusses the underlying principles of this transfer process and the restrictions / requirements that this places on the cavern operation.

Using the inputs discussed in Chapters 2 & 3 the behaviour of the cavern when subjected to a peak demand profile is reviewed in Chapter 4. With results from this, 'power generation regime' driven cavern assessment, it is then possible to undertake a focused sensitivity analysis on the cavern response to better understand the limits on cavern operation. This is discussed in Chapter 7.

An integral part of this study is also to understand how such a H₂ storage facility would support meeting the UK's low carbon targets. Chapters 5 & 6 provide an overview of the economic viability such a facility would have and the technical advancements which would be required to enhance its offering.

Chapter 2: Integrating hydrogen into power generation

2. Power generation

The integration of H₂ rich fuel streams into power generation plant is not common industry practice, where there are number of key technical and legal / regulatory constraints which require review. These are presented schematically in Figure 2-1 and are discussed in detail within the following sections where the key objectives of this chapter are to:

- I. Define baseline H₂ demand requirements to deliver a defined power output including cycles, flow rates and pressures.
- II. Identify a range of suitable GTs available on the market today suitable for H₂ operation.

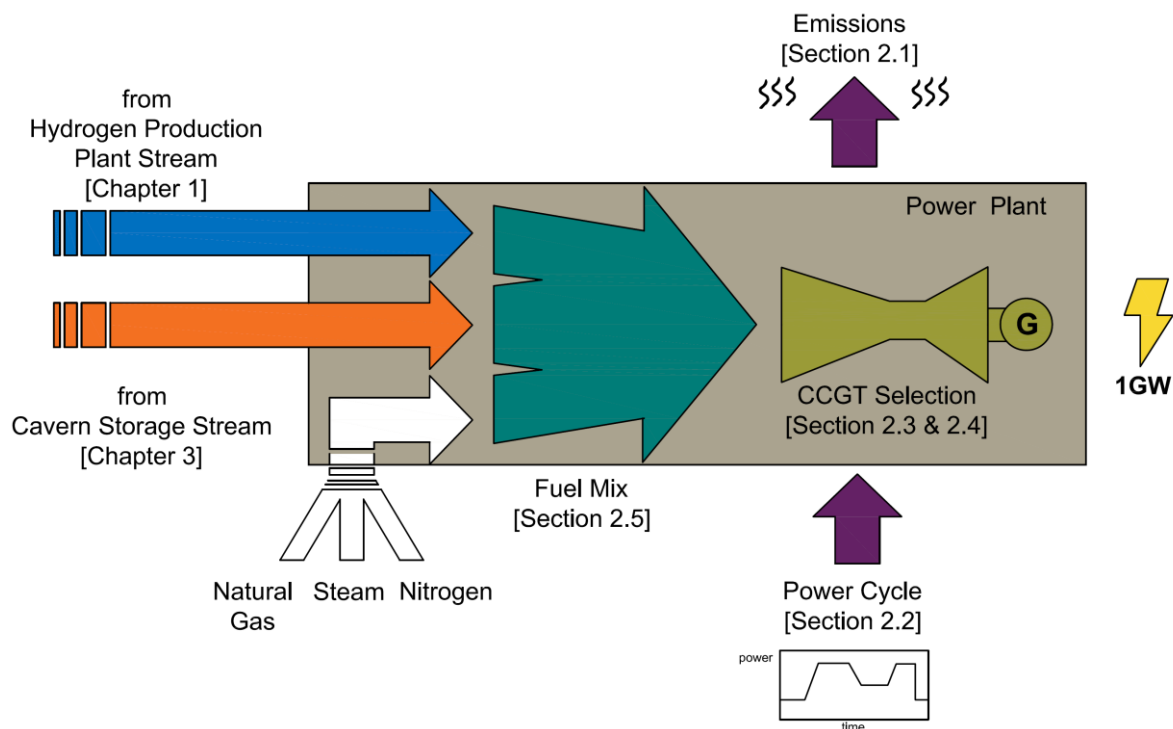


Figure 2-1: Power generation block diagram / section map

This aspect of the study has focused primarily on GT technology in combined cycle configuration where it aims to evaluate the power plant capacity, flexibility for dispatch, load ramping, technical feasibility and economics of utilising a fuel supply that incorporates an underground cavern H₂ buffer storage facility as part of an overall peak demand matching power plant. The study has performed a detailed technical assessment of the current GT range and considered the capability of proven and advanced GTs to perform with a range of fuel gases based on H₂ rich fuel gas streams.

The GT baseline demand requirements form a critical interface with the cavern storage study discussed in Chapters 3 and 4. Detailed GT performance modelling has therefore been undertaken using the fuel gas streams specified in Section 1.3 to ensure sufficient interface definition is available. An industry recognised software package, GT PRO, has been used to support this exercise where relevant assumptions and limitations of the GT PRO package are outlined in Appendix B.1.

This study considered a wide variety of GTs, which was narrowed down via a down selection exercise to ensure only the most credible GTs were considered. The down selection process included the following tasks:

- Definition of performance limits and NO_x emission constraints (Section 2.1).
- Definition of ramp rate / flexibility requirements (Section 2.2).

- Review of potential GT options and down selection to a maximum of two GTs (Section 2.3).
- Definition of CCGT arrangement (Section 2.4).
- Definition of fuel mix and power plant fuel requirements (Section 2.5).

2.1. Performance limits and NO_x emissions control

When switching from natural gas to H₂ rich fuel gas streams, one of the key constraints are the NO_x emissions. Any large combustion plant with an output of higher than 50 MW is required to comply with the EU directive emission limits. For a single GT, the NO_x emission limit values at an O₂ content of 15% are defined as follows (European Parliament, 2001):

- 50 mg/Nm³ for natural gas (~25 ppm NO_x);
- 120 mg/Nm³ for other gaseous fuel (~60 ppm NO_x).

In general, there are three methods to reduce NO_x emissions from a GT combustion chamber:

- Pre-mix Dry Low Emission (DLE) combustors, including mixes of H₂ with natural gas;
- Diffusion combustors with fuel dilution by steam, water, or N₂;
- Removal of NO_x components from exhaust gases with selective catalytic reduction (SCR).

For natural gas applications, pre-mix DLE combustors have been preferred to reduce NO_x emissions. Their basic principle is to achieve a moderate flame temperature by mixing air and fuel before the combustion. When switching to H₂ containing fuel gas streams, premix DLE combustors, used in most current GTs, are more prone to combustion instability compared to diffusion combustors. There is also a safety concern related to the wider flammability range and higher stoichiometric flame temperature of H₂ compared to the methane-rich natural gas (see Figure 1-3 for composition).

In diffusion combustors, the stoichiometric flame temperature is representative of the actual flame temperature and is strictly related to the NO_x formation rate. The higher flame temperature when firing H₂ rich fuel results in up to ~700 ppm NO_x at 15% O₂ for 95% H₂ fuel gas streams and up to ~200 ppm for natural gas (Chiesa, et al., 2005). This level of NO_x emission is unacceptable by the EU directive and industry best practice. Therefore, in diffusion combustors, dilution is used to comply with the NO_x emission limits.

DLE and diffusion combustors are further discussed below where specific considerations are given to the overall process, the potential sources of additional diluents and the impact on performance these may have.

For DLE or diffusion combustors, Selective Catalytic Recovery (SCR) may be necessary as an additional means to stay within the EU emission limits. Recent CCS project proposals identified the need for a SCR unit to remove any remaining NO_x emissions from an integrated gasification combined cycle (IGCC) with H₂ rich syngas. SCR tends to be the most expensive way of NO_x removal when aiming at such low concentrations of NO_x as 25-60 ppm, and is typically used as an additional measure rather than a low NO_x solution in its own right.

DLE combustion chambers

DLE combustion systems have seen technology advancements since the 1990s, which has helped GTs meet tighter NO_x control limits, without the need for diluents such as steam or water which was previously required. A DLE combustor uses the principle of lean premixed combustion where the fuel and the air necessary for combustion are mixed together prior to being injected into the reaction zone. All modern GTs running with natural gas are fitted with DLE.

The Siemens estimated performance, as shown in Figure 2-2, was plotted to better understand the GT performance when firing H₂ rich fuel gas streams. Siemens indicated that high H₂ concentrations on the modified current DLE burner design could be achieved by reducing the turbine inlet temperature (TIT), with a resultant reduction in power output (Michael Welch, 2016). Figure 2-2 also shows GT PRO

simulation data for SGT-800, where, compared to Siemens curves, GT PRO is configured to keep the TIT constant at a value of 1,300°C (red dotted line). As a result of this GT PRO GT power output also stays nearly constant, with only a slight rise due to the increasing calorific value of the fuel (red solid line).

GT PRO was used to estimate the TIT reduction expected with increasing H₂ fractions, based on data from the OEM. The estimated TIT reduction is shown (blue dotted line) when modelled in GT PRO against the data provided by Siemens for the same SGT-800 machine (blue solid line).

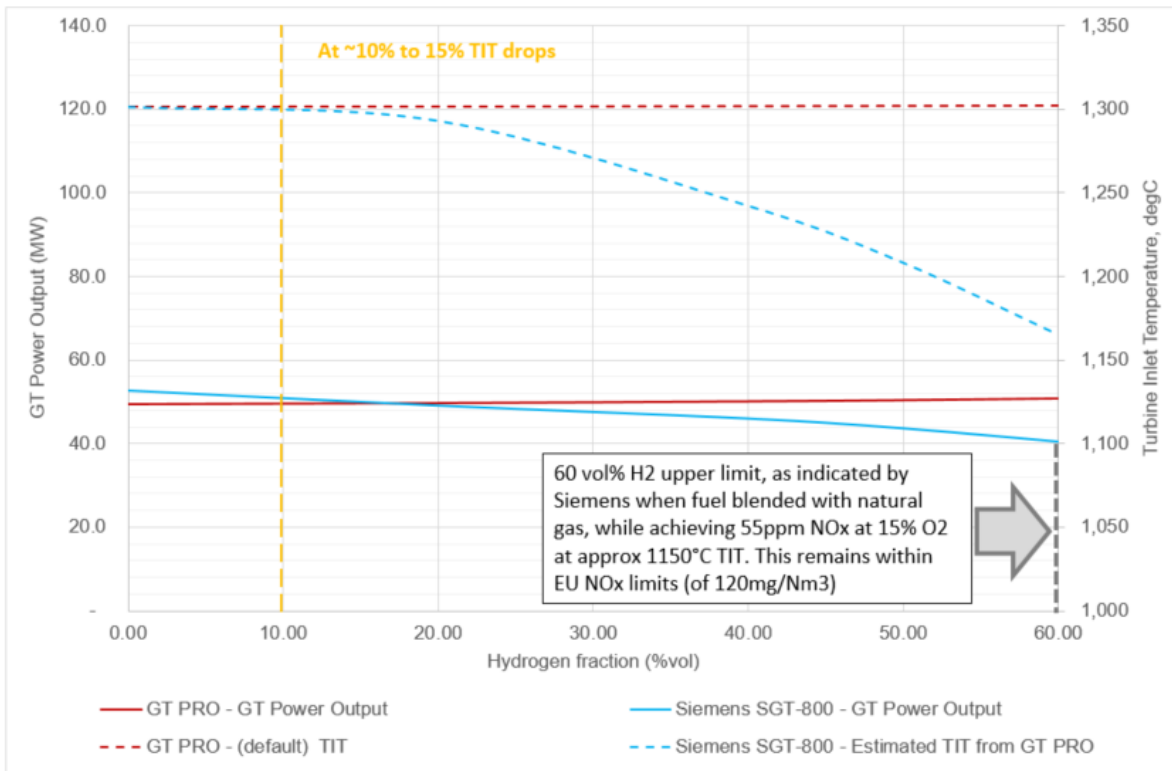


Figure 2-2: Siemens DLE combustor estimated performance

As the fraction of H₂ in the fuel increases, the TIT must be reduced to avoid flame instabilities associated with firing H₂, which also results in reduction of the GT power output. It is estimated that at approx. 60 vol% H₂, the TIT would need to reduce to about 1,150°C, which is similar to the typical operating conditions of an “E” class GT. The constraint on TIT (with adjustments of +/- 100°C in GT PRO) was later used to estimate GT performance capability with high H₂ fuels.

The results shows that there is no significant reduction in the TIT up to approx. 10-15 vol% H₂, which aligns with the OEMs indications on the current DLE burner capability to fire natural gas fuels with up to 10 vol% H₂, without significant modifications to the burner hardware.

Fuel dilution in diffusion flame combustion chambers

Diffusion burners were the standard combustor before the introduction of DLE types. The simple design allows a wide range of fuel/air mixes, but NO_x control can be more challenging due to the stoichiometric reaction temperatures, where often steam and or N₂ is used as a heat sink to reduce combustion temperatures and reduce the production of both thermal and fuel associated NO_x.

From combined research, case studies and feedback from the OEMs, it is apparent that large frame GTs with diffusion flame combustors are capable of handling higher fractions of H₂ (relative to unmodified DLE types) in the fuel by diluting the fuel with steam or N₂. Example case studies of IGCC plants operating with H₂ rich syngas with diffusion combustion (using steam or N₂ dilution for NO_x and

fuel reactivity control) are given in Appendix B.3.

For GT PRO modelled cases the source of steam has been assumed as main high pressure (HP) steam from the CCGT cycle, this reduces the plant power output and efficiency and is deemed a worst case option, although it is noted that it may be possible to use MP steam as a more efficient alternative. In practice, it would be preferential to use excess steam available from the ATR process when producing fuel gas stream 2, it is also possible to use steam generated from the heat produced in gasification process for producing fuel gas stream 1. However, if it is assumed that any excess steam from the fuel gas stream production would be fed to the CCGT steam cycle, there is an overall plant performance loss regardless of the source of the steam.

Assumptions for N₂ as a diluent are based on the production of N₂ gas from the air separation unit (ASU) as integrated to the fuel gas stream 1 gasification facility. Previous work by AmecFW (AmecFw, 2012) indicates that this production is sufficient to meet the N₂ demand required for NO_x and flame stability as outlined in Section 2.5 of this report.

In the case of gasification fuel gas stream 1 there are additional challenges for a peak demand matching power plant using N₂ as a diluent. These are primarily related to the need for N₂ to be produced and stored to match the power generation scenarios.

Natural gas blending

Through review of GT literature and OEM discussions it is apparent that, at present, the GTs offered on the market, specifically DLE types, are unable to support sustainable stable combustion of very high proportions of H₂ (more than approximately 50 vol%) without introduction of natural gas to improve the combustion stability. For example, the small scale, SGT-800 DLE GT has been tested with high fractions of H₂ (up to 60 vol%), however this relates to natural gas / H₂ blend only (Michael Welch, 2016). Indeed, there are many examples of small GTs running on up to 90 vol% H₂ with diffusion combustors with dilution to avoid uncontrolled reactivity and auto-ignition. For clarity, a summary of the requirement for natural gas in this study's application is given below:

- Natural gas is used for GT start-up, where this is most significant in Scenario 3 with two starts per day.
- Maintenance and OPEX costs are likely to be lower with Natural gas, as the maintenance regimes are well understood and proven.
- The syngas variant fuel gas stream 2 is a 'skinny' fuel relative to the LHV of natural gas seen in typical GT combustors. This suggests an additional fuel source is needed to bring the GT performance into normal natural gas ranges comparable to natural gas combustion (the LHV values are presented in Table 2-10), unless future developments allow for a greater H₂ proportion of fuel gas.
- The purer, fuel gas stream 1 is currently not combustible in GTs available on the market without significant GT modifications followed by extensive testing and / or the use of diluents.
- High H₂ fuel gas streams above those indicated (Section 2.3) are not guaranteed by OEMs regarding long term service agreements (LTSA) and are therefore currently unfeasible. A project in 2030 however, may benefit from extensive R&D in this area if the low carbon agenda pushes this technology under a 'H₂ economy' vision. This is discussed further in Chapter 6.
- The use of high diluent ratios (N₂ or steam) results in higher mass flowrates through GT. This may require compressor modifications, and / or a need to bleed off air.

Natural gas is required either during the GT start up or as a boost to the typically low LHV of the rich fuel gas streams (when mixed with required cooling diluents; steam or N₂). The natural gas would be mixed with fuel gas streams 1 or 2 post cavern storage or injected directly into the GT combustor in cases where the GT is equipped with multiple burners for syngas, natural gas and fuel oil firing.

Clearly, despite the need for Natural gas in current systems, the continued use of Natural Gas moves

away from the overarching project aspirations to be low carbon, and may prevent such projects obtaining crucial contract for difference (CfD) payments to support their financial viability.

N₂ dilution

Fuel gas stream 2 contains around 44 mol% N₂ (see Figure 1-3), so it is unlikely that further N₂ dilution would be needed. Fuel gas stream 1, contains 4 mol% N₂ and is derived from gasification, so N₂, if required would be taken from the associated air separation unit (ASU) at a supply pressure (of approx. 30barg, (AmecFw, 2012)). The ASU power consumption is a significant parasitic load as a proportion of the gross output of an integrated IGCC power plant. Dependent on the fuel gas stream source, the N₂ supply would therefore be stored (mixed with the H₂) in the cavern or, if required, as additional onsite, tanked storage to allow direct injection and increased burner control.

The use of N₂ as a diluent has been modelled with GT PRO for various fuel blends using fuel gas stream 1 and 2 as the primary fuel. The resultant mixtures chosen to be the most realistic case for the modelled GTs is given in Section 2.5.

Figure 2-3 presents the GT PRO findings for N₂ as a primary diluent to control NO_x emissions. The modelling has shown that as the ratio of H₂ to N₂ in the fuel gas at combustion decreases to below 1:1, the GT TIT and therefore GT power output decrease; indicating that the 1:1 ratio is a turning point for the “E” class GT with N₂ injection. Similar characteristics were also shown through modelling for more advanced GTs such as “F” & “H” class GTs.

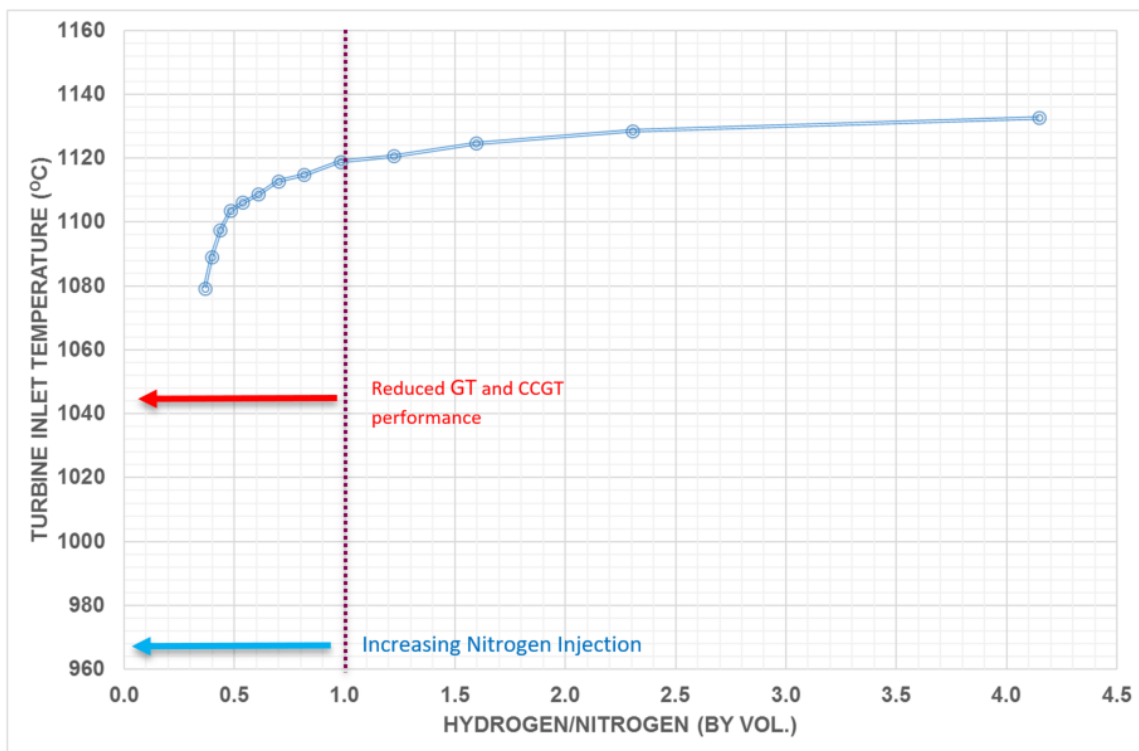


Figure 2-3: Impact of N₂ dilution effect on GT performance

* The graph is based on GT PRO simulations of SGT5-2000E GTs firing fuel gas stream 1 at ISO conditions.

The modelling indicates that high flowrates of N₂ injection, which are necessary to prevent excessive NO_x production also lead to reduced overall CCGT plant capacity and performance. Hardware modifications may be possible to circumvent this technical hurdle. For example, GT design limits on exhaust hot gas throughput mean that, in the case of increasing fuel gas flow with high fractions of N₂, it may be necessary to bleed off air from the GT compressor to prevent choking at the GT turbine inlet nozzle. In a standalone power facility, this results in a loss in power output and efficiency, unless the air

which is bled off can be used elsewhere in the cycle, for example in the ASU.

A study by Gazzani et al on using H₂ as GT fuel provides estimated results for a H₂ fuelled CCGT with diffusive flame combustor and dilution using steam or N₂. The study was based on firing pure H₂ in a GT with performance and NO_x emissions predicted by a computer code developed by the authors. The study results suggested that the NO_x emissions would be ~19 ppm (at 15% O₂) at a H₂ / N₂ ratio of 0.38:1, (Gazzani et al, 2014), which indicates a possible maximum N₂ proportion of 2.6:1 N₂ to H₂.

Steam dilution

The use of steam as a diluent has also been modelled with GT PRO for various fuel blends using fuel gas stream 1 as the primary fuel. The resultant fuel gas streams chosen to be the most realistic case for the modelled GTs is given in Section 2.5. The source of the steam is understood to be sourced from one of the following:

- The gasification process (for fuel gas stream 1).
- Steam offtake from the SMR / ATR process (for fuel gas stream 2).
- Extraction from the main high pressure or medium pressure steam header.

In the case of a stand-alone power generation plant where steam is extracted from the heat recovery steam cycle and used for dilution, there is a reduction in steam flow and power generation at the steam turbine. However, a portion of this loss is recovered by the steam exhausting through the GT.

In the case of an integrated H₂ production facility at a power plant, excess steam generated in cooling the gasifier may, for example be used instead of taking steam off the combined cycle.

For fuel gas stream 2, steam is available as a by-product from the ATR process and for fuel gas stream 1, steam is produced as part of the gasification process. There is no performance penalty for the CCGT cycle, but steam offtake is still an energy cost to the overall integrated plant.

Figure 2-4 presents results from GT PRO across a variety of H₂ to steam injection ratios for the SGT5-2000E in the combustion chamber, using fuel gas stream 1. The trend curve shows that as the fuel gas ratio of H₂ to steam in the combustor chamber decreases to below about 4:1, the GT TIT and GT performance starts to fall off significantly.

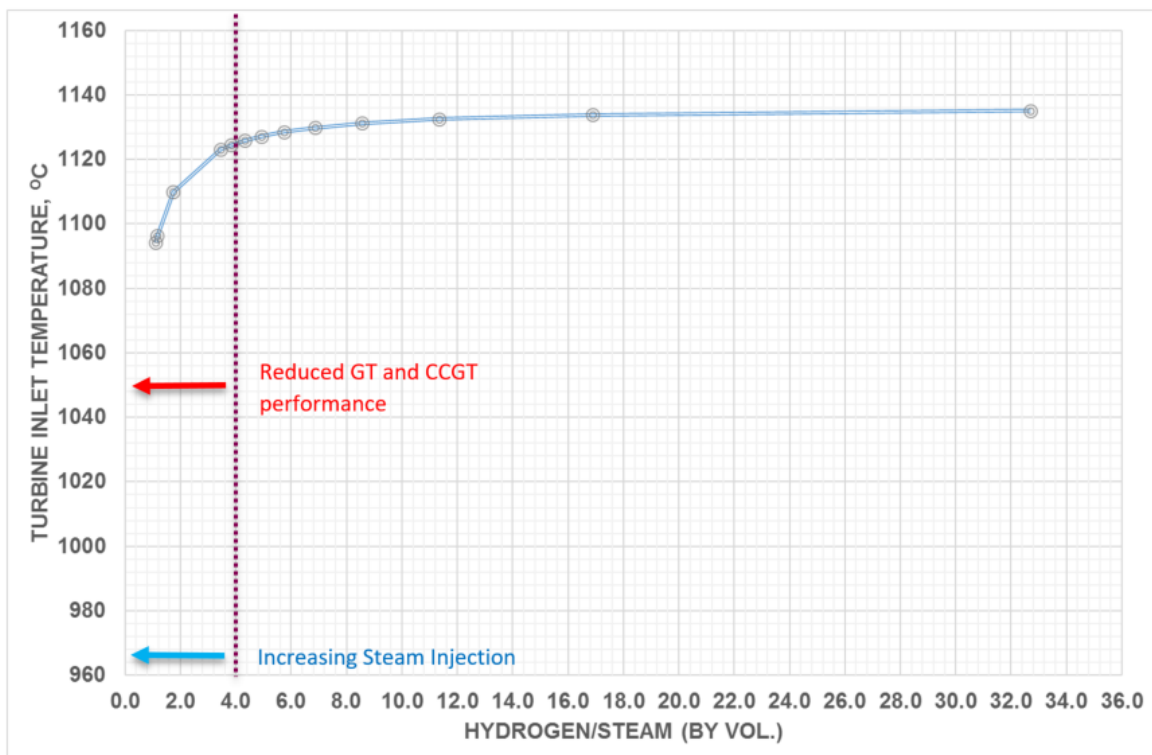


Figure 2-4: Impact of steam dilution effect on GT performance

The graph is based on GT PRO simulations of SGT5-2000E GTs firing fuel gas stream 1 at ISO conditions.

The study by Gazzani et al discussed above suggested that the NO_x emissions would be ~19 ppm (at 15% O₂) at a H₂/steam ratio of ~1.2:1 (Gazzani et al, 2014). The difference between the results of the theoretical Gazzani and GT PRO model estimates are likely to be due to disparities in the model basis and fuel composition. This study would benefit from availability of more data in regard to steam dilution, which may be available in coming years, as R&D from the OEMs becomes publicly shared.

Steam vs Nitrogen as diluent:

Nitrogen gas or steam are typically adopted as diluent gases for GT emission control in diffusion burners. Nitrogen is a by-product from the air separation units which are incorporated into the integrated gasification process, which produce H₂ from either coal or biomass. The extraction of N₂ from the ASU (of fuel gas stream 1) theoretically results in minimal direct impact or loss on generation. However, there may be some additional parasitic load to compress the N₂ leaving the ASU to the GT combustion pressure of 30 to 40 barg.

Alternatively, if steam is used this is typically extracted from the CCGT steam cycle resulting in a reduction in the generated output from the steam turbine and CCGT. Steam is also raised in the gasification process in cooling the gasifier reactor associated with the production of fuel gas stream. Importing this steam from the gasifier as an external source would result in no reduction to the CCGT output. However, in the case of an integrated plant, use of the steam raised in the gasifier would also result in a reduction in the net generation from the plant.

In terms of the effectiveness of steam compared with N₂ for emission control the GT pro modelling has demonstrated that less steam by volume is required compared with N₂. This means that GTs are less prone to choking as the throughput of hot gases increase with the addition of diluent and accordingly emission control may be achieved without the need for the compressor stage blow off.

There are apparent advantages and disadvantages in using both diluent types, which will depend on the selected fuel gas stream where a more detailed review, including the potential need for N₂ compression and storage, will need to be undertaken.

2.2. Ramp rate / flexibility

The ramp rates define the rate at which a power plant unit can be brought up and down to and from its full load operation once they are synchronised to the electricity grid system.

Depending on the power plant configuration, current CCGTs are capable of fast ramp rates, for example, a CCGT with 6 + 1 arrangement of SGT-800 GTs should be able to ramp up to full load at 73 MW/min (Siemens, 2014) and the “E” class can achieve 10-30 MW/min at ISO conditions. The fast ramp rates could be a key performance metric for a peak demand matching plant reacting to the intermittent generation demand.

Based on current GT performance data it is not considered feasible to use a H₂ fuel gas stream during GT start-up, therefore this study assumes that natural gas is used as the primary fuel for start-up. This means there will be little difference in ramp rates to those quoted for natural gas.

Post start up, there are several characteristics which will impact overall GT performance when meeting the desired power generation profile defined in Chapter 1. These include:

- Daily GT start-ups.
- GT part load operation.
- Minimum GT load to achieve environmental legislation targets.

Start-ups

The definition of hot, warm and cold starts can vary between OEMs, but primarily refers to the start classifications in terms of metal temperature at the high pressure inlet steam turbine diaphragm. Table 2-1 indicates the typical classifications for starts. The intervals shown are indicative only and actual shutdown periods are related to the steam turbine design, the materials of manufacture and the steam conditions.

Table 2-1: Definition of starts and associated times (ETI, 2016)

Start	Shutdown period
Hot	less than 8 hr
Warm	8 – 48 hr
Cold	more than 48 hr

Depending on the number of GTs in the CCGT plant configuration, the overall net plant performance can suffer, as a result of the sequential loading or deloading of GTs. It is common practice for an operator to start-up and load GTs sequentially to raise load to meet load dispatch instructions. However, as one GT reaches full load and the next is brought online and loaded, a drop in efficiency of the plant occurs which is referred to as negative overlap³.

In the case of a power block or CCGT plant, based on multiple GTs, each of relatively low capacity the impact on efficiency of the CCGT resulting from the sequential starting or de-loading of GTs is less than that for the case of a CCGT block comprising of 1 or 2 GTs. The multi GT configuration also offers a CCGT plant with an improved turndown capability whilst maintaining relatively high efficiency, compared against a CCGT with 1 or 2 GTs of higher capacity, and is therefore referred to as having a positive overlap in net efficiency.

CCGT start times are constrained by the Heat Recovery Steam Generator (HRSG) and steam turbine. Therefore, to aid CCGT flexibility the GT can be equipped with a diverter damper and bypass stack allowing open cycle operation for rapid starting and grid balancing purposes or when HRSG or steam turbine repair or maintenance is required. The diverter damper is a device that directs the GT exhaust flow to either the HRSG for combined cycle operation or to a bypass stack for OCGT operation.

For this study, a high number of starts is a requirement to meet peak demand matching, particularly in Scenario 3 defined in Chapter 1. Around 300 starts per year may be considered acceptable under normal natural gas CCGT operation. Therefore, two starts per day and up to 600 starts per year could significantly affect the operation and maintenance (O&M) efforts required. This is discussed further in Chapter 5, however the business case, and targeted revenue streams (in a peak demand matching application) would need to be considered in more detail for a future H₂ storage project.

Part load operation

The efficiency of both CCGTs and OCGTs is reduced at part load operation compared to full load. A plant configuration comprising multiple GT units ensures that plant efficiency reductions are minimised

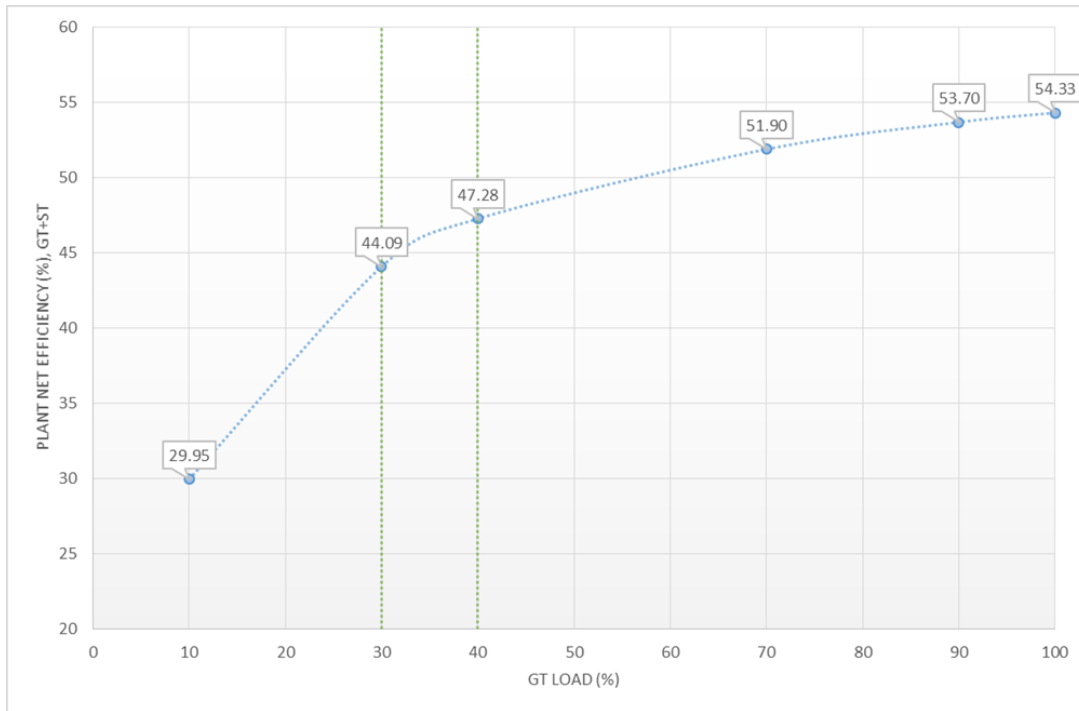
³ Negative overlap refers to a case where the overall plant output suffers a reduction in efficiency as additional GTs are brought online to meet load demand, positive overlap refers to a case where continuous ramping can be achieved.

at part load by controlling the number of units in operation and in addition provides the flexibility required for peak demand matching and load following operations. The larger “F” and “G” class GTs require fewer GTs to generate 1 GWe, which reduces the plant flexibility to undertake peak demand matching operation. Table 2-2 gives the capacity of four “F” class and one “H” class CCGT plant operating with natural gas and is based around 2 GTs in 1+1 or 2+1 configuration. For these configurations, the individual GTs would need to operate at part load to match the operation scenarios proposed.

Table 2-2: CCGT plant performance (from GT PRO results), with ACC at ISO conditions & full load

		Ansaldo	GE	MHPS	Siemens “F” class	Siemens “H” class
		KA26-1	9F-7 Series	MPCP1 (M701F4)	SCC5-4000F 1S	SCC5-8000H 1S
Gross Capacity, 2x(1+1) or 1x(2+1)	MW	984.3	1,025.7	969	908.3	1,198.3
Net Capacity, 2x(1+1) or 1x(2+1)	MW	950.4	992.2	939.8	883.8	1,169
GT capacity	MW	315.3	338.5	328	304.8	396.3
ST capacity, (1+1)	MW	176.8	174.3	156.8	149.4	202.9
ST capacity, (2+1)	MW	353.7	348.6	313.5	298.8	405.7
Gross heat rate, 2x(1+1) or 1x(2+1)	kJ/kWh	6,020	5,901	6,000	6,112	6,000
Net heat rate, 2x(1+1) or 1x(2+1)	kJ/kWh	6,228	6,112	6,196	6,133	6,164
Gross Efficiency, 2x(1+1) or 1x(2+1)	%	59.8	61.0	60.0	58.9	60.0
Net Efficiency, 2x(1+1) or 1x(2+1)	%	57.8	58.9	58.1	57.32	58.4

Figure 2-5 presents a typical curve for the relationship between the GT load and the plant net efficiency.



The graph is based on data for an “E” class GT firing fuel gas stream 1, biomass gasification fuel as modelled in GT PRO, with 25% vol% H₂

Figure 2-5: Relationship between the GT load and plant net efficiency

Therefore, the trend is for the plant minimum stable load to decrease with increasing numbers of power units or power blocks. For example, in a 2+1 CCGT block one GT can be offloaded resulting in a reduced minimum load compared to a 1+1 CCGT block. Therefore, a power plant based on several smaller capacity GTs (e.g. SGT-800) has improved plant flexibility, the ability to load follow, a lower minimum stable load and is relatively easier to peak compared with a power plant with fewer large GTs (e.g. SGT5-8000H).

Figure 2-6 illustrates the flexibility of a six GT power plant in combined cycle operation and demonstrates that such a configuration can be dispatched to optimise thermal efficiency of the plant and generation costs. Note that only Scenario 1, requires a turn down to ~40% load (as seen in Figure 1-4).

Part Load Efficiency EconoFlex6

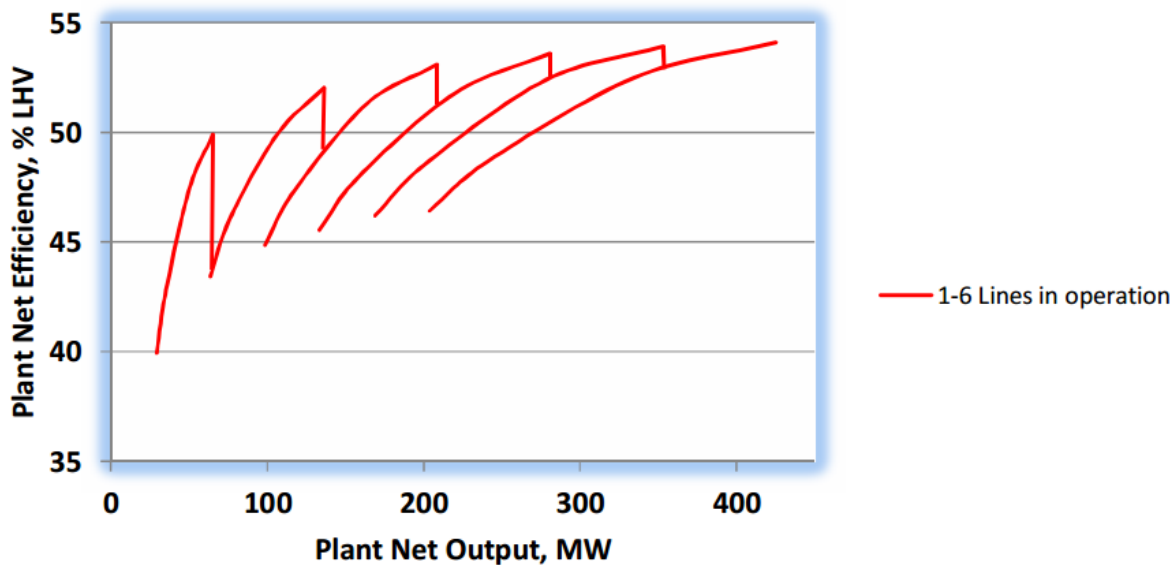


Figure 2-6: Typical part load efficiency CCGT power plant based on 6+1 'Econoflex 6' arrangement of SGT-800 (Siemens, 2014)

Minimum GT load to achieve environmental legislation targets

At less than full operating loads, down to around 60%, the levels of both NO_x and CO emissions rise marginally, however below 60% load the emissions begin to rise significantly and the minimum environmental load is the minimum load at which a GT can operate while not exceeding the emission statutory limits as set out in Section 2.1.

The minimum environmental load varies depending on the GT characteristics and the fuel composition. The current industry practice is not to operate at loads lower than about 40% because of the significant net efficiency reduction at part load described above and the likelihood of emission limit breaches at part load operation.

Operation, with syngas and low calorific value fuel gases means that the allowable statutory limits are higher (approximately double) compared with natural gas. However, the emissions are more difficult to control at varying loads and emission limit breaches more likely due to the need to balance diluent, H₂ fractions and balancing natural gas. In these cases, the industry advises that turndown does not fall below 60% load, which in turn means that larger GT fired with H₂ rich fuel gas streams are less suitable to operate in peak demand matching mode while achieving environmental legislation targets.

2.3. GT selection

During the last two decades, significant GT advancements have been made in combusting rich H₂ fuel gas streams, due to advances in both the design of integrated gasification combined cycle power plants (IGCCs) as well as progress in the development of CCS projects. Many of the case study projects are based on either, air or O₂ blown gasification to produce syngas (synthetic fuel gases), which are typically rich in H₂ and CO. Or alternatively, solid or liquid fuels produced using the Fischer-Tropsch process.

To identify the preferred GT to be implemented for this proposed H₂ storage project, it is therefore necessary to:

- Review the existing case studies of historic GTs to benchmark expected performance and operating limitations.

- Consider case study history against peak demand matching requirements and assess implications these may have on performance requirements.
- Understand the current GT performance capability that is realistic from OEM feedback and GT PRO modelling verification; i.e. understanding of flame instability, diluents needed and power outputs expected.
- Develop a set of criteria against which existing GTs can be assessed and down selected by, leaving only those that meet these criteria.

Existing case history of GTs with hydrogen rich fuel gas streams

A review of IGCC projects reveals that projects have successfully been developed for syngas fuels containing a wide range of compositions and fractions of H₂. In many cases IGCC projects are process and oil industry driven making use of refinery waste products and many of these are based on proven GT technology (e.g. GE Frame 6 and 9) and have been shown to be reliable and economic. Many of the GTs used in these projects have been smaller frame size industrial GTs (e.g. GE 6B).

Appendix B.3, Table B3-1 lists several refinery 'off-gases' and IGCC projects, in which syngas has been produced from coal and refinery bottoms and in which the aim has been to develop utility scale power generation to economic energy tariffs. The fraction of H₂ in many of these early projects has been limited to 30%, allowing "E" and "F" class technologies to be adopted with diffusion combustion. Syngas is diluted using N₂ or steam to minimise the production of thermal NO_x by lowering the TIT.

In view of the drive towards improved CCGT efficiency and higher unit capacity along with the associated economies of scale of large heavy duty utility scale GTs, more recent 'demonstrator' projects have opted for the "F" class and even, the larger "H" class technology. The integration of these advanced GT technologies in IGCC low carbon power projects is critical to bridging the gap and levelising power tariffs between CCS and existing power generation.

DLE combustion "F" class GTs are based on natural gas and unsuited for fuel gases with H₂ fractions of more than 10 vol%, with 90 vol% natural gas blending. Increasing H₂ fraction further leads to flame instability and risks HGP temperature excursion. In general, pure fuel gas streams of ~87+ vol% H₂ cannot be fired in GTs without dilution with N₂ and / or steam due to reactivity control limitations and the burners are modified to burn syngas fuels containing H₂ and CO using both DLE and diffusion combustion. Increasing the fraction of H₂ further requires either diffusion technology or will require further research to improve DLE capability.

Reports on the performance of these projects indicates that they have been less reliable and subject to more frequent inspections. In addition, it is apparent that the LHV of the fuel gas and the GT efficiency falls away with increasing N₂ fraction due to lowering of TIT. This means that for IGCC projects based on "F" class GTs the efficiency is in some cases only marginally better than that for the "E" class GTs depending on the IGCC process design and the CCGT steam cycle, indeed in several cases, combustion is supported with natural gas.

In the case of the impact on power output when burning H₂ fuel gas, this is largely dependent on the capacity of the GT control nozzles. If there is improved capacity then the power output rises as the diluent (N₂ and steam) increases because of the injection of high pressure gas at combustion without additional energy input. However, gas purge from the compressor stage may also be required to prevent surge and result in energy losses. Dilution with either, N₂, steam and blending with natural gas is required to ensure that the GT exhaust gas emissions remain within the statutory EU NO_x limits as well as sustaining stable combustion. Furthermore, several reviewed projects also needed to resort to post combustion SCR exhaust gas treatment to achieve emission limits.

In general, in the UK, technology previously purposed for base load generation using heavy duty utility scale GTs of 250 to 300 MW (CCGT 500 MW) is not ideally suited to flexible operation, daily rapid starting, loading, part load operation and load following. The efficiency of large GTs at part load tails off, as load falls, and the advantages of advanced higher efficiency technologies become less significant

because the duration of full load operation is limited.

GT down selection

Based on the discussions above, a selection criteria has been specified to down select the range of H₂ capable GTs to a handful of GTs most suited to this study's application. The criteria is defined as follows:

- Maximum allowable H₂ content in the fuel; as advised by OEMs or from experience.
- Experience on H₂ rich fuel applications; from case studies, and research papers.
- NO_x emissions; as advised by vendors, and to comply with the EU legislation (Section 2.1).
- Hot and cold start up times; response rate of GT to peak demand matching generation.
- Minimum environmental load (down to 40% load for Scenario 1)
- GT flexibility.
- No. of GTs required to meet 1 GWe target generation.
- CAPEX, OPEX and infrastructure considerations.

Appendix B.2 (page B4) presents the range of H₂ capable GTs against these criteria, where information on GT performance has been gathered through review of case history (Appendix B.3) and discussion with OEMs, including GE and Siemens. As shown in Appendix B.2, most GTs fail to meet all criteria defined and are therefore discounted from further assessment. A shortlist of the most relevant GTs is presented in Table 2-3 below:

Table 2-3: Nominal H₂ firing capability

GT model	Burner	H ₂ vol%	Net output (MW) OCGT
SGT-800	DLE	60	53
SGT5-2000E	DLE	4 - 10	171
	Diffusion	10 - 25	
SGT5-4000F	DLE	4 - 10	301
SGT5-8000H	DLE	4 - 10	425
	Diffusion	10 - 25	

In general fuel gas stream fractions of more than 10 vol% H₂ cannot be fired in a GT DLE burner without exceeding the statutory NO_x limits. While technically feasible to fire fuel with a higher fraction of H₂ this could result in higher NO_x levels, flame instability and flame outs.

The shortlisted GTs presented in Table 2-3 can be further down selected by considering the performance history of the "F" class and "H" class GTs.

- F class GTs have seen extensive experience in IGCC projects of particularly the 60Hz range. Syngas and H₂ rich fuel gas stream projects reviewed to date have been developed for base load operation and a review has not identified projects based on syngas or H₂ rich fuel gases which are primarily for peak demand matching generation.
- As discussed earlier, the efficiency of "F" class GTs are, in some cases, only marginally better than the "E" class GTs when firing H₂ rich fuel streams. Some F class GTs can burn H₂ fuel gas streams, however for H₂ fuel mixtures above 5%, flame instability prevents DLE (premix) burner operation and the GTs revert to combustion based on diffusion burner design.
- Modelling of the "F" class GTs has been limited to those cases with H₂ fuel mixtures of nominally 5% up to 7%, the remainder of the fuel being made up by natural gas. In this mode,

the “F” class machines are able to run with DLE burners with little change to the emissions compared against 100% natural gas fuel. The high levels of natural gas fuel maintain flame stability with the combustion of H₂ and prevent flame out scenarios.

- The “E” class GTs have a number of project references with a proven capability of operating reliably with a range of gaseous fuels with the composition of H₂ fractions of nominally 25% and with either N₂ or steam diluent streams.
- In the case of the “H” class GTs there is limited case history and further limitations in the GT PRO software where this type of GT is limited to modelling natural gas and distillate oil where modelling of H₂ fractions is still ongoing research and development. As such, this class of GT has not been considered further however it is noted that “H” class industrial scale GTs provide the highest power rating and efficiency. Both Siemens and GE indicated future improvements of fuel flexibility with respect to the “H” class GTs. Case studies are also available which indicate higher fractions of H₂ rich fuel gas firing are possible, though it should be noted these are often examples with low operational hours or out with EU NO_x limits. Therefore, although discounted in this study, future advancements may bring the “H” class GTs to the forefront of this field.

This study has therefore down selected the available GT to the following Siemens GTs:

- SGT-800; A robust industrial GT designed for flexibility, with long-term track record, 54 MW, and 56.7% plant efficiency achievable in CCGT mode.
- SGT5-2000E; Highly fuel flexible including low calorific fuels, heavy duty GT, proven technology and has benefited from continued development, 187 MW, and 53.3% plant efficiency achievable in CCGT mode.

These GTs are considered the most credible GTs capable of operating in the manner required to support the demand of a peak demand matching power source using a H₂ rich fuel gas stream. Furthermore, the selected GT’s allow comparisons to be drawn between an established large frame “E” class GT, with years of operational experience based on H₂ rich fuel, and small frame GTs with DLE combustors capable of burning higher H₂ fractions up to 60 vol%. Siemens machines have been chosen due to availability of OEM data within the study timescales, but other vendor GTs may be equally applicable within these GT frame classes.

2.4. CCGT arrangement

GT PRO was used to model the down selected GTs to confirm their operating performance met the underlying requirements defined in the preceding sections. Both the open cycle GT and the overall CCGT plant variants were assessed. Performance was measured against the following parameters:

- GT gross power output and efficiency at various GT loads.
- CCGT plant net power output and efficiency.
- Turbine Inlet and Exhaust Temperature.
- Compressor air bleed flow (where applicable).

OCGT performance

The expected theoretical performance of the SGT-800 and SGT5-2000E GTs running on various fractions of H₂ is summarised in Table 2-4, Table 2-5 and Table 2-6 respectively, where the SGT5-2000E GT has been modelled against both fuel gas stream 1 and 2.

Table 2-4: SGT-800 performance at various fractions of H₂ (Siemens)

	Unit	Modified Current DLE	Modified Current DLE	Modified Current DLE	Modified Current DLE	Modified Current DLE	New High H ₂ Concept	New High H ₂ Concept	New High H ₂ Concept
Fraction of H ₂	%vol	0	20	40	50	60	60	85	100
Fraction of Natural gas	%vol	100	80	60	50	40	40	15	0
Power out	MW	53	49	46	44	40	53	52	50
Efficiency at generator terminals	%	38.5	38.2	37.8	37.4	36.9	38.7	38.9	38.8
Expected NO _x (at 15% O ₂)	ppm	<15	<20	<35	<45	<55	<100	<100	<150

Notes on assumptions used in Table 2-4:

- Performance predicted at sea level, 15°C, with 10 mbar inlet and 20 mbar exhaust losses.
- All values, except 100% natural gas, are predicted only.
- The new high H₂ concept burner is envisaged to enable the GT to maintain a similar TIT to 100% natural gas operation.
- The high H₂ concept cases are aspirational only as provided by Siemens. Therefore, the values will be subject to significant planned testing. These cases will therefore not been considered until Chapter 6 of this study.
- High H₂ concentrations on the modified current DLE burner design are achieved by reducing the TIT, hence the reduction in power output.

Table 2-5: SGT5-2000E performance with fuel gas stream 1 at various fractions of H₂

	Unit	Current Diffusion	Current DLE	Ref. Case (NG only)
Mix ID		Mix 1	Mix 3	n/a
Fraction of H ₂	vol%	25	10	0
Fraction of NG	vol%	53	89	87 to 97%
Power out	MW	168	165	~187
Efficiency at generator terminals	%	34.9	34.6	~36.2
Expected NO _x (at 15% O ₂)	ppm	<25	<25	<25

Table 2-6: SGT5-2000E performance with fuel gas stream 2 at various fractions of H₂

	Unit	Current Diffusion	Current DLE	Ref. Case (NG only)
Mix ID		Mix 2	Mix 4	n/a
Fraction of H ₂	vol%	25	10	0
Fraction of NG	vol%	53	81	87 to 97%
Power out	MW	168	166	~187
Efficiency at generator terminals	%	34.9	34.7	~36.2
Expected NO _x (at 15% O ₂)	ppm	<25	<25	<25

Notes on assumptions used in Table 2-5 and Table 2-6:

- Fuel gas streams referenced in Tables 2-5 and 2-6 are described in detail in Table 2-10. These fuel gas streams were used in GT PRO modelling to estimate the GT performance on H₂.
- Performance predicted at ISO conditions.
- Given that the “E” class GT’s TIT is below 1,150°C, it was assumed that no reduction in the TIT had to be applied to the GT model.

The results presented in Tables 2-4 to 2-6 show that both GT classes have their advantages and disadvantages when operating a peak demand matching power plant. These are summarised in Table 2-7.

Table 2-7: Summary of strengths / weaknesses of selected GTs

	Strengths	Weaknesses
Large frame e.g. “E” class GTs	<ul style="list-style-type: none"> ○ Minimal modifications needed ○ Known performance ○ Good flexibility ○ Lower CAPEX 	<ul style="list-style-type: none"> ○ Lower efficiency ○ Steam / N₂ / natural gas blending requirement
Small frame e.g. SGT-800	<ul style="list-style-type: none"> ○ High flexibility/ redundancy ○ Low minimum environmental load ○ Ease of maintenance ○ More suitable for fast churn peak generation 	<ul style="list-style-type: none"> ○ Higher CAPEX ○ Its modified DLE combustion chamber works with natural gas / H₂ blend only

CCGT plant performance

The indicative CCGT performance data for the down selected GTs with natural gas as currently published by OEMs is summarised in Table 2-8.

Table 2-8: CCGT performance on natural gas [Ambient conditions - ISO 15°C & 60% relative humidity (RH) @ full load]

Model	Configuration	GT net power output	Gross efficiency
SGT5-2000E	CCGT 2 + 1	551 MW	53.3%
GE 9E	CCGT 2 + 1	430 MW	55%
GE 13E2	CCGT 2 + 1	578MW	55%
SGT-800	CCGT 2 + 1	140 MW	55.4%
SGT-800	CCGT 3 + 1	~220 MW	~55.4%
SGT-800	CCGT 6 + 1	425 MW	56.2%

There are several standard configurations offered by the OEMs for the “E” class GTs (i.e. SGT5-2000E) and smaller GTs, such as SGT-800 CCGTs, which can deliver nominally 1 GWe .

The SGT5-2000E is typically offered in 2+1 arrangement with two GTs and one steam turbine, whereas the smaller SGT-800, as an industrial GT, can be offered in various configurations including up to 8+1, However, a 6+1 arrangement is the engineered package that the OEM promotes as the Siemens ‘EconoFlex 6’ package. The ‘EconoFlex 6’ CCGT package was developed by Siemens, where fast starting, fast load following, large load range and emissions compliances are key project requirements. The ‘EconoFlex 6’ package is based on six SGT800 GTs tied to a common SST-900 steam turbine and each of the gas and steam turbines are equipped with individual generators (Siemens, 2014).

A power plant based on multiple smaller GTs (e.g. SGT-800) is more flexible to dispatch and the minimum stable load and minimum environmental load are lower than that possible with a CCGT based on larger utility scale GTs. Figure 2-7 therefore presents two configuration options for the Power Plant along with their indicative performance in Table 2-9. These show that the ‘EconoFlex 6’ can be operated in such a manner to achieve an overall plant turn down capability down to 10% and load ramping of up to 73MW/min and is most suitable for peak demand matching and meeting ancillary grid requirements.

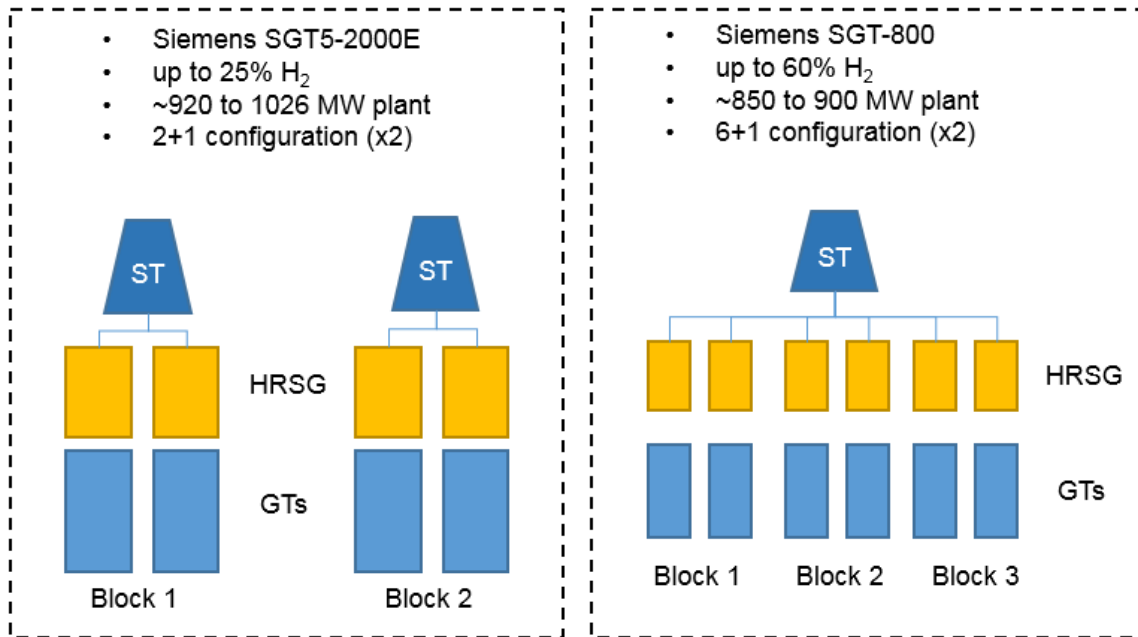


Figure 2-7: CCGT configuration for selected options

Table 2-9: CCGT block flexibility and response

Configuration	Combustor type	H ₂ limit in fuel gas *	Ramp rate	Min. CCGT load	GT start to full load	CCGT start to full load **		
						Hot	Warm	Cold
SGT5-2000E CCGT 2 + 1	Diffusion DLE	25 vol% 10 vol%	11-30 MW/min	25-30%	10-20 min	No data	~20min	No data
SGT-800 CCGT 6 + 1	DLE	60 vol%	73 MW/min	10%	10 min	30 min	65 min***	110 min
SGT-800 CCGT 2 + 1	DLE	60 vol%	24 MW/min	24%	10 min	30 min	110 min	110 min

* Maximum H₂ content in fuel within NO_x EU limits as provided directly by OEMs.

** Definition of start-up times: hot start < 8 hours; warm start 8 – 48 hours; cold start > 48 hours.

*** The difference in 6+1 to 2+1 'time to full load' from warm are due to acceptable gradients for steam turbine(ST) loading. Warming of ST during shut downs, through electrical heating can reduce cold start times by approx. 50%.

In conclusion, the two preferred GT configurations which are considered most suitable for operation with fuel gases with high H₂ fractions are:

- “E” class GTs (150 – 180 MW) in combined cycle, configured as two CCGT blocks of two GTs and a single steam turbine generator, each generating nominally 500 MW at ISO conditions and with a total plant capacity of up to ~1026 MW.
- Smaller industrial GTs (50 MW) in combined cycle configured as multiple blocks (up to four) each with either three GTs and a single steam turbine generator or alternatively six GTs and a single steam turbine generator and each generating nominally 225 MW or 425 MW at ISO conditions and a total plant capacity of up to ~900 MW.

The selection of these options has been based on firm evidence from OEMs of reliable operating performance with H₂ rich fuel gas streams. The starting and stopping of GTs to cater for dispatch requirements will inevitably impact on component life and result in GT efficiency and emission penalties, of which it is considered that the selected, more robust machines are the best GT choice to handle these requirements. One issue with more advance GTs is the cost of each start, due to single crystal turbine blades and constraints in start times governed by the steam cycle.

It is predicted that the selected configurations can deliver the flexibility required for peak demand matching and two shifting operations without incurring prohibitive operational constraints and high maintenance costs.

In the long term, it is anticipated that the OEMs will respond and develop the capability of the more advance GTs to perform reliably in the peak demand matching market for H₂ and syngas fuel gas operation and the study has also developed the performance trajectory which is believed to be achievable by 2030.

2.5. Power plant fuel requirement

Following identification of the preferred CCGT arrangement it is necessary to confirm the preferred fuel specification on which they can operate. As discussed in Section 2.1 there are several alternative fuel gas streams which can be used to improve the performance of the CCGT both in terms of efficiency and also emissions. Figure 2-8 summaries the acceptable fuel gas mixes which are suitable for combustion in either the DLE or diffusion type of GT combustor.

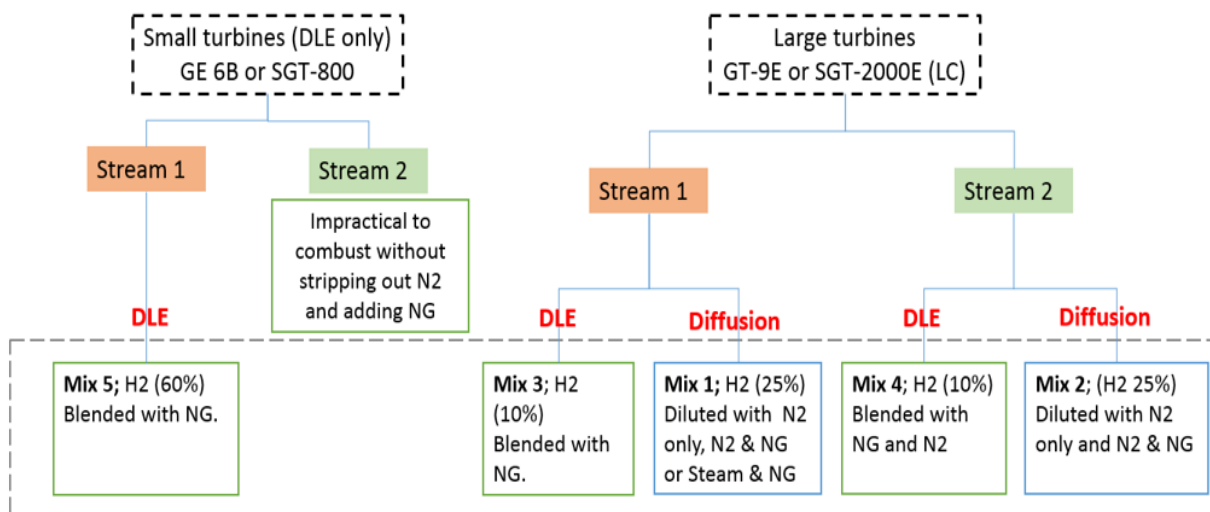


Figure 2-8: GT inlet fuel / diluent selection summary

The fuel gas streams identified in Figure 2-8 have been further refined into the eight fuel gas streams defined in Table 2-10 where a number of variants have been added to the fuel gas stream compositions. Mixes 1 to 4, with a maximum H₂ content of 10 to 25 vol%, were modelled in GT PRO for a CCGT based on four SGT5-2000E GTs.

The fuel gas stream options 1 and 2, with no added natural gas, demonstrate that these fuels have a significantly lower LHV than natural gas and results in very large fuel flowrate requirements.

As discussed in Section 2.1, the dilution of fuel gas streams 1 or 2 with N₂ (1:1 ratio of H₂ to N₂) or steam (4:1 ratio of H₂ to steam) results in a lowering of the fuel gas LHV, where TIT and performance are reduced. In practice, OEMs may offset this effect by blending with natural gas to sustain the overall LHV value.

Mix 5 is based on the Siemens data provided for a SGT-800 GT with a modified DLE combustor with a

maximum of 60 vol% H₂.

A summary description of each fuel gas stream is also provided in Table 2-10:

Table 2-10: Gas composition in the GT combustion chamber for fuel mixes (to OEM recommendations)

GT Model		SGT5-2000E	SGT5-2000E	SGT5-2000E	SGT5-2000E	SGT5-2000E	SGT5-2000E	SGT5-2000E	SGT-800
Combustion Chamber		Diffusion	Diffusion	Diffusion	Diffusion	Diffusion	DLE	DLE	DLE
Mix ID		Mix 1	Mix 1 (no NG)	Mix 1a	Mix 2	Mix 2 (no NG)	Mix 3	Mix 4	Mix 5
Description		Stream 1 blended with NG, diluted with N ₂	Stream 1 diluted with N ₂ , no NG	Stream 1 blended with NG, diluted with Steam	Stream 2 blended with NG.	Stream 2 further diluted with N ₂ , no NG	Stream 1 blended with NG in DLE combustor	Stream 2 blended with NG in DLE combustor	Stream 1 blended with NG in DLE combustor
Fuel Stream ID		Stream 1	Stream 1	Stream 1	Stream 2	Stream 2	Stream 1	Stream 2	Stream 1
Hydrogen	vol%	25.00	25.00	24.99	25.00	25.00	10.00	10.00	60.00
Carbon Monoxide	vol%	0.48	0.43	0.49	0.33	0.28	0.25	0.18	1.06
Carbon Dioxide	vol%	1.40	1.22	1.44	0.69	0.51	0.79	0.48	3.04
Nitrogen	vol%	22.39	73.20	3.61	23.05	73.68	3.73	11.41	4.11
Oxygen	vol%	0.04	0.00	0.05	0.04	0.00	0.06	0.06	0.02
Argon	vol%	0.11	0.11	0.11	0.25	0.25	0.04	0.10	0.26
Water	vol%	0.04	0.04	6.51	0.10	0.10	0.02	0.04	0.11
Methane	vol%	46.07	0.00	57.24	46.09	0.18	77.57	70.85	28.61
Ethane	vol%	4.46	0.00	5.54	4.45	0.00	7.51	6.85	2.77
Ethylene	vol%	0.02	0.00	0.02	0.02	0.00	0.03	0.02	0.01
Total	vol%	100.00	100.00	100.00	100.00	100.00	100.00	100.00	100.00
LHV	kJ/kg	30,350	2,841	41,800	30,520	2,905	46,019	40,312	43,725
Density at 0degC, 1atm	kg/Nm ³	0.7294	0.9694	0.6831	0.7247	0.9638	0.7343	0.7675	0.4264
Fraction of natural gas	by vol.	53%	0%	66%	53%	0%	89%	81%	33%
Fraction of external N ₂	by vol.	19%	72%	0%	0%	53%	0%	0%	0%
Fraction of external steam	by vol.	0%	0%	6%	0%	0%	0%	0%	0%

Note: The fraction of H₂ in the mixture is kept to the maximum as specified by the manufacturer. Also, the mixes that include significant methane proportion are still low LHV relative to natural gas (with LHV of ~46,000KJ/kg).

Mix 1; Fuel gas stream 1 blended with natural gas and diluted with N₂ in the diffusion combustion chamber. The OEM advised a limit of 25 vol% H₂ for the diffusion combustor. If fuel gas stream 1 is diluted purely with either steam or N₂, making up the remaining composition, there is not sufficient energy in the fuel gas stream to provide stable combustion. See fuel gas stream 1 with no natural gas in Table 2-10 (red highlight). Therefore, additional injection of natural gas is required.

Mix 1a; Fuel gas stream 1 blended with natural gas and further diluted with steam down to 25 vol% H₂ in the diffusion combustion chamber.

Mix 2; Fuel gas stream 2 blended with natural gas. Fuel gas stream 2 already contains significant amount of inert N₂, which acts as a diluent of H₂ in the fuel gas stream. Given that the fraction of H₂ in fuel gas stream 2 is still above 25 vol%, the stream requires further blending with natural gas, which results in a stream very similar in composition to that of fuel gas stream 1. As mentioned above, adding more N₂ or steam to fuel gas stream 2 would result in a very low LHV fuel, significantly reducing the GT and CCGT performance.

Mix 3; Fuel gas stream 1 blended with natural gas down to 10 vol% H₂ in case of a DLE combustor. This was to show an example whereby the power plant would be configured much like a CCGT peak demand matching plant, with fuel gas fraction of H₂ matching that recommended by the OEMs and without undertaking significant burner modifications. This CCGT configuration is a relatively proven technology and the design could be brought online very quickly due to the known GT capability.

Mix 4; Fuel gas stream 2 blended with natural gas down to 10 vol% H₂ in case of a DLE combustor. Mix 4 is similar in composition to Mix 3 due to the presence of N₂ in the original fuel gas stream 2.

Mix 5; Fuel gas stream 1 blended with natural gas down to 60 vol% H₂ in a SGT-800 with a modified DLE combustor. This case is based on reference data submitted by Siemens directly for a fuel gas fuel

gas stream of 60 vol% H₂ blended with natural gas.

The selected fuel gas streams defined above have enabled the GT and the combined cycle modelling to focus on a limited number of design cases to determine the plant performance for the operating scenarios. The outcomes of the assessment of the performance modelling for the CCGT based on both diffusion mode combustor and DLE burner have identified the following:

- The TIT reduction with increasing fractions of H₂ in the fuel gas stream within the combustion chamber.
- The modelling defined the optimum flowrate of N₂ and / or steam dilution for injection in the GT diffusion combustion chambers, to avoid a significant power plant performance drop and the need for further natural gas addition.
- The GT PRO modelling enabled the fuel gas demands for the power plant to be determined including the fuel gas stream 1, fuel gas stream 2, natural gas, steam and N₂ flowrates.

Of the eight Mixes presented in Table 2-10, Table 2-11 summarises the two scenarios resulting in the highest H₂ fuel gas stream flowrates to generate circa 1 GWe. The higher H₂ fraction will mean lower dependence on fuel additives or diluents and therefore make most use of the cavern storage.

- Mix 5, based on fuel gas stream 1 being blended with natural gas down to 60 vol% H₂, as required for the SGT-800 GT with a modified DLE combustor.
- Mix 2, based on fuel gas stream 2 being blended with natural gas down to 25 vol% H₂, as required for the SGT5-2000E GT with a diffusion combustor.

Table 2-11: Summary of the power plant fuel requirement

Fuel gas stream ID	Fuel gas stream 1	Fuel gas stream 2	Unit
Mix ID	Mix 5	Mix 2	
Max. fuel gas stream 1 or 2 GT inlet mass flowrate at full load + 10% design margin	16	29	kg/s
Natural gas inlet mass flowrate + 10% design margin	25	40	kg/s
Mass total flow rate + 10% design margin	41	69	kg/s
Fuel gas stream 1 or 2 GT inlet volumetric flowrate	59	41	Nm ³ /s
Natural Gas GT inlet volumetric flowrate	29	46	Nm ³ /s
Volumetric total flow rate + 10% design margin	88	87	Nm ³ /s

Values used are derived from power output of modelled GTs at calculated efficiency (see Appendix B.4 for full fuel requirement listings.)

The total volumetric flowrates of Mix 5 (fuel gas streams 1) and Mix 2 (fuel gas stream 2) shown in Table 2-11 are broadly the same, yet the mass flow rates are significantly different. This is perhaps counter intuitive and is due to the differing fuel gas stream densities. For instance, fuel gas stream 2 has a density more than twice that of fuel gas stream 1 due to the lower H₂ content and higher N₂ content than fuel gas stream 2.

2.6. Proposed plant solution

In this chapter, the current GT capability has been reviewed and the flexibility of diffusion versus DLE GTs compared. A range of GTs were reviewed and down selected to the most promising to meet the study constraints. It is clear, current machines are capable of H₂ firing in lower proportions, yet OEMs face significant technical challenges when higher H₂ flows are required. Measures can be taken to control flame instability and high temperature combustion, yet with possible knock-on effects on performance and emissions.

Final power plant configuration (current GT capability)

Figures 2-9 and 2-10 present the two proposed power plant configurations which are based on current technology capability and are considered to provide the necessary flexibility and efficiency to meet the requirements defined in Chapter 1.

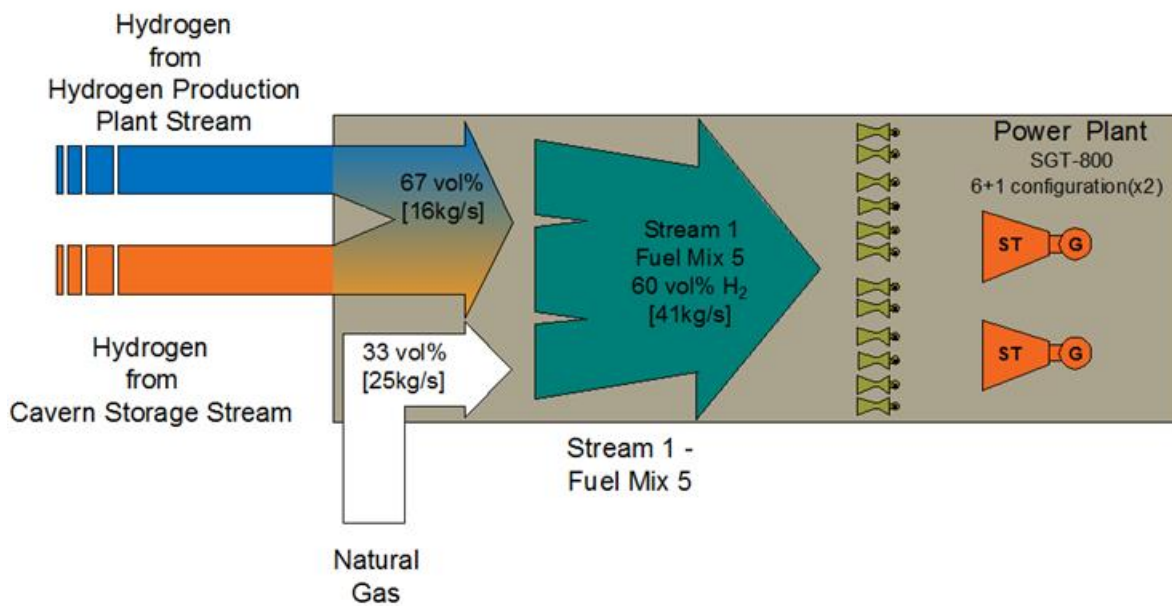


Figure 2-9: Small frame GT power plant arrangement at full load

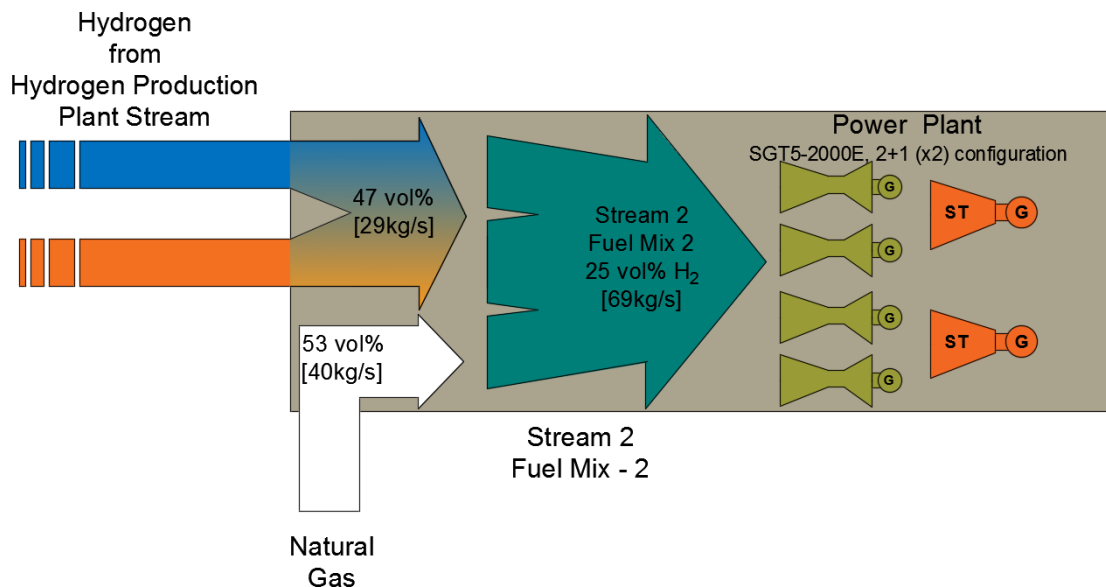


Figure 2-10: "E" class GT power plant arrangement at full load

Chapter 3: Supply of hydrogen to power plant

3. Supply of hydrogen to power plant

Given the power generation fuel requirements specified in Chapter 2, and summarised in Table 3-1, it is now possible to define the required flow path for transferring H₂ from the cavern to the power plant. These are presented schematically in Figure 3-1 and are discussed in detail within the following section where the key objectives of this chapter are to:

- I. Define anticipated split of supply from H₂ production plant and cavern storage.
- II. Define process requirements for conditioning of H₂ from cavern and identify constraints
- III. Outline well design constraints at each location (Teesside, Cheshire and East Yorkshire)
- IV. Define well design to meet required fuel requirements
- V. Specify cavern operating requirements including flow rates and injection / production cycles to be used to assess cavern integrity.

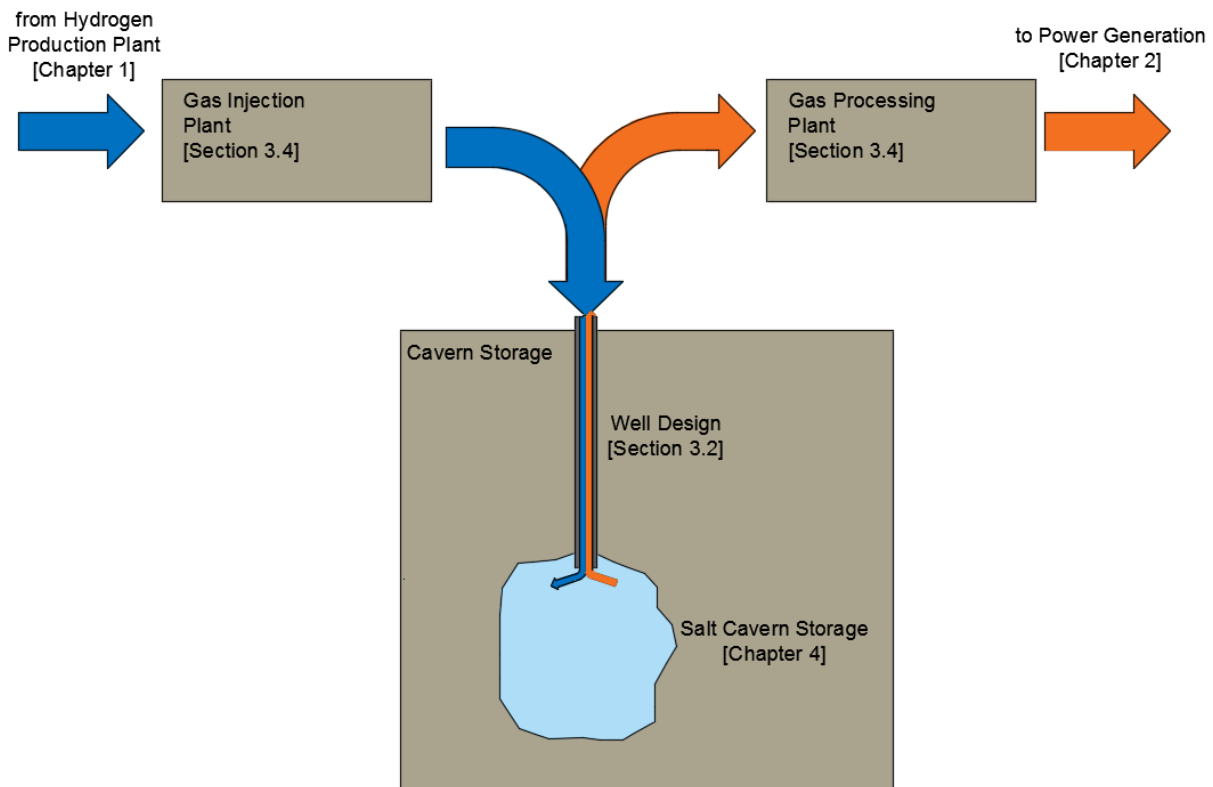


Figure 3-1: H₂ supply block diagram

Table 3-1: Summary of the power plant fuel requirement of fuel gas streams

Fuel gas stream ID	Unit	Fuel gas stream 1	Fuel gas stream 2
Mix ID		Mix 5	Mix 2
(fuel gas stream 1 or 2) Maximum GT inlet mass flowrate at full load + 10% design margin	kg/s	16	29
Natural gas GT inlet mass flowrate + 10% design margin	kg/s	25	40

See Appendix B.4 for GT PRO outputs of the fuel requirement for each fuel mix.

3.1. Plant summary under daily cycle

As defined in Chapter 1, there are three power plant generation scenarios which are representative of the overall loading cycle that a H₂ storage based power generation plant would be required to meet. These have been used to determine the overall requirements for the H₂ production plant and cavern injection / extraction flow rates by correlating the specified fuel requirements against them.

As shown in Figure 3-2, due to the fixed constraints outlined in Chapter 1, and the constant H₂ supply, it was necessary to use an iterative process to:

- Balance the daily fill / emptying cycle of the cavern with the gasifier size.
- Balance cavern performance to ensure cavern integrity is not impacted due to temperature changes through injection / extraction.
- Balance cavern performance to prevent inadvertently filling the cavern before demand is required (impacting overall plant efficiencies).

Figure 3-3, 3-4 and 3-5 present summaries of the operating scenarios and the identified gasifier, GT and fuel gas stream requirements.

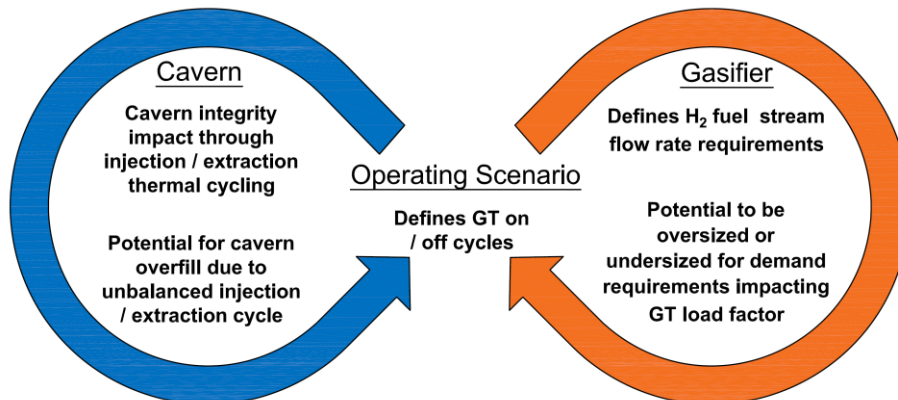


Figure 3-2: Operating scenario considerations and interfaces

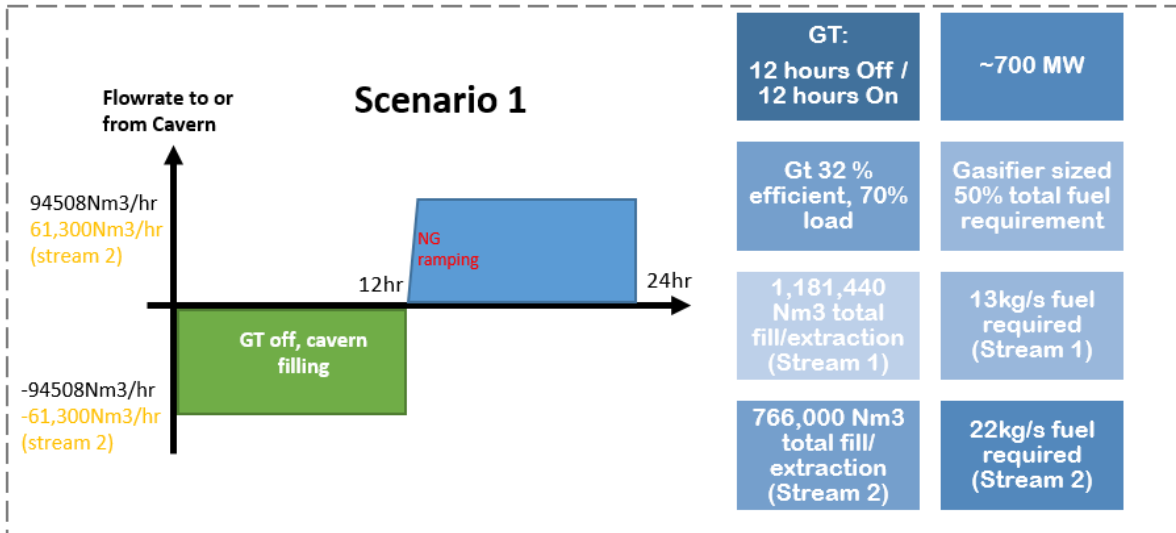


Figure 3-3: Scenario 1 daily profile

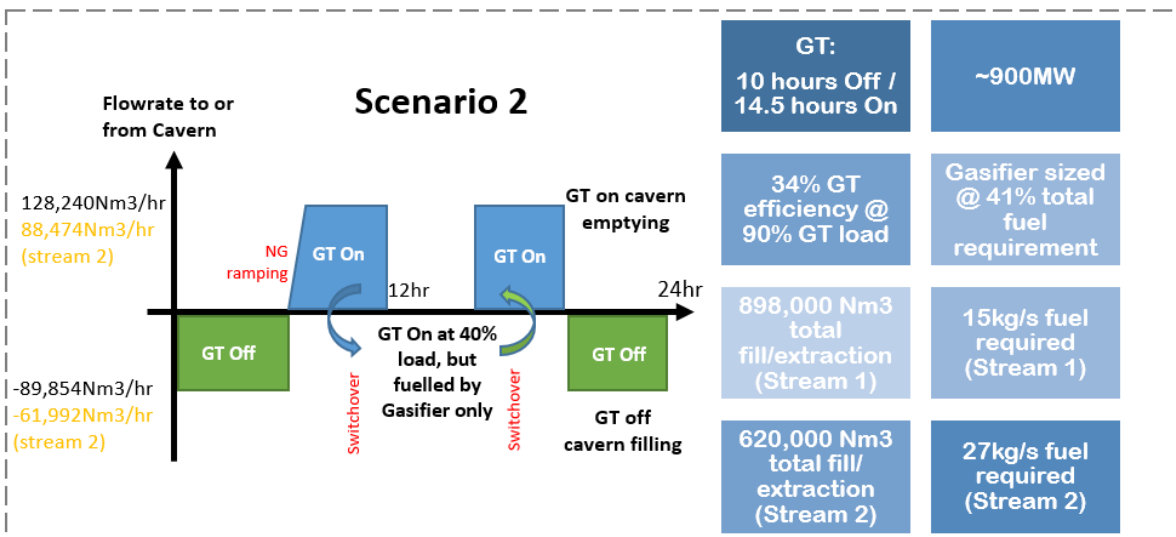


Figure 3-4: Scenario 2 daily profile

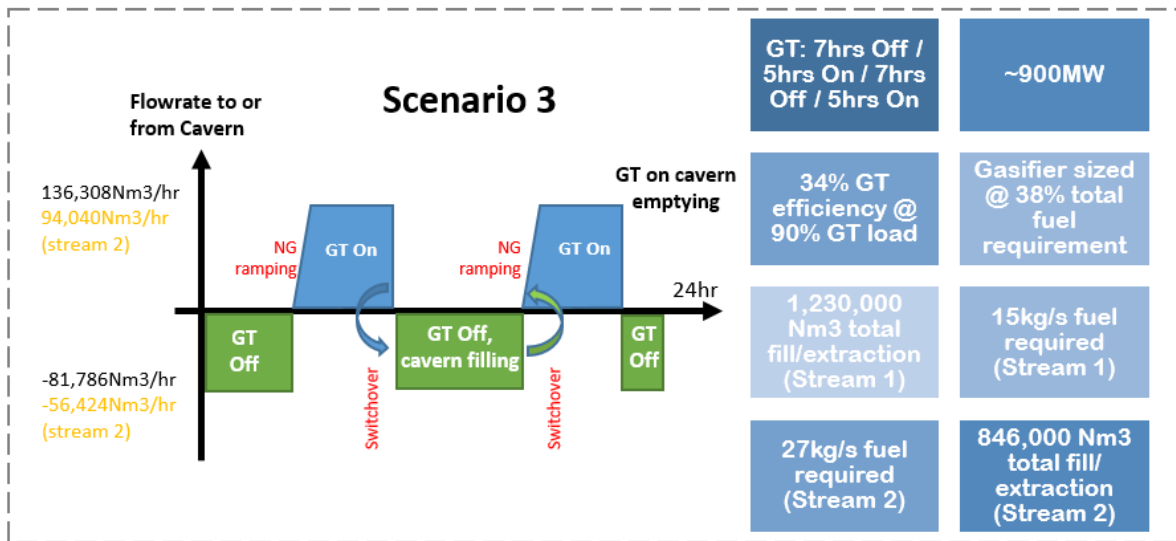


Figure 3-5: Scenario 3 daily profile

Through refinements in the operating cycle and feedback from the initial cavern modelling (discussed in Chapter 4) the following conclusions were reached:

- To balance the filling / empty cycles of H₂ to / from the cavern, the H₂ production plant / gasifier output should be sized at approximately the size of required injection (e.g. in Scenario 2, the injection cycle is approx. 10 hours or 41% of the time and therefore gasifier should be sized at ~41% of GT total fuel flowrate).
- Scenario 3 is deemed the worst case for the GTs and well completion, as it has the largest injection / extraction in each daily cycle, and has the highest number of cycles / starts. The impact of this scenario on the cavern is further explored in Chapter 4.
- A 30 min start up window, where the GT would operate on natural gas has been included in the modelling scenarios. For Scenario 2 this is omitted, as the GT runs at 40% load fuelled (from the gasifier) and is then ramped back up to 90% load.
- The given fuel required in kg/s is the maximum fuel requirement of that GT at the given load (i.e. 40%, 70%, or 90%) and over an average period the GT fleet would be able to deliver higher peak power outputs nearer the circa 1GW.

It is noted that the scenarios have not been modelled to the 100% load factors modelled in Chapter 2 where it is necessary to provide a level of flexibility in the overall arrangement. Furthermore, the weekly and monthly demand variations have not been modelled in detail. As the main drivers for this plant are to meet peak demand matching operation, it is assumed that seasonal variations would have little impact on the overall basis for the study and plant sizing.

Scenario 3 has been selected by this study as the worst case operating regime for cavern integrity therefore the associated parameters for this scenario will be used to confirm cavern impact. However, before this can be determined it is necessary to align these with the ability of the wells to deliver the required flow rates. The following parameters are therefore taken forward into Section 3.2:

Table 3-2: Scenario 3 parameters**

Parameter	Unit	Fuel gas stream 1	Fuel gas stream 2
Mol% H ₂		89%	53%
Density of gas at 0°C, 1 atm	kg/Nm ³	0.2476	0.646
Power Generation Period per 24 hours (Cavern being emptied)	hrs	9	
Cavern Filling Period per 24 hours (no power generation) *	hrs	15	
Split from gasifier direct to GT (when generating)		38%	
Supply from cavern (when generating)		62%	
Extraction rate required from wells to Power Plant when generating (90% load)	kg/hr	33,750	60,750

Notes: *15 hour no power generation value is derived from 14 hour no power generation (as defined in Figure 3-5) plus two 30 minute ramp up durations using purely natural gas.

**Schematics on the overall operating regime are given and discussed later in section 3.5.

3.2. Well design

The well(s) effectively acts as the conduit for the H₂ fuel gas streams between the cavern and surface. As such, its design is a key constraint on the ability of the cavern to deliver the required flow rates. It is therefore important to determine realistic dimensional parameters which can be used to derive the flow rates experienced by the cavern at depth.

Furthermore, where flow rates cannot be achieved by a single well there are options to drill additional wells and potentially additional caverns. However, to ensure the most cost effective options are considered by this study the number of caverns and wells should be minimized. Essentially, the wells should be designed in such a way as to maximise extraction / injection flowrates from the caverns for delivery to the power plant.

The key aims of this section are therefore to:

- I. Outline the most cost effective well design for each site, where it is noted that, unlike the surface plant equipment, the design of wells will vary from location to location.
- II. Determine the flow rates which can be delivered by the wells at each location
- III. Determine the number of wells required to deliver the required flow rate to the surface plant.

Before considering well design further it is important to note that the use of existing wells by repurposing them for H₂ storage has been discounted due to several limitations and disadvantages which are outlined in Table 3-3 below. To be clear, this report uses the geometry of existing, representative, caverns as a basis for validating their capability for H₂ storage where it is assumed that the representative cavern is applicable to existing or new caverns. However as outlined below it is not proposed to reuse any existing wells therefore in either existing or new caverns it will be necessary to drill new wells (this does not preclude the reuse of existing caverns as default):

Table 3-3: New versus old caverns and wells

Operation	Advantages	Disadvantages
<p>Use existing Caverns/ Wells (including remediation of wells or drilling of new wells)</p>	<ul style="list-style-type: none"> • Potentially lower CAPEX cost due to caverns/wells already being constructed 	<ul style="list-style-type: none"> • Casing and tubing already corroded and limits design life • Potentially limited flowrates due to well ID's compared to new well design • Steel casing and tubing potentially not suitable for H₂ service • Increased risk of well integrity issues with ageing asset • Existing last cemented casing shoes that have not being subjected to a Mechanical Integrity Test (MIT) for H₂ service and may not have had any form of MIT carried out • Existing Wellhead and Production tree components would need replaced • Intermediate casing and old production casing hangers cannot be replaced • Higher Risk well workovers required (section milling, under reaming, cementing) • Costs for remedial / workover operations are historically hard to predict • Possible abandonment of existing wells required prior to drilling new wells
<p>Use new Caverns/ Wells (up to 2 wells per cavern)</p>	<ul style="list-style-type: none"> • Cavern solution mined using latest technologies, likely good control of size and shape • Control over full well design • Entire well built with new equipment suitable for H₂ service • Likely to achieve larger completion ID resulting in higher flowrates per well • Costs easier to predict in drilling of new well over remedial works • More likely to achieve a quality cemented LCCS compared to an existing well or the re-lining of an existing well 	<ul style="list-style-type: none"> • CAPEX costs and time for leaching new caverns • Multiple wells entering cavern roof potentially increases stability issues and potential leak paths

New conceptual well designs for each of the three sites need to be defined to allow flowrates to be calculated. In order to create conceptual designs, the operating pressures, lithologies and cavern depths are required. These are presented in the following sections where a number of assumptions have been made as baseline well design requirements.

A minimum of three casing strings is recommended as follows:

- **Conductor** – provide structural support to the subsequent casing strings and surface valves and isolates the unconsolidated tertiary layers (glacial till).
- **Surface casing** – case off and isolate fresh water zones while allowing sufficient kick tolerance to drill the next section to the target depth.
- **Production casing** – isolate any shallower permeable formations above the cavern, seal around the cavern neck and provide a gas tight seal as part of the primary and secondary barrier envelopes.

As a minimum, the design should have two barriers between the cavern inventory and the atmosphere and strata. These are required to satisfy the Borehole and Design and Construction Regulations (DCR) regulations to an as low as reasonably practical (ALARP) level. For the purposes of this study and without full metallurgy analysis of H₂ in wells it has been assumed that grades of casing selected are suitable for H₂ service. Softer grades of steel have been chosen where acceptable mechanically as it is known that harder steels are more likely to be subjected to H₂ embrittlement. All naturally flowing wells should incorporate a Sub Surface Safety Valve into their completion design as an emergency barrier. Finally it is noted that the last cemented casing shoe should be located in the salt formation with sufficient depth to top of salt to ensure integrity of seal and also sufficiently above the cavern roof for the cavern neck to offer protection against cavern roof movements.

East Yorkshire

The East Yorkshire caverns are the deepest of the three proposed sites. The deeper cavern depth allows higher operating pressures however this means that the casing design must be capable of withstanding higher design loads. The proposed design for the East Yorkshire site is shown in Figure 3-6:

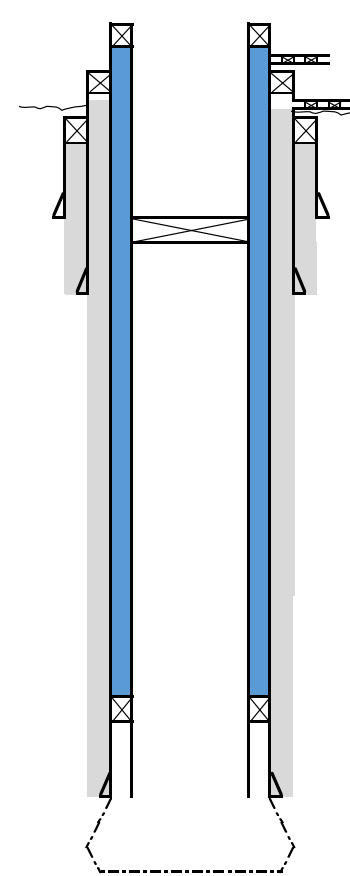
Indicative East Yorkshire Site Well Schematic					
DEPTH MD (m)	SCHEMATIC	LITHOLOGY	DESCRIPTION	OD (inch)	
			Note: Production Tree not included in schematic		
			Glacial Till	Glacial Till (0-35m BGL)	
40			Chalk Group	26" Conductor Shoe Chalk Group (35-561m BGL) Sub-surface safety valve	26.000
550			Lower Liassic Shales	20" Surface Casing Shoe Lias Group Shales (561-591m BGL)	20.000
			Penarth Shales	Penarth Shales (591-608m BGL)	
			Mercia Mudstone	Mercia Mudstone (608-931m BGL)	
			Sherwood Sandstone	Sherwood Sandstone (870-1400m BGL)	
			Eskdale Group	Eskdale Group (1400-1490m BGL)	
			Zechstein Formations Z4 Cycle	Z4 Cycle (1490-1570m BGL)	
			Zechstein Formation Z3 Cycle	9 5/8" Production Packer Z3 Cycle (1570-1695m BGL)	
1710			Zechstein Formation Z2 Cycle	9 5/8" Production tubing 13-3/8" Production Casing Shoe Z2 Cycle (1695-1830m BGL)	9.625 13.375
1830				Solution mined cavern - +/-250,000m2	

Figure 3-6: East Yorkshire conceptual well design

The conceptual well design comprises three casing strings, conductor, surface and production. The production tubing is installed inside the production casing and anchored with a packer to give the design a secondary barrier envelope and to allow monitoring of the primary barrier envelope.

To maximise the possible flowrates, the production tubing through bore should be designed with as large an ID as possible. A review of the available completion designs identified that there were two alternatives realistically available; either 10 3/4" or 9 5/8" diameter tubing. The 10 3/4" diameter tubing would allow the majority of the through bore to be larger than the 9 5/8" option however the completion packer is not available as a full bore option and therefore would cause a choke point in the tubing resulting in a reduced gas flowrate that would likely be similar to the 9 5/8" option. Furthermore, from the research undertaken there does not appear to be a standard sub-surface safety valve (SSSV) available in the 10 3/4" size.

The 9 5/8" option has been developed for use at gas storage sites to provide a full bore packer and SSSV design resulting in negligible choke points. This option has been used extensively for the gas storage market over recent years including large sites in East Yorkshire and Northern Germany. It is therefore concluded that the most suitable conceptual design is a 9 5/8" full bore design with production packer and SSSV as per Figure 3-6.

With the casing and tubing sizes selected the exact wall thickness of the production tubing needs to be assessed based on operating pressures and realistic design loads. This would be done for all the casing

sizes in detailed design however it is only important at this stage for the production tubing in order to calculate flowrates to feed in to the cavern modelling (Chapter 4) and cost estimates for the number of caverns and wells required (Chapter 5). The exact grades and wall thickness of the other casing string will not directly affect the completion tubing size. The tubing needs to withstand the operating pressures of the cavern throughout the design life of the assets. The following load cases have been assumed as the burst and collapse load cases:

- **Burst** - Maximum pressure internally at surface, zero pressure externally.
- **Collapse** - Minimum pressure internally just above production packer, 10 pounds per gallon (ppg) Annulus Fluid column externally.

The selected specification for the 9 5/8" tubing at East Yorkshire is shown in Table 3-4 below:

Table 3-4: 9 5/8" Tubing grade selection for East Yorkshire

Tubing OD Size (inches)	Tubing Grade	Weight (lb/ft)	Nominal ID (inches)	Burst Yield (barg)	Collapse yield (barg)
9 5/8"	L-80	53.5	8.535	545	455

Assuming a 0.1mm/year corrosion rate and 20% safety factor Table 3-5 below checks the casing is suitable for the project life with the desired operating pressure. All burst and collapse ratings have been calculated using "PD CEN ISO/TR 10400:2011 Petroleum and natural gas industries — Equations and calculations for the properties of casing, tubing, drill pipe and line pipe used as casing or tubing".

Table 3-5: 9 5/8" Tubing grade design life check for East Yorkshire

Casing / Tubing	Design Load Burst (barg)	Design Load Collapse (barg)	Operating Pressure (barg)	New Burst ratings (barg)*	New Collapse ratings (barg)*	End of life Burst ratings (barg)*	End of life Collapse ratings (barg)*
9 5/8"	271	80	120 to 271	436	364	342	199

*Ratings include a 20% safety factor

Table 3-5 shows that L-80, 53.5lb / ft 9 5/8" casing is suitable for the 30 year design life and will be used to calculate flowrates for East Yorkshire.

Teesside

The caverns at Teesside are wet storage compared to dry storage at the other two locations. This means that there is an internal brine string which displaces the gas out of the cavern while maintaining a constant pressure in the cavern. The large volumes of brine are stored in a surface open top reservoir. Based on a wet storage cavern the proposed conceptual design is show in Figure 3-7 below:

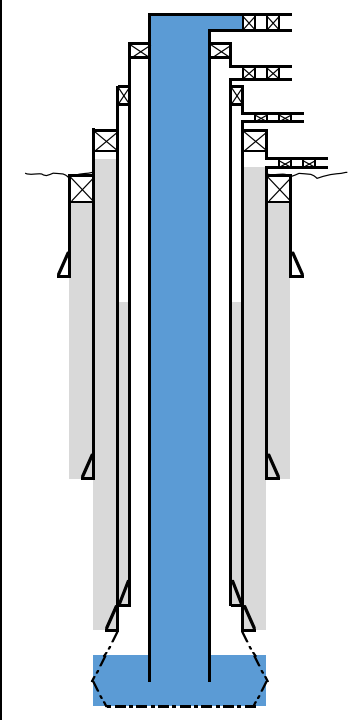
Indicative Wilton Site Well Schematic				
DEPTH MD (m)	SCHEMATIC	LITHOLOGY	DESCRIPTION	OD (inch)
30		Glacial Till	Brine flow Gas flow A-annulus valves B-annulus valves Ground Level - Well Datum <i>Boulder Clay (0-16m BGL)</i>	26.000
		Lower Liassic Shales	<i>Lower Liassic Shales (16-104m BGL)</i>	
		Penarth Shales	26" Conductor Shoe <i>Penarth Shales (104-116m BGL)</i>	
		Keuper Marl	<i>Keuper Marl (116-322m BGL)</i>	
341		Sherwood Sandstone	20" Surface Casing Shoe <i>Sherwood Sandstone (322-570m BGL)</i>	20.000
630		Zechstein Formations Z4 Cycle	<i>Roxby Formation - Upper Permian (570-646m BGL)</i> <i>Sherburn Anhydrite (646-650m BGL)</i> <i>Carnalitic Marl (650-659m BGL)</i>	10.750
635		Zechstein Formation Z3 Cycle	10 3/4" Production liner (second barrier between flow & strata) 13-3/8" Production Casing Shoe <i>Boulby Halite (659-692m BGL)</i>	
685		Zechstein Formation Z3 Cycle	7 5/8" Brine tubing Solution mined cavern - +/-50,000m2	13.375

Figure 3-7: Teesside conceptual well design

The conceptual well design at Teesside comprises four casing strings, conductor, surface and two production strings. The reason for the “double skinned’ production casing is to achieve two barriers between the strata and the production flow. This is different to the dry storage wells as the A annulus is essentially the production conduit and so primary and secondary barrier envelopes cannot be created in the same way (i.e. using a production packer). This is a different design to the older existing wells at Teesside however it is best practice for wet storage as per the UK regulation ALARP principles. Furthermore, the doubled skinned production string is becoming common place in continental Europe where authorities are pushing operators to reline older wells with an extra production string. The production casing strings selected are 13 3/8" as the primary string which would provide a seal at the cavern neck and a 10 3/4" casing. The 10 3/4" casing string will be cemented back around ±300m from the shoe with the remainder of this annulus filled with fluid. The annulus fluid will allow monitoring of the A annulus providing a positive indicator in the event of a casing leak allowing remedial measures to be planned.

The 7 5/8" brine tubing is installed inside the production casing down to the cavern sump area in order to maintain a permanent water leg and prevent gas migration up the tubing. Due to the additional production casing string the brine tubing OD is limited to 7 5/8". The feed rate of the brine is the limiting factor for the flow rate of gas from the 10 3/4" x 7 5/8" annulus. The brine velocity is limited to 4.5m/s (an industry rule of thumb) in order to stop vibrational effects on the free hanging brine tubing.

It is noted that the wet storage arrangement does not include an SSSV where the gas flow is via the annulus and is driven by fluid flow through the production tubing. An annulus safety valve could be deployed which would shut-off gas flow up the annulus in a similar manner to the tubing SSSV however even in its unoperated condition this would restrict flow and impair overall performance of the well. Ultimately the requirement for a SSSV is hazard driven and in this case it is considered overly conservative where alternative arrangements could be made at surface (however this would be subject

to assessment at the development stage).

With the casing and tubing sizes selected the exact wall thickness of the production tubing and casing need to be assessed based on operating pressures and realistic design loads. Again, this would be done for all the casing sizes in detailed design however it is only important at this stage for the production tubing and casing in order to calculate flowrates to feed in to the cavern modelling and the cost estimates for the number of caverns and wells required. The tubing and casing needs to withstand the operating pressures of the cavern throughout the design life of the assets. The following load cases have been assumed as the burst and collapse load cases:

Production Casing Burst - Maximum pressure internally at surface zero pressure externally.

- **Production Casing Collapse** - Min pressure internally just above top of cement / 10ppg Annulus Fluid column externally.
- **Brine Tubing Burst** - Max pressure internally at brine / gas interface atmospheric pressure externally.
- **Brine Tubing Collapse** - Zero pressure internally max pressure externally at surface.

The selected specifications for the 10 3/4" casing and 7 5/8" tubing are shown in Table 3-6 below:

Table 3-6: Tubing and casing grade selection for Teesside

Casing / Tubing	OD Size (inches)	Tubing Grade	Weight (lb/ft)	Nominal ID (inches)	Burst Yield (barg)	Collapse Yield (barg)
10 3/4" Production Casing	10 3/4	L-80	51	9.85	404	222
7 5/8" Brine Tubing	7 5/8	L-80	29.7	6.875	475	330

Again, assuming a 0.1mm/year corrosion rate and 20% safety factor Table 3-7 below checks the 7 5/8" tubing and 10 3/4" production casing are suitable for the project life with the desired operating pressure.

Table 3-7: 10 3/4" casing and 7 5/8" tubing grade design life checks for Teesside

Casing / Tubing	Design Load Burst (barg)	Design Load Collapse (barg)	Operating Pressure (barg)	New Burst rating* (barg)	New Collapse rating* (barg)	End of life Burst ratings* (barg)	End of life Collapse ratings* (barg)
10 3/4" Production Casing	76.5	40	76.5	323	177	238	81
7 5/8" Brine Tubing	80	76.5	76.5	380	264	260	106

*Ratings include a 20% safety factor

Table 3-7 shows that the selected casing and tubing strings are suitable for the 30 year design life and will be used to calculate flowrates at Teesside.

Cheshire

The caverns at Cheshire will be operated as dry gas storage similar to East Yorkshire however due to the shallower depth of the caverns they will have a reduced operating pressure in comparison. None the less the same practices apply to the design at Cheshire which can be seen in Figure 3-8 below.

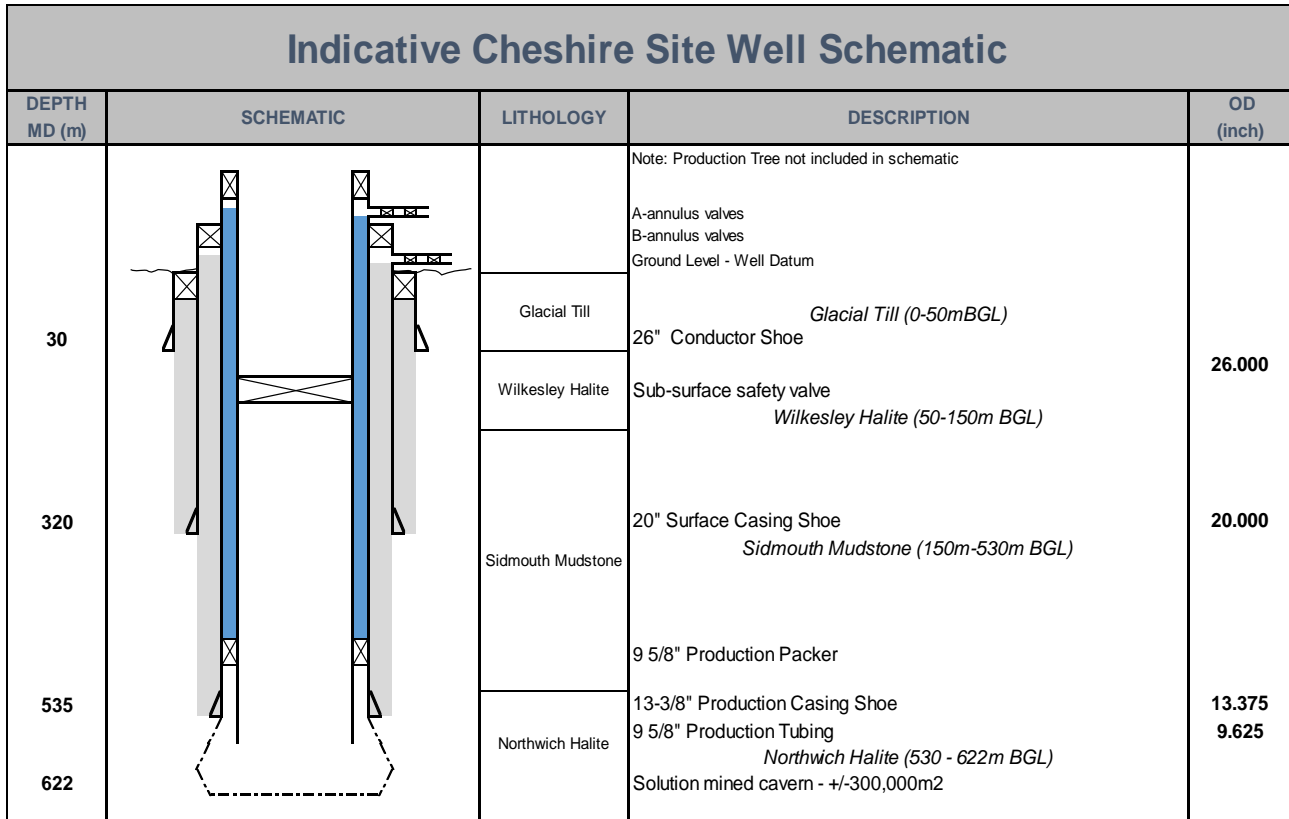


Figure 3-8: Cheshire conceptual well design

The conceptual well design at Cheshire comprises three casing strings, conductor, surface and production. The production tubing is installed inside the production casing and anchored with a packer to give the design a secondary barrier envelope.

Again, as with the East Yorkshire design in order to maximise the production flow rate a full bore 9 5/8" completion has been selected. The tubing and casing needs to withstand the operating pressures of the cavern throughout the design life of the assets. The following load cases have been assumed as the burst and collapse load cases:

- **Production Tubing Burst** - Maximum pressure internally at surface zero pressure externally.
- **Production Tubing Collapse** - Min pressure internally just above production packer / 10ppg Annulus Fluid column externally.

The selected specifications for the 9 5/8" tubing at Cheshire are shown in Table 3-8 below:

Table 3-8: 9 5/8" Tubing grade selection for Cheshire

Tubing OD Size (inches)	Tubing Grade	Weight (lb/ft.)	Nominal ID (inches)	Burst Yield (barg)	Collapse yield (barg)
9 5/8"	L-80	40	8.835	396	213

Again, assuming a 0.1mm/year corrosion rate and 20% safety factor Table 3-9 checks the 9 5/8" production casing is suitable for the project life with the desired operating pressure.

Table 3-9: 9 5/8" Tubing grade design life check for Cheshire

Tubing OD Size (inches)	Design Load Burst (barg)	Design Load Collapse (barg)	Operating Pressure (barg)	New Casing Burst ratings* (barg)	New Casing Collapse ratings* (barg)	End of life Burst ratings* (barg)	End of life Collapse ratings* (barg)
9 5/8"	95	29	30 to 95	317	170	222	66

*Ratings include a 20% safety factor

Table 3-9 shows that L-80, 40lb/ft, 9 5/8" casing is suitable for the 30 year design life and will be used to calculate flowrates at Cheshire:

Number of wells per cavern

A potential method of reducing the number of caverns required to meet the power demand is to have multiple wells per cavern. Whilst in theory this will reduce the costs of the project, having several wells per cavern is not recommended.

The main reason for this is that the interface between the cavern roof and last cemented casing shoe (LCCS) is an extremely important part of the well construction and its implementation needs to be successful in order to safely contain the inventory of gas. The interface needs to be verified as gas tight to put the cavern into commercial service and this is only achieved through good engineering design and execution.

The practice of pumping cement down a casing string to cement it in place is never guaranteed to be successful due to the nature of the operations and the uncertainties and quality controls that exist with an asset hundreds of meters below ground. The cemented seal is confirmed during the construction phase by completing a mechanical integrity test (MIT) test once the cavern has been leached.

In the event a failure of the LCCS was encountered during an MIT the well would have to be repaired and retested or if it was unrepairable the cavern and all wells drilled in to that particular cavern would have to be abandoned.

By using multiple wells in a single cavern the risk profile is increased. For example, if one of multiple wells drilled into a cavern is leaking (fails an MIT) the cavern cannot be put into commercial service and all of the wells would need to be plugged and abandoned. Furthermore, there are operational limits where any planned or unplanned maintenance on a single well (e.g. caliper surveys or production tubing replacement) would preclude the use of the cavern, and other associated wells, until the maintenance was completed.

In an idealised project, only one well would be drilled per cavern to minimise the implementation risk, however it is accepted that to help reduce costs, a small amount of increased risk can be accepted. For this reason, it has been assumed that a maximum of 2 wells per cavern is feasible.

3.3. Flowrates for cavern modelling

The flowrates from the wells will be subject to three high level boundary conditions, one of which will limit the flowrate for each well:

- I. The required flowrate to help achieve 1 GWe of energy assuming the H₂ production facility will continually supply a portion of the fuel. This has been calculated in Chapter 2.
- II. The maximum achievable flowrates assuming a maximum velocity limitation.
- III. The maximum allowable flowrates to maintain cavern stability for the life of the project.

In addition to these boundary conditions several parameters and limitations have been assumed to allow the flowrates to be calculated. These are listed below:

- The production flow area for each well. Calculated as per the well designs in Section 3.2 for each location.
- The minimum and maximum cavern operating pressures. As per Chapter 1
- The gas temperature in the cavern. The geothermal temperatures are known for each of the sites.
- The gas compositions and densities for fuel gas stream 1 and 2.
- The maximum gas flow velocity (30 m/s) in the well. Limited to reduce potential erosion and vibration in the well.
- The maximum brine feed velocity for Teesside (4.5 m/s). This is to limit vibrational effects from the free hanging brine tubing.

Using these parameters, the maximum achievable extraction flowrates, boundary condition 2, from a well for East Yorkshire and Cheshire were calculated using HYSYS software (see Table 3-10).

Table 3-10: Flow rates for power generation Scenario 3

Power Generation Scenario #3 which was worst case		East Yorkshire		Cheshire 1		Teesside	
		1	2	1	2	1	2
Stream No							
Mol% H ₂		89%	53%	89%	53%	89%	53%
Density of gas at 0degC, 1 atm	kg/Nm ³	0.2476	0.646	0.2476	0.646	0.2476	0.646
Max Cavern Pressure	barg	271	271	95	95	76	76
Min Cavern Pressure	barg	120	120	30	30	76	76
Power Generation Period (Cavern being emptied)	hrs	9	9	9	9	9	9
Cavern Filling Period (No Power Generation)	hrs	15	15	15	15	15	15
Extraction rate required from wells to Power Plant when generating	kg/hr	33750	60750	33750	60750	33750	60750
Injection rate required to wells when no Power Generation	kg/hr	20250	36450	20250	36450	20250	36450
Max allowable flowrate from well at given site (based on 30m/s limit)	kg/hr	94,468	248,179	29,534	77,487	6,394	16,802
Max required flowrate from wells assuming 1 Cavern with 2 wells	kg/hr	16,875	30,375	16,875	30,375	16,875	30,375
Check if one cavern with 2 wells is feasible		Yes	Yes	Yes	Yes	No	No
Max required flowrate from wells assuming 2 Cavern with 3 wells total	kg/hr	N/A	N/A	N/A	N/A	11,250	20,250
Number of caverns required for Teesside (wet storage)		N/A	N/A	N/A	N/A	No	No
Max required flowrate from wells assuming 2 Cavern with 4 wells total	kg/hr	N/A	N/A	N/A	N/A	8,438	15,188
Number of caverns required for Teesside (wet storage)		N/A	N/A	N/A	N/A	No	Yes
Max required flowrate from wells assuming 3 Cavern with 5 wells total	kg/hr	N/A	N/A	N/A	N/A	6,750	N/A
Number of caverns required for Teesside (wet storage)		N/A	N/A	N/A	N/A	No	N/A
Max required flowrate from wells assuming 3 Cavern with 6 wells total	kg/hr	N/A	N/A	N/A	N/A	5,625	N/A
Number of caverns required for Teesside (wet storage)		N/A	N/A	N/A	N/A	Yes	N/A
Total Cavern Required		1	1	1	1	3	2
Total number of wells required		2	2	2	2	6	4
Planned extraction rate for a single well	kg/hr	16,875	30,375	16,875	30,375	5,625	15,188
	Nm ³ /hr	68,154	47,020	68,154	47,020	22,718	23,510
Planned injection rate for a single well	kg/hr	10,125	18,225	10,125	18,225	3,375	9,112.50
	Nm ³ /hr	40,893	28,212	40,893	28,212	13,631	14,106

The flowrates were calculated assuming the cavern is at full operating pressure at the start of the

extraction period. The flowrates for the wet storage cavern at Teesside was calculated based on the maximum extraction / injection rate being limited by the 4.5 m/s brine flow limitations. The results are shown in Table 3-11.

Table 3-11: Maximum achievable flowrates from a single well

Site	East Yorkshire	East Yorkshire	Cheshire	Cheshire	Teesside	Teesside
Fuel gas stream	1	2	1	2	1	2
Max flowrate (kg/hr)	94,468	248,179	29,534	77,487	6,394	16,802

In order to calculate boundary condition 1, the required flowrates to produce the power requirement for the operating scenario is required. As discussed in Section 3.1, scenario 3 is considered the most intense cycling scenario and was selected as a worst case to model the stability of the cavern. Based on the daily mass balance, the calculated flowrates are as per Table 3-12.

Table 3-12: Required flowrates for load profiles

Fuel gas stream	1	2	1	2
	Required Extraction (kg/hr)		Required injection (kg/hr)	
Scenario 3	33,750	60,750	20,250	36,450

Knowing the maximum flowrate per well and the required total flowrate to provide the required power output allows an assessment to be made on how many wells and caverns are required at each site.

The extraction flowrates for modelling were calculated using Tables 3-11 and 3-12 above and were used in the initial cavern modelling runs, boundary condition 3. However, after initial cavern thermodynamic modelling, using one well per cavern, it was apparent that the temperature changes in the cavern due to the flowrate were going to have a detrimental effect on the caverns and so the decision was made to model each cavern with two wells to minimise the flowrates for the extraction / injection cycles. It was assumed that by creating two wells of identical design in each cavern the flowrates could be halved to deliver the required flow via two wells. Table 3-13 below shows the flowrates used for the cavern modelling and how many cavern and wells would be required based on these flowrates.

Table 3-13: Required flowrates based on initial modelling

Power Generation Scenario 3	East Yorkshire		Cheshire		Teesside	
Fuel gas stream	1	2	1	2	1	2
Planned extraction rate for a single well* (kg/hr)	16,875	30,375	16,875	30,375	5,625	15,188
Planned injection rate for a single well* (kg/hr)	10,125	18,225	10,125	18,225	3,375	9,112
Total number of cavern required	1	1	1	1	3	2
Total number of wells required	2	2	2	2	6	4

*Assumes 2 wells per cavern to minimise temperature effects on cavern

3.4. Surface processing plant

Surface equipment upstream of the Power Plant is required to process the H₂ fuel gas stream extracted from the underground cavern(s) buffer store to meet the inlet fuel gas specification for the power plant GTs. An appreciation of such a facility is required to understand the overall process requirements and support definition of CAPEX / OPEX costs discussed further in Chapter 5.

As stated in Chapter 2, H₂ fuel gas streams 1 and 2, when blended with natural gas meet an acceptable gas composition quality to be fed directly to the GTs, providing that the fuel gas temperature is at least 20°C above the dew-point. The conditioning treatment of the H₂ fuel gas stream extracted from the underground cavern buffer store is therefore primarily required to remove excessive moisture, hydrates and contaminants that occur during storage.

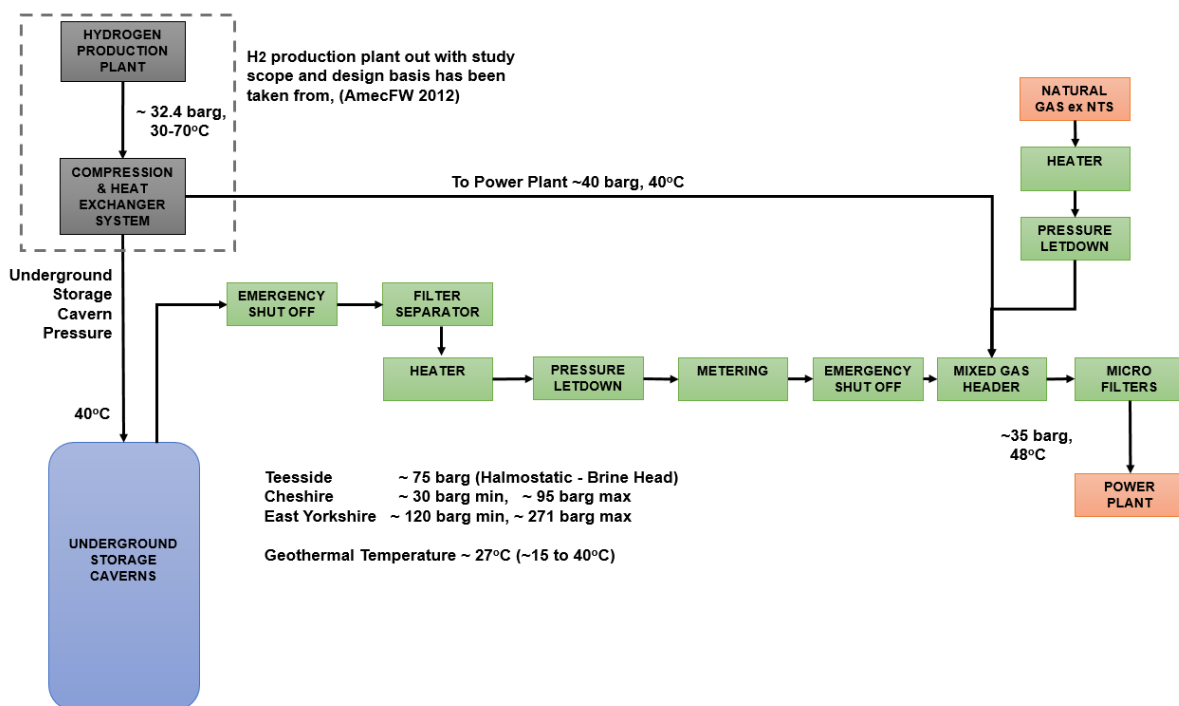


Figure 3-9: Block Flow Diagram: Surface Processing Plant

Figure 3-9 presents the anticipated arrangement of the surface processing facility, including mixing header for mixing the fuel gas streams with natural gas, metering stations and inlet compressors (if required). The requirements of such a surface plant facility have been considered in previous ETI works, (AmecFw, 2012), where a high level breakdown of the key parts are provided in Appendix C. For this report the previous works conducted for the ETI, (AmecFw, 2012), have been considered as the basis for CAPEX and OPEX costs.

Due to the innovative nature of H₂ storage the specific details of the surface plant require further investigation and development where Figure 3-9 is considered a simplified schematic. For example, it is common in existing gas storage facilities for the surface plant to include multiple gas trains as this provides system flexibility, reduces pipeline diameter and also provides a level of redundancy. Features such as this would require to be confirmed during the development stage and are therefore not presented in Figure 3-9.

Furthermore, the details of some aspects of the surface plant will vary from site to site depending on operating method and pressures.

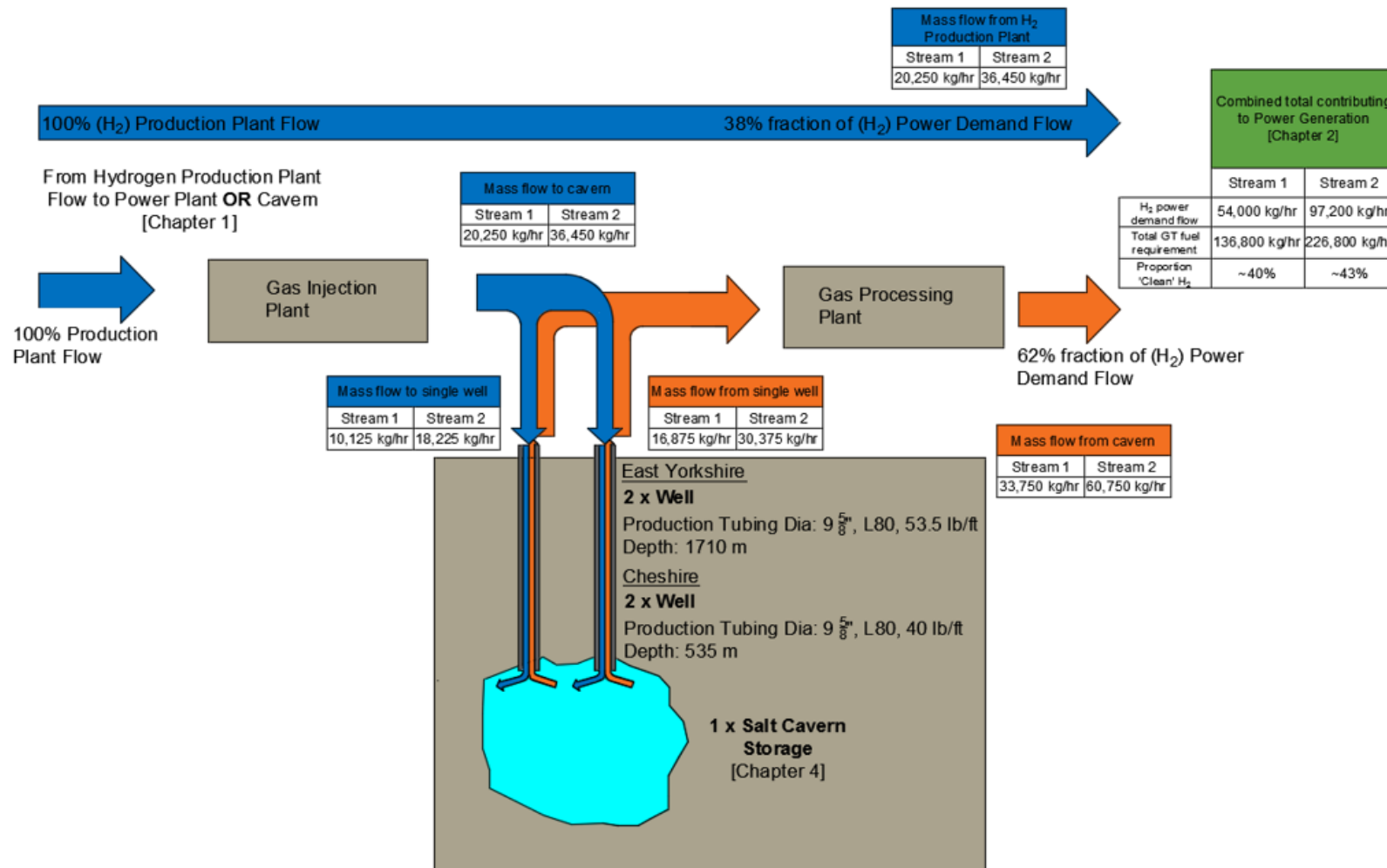
- **Wet Storage** – As stated in Section 3-2 it is proposed that a H₂ storage plant would operate

as a wet storage facility at the Teesside location. This would have a constant operating pressure of ~75 barg based on the halmostatic pressure at cavern depth. This type of operation requires additional surface plant facilities not shown in Figure 3-9 such as a brine reservoir and brine pump to ensure H₂ is efficiently displaced from the cavern during brine injection / H₂ extraction periods. It is assumed brine heating wouldn't be required where the production of H₂ hydrates is not considered to occur at these operating pressures. It is noted that the previous ETI works, (AmecFw, 2012), assumed that all locations, including Teesside, would adopt a dry storage method. Although this is considered suitable for Cheshire and Yorkshire it is not considered viable at the Teesside location. The CAPEX and OPEX costs presented in this report have therefore factored the previously defined costs at Teesside to account for the difference in method of storage.

- **Compression** – Due to the different operating pressures at each location there are varying levels of compression required where the East Yorkshire location, with a maximum pressure of 271 barg, will have a much larger energy penalty than compared to the Teesside location where minimal compression would be required due to the wet storage operation.
 - A key consideration in the design of the surface plant is therefore the offset between the compression required to achieve maximum pressure (and therefore maximum H₂ storage capacity) versus the energy loss to reduce the pressure down to a satisfactory pressure for GT operation (e.g. 35 barg).
 - It is further noted that in the case of the Cheshire location there may be a requirement for additional compression at the cavern outlet where the minimum cavern operating pressure is below the GT minimum operating pressure. This requirement could be removed by increasing the cavern minimum pressure to equal GT requirements however this would then reduce the overall cavern storage volume.
 - Compression would be required at the Teesside facility to displace the brine at halmostatic pressure during H₂ injection operations.
- **Pressure Let Down** – The use of a turboexpander will address some of the inefficiencies in the high pressure storage operation where, as a by-product of reducing pressure, power is generated through the use of an expansion turbine. The previous works assumed the Cheshire and Yorkshire locations would have 1x 14.6 MW and 2 x 16 MW expansion turbines respectively. It was however assumed that the Teesside location would not benefit from an expansion turbine due to the assessed operating pressure of 45 bar (based on a cavern depth of 300-400 m). As presented within this report this is considered overly conservative where a wet storage facility would operate at ~75 barg (based on cavern depth of ~650 m). It is estimated that the power generated by the turbo-expander reducing H₂ fuel gas streams at the Teesside location from 75 barg to 40 barg would be 2.6 MWe for fuel gas stream 1 - (based on estimated flow of 40 t/h) and 1.7 MWe for fuel gas stream 2 (based on an estimated detailed flow of 70 t/h). The benefits of investing in a turboexpander at each site would need to be subject to a detailed assessment during design development where additional requirements such as heating would also be required to ensure product temperature into the CCGT was satisfactory.

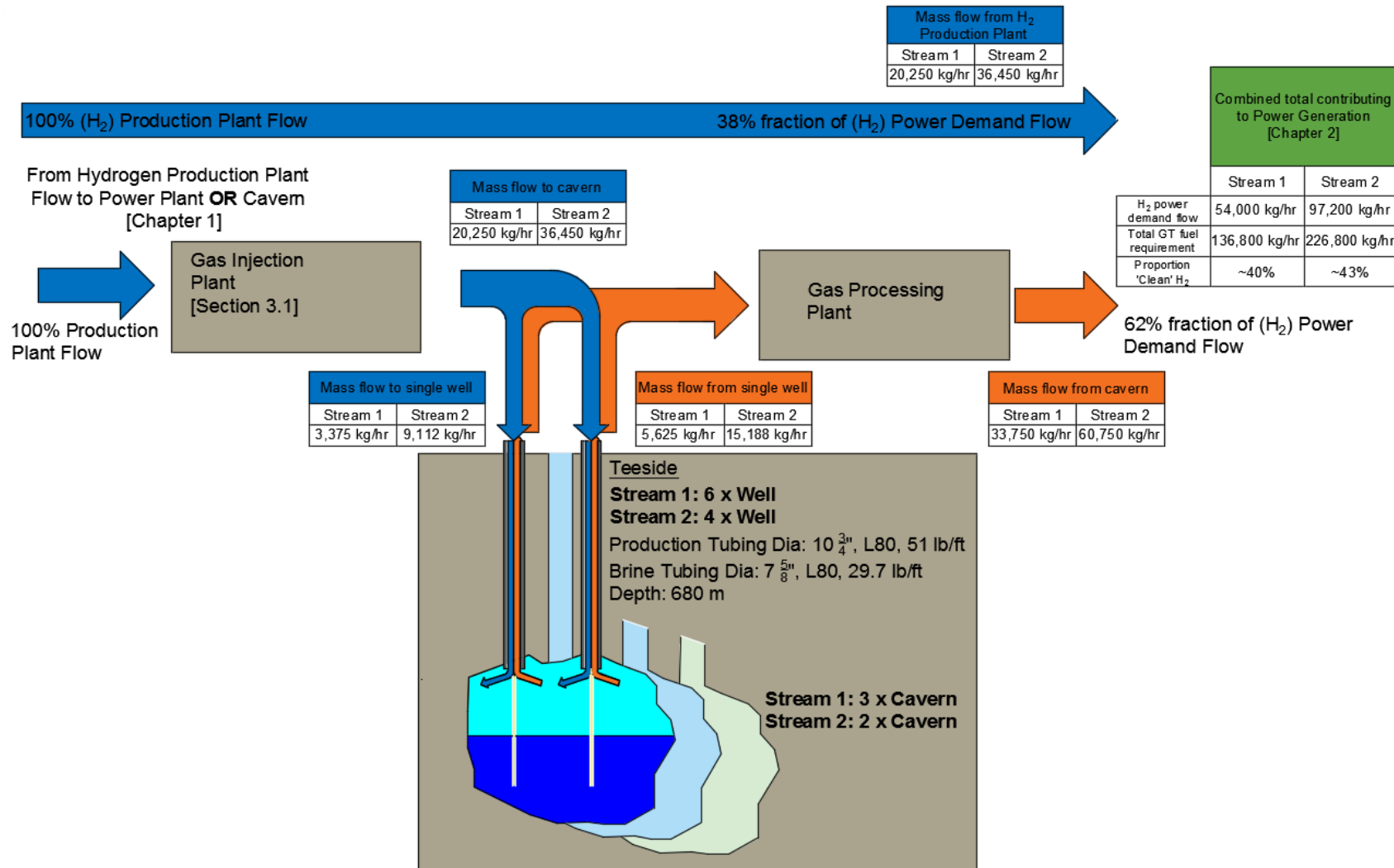
3.5. Proposed hydrogen supply arrangement

Figures 3-10 and 3-11 present the proposed H₂ supply arrangements at East Yorkshire, Cheshire and Teesside respectively. These arrangements and associated flow rates will be used in Chapter 4 to assess the ability of the salt caverns to meet the defined requirements. It should be noted that during GT operation there is a direct feed of fuel gas stream (1 or 2) from the H₂ production source to the power generation plant (shown by blue arrow). This supply combines with the fuel gas stream (1 or 2) supplied from the cavern (shown by orange arrows) to meet the 'clean' proportion of the 'Power Demand Flow'.



* Flowrates presented exclude 10% design margin used in cavern modelling. The fuel requirement is based on the E class machine at 90% load.

Figure 3-10: Block flow diagram East Yorkshire and Cheshire arrangements (Scenario 3)



* Flowrates presented exclude 10% design margin used in cavern modelling. The fuel requirement is based on the E class machine at 90% load.

Figure 3-11: Teesside mass flow rate block diagram (Scenario 3)

ATKINS

Chapter 4: Storing hydrogen in salt caverns



4. Cavern storage

Based on the output of Chapters 2 and 3 the demand requirements for caverns operating in a H₂ power generation process at each of the three locations have now been defined. It is now necessary to confirm that representative caverns at these locations can meet these requirements. The objectives of this section are therefore:

- I. Review cavern performance when subject to the demand profile.
- II. Confirm cavern capability as an H₂ store.

4.1. Introduction

As identified by Pellizzarro et al (2011), the stability of a solution-mined cavern used for underground storage of gaseous products is dependent upon the state of stress in the salt surrounding the cavern. This state of stress depends on the original in-situ stresses in the salt and the way they are modified by the gas pressure and temperature cycles in the cavern. The gas pressure in the cavern and the injection/withdrawal rates play a major role on the state of stress in the salt surrounding the cavern. The temperature of the gas in the cavern varies too, for thermodynamic and heat exchange reasons. These gas thermal changes are transmitted to the salt but remain generally limited to the immediate vicinity of the cavern. However, as salt has a relatively high coefficient of thermal expansion, small temperature changes in the salt may induce relatively large stress changes, and therefore may affect salt integrity.

The thermo-mechanical analysis employed in this work, aims at assessing the stability of the investigated caverns regarding usual mechanical criteria, and evaluates the probable consequences related to the thermal loading of the salt mass that surrounds the caverns. Thermodynamic computations in the cavern are performed employing the Salt Cavern Thermal Simulator (SCTS) (Nieland, 2004), a program developed by PB Energy Storage Services, Inc. and RESPEC for simulating the thermodynamics and heat transfer related to the storage of natural gas in underground salt caverns.

The SCTS software accounts for the thermal effects associated with gas compression and expansion; the mass transfer during injection and withdrawal; and the heat transfer between the gas and its surroundings, both in the wellbore and in the cavern. SCTS has been used in this work to estimate the cavern temperatures during cavern development, dewatering, and throughout the simulated storage operations. The current version of SCTS only simulates natural gas storage, for this reason, the derived results were corrected by employing a benchmarking process using the TDFD program developed in the University of Newcastle (Thompson, 1973) to allow the simulation of H₂ storage.

The SCTS software models the wellbore and the cavern separately because the dominant modes of heat transfer are different in these two regions. Naturally, the two regions are connected in that the temperature of the gas entering the cavern model is the temperature of the gas exiting the wellbore model during injection. Similarly, the temperature of the gas entering the wellbore model is the temperature of the gas exiting the cavern model during withdrawal. Because the temperature gradients in the direction of the flow are expected to be small, in the thermodynamic modelling of the wellbore the heat transfer by conduction is neglected in the vertical direction.

In SCTS, the heat transfer between the stored gaseous product in the cavern and the surrounding salt formation is estimated using a one-dimensional spherical heat transfer model containing a single material that corresponds to the surrounding salt. SCTS uses the parameter “volume-to-area ratio” to modify the spherical model to approximate the actual shape of the cavern. The heat transfer between the stored gaseous product in the wellbore and surrounding rock is estimated using a stacked series of one-dimensional radial heat transfer models with properties assigned based on the surrounding rock formations. SCTS calculates the cavern temperature and the cavern pressure as functions of time, which are subsequently applied as a boundary condition to the geomechanical model that investigates the

thermo-mechanical response of the salt surrounding the cavern as a function of time.

The thermo-mechanical coupled calculations are implemented by a computer aided numerical technique that models the response of the H₂ storage caverns, by employing the finite difference method. The particular code used is the FLAC (Fast Lagrangian Analysis of Continua) (Itasca Consulting Group, 2011b) which is considered to be the most well-known stress analysis computer code for engineering problems that employs the finite difference technique, and is based upon a ‘Lagrangian’ calculation scheme. This scheme is well suited for modelling large distortions, primarily encountered in geomechanical applications in salt formations.

During the modelling process the salt caverns are subjected to the specified operating conditions required to meet the power production demands. The deliverability of cavern/GT systems in meeting diurnal power demand profiles is based on the worst possible case resulting from the power generation Scenario 3 which led to the flowrates shown in Table 3-10.

In the thermodynamic simulations, properties of the brine and the H₂ rich fuel gas streams are calculated in SCTS based on the molecular composition of the gaseous product, or the salinity of the brine, and are functions of the temperature and pressure. These properties include density, compressibility, thermal conductivity, specific heat, and viscosity. The composition of the H₂ rich fuel gas streams (no.1 and no.2) are given in Appendix A.1.

Assessment of the results presented in Table 3-10, identified that during the cyclic operation of the caverns the flowrates, for both East Yorkshire and Cheshire, correspond to the pattern shown in Table 4-1.

Table 4-1: Cyclic operations flowrates, corresponding to power generation Scenario 3, for the East Yorkshire and Cheshire caverns (expressed in Nm³/d).

Time interval [hrs]	Operation	Fuel gas stream 1	Fuel gas stream 2
5½	injection	981,408	677,088
4½	withdrawal	1,635,696	1,128,480
7½	injection	981,408	677,088
4½	withdrawal	1,635,696	1,128,480
2	injection	981,408	677,088

4.2. Thermodynamic analysis for East Yorkshire and the Cheshire representative caverns

The thermodynamic analysis was carried out only for the East Yorkshire and the Cheshire sites where the salt caverns are functioning by employing dry storage operations. In contrast, the Teesside caverns are functioning by employing wet storage operations and as such there is no need to consider the thermodynamic response, as with a near constant pressure they operate near isothermally.

East Yorkshire

The stratigraphy used in the simulations of the wellbore heat transfer for the East Yorkshire analysis is based on the local geology described in Appendix A.2.1. The densities for the rock units and the corresponding thermal properties are listed in Appendix D.2.

The ratio of the volume to surface area of the investigated East Yorkshire representative cavern is 15.64 m³/m². The thermodynamic simulation was preceded by leaching and dewatering of the cavern. The leaching was simulated over 1,505 days with a flow rate of 1.8 m³/min. A freshwater injection

temperature of 10°C at the wellhead was assumed during leaching.

To de-brine the cavern in line with standard practices while maintaining its integrity, the cavern de-brining operation is expected to take at least 3 months. On this basis, the calculated required gas rate will be very low at circa 450,000 Nm³/day. This rate is well below the production rate of the H₂ production plant and any sensible/practical design turndown rate (it would be running at circa 10% capacity).

The options to allow this 450,000 Nm³/day de-brining rate are as follows:

- Commission the H₂ production plant and the power generation plant. Operate the power plant fully at say 70% load for 100 days whilst sending a bleed of H₂ from the H₂ production plant at 450,000 Nm³/day to the cavern.
- De-brine the cavern using natural gas.
- Use H₂ trailers which are available at high pressure (likely impractical).
- Use N₂ trailers (likely impractical).
- Design H₂ production plant in such a way that it can run at 450,000 Nm³/day (likely impractical).

Careful consideration and assessment of the advantages and disadvantages of the available options resulted in choosing to de-brine the cavern using natural gas, taking into account that:

- A natural gas supply will be required to the facility anyway.
- At the end of the de-brining operation, the cavern will be full of natural gas.
- Natural gas is available in the cavern for any testing of the power generation equipment.
- Start up the H₂ production plant and the power generation plant, feeding the power generation plant with a mixture of H₂ (direct from the plant) and natural gas (direct from the caverns).
- When the power generation plant is offline, the cavern will be filled with H₂ from the H₂ production plant. Over time the cavern will be depleted of natural gas and will be full of the H₂ composition.

The complications this may add to the design are:

- A compressor may be required to compress the natural gas for de-brining. This could be the same compressor needed for the H₂ plant.
- Some GTs in the power gen plant would be designed to run on a mix of H₂ and natural gas however, this may well be the case anyway.

Accordingly, after leaching, the cavern is dewatered and filled with natural gas at a wellhead pressure of 25 MPa g.

Because the salt immediately around the cavern is cooled during leaching, the cavern gas temperature is initially lower than that of the surrounding salt layer and gradually warms with time. As a result of this gradual warming of the cavern, the pressure in the cavern will gradually increase with time, even if we adopt the cyclic loading specified in Table 4-1 whereby, a perfect mass balanced approach is employed since in each cycle the injected gaseous mass is fully withdrawn before the next cycle commences.

To avoid building up the pressure to an unacceptable level, i.e. higher than the maximum permissible pressure at the last cemented casing shoe, a net outflow of gas was assumed initially. This was modelled by reducing injection by two hours for a period of approximately six months.

In following this approach, the cavern is de-pressurised to about 19.5 MPa g at the last cemented casing shoe, which corresponds approximately to the middle of the range defined by the maximum and minimum allowable pressure ($P_{max} = 27.1$ MPa g and $P_{min} = 12.0$ MPa g). The conditions at this point were used as the starting point for the cavern thermodynamic simulations that follow the specified cyclic loading shown in Table 4-1.

Comparison of the flowrates for fuel gas stream 1 and fuel gas stream 2, shown in Table 4-1, suggests that fuel gas stream 1 is expected to result in a more “aggressive” cyclic loading since its higher flow

rates (the flow rates for fuel gas stream 1 are approximately 1.45 times higher than the corresponding rates for fuel gas stream 2) will result in a higher width of the developing temperature range.

Indeed, the resulting temperature histories for fuel gas stream 1 and fuel gas stream 2, shown in Figure 4-1, that relates to the depressurisation of the cavern to about 19.5 MPa g, confirm that the worst possible case corresponds to the use of fuel gas stream 1.

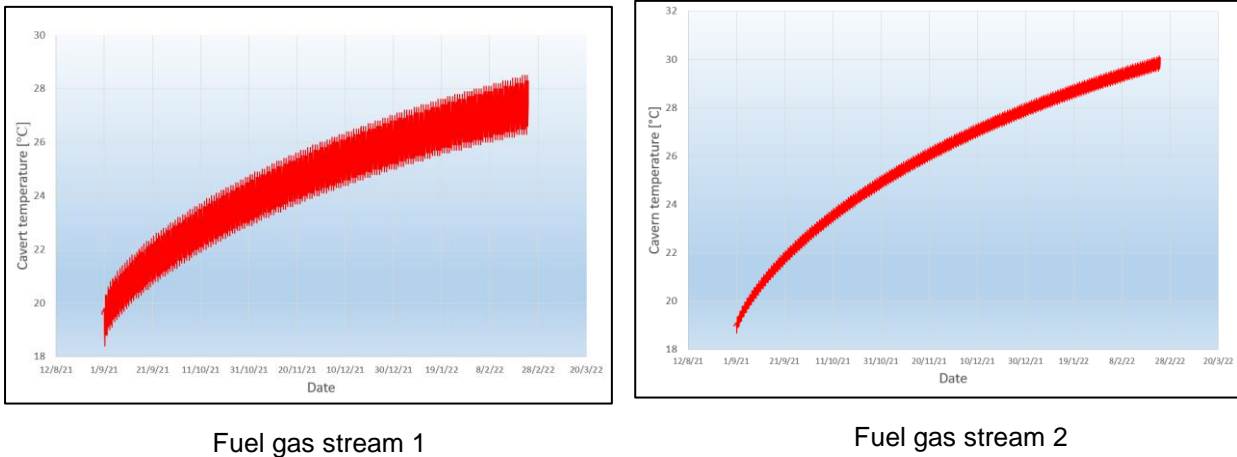


Figure 4-1: Comparison of the effect of fuel gas stream 1 and fuel gas stream 2 on the resulting cavern temperature history

Consequently, the thermodynamic analysis of the East Yorkshire representative cavern was carried out by employing the fuel gas stream 1 molecular composition and its respective flow rate, as specified in Table 4-1.

The results of the thermodynamic analysis for a cyclic loading that lasted five years, are presented in Figure 4-2 as the cavern temperature history and in Figure 4-3 as the respective cavern pressure history.

The solution mining of the cavern was modelled by gradually reducing the internal pressure of the cavern from the original undisturbed mean geostatic stress to the intensity that corresponds to the exerted halmostatic pressure (Oliver, 1982). As a result, the cavern pressure history (shown in Figure 4-3) starts from point G that refers to the pressure that corresponds to the equivalent geostatic stress, which existed prior to the creation of the cavern.

Over the period that it has taken to solution mine the cavern (i.e. over a period of 1,505 days), the cavern pressure was reduced by following the ramp (shown in Figure 4-3) from point G to point S, which corresponds to the halmostatic pressure. A similar pattern, to the one exhibited by the cavern pressure history, is demonstrated by the change in the cavern temperature. Before the creation of the cavern, as shown in Figure 4-2, the temperature history starts from point G that corresponds to the geothermal temperature at cavern depth, which is taken to be equal to 56°C. As the solution mining of the cavern proceeds, by injecting sea water with a 10°C temperature, the salt mass that surrounds the caverns cools down and the cavern temperature drops gradually to 12.7°C indicated in Figure 4-2 by point S.

After a short time, that lasted a month, the de-brining process started and was completed when the cavern pressure reached point D (as shown in Figure 4-3), which is very close to, but never higher than, the maximum allowable pressure in the cavern (P_{max}). Following a similar pattern, the temperature in the cavern increased from point S to point D as consequence of the injection of warm gas during the de-brining phase.

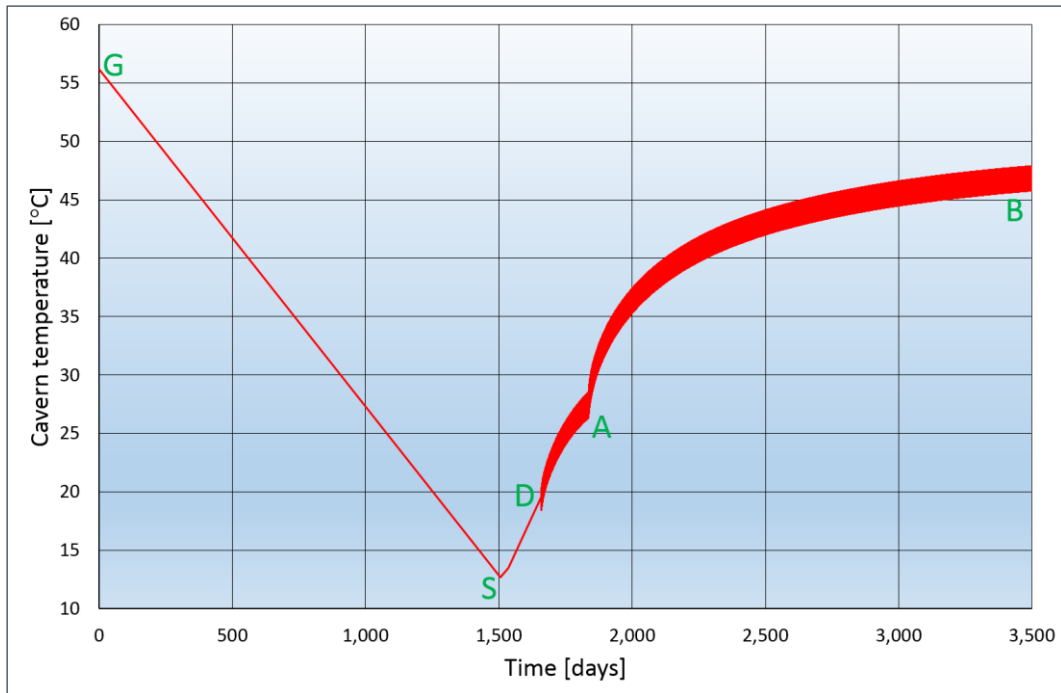


Figure 4-2: Cavern temperature history for the East Yorkshire cavern

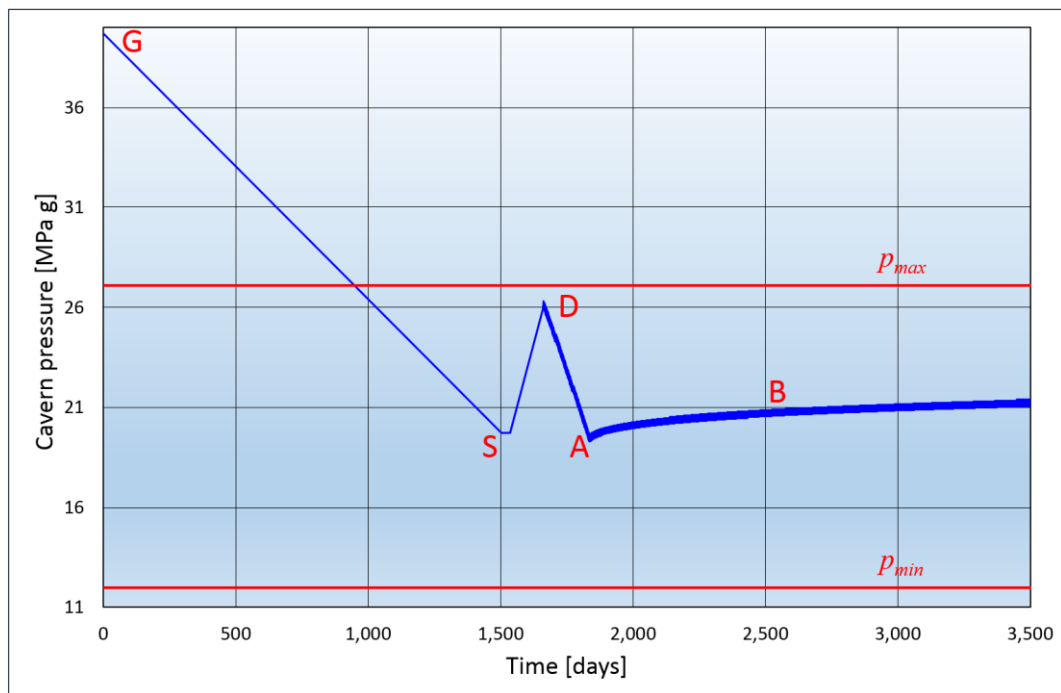


Figure 4-3: Cavern pressure history for the East Yorkshire cavern

In an attempt to prevent the building of the cavern pressure to an unacceptable level, as explained earlier, the early storage cycles skipped the injection of H₂ for two hours every cycle. Consequently, the cavern pressure gradually reduced from point D (i.e. end of de-brining) to point A over a period of six months. This time, the history of the cavern temperature did not follow the same trend as the one exhibited by the cavern pressure. Instead, after the end of de-brining (i.e. point D in Figure 4-2), the temperature in the cavern gradually increased as a consequence of the applied H₂ storage operations.

The increase in the caverns temperature up to point A, did not take place at a fast rate essentially because the injection of H₂ in every cycle, was prevented for two hours.

From point A and forward, the injection/withdrawal cycles continued by conforming to the pattern specified in Table 4-1, and resulted in a gradual increase in the cavern pressure typically represented by point B (shown in Figure 4-3). Similarly, as shown in Figure 4-2, the temperature in the cavern increased at a faster rate than the one that typified the transition from point D to point A, basically because the skipping of the two hours' injection step was revoked and the cavern was subjected to a complete storage operation cycle.

Aspects of the thermodynamic results that are shown in Figures 4.2 and 4.3 are discussed in Appendix D.9 where details of the cavern's pressure and temperature histories near points A and B are analysed. Examination of Figure D9-4 indicates that during the cavern de-pressurisation steps, included in the cyclic pressurisation of the cavern, the corresponding temperature changes were of the order of 2°C. These relatively small temperature fluctuations are attributed to the fact that, in terms of H₂ flows, the East Yorkshire cavern is not overstressed.

Cheshire

The stratigraphy used in the simulations of the wellbore heat transfer for the Cheshire analysis is based on the local geology described in Appendix A.2.3. The densities for the rock units and the corresponding thermal properties are listed included in Appendix D.3.

The ratio of the volume to surface area of the investigated Cheshire representative cavern is 18.72 m³/m². The thermodynamic simulation was preceded by leaching and dewatering of the cavern. The leaching was simulated over 1,590 days with a flow rate of 1.53 m³/min. A freshwater injection temperature of 16.5°C at the wellhead was assumed during leaching.

To de-brine the cavern, in line with conclusions reached in above, natural gas was used to displace the brine in the cavern. Accordingly, after leaching, the cavern is dewatered and filled with natural gas at a wellhead pressure of 8.33 MPa g.

To avoid building up the pressure to an unacceptable level, i.e. higher than the maximum permissible pressure at the last cemented casing shoe, a net outflow of gas was assumed initially. This was modelled by reducing injection by two hours for a period of approximately three months.

In following this approach, the cavern is depressurised to about 6 MPa g at the last cemented casing shoe, which corresponds approximately to the middle of the range defined by the maximum and minimum allowable pressure ($P_{max} = 9.5$ MPa g and $P_{min} = 3.0$ Mpa g). The conditions at this point were used as the starting point for the cavern thermodynamic simulations that follow the specified cyclic loading shown in Table 4-1.

In line with conclusions reached above for East Yorkshire, the thermodynamic analysis of the Cheshire representative cavern was carried out by employing the fuel gas stream 1 molecular composition and its respective flow rate, as specified in Table 4-1.

The results of the thermodynamic analysis for a cyclic loading that lasted five years, are presented in Figure 4-4 as the cavern temperature history and in Figure 4-5 as the respective cavern pressure history.

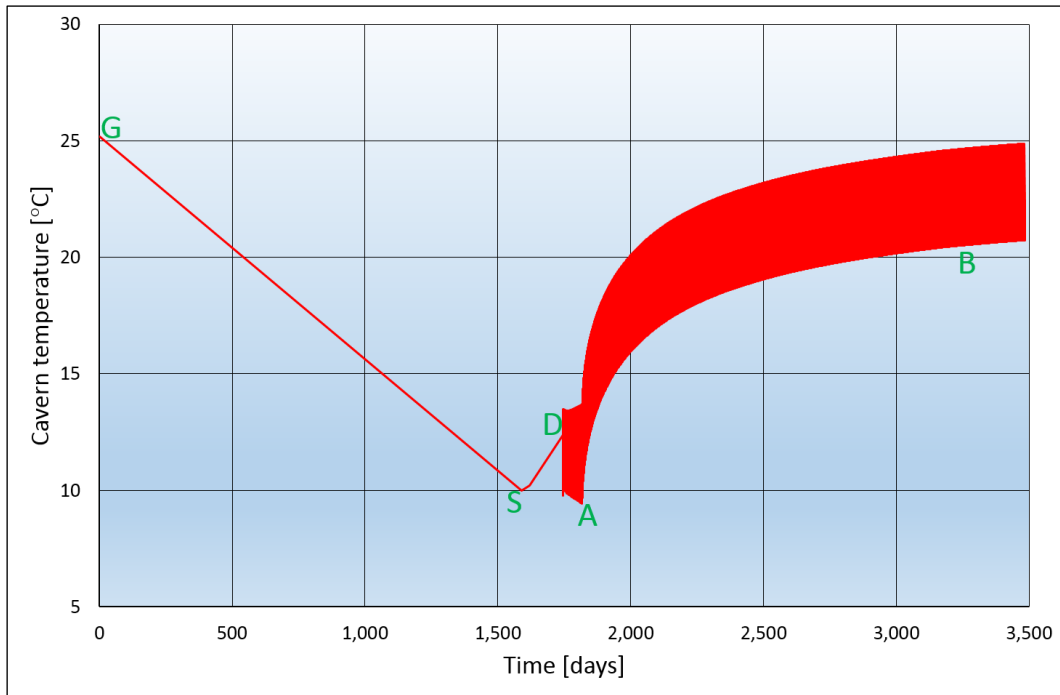


Figure 4-4: Cavern temperature history for the Cheshire representative cavern

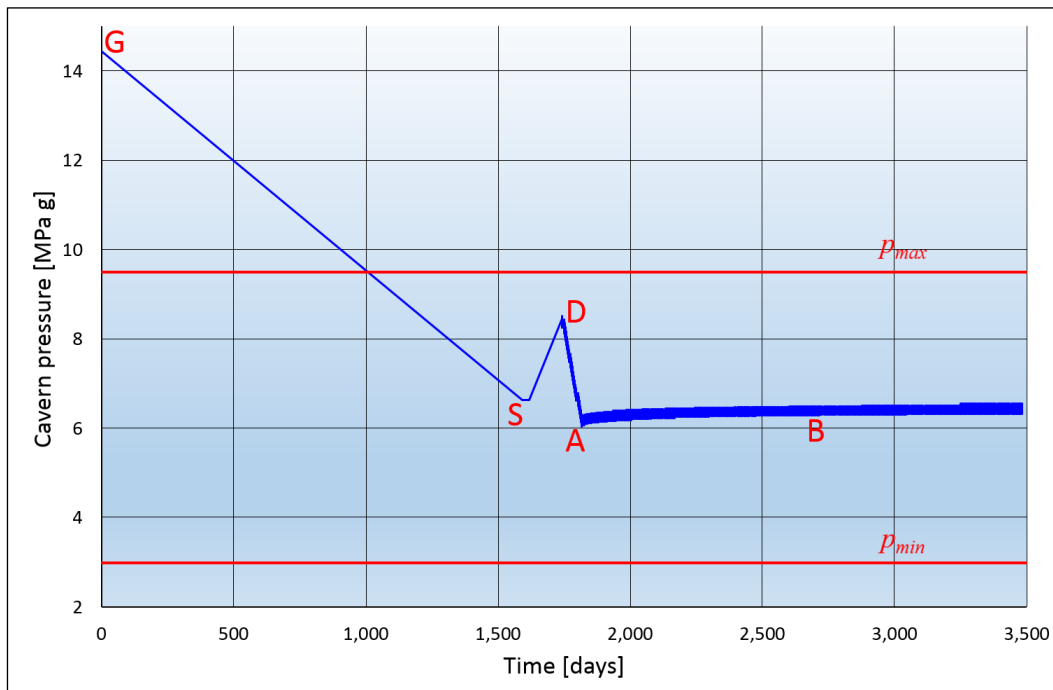


Figure 4-5: Cavern pressure history for the Cheshire cavern

The progression of the pressure and temperature histories for Cheshire representative cavern, from point G, to point B, including points S, D and A, may be evaluated by following the same discussion and description that was presented for the East Yorkshire representative cavern. The only differences are:

- the solution mining of the cavern (i.e. the time taken to progress from point G to point S, in

- Figures 4-4 and 4-5) lasted for 1,590 days, instead of 1,505 days;
- the geothermal temperature at cavern depth (i.e. point G in Figure 4-4), is 25.2°C, instead of 56°C;
 - during the solution mining phase the injecting fresh water had a temperature of 16.5°C, instead of 10°C; and
 - at the end of the solution mining phase (indicated in Figure 4-4 by point S), the cavern temperature dropped to 10°C, instead of 12.7°C;

Aspects of the thermodynamic results that are shown in Figures 4-4 and 4-5 are discussed in Appendix D.10 where details of the cavern's pressure and temperature histories near points A and B are analysed. Examination of Figure D10-4 indicates that during the cavern de-pressurisation steps, included in the cyclic pressurisation of the cavern, the corresponding temperature changes were of the order of 4°C. These relatively small temperature fluctuations are attributed to the fact that, in terms of H₂ flows, the Cheshire representative cavern is not overstressed.

4.3. Coupled thermo-geomechanical analysis for East Yorkshire & Cheshire representative caverns

East Yorkshire

Technical approach

There are no direct stress measurements available for the *in situ* stress field in the East Yorkshire area and therefore the assessment of the geostatic stress field relied on the review of the regional stress information taking into account the lithology, the thicknesses and depths of the identified geological formations.

The geostatic vertical stress has been estimated based on the superincumbent strata and it is assumed that the horizontal stress is uniform and related to the vertical. Finally, based on long-term creep results of laboratory testing of Fordon Evaporites Salt core specimens taken from the Atwick gas storage site (Horseman & Passaris, 1981) and taking into consideration the depth of the representative cavern (~ 1.8 km), the ratio of the horizontal to the vertical geostatic stress is expected to approach unity whereby the *in situ* stress state of the salt is assumed to be isotropic showing no differences in horizontal and vertical directions.

In the coupled thermo-mechanical analysis of the salt cavern, its sump is represented as being occupied by the stored H₂ mixture. In real terms, the sump collects insoluble materials during the solution mining process and although these insoluble materials will provide some support to the cavern walls, the sump of the cavern is modelled as being devoid of such material. This approximation lends conservatism to the model, although the overall response of the modelled cavern will be little influenced by the approach used to represent the pressure exerted at the walls of the sump.

Over the period that it has taken to develop the cavern (i.e. over a period of 1,505 days), the solution mining of the cavern was modelled by gradually reducing the internal pressure of the cavern from the original undisturbed mean geostatic stress to the intensity that corresponds to the exerted halmostatic pressure (Oliver, 1982).

To investigate the thermo-mechanical response of the East Yorkshire representative cavern, when the cavern internal boundary is modelled in accordance with the temperature and pressure histories specified in Section 4.2 use was made of the software package FLAC. Three components were specified for the system configuration employed in the coupled thermo-mechanical modelling:

- The constitutive behaviour, the strength characteristics, the physical (as shown in Appendix D.11) and the thermal properties of the geological materials that influence the structural response of the cavern to the imposed disturbances.

- A model grid defining the geometry of the problem (shown in Figure 4-6).
- The boundary and initial conditions corresponding to the *in situ* geomechanical state.

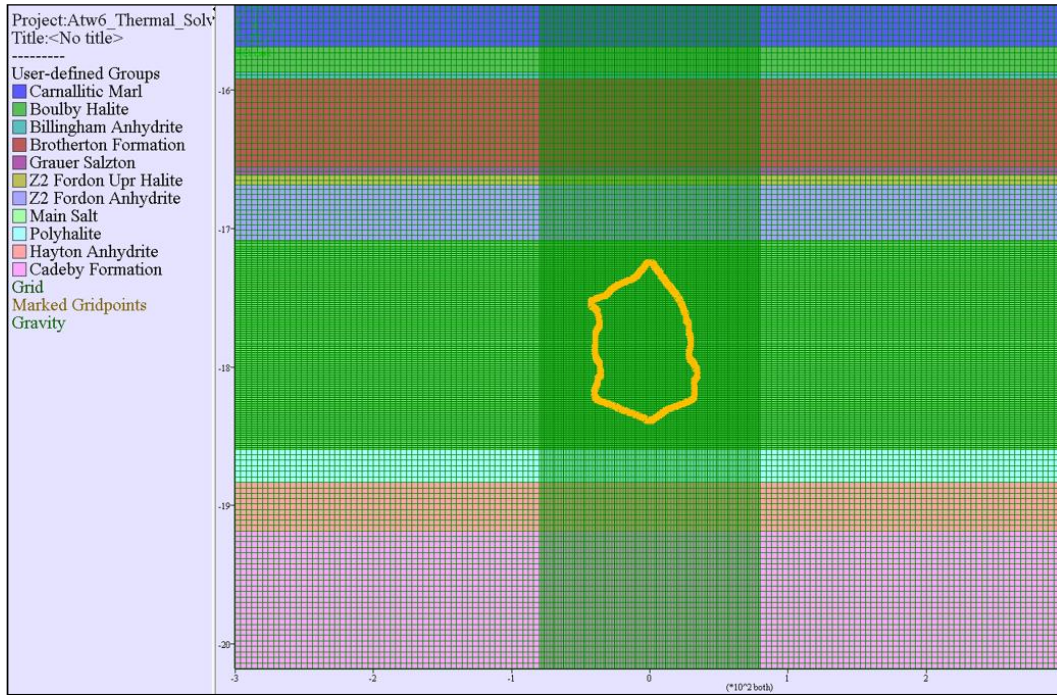


Figure 4-6: Finite difference grid used in the modelling of the East Yorkshire cavern

Examination of Figure 4-7 indicates that, in the region immediately surrounding the cavern, the finite difference grid was finely subdivided to improve the accuracy of the analysis near the cavern roof and side walls where high stress gradients were anticipated.

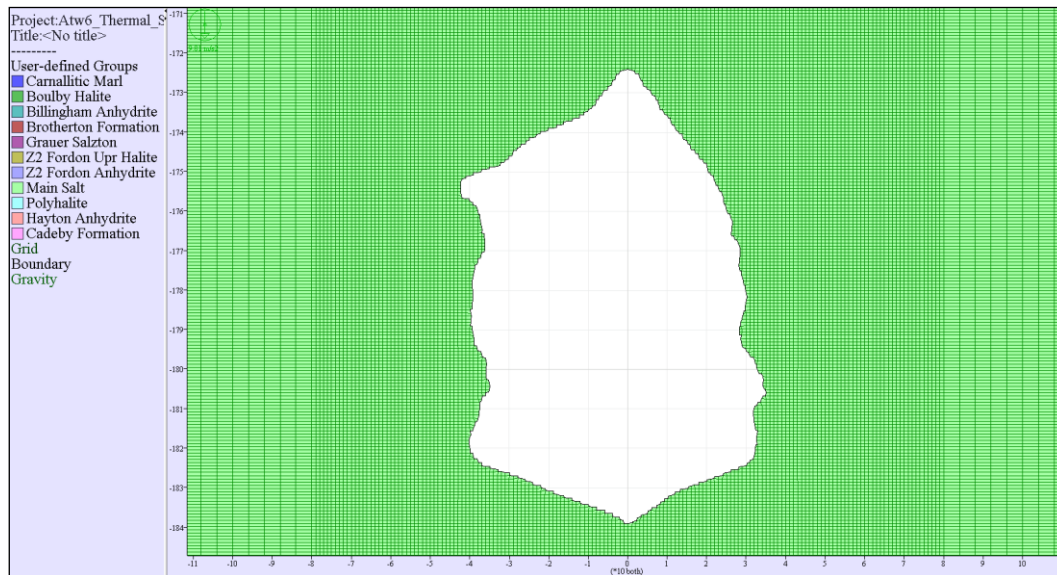


Figure 4-7: Details of the finite difference grid used in the modelling of the East Yorkshire cavern

As shown in Figure 4-6, the finite difference model of the cavern employed the stratigraphy identified in Appendix A.2. The sequence of layers above the Carnallitic Marl was not explicitly modelled; instead the overburden loading that corresponds to the gravitational loading of these beds was applied as a uniform vertical pressure to the top end of the model.

During the thermo-mechanical analysis, the modelled ground was pre-stressed in accordance to the *in situ* geostatic stress field. It is important to take into consideration that, in addition to the horizontal σ_{11} and vertical σ_{22} geostatic stress components, σ_{33} (the component acting normal to the plane-strain grid) was also initialised while using FLAC, since the employed constitutive models take it into account. If omitted, it would have defaulted to zero, which may have caused failure to occur in the out-of-plane direction.

After this pre-stressing stage, the resulting horizontal (u_x) and vertical (u_y) displacement components were zeroed in order to only record the deformation behaviour of the cavern during the solution mining process and the subsequent storage operations. This technique did not affect the calculations since the FLAC finite difference modelling does not require displacements in the calculation sequence; they are kept simply as a convenience to the user.

The upper boundary of the finite difference model was placed at the top of the Carnallitic Marl layer at a depth of 1,538 m bgl, as obtained from the stratigraphy data. The layers overlying the modelled upper boundary were represented as a uniform vertical pressure equal to 33.9 MPa, which corresponds to the vertical geostatic stress at that depth.

The bottom boundary of the finite difference model was subjected to a vertical fixity (i.e. restricting all the bottom boundary grid nodes from moving along the vertical direction), that was placed approximately 179 m below the bottom of the cavern sump at a depth of 2,018 m bgl. In addition, the kinematic boundary conditions along the sides of the finite difference model, specified no horizontal displacement along the two vertical sides of the model while the upper horizontal surface of the model was free to move both in the horizontal and vertical directions.

Results of the coupled thermo-mechanical analysis

The geomechanical stability of the East Yorkshire representative cavern was considered by comparing stress states, predicted by the coupled thermo-mechanical analysis, to criteria developed from the rock mechanics testing of the relevant geological materials. States of stress in the walls and the roof of the cavern were analysed to determine whether the investigated temperature and pressure histories could initiate rock failure in the geological formations that surround the cavern.

Therefore, the primary goal of the thermo-mechanical analysis is to investigate, *inter alia*, the potential of:

- tensile failure that may be introduced at the roof and walls of the cavern, and/or
- shear failure of the cavern's walls, including its roof.

Cavern structural stability in this context is defined as the condition that prevents any potential shear and/or tensile failure to develop deeper than approximately 1 m inside the salt mass that surrounds the cavern.

The geomechanical stability of the modelled cavern was assessed by generating contour diagrams for:

- the ground temperature;
- the minor σ_3 and major σ_1 principal stresses;
- the von Mises stress component σ_{vm} ; and
- the vertical displacement components u_y .

The von Mises or Equivalent stress component is defined by the following expression:

$$\sigma_{vm} = \sqrt{3J_2} \quad \text{Equation 4.1}$$

where J_2 is the second invariant of the deviatoric stress tensor that has been defined by Equation D8 (in Appendix D.7)

and where σ_2 is the intermediate principal stress that satisfies the following relationship:

$$\sigma_3 \leq \sigma_2 \leq \sigma_1 \quad \text{Equation 4.2}$$

When a plane strain analysis is employed for the geomechanical modelling of a geo-structure, the physical equivalent of the von Mises component corresponds to the difference of the maximum and minimum principal stresses. To determine the progressive development of temperature, σ_1 , σ_3 , σ_{vm} and u_y , the corresponding contour diagrams were produced at the end of the cavern de-pressurisation (depicted as point A in Figure 4-2) and also at the end of the 5 years modelling of the cyclic operation of the cavern. The contour diagrams of temperature, σ_1 , σ_3 , σ_{vm} and u_y derived from the coupled thermo-mechanical modelling of the East Yorkshire representative cavern are included in Appendix D.4.

The initial temperature in the salt mass surrounding the East Yorkshire representative cavern which is linked to a geothermal gradient of 0.026°C/m (British Geological Survey, 1986), is proportional to the depth and is about 329 K (56°C) at cavern mid-height. At the end of the cavern de-pressurisation, the distribution of the temperature in the surrounding salt mass, shown in Figure D4-1 (included in Appendix D.4), indicates that the applied cavern temperature of 301 K (28°C) gradually increases to the geothermal grade within 20 m from the walls of the cavern. Following the completion of five years of cyclic loading, the distribution of the temperature in the surrounding salt mass, shown in Figure D4-6 (included in Appendix D.4), indicates that the applied cavern temperature of 321 K (48°C) gradually increases to the geothermal grade within 45 m from the walls of the cavern.

Examination of both Figures D4-1 and D4-6 indicates that the part of the cavern that corresponds to the sump is not affected by the applied cavern temperature changes. This is because, the mixture of brine and insoluble materials present in the cavern sump is characterised by a typical thermal conductivity of 0.62 W/(m K) (Ozbek & Phillips, 1980) and a specific heat capacity of 3,300 J/(kg K) (Ramalingam & Arumugam, 2012), which causes the mixture to act as an insulating medium. As a result, the development of thermal stresses is essentially restricted to the roof and the walls of the cavern that are exposed to the stored H₂ mixture.

Examination of the distribution of the minor principal stress σ_3 in the salt mass that surrounds the modelled cavern, which was subjected to temperature and pressure changes associated with:

- the end of the cavern de-pressurisation (shown in Figure D4-2 included in Appendix D.4), and
- the completion of five years of cyclic loading (shown in Figure D4-7 included in Appendix D.4),

indicates the complete absence of any tensile stresses. This provides evidence that the walls of the East Yorkshire representative cavern are everywhere in compression as shown in the minor principal stress σ_3 contours presented in the aforementioned Figures D4-2 and D4-7, where the negative sign of the stress components implies compression.

The distribution of the major principal stress σ_1 around the East Yorkshire representative cavern indicates that the majority of the salt mass that forms the immediate surrounding of the cavern is tolerably compressive. In particular, at the end of the cavern de-pressurisation, σ_1 varies from location to location around the cavern between 25 MPa and 75 MPa (as shown in Figure D4-3 included in Appendix D.4). Moreover, following the completion of five years of cyclic loading the major principal stress varies, from location to location around the cavern, between 23 MPa and 53 MPa (see Figure D4-8 in Appendix D.4).

In assessing the effect of the development of high stress concentrations at the roof and the walls of the cavern, it is important to consider the combined effect of σ_1 and σ_3 rather than simply assessing their individual magnitudes. By plotting in the graph of the Fordon Evaporites Salt shear strength envelope (shown in Figure 4-8), which was derived from laboratory experimental data (RESPEC, 2008), the clusters of the *loci* of the effective stress concentrations that correspond to:

- the end of the cavern de-pressurisation (shown as cluster A and referring to point A in Figure 4-2), and
- the completion of five years of cyclic loading (shown as cluster B),

it is evident that the shear strength of the salt surrounding the cavern is not compromised.

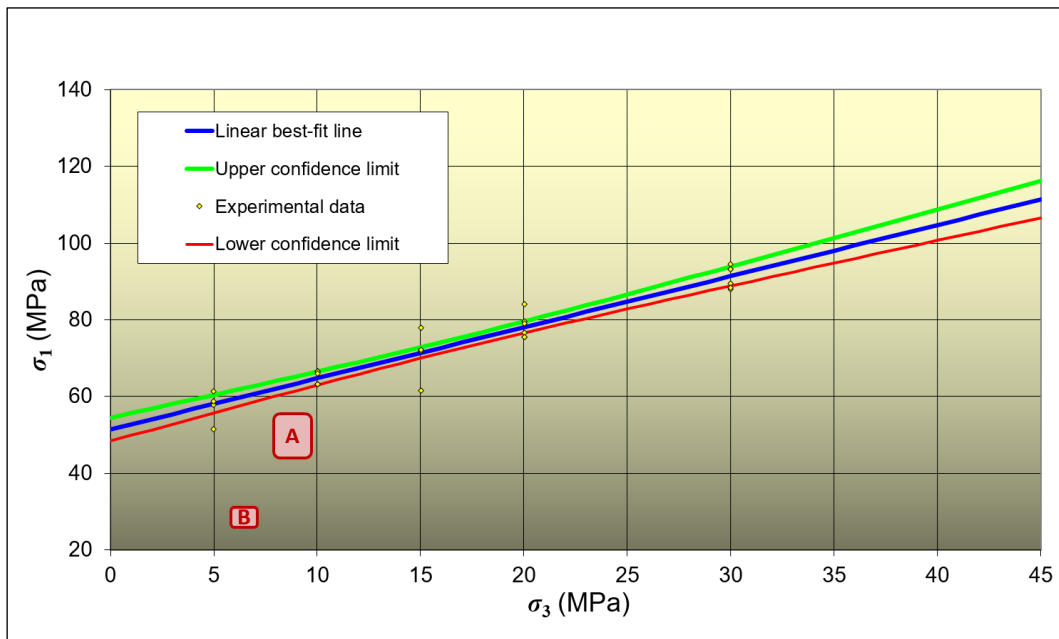


Figure 4-8: Shear strength envelope for Fordon Evaporites Salt, expressed in terms of σ_1 and σ_3 .

This shows the clusters of the *loci* of the effective stress concentrations that develop around the East Yorkshire representative cavern. Confidence limits were determined according to Snedecor & Cochran (1989)

A complementary way of assessing the potential shear stress intensity of the salt surrounding the East Yorkshire representative cavern is to investigate the magnitude of the von Mises stress (σ_{vm}) or the square root of the second invariant of the deviatoric stress tensor $\sqrt{J_2}$ (which is equal to $(\sigma_{vm}/\sqrt{3})$).

At the end of the cavern de-pressurisation, the peak value of σ_{vm} at the roof and the sides of the cavern is 35 MPa (as shown in Figure D4-4 included in Appendix D.4). In addition, following the completion of five years of cyclic loading, the peak value of σ_{vm} at the roof and the sides of the cavern is 22.5 MPa (as shown in Figure D4-9 included in Appendix D.4).

Taking into consideration that the potential shear failure of salt has been modelled by employing the Drucker Prager failure criterion (as described in Appendix D.7), the severity of the loading of the salt may be ascertained by plotting $\sqrt{J_2}$ against the first invariant of the stress tensor I_1 (as defined by Equation D7 of Appendix D.7) in the graph of the Fordon Evaporites Salt shear strength envelope (shown in Figure 4-9), the relative positions of the clusters of the *loci* of the effective stress concentrations that correspond to:

- The end of the cavern de-pressurisation (shown as cluster A and referring point A in Figure 4-3).
- The completion of five years of cyclic loading (denoted as cluster B),

These indicate that the shear strength of the salt surrounding the cavern is not compromised.

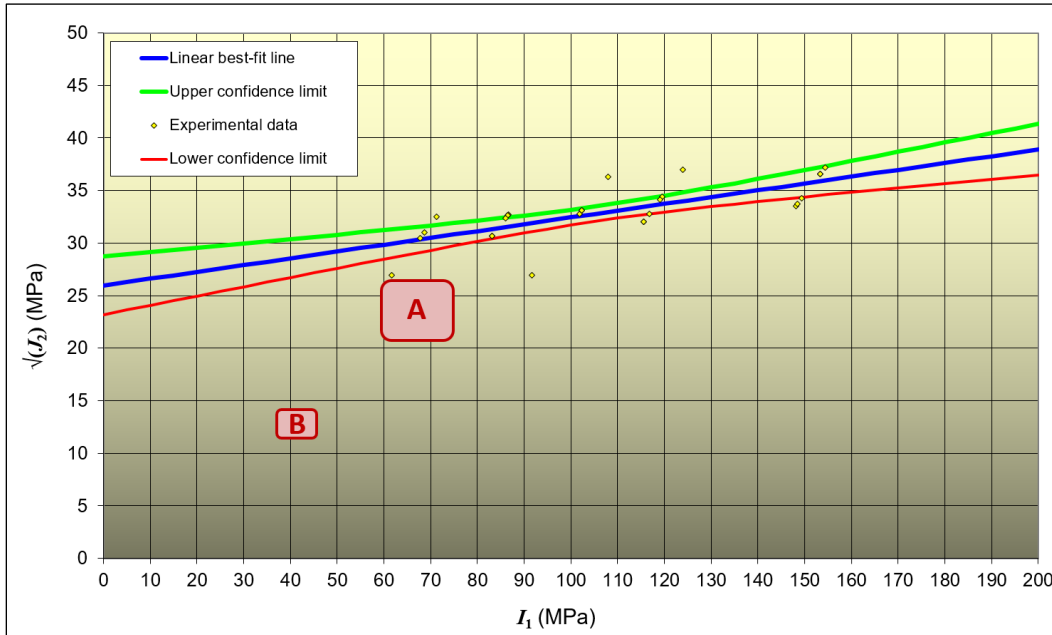


Figure 4-9: Shear strength envelope for Fordon Evaporites Salt, expressed in terms of $\sqrt{I_2}$ and I_1 ,

This shows the clusters of the *loci* of the effective stress concentrations that develop around the East Yorkshire representative cavern. Confidence limits were determined according to Snedecor & Cochran (1989)

To investigate the deformation of the East Yorkshire representative cavern, the contour diagrams of the distribution of the vertical displacements that develop around the cavern are examined. As shown in Figure D4-5 (included in Appendix D.4) at the end of the cavern de-pressurisation, the vertical creep closure of the cavern occurs primarily in the cavern roof (downwards) and the cavern sump (upwards). The vertical displacements u_y at the roof of the cavern are of the order of 0.12 m, which are considered acceptable when compared with the u_y derived from the investigations carried out concerning the operating gas storage caverns in East Yorkshire (Passaris et al, 2015). As is evident from Figure D4-5, part of the closure of the cavern is taking place in the sump area of the cavern, where the uplift is of the order of 0.04 m.

Following the completion of five years of cyclic loading, as shown in Figure D4-10 (included in Appendix D.4), the vertical creep closure of the cavern occurs primarily in the cavern roof (downwards) and the cavern sump (upwards). The vertical displacements u_y at the roof of the cavern are of the order of 0.4 m, while the uplift at the sump of the cavern is of the order of 0.15 m. Once more, these vertical displacements are considered acceptable and their effect has no particular significance on the long term structural stability of the cavern.

Cheshire

Technical approach

In the absence of direct stress measurements for the *in situ* stress field in the Cheshire area, the assessment of the geostatic stress field relied on the review of the regional stress information taking into account the lithology, the thicknesses and depths of the identified geological formations.

The geostatic vertical stress has been estimated based on the superincumbent strata and it is assumed that the horizontal stress is uniform and related to the vertical. Finally, based on creep results of laboratory testing of Northwich Halite core specimens (as specified in Appendix A.2) and taking into consideration the depth of the representative cavern (~600 m), the ratio of the horizontal to the vertical geostatic stress is expected to approach unity whereby the *in situ* stress state of the salt is assumed to

be isotropic showing no differences in horizontal and vertical directions.

In the coupled thermo-mechanical analysis of the salt cavern, its sump is represented as being occupied by the stored H₂ mixture. In real terms, the sump collects insoluble materials during the solution mining process and although these insoluble materials will provide some support to the cavern walls, the sump of the cavern is modelled as being devoid of such material. This approximation lends conservatism to the model, although the overall response of the modelled cavern will be little influenced by the approach used to represent the pressure exerted at the walls of the sump.

Over the period that it has taken to develop the cavern (i.e. over a period of 1,590 days), the solution mining of the cavern was modelled by gradually reducing the internal pressure of the cavern from the original undisturbed mean geostatic stress to the intensity that corresponds to the exerted halmostatic pressure (Oliver, 1982).

To investigate the thermo-mechanical response of the Cheshire representative cavern, when the cavern internal boundary is modelled in accordance with the temperature and pressure histories specified in Section 4.2., use was made of the software package FLAC. Three components were specified for the system configuration employed in the coupled thermo-mechanical modelling:

- the constitutive behaviour, the strength characteristics, the physical properties (as shown in Appendix D.12) and the thermal properties of the geological materials that influence the structural response of the cavern to the imposed disturbances;
- a model grid defining the geometry of the problem (shown in Figure 4-10); and
- the boundary and initial conditions corresponding to the *in situ* geomechanical state.

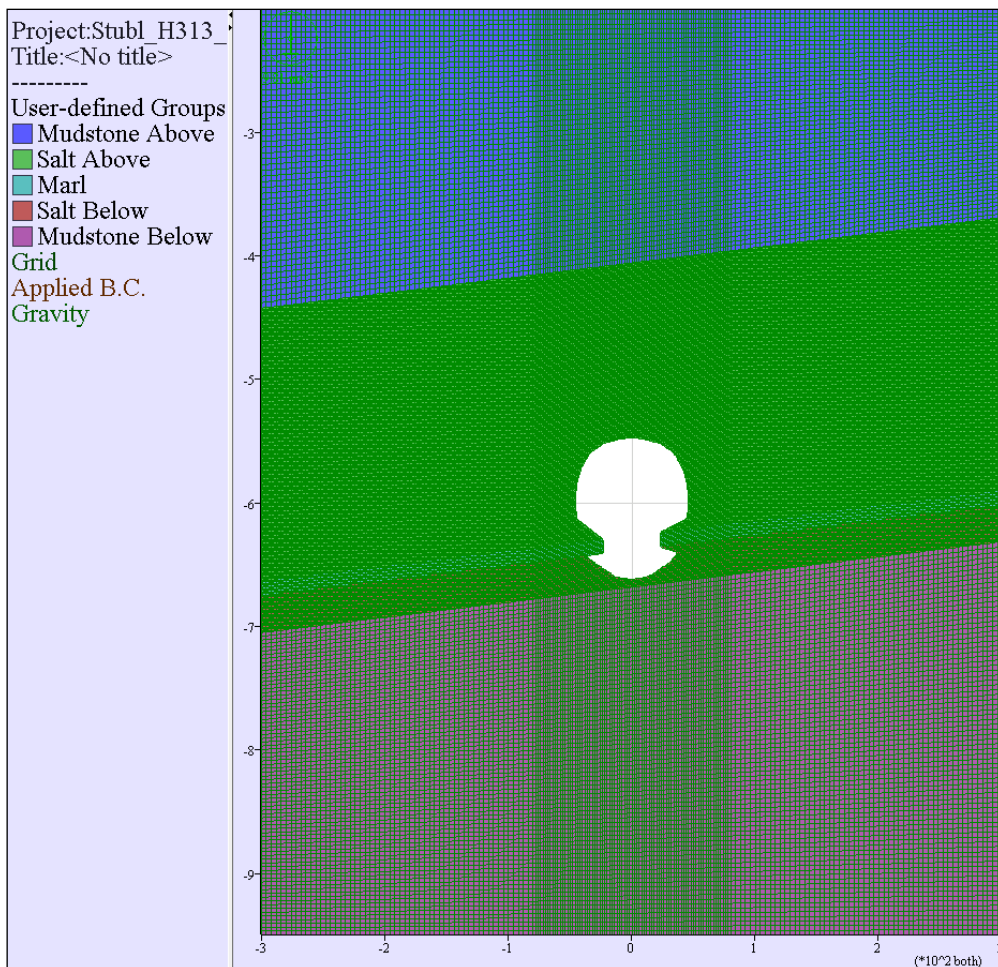


Figure 4-10: Finite difference grid used in the modelling of the Cheshire cavern

Examination of Figure 4-11 indicates that, in the region immediately surrounding the cavern, the finite difference grid was finely subdivided to improve the accuracy of the analysis near the cavern roof and side walls where high stress gradients were anticipated.

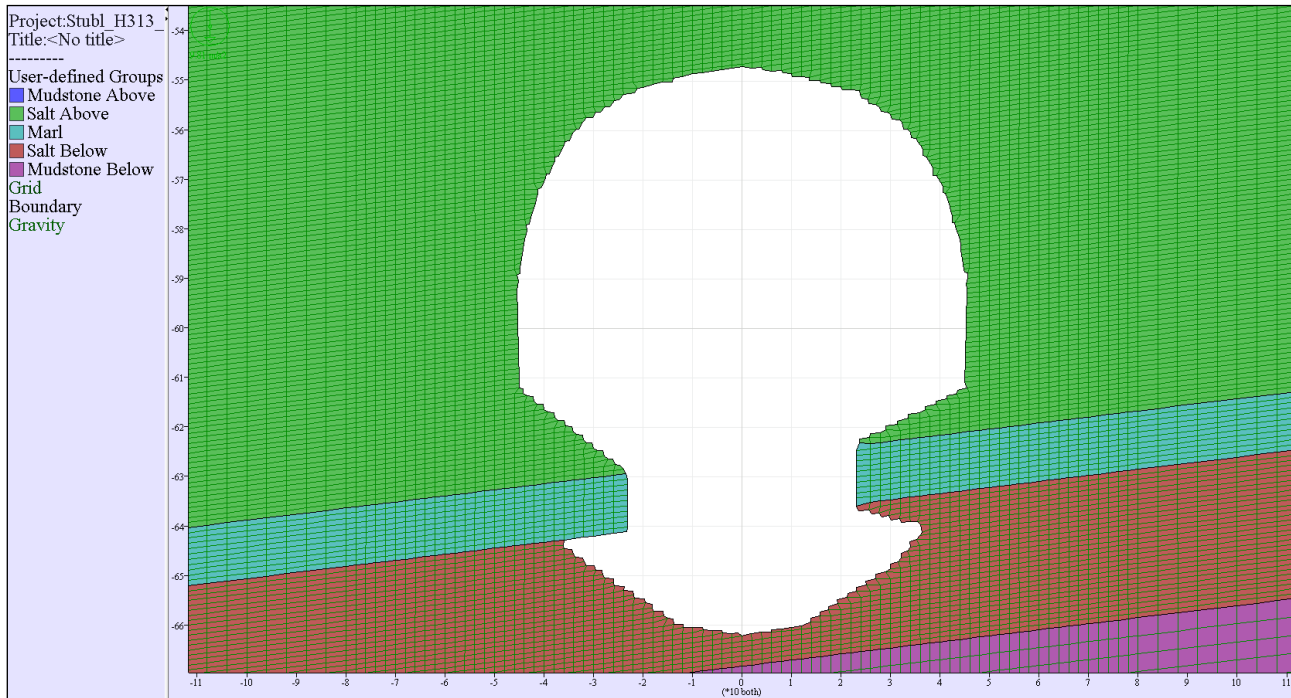


Figure 4-11: Details of the finite difference grid used in the modelling of the Cheshire cavern

As shown in Figure 4-10, the finite difference model of the cavern employed the stratigraphy identified in Appendix A.4. The sequence of layers up to the ground surface was not explicitly modelled; instead the overburden loading that corresponds to the gravitational loading at a depth of 200 m bgl was applied as a uniform vertical pressure to the top end of the model.

During the thermo-mechanical analysis, the modelled ground was pre-stressed in accordance to the *in situ* geostatic stress field. It is important to take into consideration that, in addition to the horizontal σ_{11} and vertical σ_{22} geostatic stress components, σ_{33} was also initialised while using FLAC, since the employed constitutive models take it into account. If omitted, it would have defaulted to zero, which may have caused failure to occur in the out-of-plane direction.

After this pre-stressing stage, the resulting horizontal (u_x) and vertical (u_y) displacement components were zeroed in order to only record the deformation behaviour of the cavern during the solution mining process and the subsequent storage operations. This technique did not affect the calculations since the FLAC finite difference modelling does not require displacements in the calculation sequence; they are kept simply as a convenience to the user.

The upper boundary of the finite difference model was placed at a depth of 200 m bgl and the layers overlying the modelled upper boundary were represented as a uniform vertical pressure equal to 4.79 MPa, which corresponds to the vertical geostatic stress at that depth.

The bottom boundary of the finite difference model was subjected to a vertical fixity (i.e. restricting all the bottom boundary grid nodes from moving along the vertical direction), that was placed approximately 288 m below the bottom of the cavern sump at a depth of 950 m bgl. In addition, the kinematic boundary conditions along the sides of the finite difference model, specified no horizontal displacement along the two vertical sides of the model while the upper horizontal surface of the model was free to move both in the horizontal and vertical directions.

Results of the coupled thermo-mechanical analysis

The geomechanical stability of the Cheshire representative cavern was considered by comparing stress states, predicted by the coupled thermo-mechanical analysis, to criteria developed from the rock mechanics testing of the relevant geological materials. States of stress in the walls and the roof of the cavern were analysed to determine whether the investigated temperature and pressure histories could initiate rock failure in the geological formations that surround the cavern.

Therefore, the primary goal of the thermo-mechanical analysis is to investigate, *inter alia*, the potential of:

- tensile failure that may be introduced at the roof and walls of the cavern, and/or
- shear failure of the cavern's walls, including its roof.

Cavern structural stability in this context is defined as the condition that prevents any potential shear and/or tensile failure to develop deeper than approximately 1 m inside the salt mass that surrounds the cavern.

The geomechanical stability of the modelled cavern was assessed by generating contour diagrams for:

- the ground temperature;
- the minor σ_3 and major σ_1 principal stresses;
- the von Mises stress component σ_{vm} ; and
- the vertical displacement components u_y .

To determine the progressive development of temperature, σ_1 , σ_3 , σ_{vm} and u_y , the corresponding contour diagrams were produced at the end of the cavern de-pressurisation (depicted as point A in Figure 4-4) and also at the end of the 5 years modelling of the cyclic operation of the cavern. The contour diagrams of temperature, σ_1 , σ_3 , σ_{vm} and u_y , derived from the coupled thermo-mechanical modelling of the Cheshire representative cavern are included in Appendix D.5.

The initial temperature in the salt mass surrounding the Cheshire representative cavern which is linked to a geothermal gradient of 0.026°C/m (British Geological Survey, 1986), is proportional to the depth and is about 298 K (25°C) at cavern mid-height. At the end of the cavern de-pressurisation, the distribution of the temperature in the surrounding salt mass, shown in Figure D.5-1 (included in Appendix D.5), indicates that the applied cavern temperature of 285 K (12°C) gradually increases to the geothermal grade within 20 m from the walls of the cavern. Following the completion of five years of cyclic loading, the distribution of the temperature in the surrounding salt mass, shown in Figure D.5-6 (included in Appendix D.5), indicates that the applied cavern temperature of 295 K (22°C) gradually increases to the geothermal grade within approximately 45 m from the side walls of the cavern.

Examination of both Figures D5-1 and D5-6 indicates that the part of the cavern that corresponds to the sump is not affected by the applied cavern temperature changes. This is because, the mixture of brine and insoluble materials present in the cavern sump acts as an insulating medium. As a result, the development of thermal stresses is essentially restricted to the roof and the walls of the cavern that are exposed to the stored H₂ mixture.

Examination of the distribution of the minor principal stress σ_3 in the salt mass that surrounds the modelled cavern, which was subjected to temperature and pressure changes associated with:

- the end of the cavern de-pressurisation (shown in Figure D5-2 included in Appendix D.5), and
- the completion of five years of cyclic loading (shown in Figure D5-7 included in Appendix D.5),

indicates the complete absence of any tensile stresses. This provides evidence that the walls of the Cheshire representative cavern are everywhere in compression as shown in the minor principal stress σ_3 contours presented in the aforementioned Figures D5-2 and D5-7, where the negative sign of the stress components implies compression.

The distribution of the major principal stress σ_1 around the Cheshire representative cavern indicates that the majority of the salt mass that forms the immediate surrounding of the cavern is tolerably compressive. In particular, at the end of the cavern de-pressurisation, σ_1 varies from location to location around the cavern between 12.5 MPa and 15 MPa (as shown in Figure D5-3 included in Appendix D.5). Moreover, following the completion of five years of cyclic loading the major principal stress varies, from location to location around the cavern, between 12.5 MPa and 15 MPa (see Figure D5-8 in Appendix D.5).

In assessing the effect of the development of high stress concentrations at the roof and the walls of the cavern, it is important to consider the combined effect of σ_1 and σ_3 rather than simply assessing their individual magnitudes. By plotting in the graph of the Northwich Halite shear strength envelope (shown in Figure 4-12), which was derived from laboratory experimental data (Hadj-Hassen, 2009), the clusters of the loci of the effective stress concentrations that correspond to:

- the end of the cavern de-pressurisation (denoted as cluster A that refers to point A in Figure 4-5), and
- the completion of five years of cyclic loading (denoted as cluster B5),

it is evident that the shear strength of the salt surrounding the cavern is not compromised.

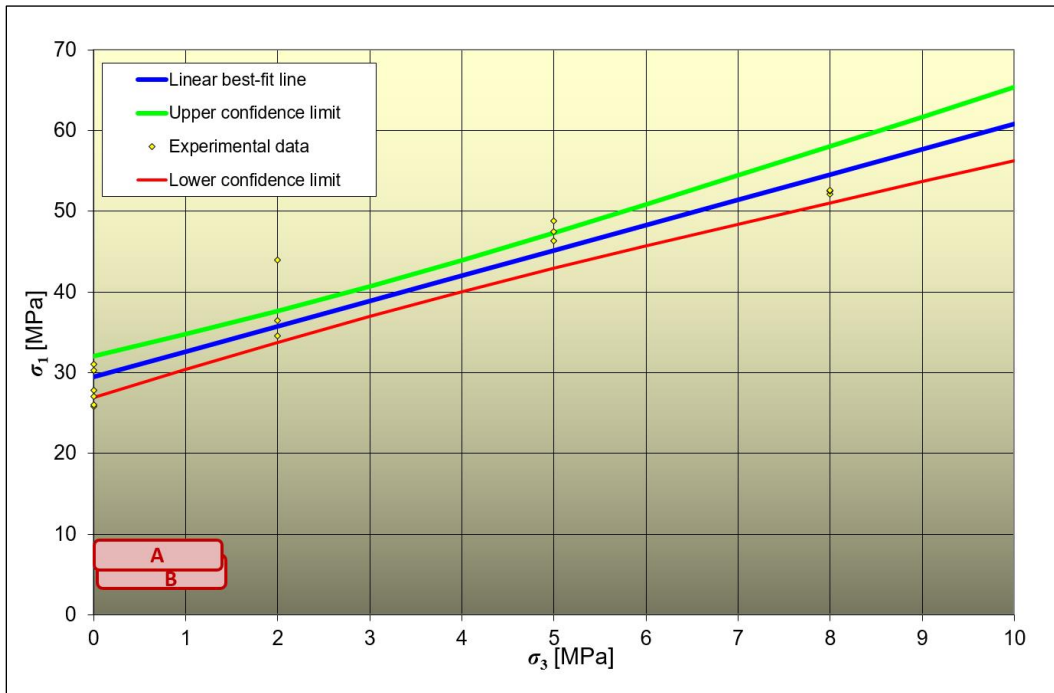


Figure 4-12: Shear strength envelope for Northwich Halite, expressed in terms of σ_1 and σ_3 .

This shows the clusters of the *loci* of the effective stress concentrations that develop around the Cheshire representative cavern. Confidence limits were determined according to Snedecor & Cochran (1989)

A complementary way of assessing the potential shear stress intensity of the salt surrounding the Cheshire representative cavern is to investigate the magnitude of the von Mises stress (σ_{vm}) or the square root of the second invariant of the deviatoric stress tensor $\sqrt{J_2}$.

At the end of the cavern de-pressurisation, the peak value of σ_{vm} at the roof of the cavern is 9 MPa while at the sides of the cavern is 5 MPa (as shown in Figure D5-4 included in Appendix D.5). In addition, following the completion of five years of cyclic loading, the peak value of σ_{vm} at the roof of the cavern is 7 MPa while at the sides of the cavern is 5 MPa (as shown in Figure D5-9 included in Appendix D.5).

When $\sqrt{J_2}$ is plotted against the first invariant of the stress tensor I_1 in the graph of the Northwich Halite

shear strength envelope (shown in Figure 4-13), the relative positions of the *loci* of the effective stress concentrations that correspond to:

- the end of the cavern de-pressurisation (denoted as cluster A that refers to point A in Figure 4-5), and
- the completion of five years of cyclic loading (denoted as cluster B),

indicate that the shear strength of the salt surrounding the cavern is not compromised.

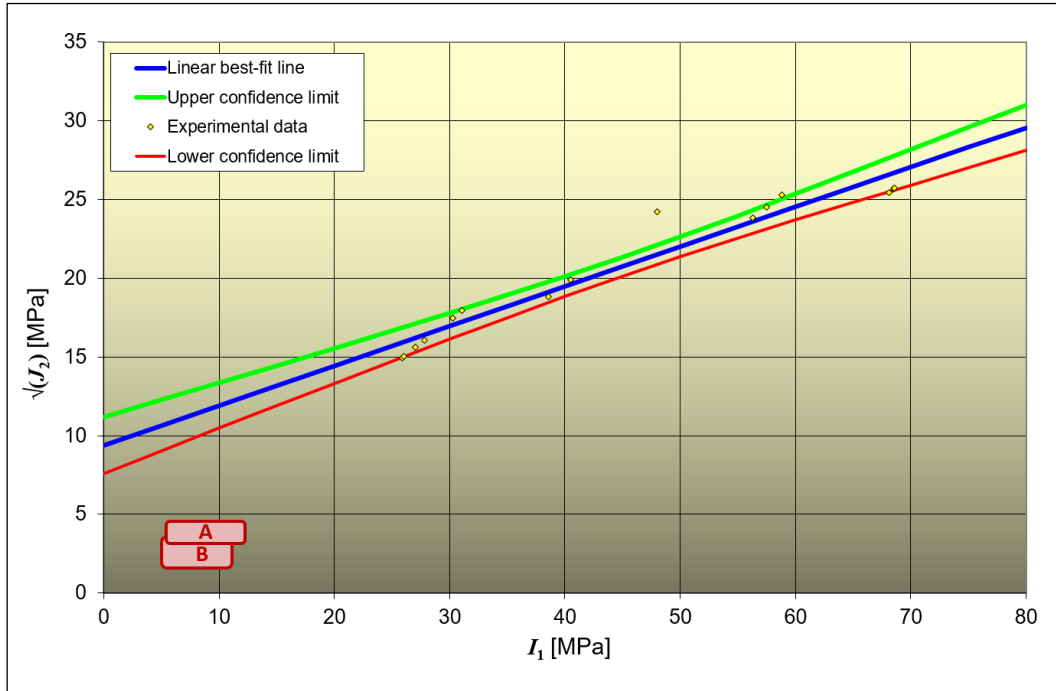


Figure 4-13: Shear strength envelope for Northwich Halite, expressed in terms of $\sqrt{J_2}$ and I_1 .

This showing the clusters of the loci of the effective stress concentrations that develop around the Cheshire representative cavern. Confidence limits were determined according to Snedecor & Cochran (1989)

To investigate the deformation of the Cheshire representative cavern, the contour diagrams of the distribution of the vertical displacements that develop around the cavern are examined. As shown in Figure D5-5 (included in Appendix D.5) at the end of the cavern de-pressurisation, the downward vertical creep closure of the cavern occurs primarily in the cavern roof. The vertical displacements u_y at the roof of the cavern are of the order of 0.06 m, while at the cavern sides the vertical displacements are reduced to 0.01 m. These relatively small displacements which are of the order of millimetres are considered acceptable and have no significance on the long term structural stability of the cavern.

Following the completion of five years of cyclic loading, as shown in Figure D5-10 (included in Appendix D.5), the downward vertical creep closure of the cavern occurs primarily in the cavern roof. The vertical displacements u_y at the roof of the cavern are of the order of 0.08 m, while at the cavern sides the vertical displacements are reduced to 0.02 m. Once more, these vertical displacements are considered acceptable and their effect has no effect on the long term structural stability of the cavern.

Comparison of caverns with sumps developed above and below the ‘Thirty Foot’ Marl

As a result of the particular geological conditions that exist in Cheshire, concerning the presence of the ‘Thirty Foot’ Marl band which is intercalated in the Northwich Halite, in addition to the Cheshire representative cavern, an alternative cavern type has also been considered.

The differences between the Cheshire representative cavern (also referred to as Stublach cavern) and the type of cavern that may be developed in the Holford site (the cavern site adjacent to Stublach site)

are graphically shown in Figure 4-14, where it is shown that the Stublach caverns are developed with their sump located below the ‘Thirty Foot’ Marl, while in Holford there is opportunity to develop the caverns with their sump above the ‘Thirty Foot’ Marl.

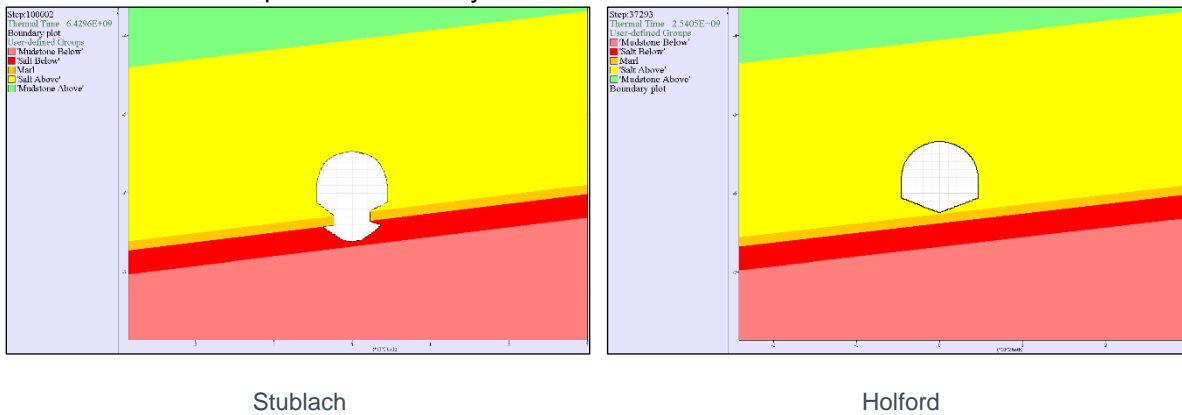


Figure 4-14: Comparison between the Stublach and Holford caverns

To investigate the potential influence of the ‘Thirty Foot’ Marl band on the geomechanical response of the caverns, the two cavern types were subjected to the same pressure (i.e. 6.6 MPa) and temperature (i.e. 10°C = 283.15 K) conditions.

Comparison of the temperature distribution in the immediate vicinity around the caverns, to a distance of approximately 70 m from the cavern periphery, indicates the lack of any significant differences (see Figure 4-15).

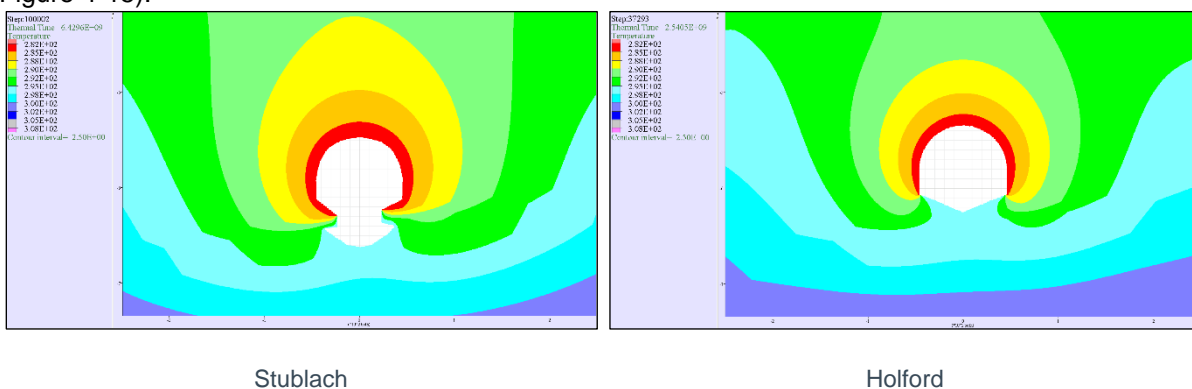
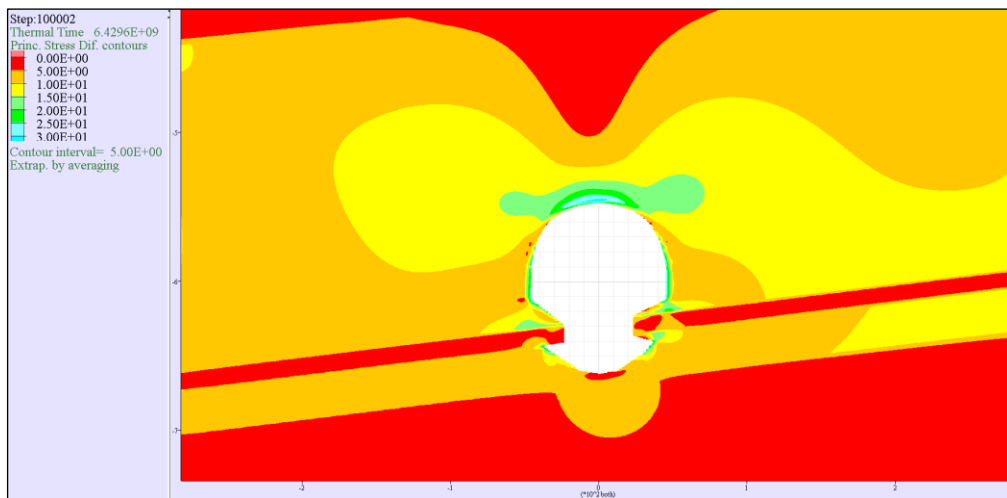


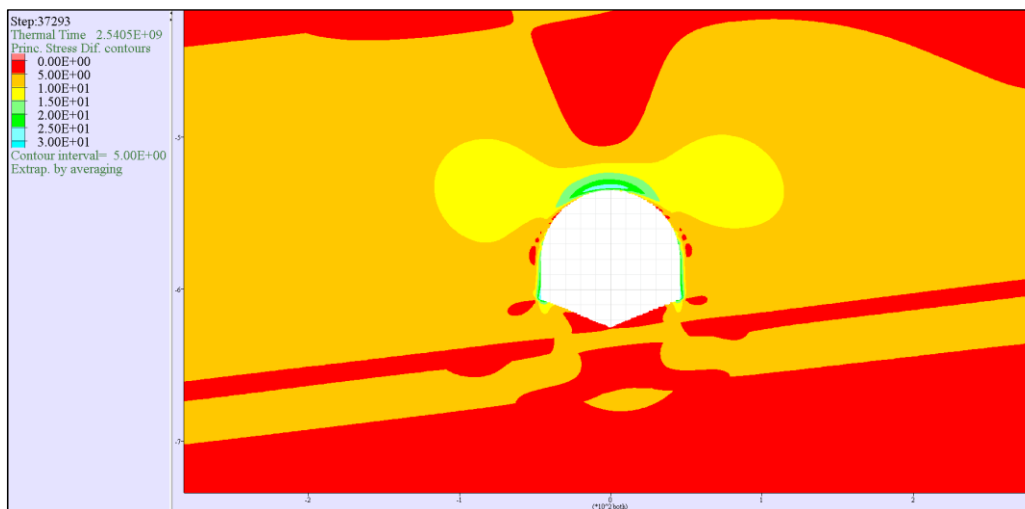
Figure 4-15: Comparison the temperature distribution around the Stublach and Holford caverns

To assess the development of shear stress concentrations at the roof and the walls of the caverns, resulting from the combined effect of thermal and pressure loading, consideration was given to the collective effect of σ_1 and σ_3 by plotting the contours of the stress difference ($\sigma_1 - \sigma_3$) component. As shown in Figure 4-16, although there is a difference in the distribution of the stress concentrations at the sumps of the caverns, the caverns’ walls and roofs which are subjected to the conditions exerted by the stored H₂ mixture, are characterised by similar stress concentrations.

This lack of significant differences in the geomechanical response of the Stublach and Holford caverns is attributed to the mixture of brine and insoluble materials at the cavern sumps, that acts as an effective insulator.



Stublach



Holford

Figure 4-16: Comparison the $(\sigma_1 - \sigma_3)$ distribution around the Stublach and Holford caverns

4.4. Geomechanical analysis of Teesside representative cavern

Technical approach

There are no direct stress measurements available for the *in situ* stress field in the Teesside area and therefore the assessment of the geostatic stress field relied on the review of the regional stress information taking into account the lithology, the thicknesses and depths of the identified geological formations.

The geostatic vertical stress has been estimated based on the superincumbent strata and it is assumed that the horizontal stress is uniform and related to the vertical. Finally taking into consideration the creep behaviour of the Boulby Halite and the depth of the representative cavern (~640 m), the ratio of the horizontal to the vertical geostatic stress is expected to approach unity whereby the *in situ* stress state of the salt is assumed to be isotropic showing no differences in horizontal and vertical directions.

In the geomechanical analysis of the salt cavern, its sump is represented as being occupied by the

stored H₂ mixture. In real terms, the sump collects insoluble materials during the solution mining process and although these insoluble materials will provide some support to the cavern walls, the sump of the cavern is modelled as being devoid of such material. This approximation lends conservatism to the model, although the overall response of the modelled cavern will be little influenced by the approach used to represent the pressure exerted at the walls of the sump.

The thickness of the salt formation and the resulting shape of the caverns at Teesside (i.e. large roof span), coupled with the proximity of the Carnallitic Marl above the cavern roof, requires that the Teesside caverns function as wet storage facilities. Therefore, the caverns at Teesside operate by brine displacement and are subjected continuously to a nearly constant internal pressure that corresponds to the full brine head also known as halmostatic pressure. The normal cavern pressure conditions are consistent with a pressure maintained by the full head of brine characterized by a density of 1.205 Mg/m³. Consequently, the modelling of the cavern's internal pressure was implemented by employing a hydrostatic loading, acting normal to the cavern's boundary, corresponding to a gradient of 0.0118 MPa/m (= 9.81×1.205/1000). Taking into consideration that the depth of the roof of the Teesside representative cavern is 647 m the halmostatic pressure at the cavern roof is estimated to be 7.65 MPa.

To investigate the geomechanical response of the Teesside representative cavern, when the cavern is subjected to the applied halmostatic pressure use was made of the finite element package RS² that has been developed by Rocscience Inc. (Rocscience, 2017).

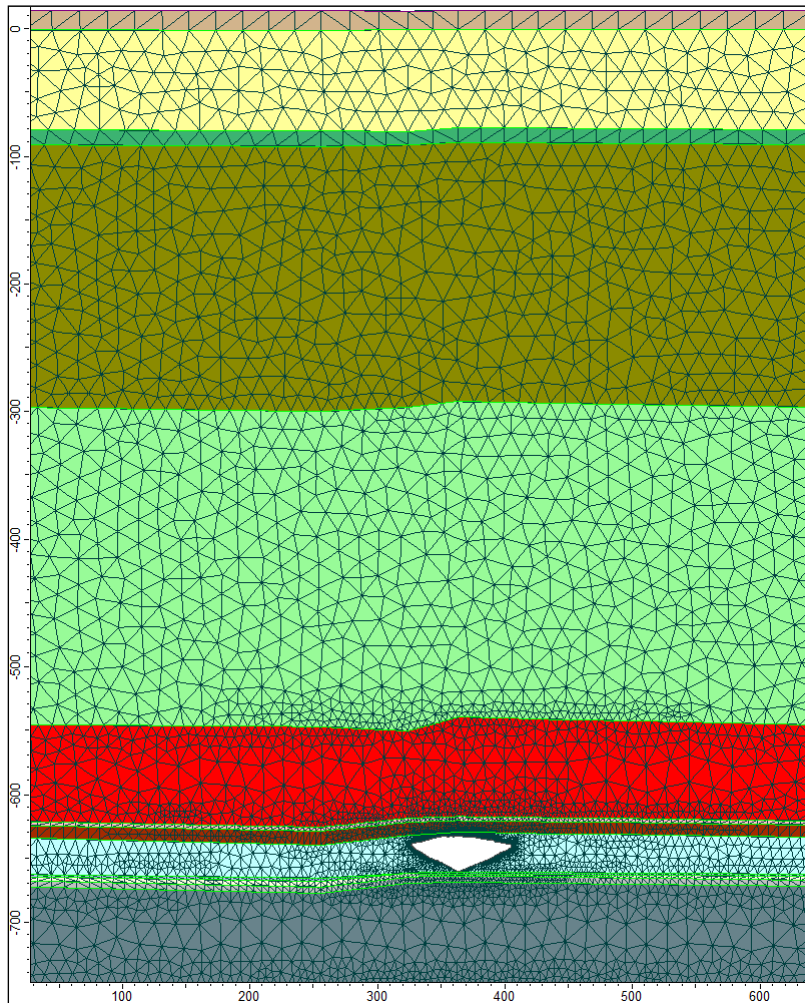


Figure 4-17: Finite element mesh used in the modelling of the Teesside representative cavern

Three components were specified for the system configuration employed in the geomechanical modelling:

- I. The constitutive behaviour, the strength characteristics and physical properties of the geological materials (as shown in Appendix D.13) that influence the structural response of the cavern to the imposed disturbances;
- II. A model grid defining the geometry of the problem (shown in Figure 4-17); and
- III. The boundary and initial conditions corresponding to the *in situ* geomechanical state.

Examination of Figure 4-18 indicates that, in the region immediately surrounding the cavern, the finite element mesh was finely subdivided to improve the accuracy of the analysis near the cavern roof and side walls where high stress gradients were anticipated.

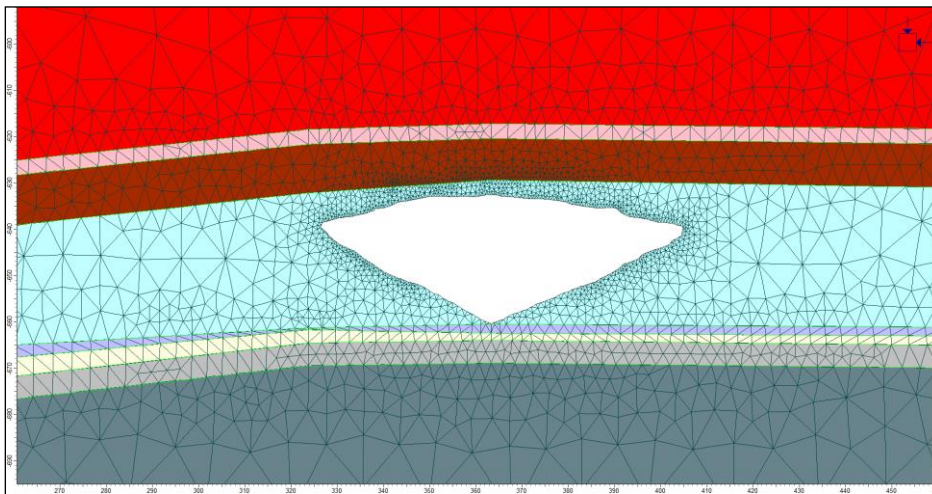


Figure 4-18: Details of the finite element mesh used in the modelling of the Teesside cavern

During the geomechanical analysis the modelled ground was pre-stressed in accordance to the *in situ* geostatic stress field. It is important to take into consideration that, in addition to the horizontal σ_{11} and vertical σ_{22} geostatic stress components, σ_{33} (the component acting normal to the plane-strain grid) was also initialised while using RS², since the employed constitutive models take it into account. If omitted, it would have defaulted to zero, which may have caused failure to occur in the out-of-plane direction.

The upper boundary of the finite element model corresponds to the ground surface, while the bottom boundary of the model was subjected to a vertical fixity (i.e. restricting all the bottom boundary nodes from moving along the vertical direction) that was placed approximately 90 m below the bottom of the cavern sump at a depth of 750 m bgl. In addition, the kinematic boundary conditions along the sides of the finite difference model, specified no horizontal displacement along the two vertical sides of the model while the upper horizontal surface of the model was free to move both in the horizontal and vertical directions.

Results of the geomechanical analysis

The geomechanical stability of the Teesside representative cavern was considered by comparing stress states, predicted by the geomechanical analysis, to criteria developed from the rock mechanics testing of the relevant geological materials. States of stress in the walls and the roof of the cavern were analysed to determine whether the investigated storage pressure could initiate rock failure in the geological formations that surround the cavern.

Therefore, the primary goal of the geomechanical analysis is to investigate, *inter alia*, the potential of:

- tensile failure that may be introduced at the roof and walls of the cavern, and/or
- shear failure of the cavern's walls, including its roof.

Cavern structural stability in this context is defined as the condition that prevents any potential shear and/or tensile failure to develop deeper than approximately 1 m inside the salt mass that surrounds the cavern.

The geomechanical stability of the modelled cavern was assessed by generating contour diagrams for:

- the minor σ_3 and major σ_1 principal stresses;
- the von Mises stress component σ_{vm} ;
- the vertical displacement components u_y , and
- the Strength Factor.

In addition to the stresses and displacements around the cavern, the employed finite element analysis calculates the *Strength Factor* corresponding to the implemented failure criteria for tensile and shear strength. The program starts by checking, in every finite element, whether the minor principal stress σ_3 is less than or equal to the negative stress that corresponds to the tensile strength of the geological material, (i.e. if $\sigma_3 \leq -\sigma_t$). If this is the case, then the *Strength Factor* for that particular element is set equal to -1 indicating that tensile failure has occurred. If on the other hand, $\sigma_3 > -\sigma_t$ then the program investigates the potential shear failure by calculating the *Strength Factor* in the element as shown in Equation 4.3 by dividing the shear strength of the geological material (based on the Mohr-Coulomb failure criterion described in Appendix D.8) by the induced shear stress:

$$\text{Strength Factor} = \frac{\sigma_3 - \sigma_3 N_\phi - 2c\sqrt{N_\phi}}{\sigma_3 - \sigma_1} \quad \text{Equation 4.3}$$

where N_ϕ has been defined by Equation D13 (in Appendix D.8) and c is the material's peak cohesion.

If the *Strength Factor* is greater than 1, it indicates that the material's shear strength is greater than the induced shear stress and as such no shear failure occurs. However, if $0 < \text{Strength Factor} \leq 1$, then it is implied that the shear stress in the material exceeds the material's shear strength signifying that shear failure may occur.

To determine the development of σ_1 , σ_3 , σ_{vm} , u_y and *Strength Factor* the corresponding contour diagrams were produced as derived from the geomechanical modelling of the Teesside representative cavern and are included in Appendix D.6.

Examination of the distribution of the minor principal stress σ_3 in the salt mass that surrounds the modelled cavern indicates the complete absence of any tensile stresses. This provides evidence that the walls of the Teesside representative cavern are everywhere in compression as shown in the minor principal stress σ_3 contours presented in Figure D6-1, where the positive sign of the stress components implies compression.

The distribution of the major principal stress σ_1 around the Teesside representative cavern indicates that most the salt mass that forms the immediate surrounding of the cavern is tolerably compressive. In particular, σ_1 varies from location to location around the cavern between approximately 12 MPa and 90 MPa (as shown in Figure D6-2 included in Appendix D.6).

The likelihood of shear failure, as a consequence of high compressive stresses, cannot be assessed by simply considering the values of the major principal stress σ_1 (i.e. the most compressive stress component). Instead, it is more useful to examine the corresponding von Mises stress and the distribution of the resulting *Strength Factor*. The distribution of the von Mises stress for the investigated cavern is portrayed in the contour diagram of Figure D6-3 in Appendix D.6, where it is evident that the shear stresses are in general relatively low and typically below 45 MPa.

However, at a depth of approximately 640 m bgl, where the cavern's maximum diameter extends; limited areas characterised with a von Mises of the order of 60 MPa which may be prone to potential structural

failure, have been identified. These high stress concentrations develop because the creep response of the salt at Teesside is negligible (the material behaves in a non-linear elasto-plastic manner as specified in Appendix D.13), consequently there is no time-dependant stress relaxation which inevitably results to stress concentrations of the order of 60 MPa. Nevertheless, the extent of these potential structural failures is insignificant and the consequences are expected to have a purely superficial effect that may simply contribute in a slight time-dependent increase of the maximum diameter of the cavern. These restricted areas, where the cavern's maximum diameter extends, are essentially subjected to a so-called skin effect of excessive stress concentrations resulting in *Strength Factor* values less than 1 (see Figure D6-5 in Appendix D.6).

To investigate the deformation of the Teesside representative cavern, the contour diagram of the distribution of the vertical displacements that develop around the cavern are examined. As shown in Figure D6-4 (included in Appendix D.6), the vertical convergence of the cavern occurs primarily in the cavern roof (downwards) and the cavern sump (upwards). The vertical displacements u_y at the roof of the cavern are of the order of 0.04 m, while part of the closure of the cavern is taking place in the sump area of the cavern, where the uplift is of the order of 0.01 m. These relatively small displacements which are of the order of millimetres are considered acceptable and have no significance on the long term structural stability of the cavern.

4.5. Conclusions

During the geomechanical analysis of the East Yorkshire, Cheshire and Teesside representative caverns the salt caverns were subjected to the specified operating conditions required to meet the power production demands. The deliverability of cavern/GT systems in meeting diurnal power demand profiles was based on the worst possible case resulting from the power generation Scenario 3 which led to the specific flowrates that were used to model the cyclic operation of the caverns.

As part of the geomechanical analysis of the investigated representative caverns a thermodynamic analysis was carried out only for the East Yorkshire and the Cheshire sites where the salt caverns are functioning by employing dry storage operations. In contrast, there was no need to consider the thermodynamic response of the Teesside representative cavern since in Teesside the caverns are functioning by employing wet storage operations.

East Yorkshire and Cheshire representative caverns

The salt around the cavern is cooled during leaching, consequently, the cavern gas temperature gradually warms with time during thermodynamic simulation.

As a result of this gradual warming of the cavern, the pressure in the cavern will gradually increase with time, even when a perfect mass balanced approach is adopted whereby in each cycle the injected gaseous mass is fully withdrawn before the next cycle commences. To avoid building up the pressure to an unacceptable level, i.e. higher than the maximum permissible pressure at the last cemented casing shoe, a short time interval of injection was skipped over a period of approximately 6 months. In following this approach, the investigated caverns are depressurised to approximately to the middle of the range defined by the maximum and minimum allowable pressure.

The thermodynamic analysis of the East Yorkshire and Cheshire representative caverns was carried out by employing the fuel gas stream 1 molecular composition and its respective flow rate. This option was pursued after it was ascertained that fuel gas stream 1, in comparison with fuel gas stream 2, results in a more "aggressive" cyclic loading primarily because of its higher flow rates (the flow rates for fuel gas stream 1 are approximately 1.45 times higher than the corresponding rates for fuel gas stream 2).

During the thermodynamic analysis of the East Yorkshire representative cavern the applied cyclic pressure loading over a period of five years resulted in cyclic temperature steps of the order of 2°C. Extrapolation of the temperature and pressure histories, over a period of 30 years, has shown that both

the cavern temperature and the cavern pressure are considered to be acceptable. In particular, the cavern temperature for the East Yorkshire representative cavern reaches asymptotically 53.5°C (noting that the geothermal temperature at cavern is approximately 56°C), while the cavern pressure follows a similar trend reaching asymptotically 22.4 MPa g (well below the maximum allowable pressure of 27.1 MPa g).

During the thermodynamic analysis of the Cheshire representative cavern the applied cyclic pressure loading over a period of five years resulted in cyclic temperature steps of the order of 4°C. Extrapolation of the temperature and pressure histories, over a period of 30 years, has shown that both the cavern temperature and the cavern pressure are considered to be acceptable. In particular, the cavern temperature for the Cheshire representative cavern reaches asymptotically 24.1°C (noting that the geothermal temperature at cavern is approximately 25.2°C), while the cavern pressure follows a similar trend reaching asymptotically 6.6 MPa g (well below the maximum allowable pressure of 9.5 MPa g).

The coupled thermo-mechanical numerical analysis of the East Yorkshire and Cheshire representative caverns was undertaken by carrying out a finite difference creep analysis using isotropic boundary conditions. The employed cyclic temperature and pressure storage operating conditions were derived from the undertaken respective thermodynamic analyses. The modelling incorporated, in the first instance, the early temperature and pressure history of the caverns, which included the solution mining and the de-brining of the caverns and eventually the cavern boundary conditions derived from the investigated storage operating conditions.

Examination of the distribution of the minor principal stress σ_3 , above the roof of the East Yorkshire and Cheshire representative caverns indicates that σ_3 is always compressive and as such no tensile stresses may develop. Consequently, the possibility of developing conditions that may lead to tensile failure in the roof of the caverns is highly unlikely.

Moreover, the lack of any positive values (i.e. implying tension) in the distribution of the minor principal stresses, in the salt mass that surrounds the investigated caverns, indicates the complete absence of any tensile stresses. Assessment of the shear stress concentrations that develop around the East Yorkshire and Cheshire representative caverns, indicates that the calculated stress concentrations at the roof and the walls of the caverns were relatively low in comparison with the shear strength of the salt formation that surrounds the caverns. In evaluating the cavern creep convergence results, the identified vertical displacements at the roof of the caverns were considered acceptable and essentially their effect has no effect on the long term structural stability of the East Yorkshire and Cheshire representative caverns.

Teesside representative cavern

The Teesside representative cavern functions as a wet storage facility and operates by brine displacement; therefore, the cavern is subjected continuously to a nearly constant internal pressure equal to the halmostatic pressure that corresponds to the full brine head.

Examination of the distribution of the minor principal stress σ_3 , above the roof of the Teesside representative cavern indicated that since the storage pressure in the cavern is maintained equal to the corresponding hydrostatic full brine head, σ_3 is compressive and as such no tensile stresses may develop as a consequence of the current structural conditions of the caverns.

Assessment of the distribution of the von Mises stress and the *Strength Factor*, that develop around the Teesside representative cavern, indicates that no significant shear stresses arise in the geological materials that surround the investigated cavern. However, at the depth where the cavern's maximum diameter extends; limited areas with high stress concentrations may be prone to potential structural failure. Nevertheless, the extent of these potential structural failures is insignificant and the consequences are expected to have a purely superficial effect that may simply contribute in a slight time-dependent increase of the maximum diameter of the cavern.

ATKINS

Chapter 5: Economic viability



5. Economic viability

In Chapters 1 to 4 a technologically feasible solution has been identified. Throughout the duration of this study all aspects from cavern, wells and surface plant to GTs were explored in depth to allow an assessment of current technology to provide a low carbon energy source for the future. Having established the technical feasibility, the following chapter outlines the economic characteristics and considerations for such a solution. This includes:

- I. CAPEX costs - long-term investment costs in permanent assets.
- II. OPEX costs - continuous costs for operating and maintaining assets.
- III. Permitting and Legislation - constraints on local area which would impact development.

For simplicity, the estimates have been sub-divided into the three key areas; caverns and wells, surface processing plant and GT. In addition, the following assumptions have been used to develop the estimates where these are valid for all three locations. Specific assumptions, relevant only to the area considered, are identified in the preceding sections.

General assumptions:

1. The level of definition of the H₂ storage facility is at an early conceptual level therefore costs presented are to an order of magnitude only, with an accuracy commensurate with an ACE5 level (-50% to +100%).
2. The scope of study encompasses the wells completion, solution mined cavern & surface processing plant (as shown in Figure 3-9). The CAPEX estimates therefore do not include the H₂ production plant or associated requirement for compression, heat exchange.
3. The presented CAPEX costs relate to the following scope:
 - a. The creation of salt cavern stores through drilling of wells into the salt layer and leaching of a void including supporting process equipment such as brine pipework, pumps etc.
 - b. The construction of a surface processing plant and GT arrangement to produce 1 GWe of electricity from a H₂ production plant on site.
 - c. It does not include the development of the H₂ production plant or associated process.
4. Land purchasing costs have not been included.
5. Costs for permitting and approvals have not been included.
6. Costs are based on 2017 prices, inflation has not been factored for a future case unless stated.
7. The presented OPEX costs do not include fuel costs (e.g. natural gas, electricity). These are variable depending on price of fuel at time of use and are therefore excluded for simplicity. It is not within this scope or works to undertake a full economic simulation of the H₂ storage facility.
 - a. It has been assumed that new facility would have a 30-year design life.
 - b. The new facility would have a fixed staff cost of approximately 70 personnel with an average salary of £30k.
8. Contingency costs have not been included. Risks such as adverse weather, adverse ground conditions and non-productive time could lead to delay and increased costs however these are not considered relevant for this level of estimate.
9. Decommissioning costs are generally excluded from the CAPEX and OPEX estimate. However, in the case of the wells and caverns, it is considered essential that decommissioning costs are accounted for due to the potential impact this could have on the site owners / developers.
 - a. Decommissioning of solution mined caverns is subject to regulatory requirements where it is necessary to ensure that the cavern is abandoned safely, preventing any potential for H₂ return to surface (typically accomplished by filling the cavern with brine

and setting cement plugs in the well). The liability of any future failure of the abandonment remains in perpetuity.

- b. Prior to final abandonment (i.e. cement plugging) it is necessary to allow the cavern time to equalise pressure (where temperature of brine equalises with formation) where these times can extend from 3 years to potentially 25 years depending on cavern depth (formation temperature varies with depth) and temperature of rewatering fluid.

5.1. Caverns and wells

For each site, and fuel gas stream, CAPEX and OPEX have been estimated. In total, there are two different fuel gas streams and three different locations as set out in Chapter 1. This results in four different well configurations, due to the cavern and well requirements for fuel gas streams 1 and 2 being the same at East Yorkshire and Cheshire. Tables 5-1, 5-2, 5-3 and 5-4 provide details of the cost models for these four configurations considering the assumptions below:

General assumptions:

1. Solution mining times for each site have been estimated using data from previously developed caverns within the areas.
2. Solution mining pump requirements based on notional ~100 m³/hr at 50 barg (minimum of 115kW).
3. L-80 grade steel casing and tubing used.
4. MIT assumed as a 20-day operation.
5. OPEX assumes:
 - a. annual wellhead maintenance,
 - b. 5 yearly sonar surveys of caverns,
 - c. 10 yearly calliper surveys of the wells
6. Decommissioning costs assume pumps and brine lines still intact from construction to fill caverns and cost to decommission reservoirs at Teesside are negligible. Furthermore, the decommissioning costs assume:
 - a. 3 years at Teesside for cavern equalisation prior to well abandonment.
 - b. 10 years at Cheshire for cavern equalisation prior to well abandonment.
 - c. 25 years at East Yorkshire for cavern equalisation prior to well abandonment.
 - d. OPEX during cavern equalisation prior to abandonment assumed to be 50% of normal OPEX.

It is noted that the liability of decommissioning cost may not be directly realised by the operator however this is dependent on specific site arrangements and requires further discussion and refinement with all stakeholders including regulator. Costs presented are considered full life costs independent of ownership.

The model includes the following costs:

1. Assumes £100,000 per well cost for helium during the MIT, which is necessary for this integrity test to detect any leak through the casing shoe.
2. The construction costs include the groundworks required for well pad and surface pumping equipment.
3. The drilling cost includes 8 days' mobilisation / demobilisation time.

The model excludes the following costs:

1. No costs for seismic surveys to select a geological location have been included.

Cost modelling

The cost models for wells and caverns have been calculated using known tangible, rental and equipment costs based on experience of these construction operations. The timings for the operations have been calculated based on historical data and experience at site. The knowledge of timings, rental and personnel costs allows a good estimate of overall project costs to be built up.

East Yorkshire

Following the modelling work undertaken for GTs, surface plant, caverns and wells, as set out in Chapters 2, 3 & 4, the storage and well requirements for East Yorkshire were determined to be one cavern with two wells for both fuel gas stream 1 and 2. The CAPEX and OPEX for this arrangement are detailed in Table 5-1 below.

Table 5-1: Cost estimate for East Yorkshire site for fuel gas streams 1 or 2

Costs - East Yorkshire Site - Stream 1 & Stream 2 (1 Cavern 2 Wells)					
SEQUENCE	PHASE	Estimated times per well / cavern	Quantity	Cost (£) per well / cavern	Totals
1	Drill wells to ±1,800m	30 days	2	£3,750,000	£7,500,000
2	Leach ±275,000m ³ Cavern	1500 days	1	£5,750,000	£5,750,000
3	MIT's, Run completions & 1st Gas fills	45 days	2	£2,000,000	£4,000,000
4	30 year OPEX Costs	30 years	1	£9,300,000	£9,300,000
5	Decommissioning Costs	30 years	1	£8,150,000	£8,150,000
Total Cost (Per Cavern) :					£34,700,000

Cheshire

Following the modelling work undertaken for GTs, surface plant, caverns and wells, as set out in Chapters 2, 3 & 4, the storage and well requirements for Cheshire were determined to be one cavern with two wells for both fuel gas stream 1 and 2. The CAPEX and OPEX for this arrangement are detailed in Table 5-2 below.

Table 5-2: Cost estimate for Cheshire site for fuel gas streams 1 or 2

Costs - Cheshire Site - Stream 1 & Stream 2 (1 Cavern 2 Wells)					
SEQUENCE	PHASE	Estimated times per well / cavern	Quantity	Cost (£) per well / cavern	Totals
1	Drill wells to ±625m	24 days	2	£2,000,000	£4,000,000
2	Leach ±300,000m ³ Cavern	1650 days	1	£6,000,000	£6,000,000
3	MIT's, Run completions & 1st Gas fills	40days	2	£1,500,000	£3,000,000
4	30 year OPEX Costs	30 years	1	£8,400,000	£8,400,000
5	Decommissioning Costs	10 years	1	£3,900,000	£3,900,000
Total Cost (Per Cavern) :					£25,300,000

Teesside

Following the modelling work undertaken for GTs, surface plant, caverns and wells, as set out in Chapters 2,3 & 4, the storage and well requirements for Teesside were determined to be three caverns with six wells for fuel gas stream 1 and two caverns with four wells for fuel stream 2. The CAPEX and OPEX for these arrangements are detailed in Table 5-3 and Table 5-4 below.

Table 5-3: Cost estimate for fuel gas stream 1 at Teesside

Costs - Wilton Site - Stream 1 (3 Cavern 6 Wells)					
SEQUENCE	PHASE	Estimated times per well / cavern	Quantity	Cost (£) per well / cavern	Totals
1	Drill wells to ±650m	24 days	6	£2,000,000	£12,000,000
2	Leach ±50,000m ³ Caverns	425 days	3	£3,250,000	£9,750,000
3	MIT's, Run completions & 1st Gas fills	40 days	6	£1,500,000	£9,000,000
4	30 year OPEX Costs	30 years	1	£18,600,000	£18,600,000
5	Decommissioning Costs	3 years	1	£8,430,000	£8,430,000
Total Cost :					£57,780,000

Table 5-4: Cost estimate for fuel gas stream 2 at Teesside

Costs - Wilton Site - Stream 2 (2 Cavern 4 Wells)					
SEQUENCE	PHASE	Estimated times per well / cavern	Quantity	Cost (£) per well / cavern	Totals
1	Drill wells to ±650m	24 days	4	£2,000,000	£8,000,000
2	Leach ±50,000m ³ Caverns	425 days	2	£3,500,000	£7,000,000
3	MIT's, Run completions & 1st Gas fills	40 days	4	£1,500,000	£6,000,000
4	30 year OPEX Costs	30 years	1	£15,600,000	£15,600,000
5	Decommissioning Costs	3 years	1	£5,780,000	£5,780,000
Total Cost:					£42,380,000

5.2. Surface processing plant

The surface processing plant is the conduit for the fuel gas streams from the H₂ production plant and the cavern and will condition the fuel gas stream going into the GTs. The processing plant is described in Chapter 3, detailing the different parts of the system and their functions.

General assumptions:

1. Surface plant costs have been derived from previous works undertaken for the ETI (AmecFw, 2012).
2. Cost of H₂ supply and associated facility is out with the scope of this work. It is assumed fuel gas stream 1 or 2 are provided at a pressure of 32.4 barg ready for injection.

The cost model includes the following costs based on details from (AmecFw, 2012):

1. Major equipment inclusive of costs up to delivery to site.
2. Direct bulk materials including piping, electrical, catalyst and chemicals, spares and shipping costs.
3. Direct material & labour contracts including civil, steelwork, building and protective cover.
4. Labour only contracts including mechanical, electrical, instrumentation, pre-commissioning trade labour support and scaffolding labour costs.
5. Indirect costs including temporary facilities, heavy lifts, commissioning services and vendors engineering.
6. EPC contracts including engineering, procurement and construction management.

The cost model excludes the following costs:

1. Decommissioning costs.

Cost modelling

CAPEX

As stated above, the CAPEX of the surface processing plant is based on the costs presented in the previous ETI work (AmecFw, 2012). Some aspects of these have been factored to account for variances in the operating concepts. Table 5-5 presents the baseline costs used in this assessment where specific considerations are:

1. Two potential storage options were considered in the previous works, 1) multiple cavern storage where each cavern stores pure components (e.g. 1 x H₂ cavern and 1 x N₂ cavern if N₂ mix considered) and these are then mixed after storage, 2) single cavern filled with premixed source. In this case it is assumed that the single source cavern cost is the most applicable option where it is not proposed to develop additional caverns for mix fuel gas streams.
2. Cost associated with Teesside have been factored to account for differences between the wet storage method discussed in this report and dry storage presented in the previous works.
3. Only the surface plant costs have been taken from the previous works. It is acknowledged that costs were also developed for cavern development and CCGT however these are superseded by works undertaken as part of this report.
4. The previous works specified expansion turbines for the Cheshire and East Yorkshire regions however did not include this function at the Teesside region. As stated in Section 3 it is considered feasible that an expansion turbine could be used however this will be subject to review at the next phase of development and therefore cost for an expansion turbine at the Teesside location has not been included.
5. It is assumed the facility would have a maximum 10km pipeline for transport of fluid/gas from H₂ plant to cavern and cavern to GT location.

Table 5-5: Surface plant cost estimates for East Yorkshire, Cheshire and Teesside

Case ref (Amec, 2012)	Description	Teesside	Cheshire	Yorkshire
		45barg	105barg	270barg
single cavern facility (case 3)	Above ground facility in syngas unit (compressor)	£ 34,917,400	£ 61,433,400	£ 94,327,800
	Above ground facility in salt cavern site	£ 9,431,800	£ 9,431,800	£ 10,087,000
	Pipeline 10km	£ 17,234,000	£ 11,354,000	£ 13,664,000
	Brine facility factor (50%) (Wet Storage only)	£ 17,458,700	N/A	N/A
Sub Total		£ 79,041,900	£ 82,219,200	£ 118,078,800
Outlet facility (case 4)	Above ground facility in salt cavern site	£ 57,160,600	£ 65,716,000	£ 76,811,000
	Above found facility in power island (expansion turbine)	£ -	£ 22,951,600	£ 79,713,200
	Pipeline 10km	£ 17,234,000	£ 11,354,000	£ 13,664,000
Sub Total		£ 74,394,600	£ 100,021,600	£ 170,188,200
TOTAL		£ 153,436,500	£ 182,240,800	£ 288,267,000

Notes

- 1) Costs from *Hydrogen Storage and Flexible Turbine Systems WP2 - Hydrogen Storage (Amex Foster Wheeler - ETI)*.
- 2) * assume no turbo expander at Teesside subject to review at next phase.
- 3) Brine facility assumes requirement to develop new brine reservoir, brine pumps and pipeline

OPEX

Although annualised OPEX costs were developed in (AmecFw, 2012), these are not considered to be appropriate for this report where they were combined costs for differing numbers of caverns, wells and GT. It is however noted that the surface plant OPEX estimates were typically based on a factor of the capital cost, as shown below:

- 2.5% of the installed capital cost for gaseous and liquid handling units
- 10% of the major equipment cost for utilities and offsites

In this instance, it is assumed acceptable to adopt the lesser factor of 2.5% to develop OPEX cost for the specific surface plant capital costs presented in Table 5-5 where they will be combined with the other OPEX estimates for the cavern, wells and GT. The OPEX estimates are therefore presented in Table 5-6.

Table 5-6: Surface plant cost estimates for East Yorkshire, Cheshire and Teesside

Description	Teesside	Cheshire	Yorkshire
	45barg	105barg	270barg
Cavern Facility CAPEX	£ 79,041,900	£ 82,219,200	£ 118,078,800
Outlet Facility CAPEX	£ 74,394,600	£ 100,021,600	£ 170,188,200
OPEX Factor 2.50%	£ 3,835,913	£ 4,556,020	£ 7,206,675
Annual OPEX Cost	£ 3,835,913	£ 4,556,020	£ 7,206,675

5.3. Gas Turbine

The costing for the GTs compares the CAPEX and OPEX of the preferred CCGT technologies which have been identified for the fuel gas stream 1 and 2.

General assumptions:

1. Although the surface process plant may vary at each site, the GT arrangement and plant layout is identical at each of the three locations.
2. Discussions with OEMs indicated that there would be few changes to the overall design of the GT itself due to H₂ operation, with the exception that the burners and combustion can would differ significantly to fire the H₂ rich fuel gas streams. It is predicted that this will lead to increased CAPEX and a contingency of up to 10% of the GT plant costs, which has been included in the cost modelling.
3. The grid interconnection substation is assumed to be of GIS design.
4. OPEX service costs estimates are based on “E” class case study examples.
5. Equivalent operating hours are based on hours generating annually from Scenario 3.
6. There is assumed to be no gasifier outage in the first 3 years, but required thereafter due to H₂ production source being fuel gas stream 1.
7. Forced outage rate assumed at 3 days per year, but 10 days in the 1st year of operation to reflect plant shakedown (initial defects etc.).
8. Gasifier maintenance costs have been included.
9. A midlife major overall cost of ~£19m has been included per unit, includes cost of rotor assumed at approx. ~£11m.
10. Assume hot gas path inspection required after 1200 starts per unit and major overhaul after 2400 starts per unit.

The cost model includes the following costs:

1. Fixed costs for the grid interconnection substation, insurance requirements and staff.
2. Owner’s costs for development and project management.
3. Civil and structural engineering and construction costs for all buildings.
4. Installation of the connection facilities to the national gas grid:
 - a. Pressure reduction terminal (PRT).
 - b. Fiscal / tariff metering facilities for supply of natural gas to the surface and GT plant required for both start-up and flame stabilisation.
5. Construction costs have been included and cover the groundworks required.
6. Cost includes mobilisation / demobilisation time.

7. Development costs included for project mobilisation, e.g. environmental assessments and planning applications.

The cost model excludes the following costs:

1. Additional CAPEX necessary if stack heights need to be raised to meet ground level air quality standards.
2. Decommissioning costs.

Cost modelling

CAPEX

The CAPEX for the main CCGT plants under consideration are presented in Table 5-7 and in all cases the CAPEX relates to the target capacity of approx. 1 GWe. Table 5-7 includes the “E” class heavy duty utility power generation technologies based on GE 9E, Siemens SGT5-2000E and GE 13E2 as well as the smaller industrial Siemens SGT-800 GTs, which have a proven operating history with H₂ rich fuel gas streams. As a comparison, the more advanced SGT5-4000F GTs CAPEX is also included.

Any variations in grid connection costs relate to the need for a GIS breaker for each generator, which escalates the costs for the smaller industrial machines requiring a substation equipped with more breakers for each of the GTs.

Due to the inherent efficiency savings and economies of scale the lowest CAPEX is associated with the larger frame GTs benchmarks 2, 3 & 5 (see Table 5-7, which in combined cycle can generate at efficiencies of 55% in the case of the SGT5-2000E and the GE-13E2 and 59% for the SGT5-4000F (note, output relates to performance with natural gas).

The “E” class CCGT development options GE9E, 13E2 and SGT5-2000E are configured as two blocks of 2+1, which provides excellent peak demand matching ability of four GTs in combined cycle whilst allowing part load operation without significant falloff in efficiency.

For optimum power plant flexibility, the option of exhaust gas bypass stacks for each GT should be considered allowing operation in combined and open cycle and providing an option for fast starting as well as conventional start-up. However, the CAPEX of the blast stack and damper is circa. £5-6m for the “E” class technology and up to £8m for the advanced class GTs.

Table 5-7: GT plant Cost estimate for fuel stream 2 (excludes 10% increase due to high H₂)

	Benchmark 1		Benchmark 2		Benchmark 3		Benchmark 4		Benchmark 5	
GT Power Equipment	General Electric 9E, 2 x 2+1		Siemens, SGT5 - 2000E 2 x 2+1		General Electric 13E2 2 x 2+1		Siemens, SGT - 800: 2 x 6+1 / 4 x 3+1		Siemens, SGT5 - 4000F: 2+1 [with natural gas]	
Output MWe @ ISO site Conditions 15 degC & 60 RH	900		1050		1110		900		950	
	£M	percentage	£M	percentage	£M	percentage	£M	percentage	£M	percentage
CIVIL	58£M	10.3%	61£M	10.1%	65£M	10.2%	72£M	10.4%	53£M	9.9%
MECHANICAL	258£M	45.3%	276£M	45.4%	290£M	45.7%	312£M	44.6%	239£M	44.8%
ELECTRICAL & C&I	75£M	13.3%	86£M	14.1%	86£M	13.6%	97£M	13.8%	66£M	12.4%
FUEL	6£M	1.0%	7£M	1.1%	7£M	1.1%	6£M	0.8%	7£M	1.3%
Hydrogen Fuel Receiving Skids	1£M	0.2%	1£M	0.2%	1£M	0.2%	1£M	0.1%	1£M	0.2%
ELECTRICAL GRID CONNECTION FACILITIES	22£M	3.8%	22£M	3.6%	24£M	3.8%	32£M	4.6%	18£M	3.5%
ENGINEERING CONSTRUCTION & COMMISSIONING	46£M	8.0%	48£M	7.8%	51£M	8.1%	65£M	9.3%	46£M	8.7%
PROJECT MANAGEMENT	20£M	3.5%	20£M	3.4%	21£M	3.2%	24£M	3.4%	20£M	3.8%
TRANSPORT FREIGHT	11£M	1.9%	12£M	2.0%	13£M	2.0%	11£M	1.6%	11£M	2.0%
MISCELLANEOUS, Insurance, Bonds, Taxes etc.	17£M	2.9%	19£M	3.1%	21£M	3.3%	24£M	3.4%	16£M	3.0%
Owners Costs	56£M	9.9%	56£M	9.2%	56£M	8.9%	56£M	8.0%	56£M	10.5%
TOTAL	569£M	100.0%	609£M	100.00%	633£M	100.00%	699£M	100.00%	532£M	100.00%
£/KW	632.03		579.56		570.52		776.60		560.11	

*The benchmarks 1,2,3 & 5 were derived from past project experience and cross checked against GT PRO, PEACE output. An average of these benchmarks costs was used as the basis for the "E" class CCGT CAPEX. Benchmark 4 was derived from CAPEX data provided by Siemens for the SGT-800.

Table 5-8: Cost estimate, sector package details

Sector	Includes:
CIVIL	Structure GTG, Buildings STG, Structure HRSG, General Buildings, Control Building, Warehousing, Administration, Piling, Ground Reinforcements
MECHANICAL	Mechanical Power Island incl. : Gas Turbines GTGs, Steam Turbines STGs, Waste Heat Recovery Blr 1 Press, DCS Control System, Inlet Air Cooling System, Intake, Filters & Stacks, Mechanical BOP Packages incl. : Make-up, Service & Potable Water , HVAC, Compressed Air, Fire Fighting Packages inc Fire Tenders ambulance etc. Mechanical Equipment & Material incl. : Air Cooled Condenser, Closed Circuit Cooling System, Lifting Equipment
ELECTRICAL & C&I	Generator to Grid Interconnection, Plant Auxiliary Supply, Plant Emergency Supply, Instrumentation & Control Equip
FUEL	Natural Gas Receiving PRT Includes: Pressure Reducing Station, Separator, Metering & Settlement System, Chromatograph, Shut Off Valves
Hydrogen Fuel Receiving Skids	Pressure Reducing Station, Separator, Metering & Settlement System, Shut Off Valves
ELECTRICAL GRID CONNECTION FACILITIES	Construction of Electrical Special Facilities: 400kV GIS Substation, Civils cable trenches, building, 400kV Cabling 6 Circuits 0.4km, 400kV Cabling 14 Circuits 0.4km
ENGINEERING CONSTRUCTION & COMMISSIONING	Includes: Engineering, Construction, Commissioning
PROJECT MANAGEMENT	Project Management incl. : Project Planning, Procurement, Construction supervision, Site HSE, Infrastructure, Services, Commissioning Supervision

OPEX

Maintenance costs and GT availability are of great significance to the operation of a power plant, particularly in this case as a secondary process of CCS in the continuous production of H₂.

The OPEX of the surface processing plant has been determined at £31m (average) per annum and is based on annual visual inspections and periodic in-depth tests in line with the GT operation and maintenance regime. A summary of the inspections and tests which have been considered for this project, and underpin the averaged figure of £31m, are presented in Appendix E⁴ and summarised graphically in Figure 5-1 below. The slow ramp up in costs is due to no gasifier outages in first 3 years, and staggered unit commissioning. The midlife peak is due to major overhaul costs included half way through the design life.

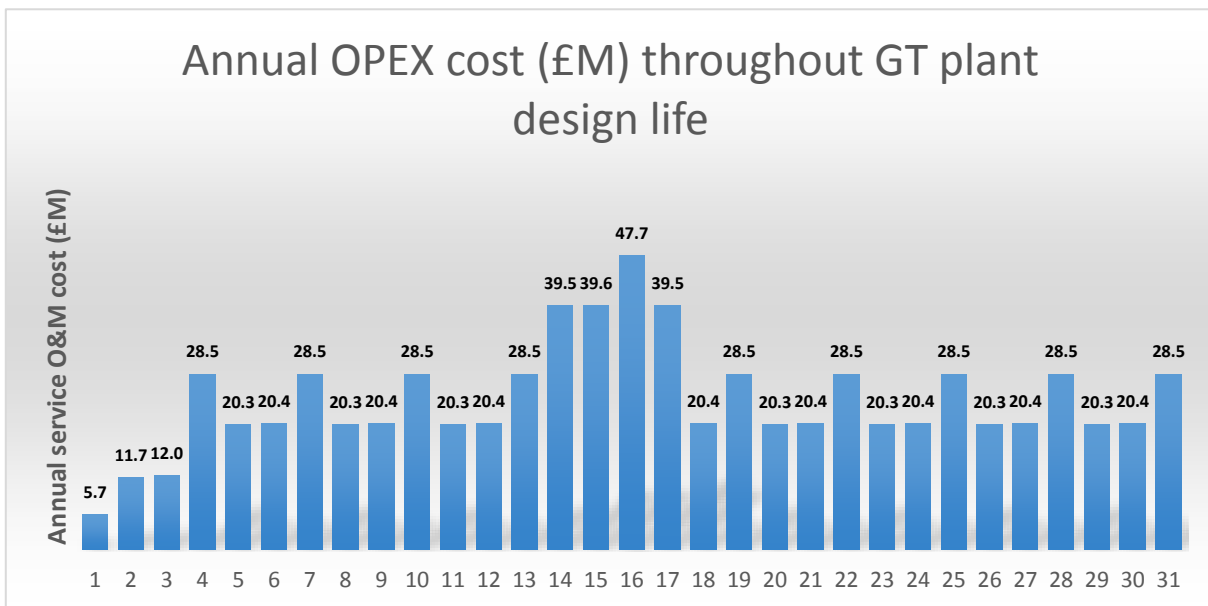


Figure 5-1: Annual Opex cost through GT Plant Design Life

The majority of advanced GT projects based on “F” or “H” class technology is tied to Long Term Service Agreements (LTSA) and the OEM takes on the management responsibility for oversight and recommendations during inspections and major outages. Many components are assigned an operational life based on factored or equivalent operating hours and the OEM requires the replacement or refurbishment of these once the factored hours are met.

Many of the older “E” class technology GTs utilise components such as the HGP and blading which can be fully re-furbished. This typically involves NDT inspection for cracking, repair and reprofiling and recoating of blade sets. “E” class GT blading can on average be refurbished up to three times. However, the “F”, “G” and “H” class GTs utilise single crystal blades for 1st and 2nd stage buckets and it is not possible to refurbish these components. The impact of this is a significant increase (typically 50%) in O&M costs for “F” and “H” class technology compared to “E” class GTs. This however is not an inhibitive overall cost increase when taking the savings in natural gas consumed as a result of the increased efficiency of the more advanced GT (between 5 to 7%) into account. However, for H₂ combustion in “F” or “H” class GTs the technical data and review findings indicate that the performance of the GT is generally de-rated due to the H₂ / N₂ fuel gas streams and lower TITs than for natural gas.

The presence of trace syngas impurities, water for NO_x control and highly reactive H₂ means that

⁴ with conversion of \$ to £ at 0.77, July 2017

although there may be a marginal impact on coating life this is offset by the slightly lower TIT. Technical discussions with the GT OEMs indicated that it was not expected that H₂ rich fuel gas streams or syngas fuels would have a material impact on the frequency or the costs of inspections. The OEMs however noted that the LTSAs for such projects would be agreed on a case by case basis and be highly dependent on the mode of operation as well as the primary fuels to be used.

5.4. Overall project costs

The overall project costs are dependent on the chosen location for the plant, which is driven by multiple factors discussed throughout this report, as well as the GT technology chosen. The below figures give an overview of the theoretical CAPEX when matching up small and larger frame GTs with the cavern stores at each location. The following cost cases are depicted in Figure 5-2 to Figure 5-4 below where the cost is presented in both a combined cost and also £/kW to allow direct comparison between GT selection. In addition, Figure 5-6 presents the anticipated OPEX cost for operating a H₂ facility at each of the locations.

- 1) Case 1a:
 - a) Fuel: Fuel gas stream 2
 - b) Location: East Yorkshire
 - c) GT option: Representative “E” class machine
- 2) Case 1b:
 - a) Fuel: Fuel gas stream 1
 - b) Location: East Yorkshire
 - c) GT option: Siemens SGT-800
- 3) Case 2a:
 - a) Fuel: Fuel gas stream 2
 - b) Location: Cheshire
 - c) GT option: Representative “E” class machine
- 4) Case 2b:
 - a) Fuel: Fuel gas stream 1
 - b) Location: Cheshire
 - c) GT option: Siemens SGT-800
- 5) Case 3a:
 - a) Fuel: Fuel gas stream 2
 - b) Location: Teesside
 - c) GT option: Representative “E” class machine
- 6) Case 3b:
 - a) Fuel: Fuel gas stream 1
 - b) Location: Teesside
 - c) GT option: Siemens SGT-800

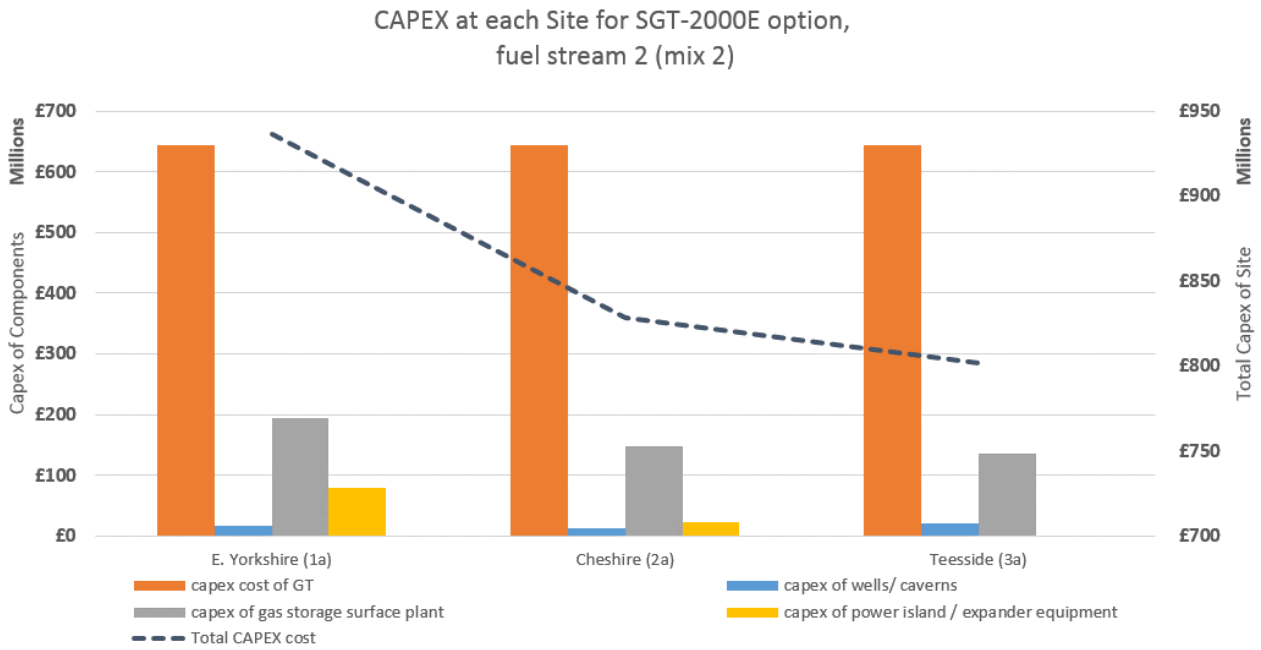


Figure 5-2: CAPEX for SGT-2000E, fuel gas stream 2

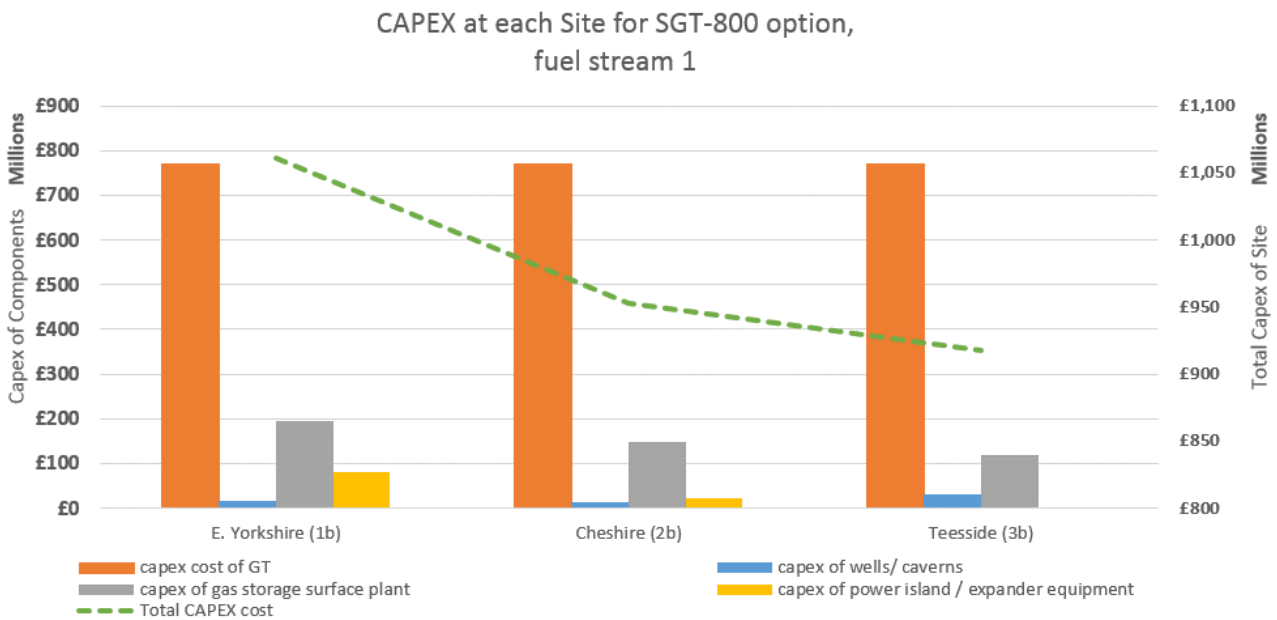


Figure 5-3: CAPEX for SGT-800, fuel gas stream 1

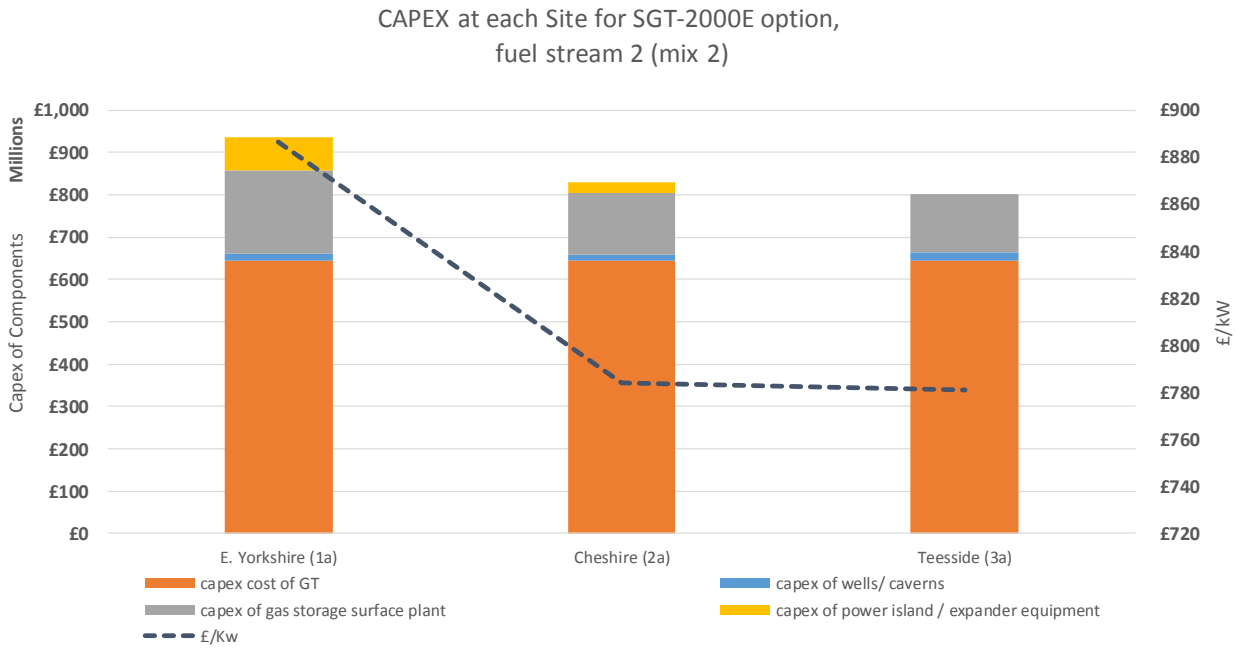


Figure 5-4: CAPEX for SGT-2000E (fuel gas stream 2) in £/kW

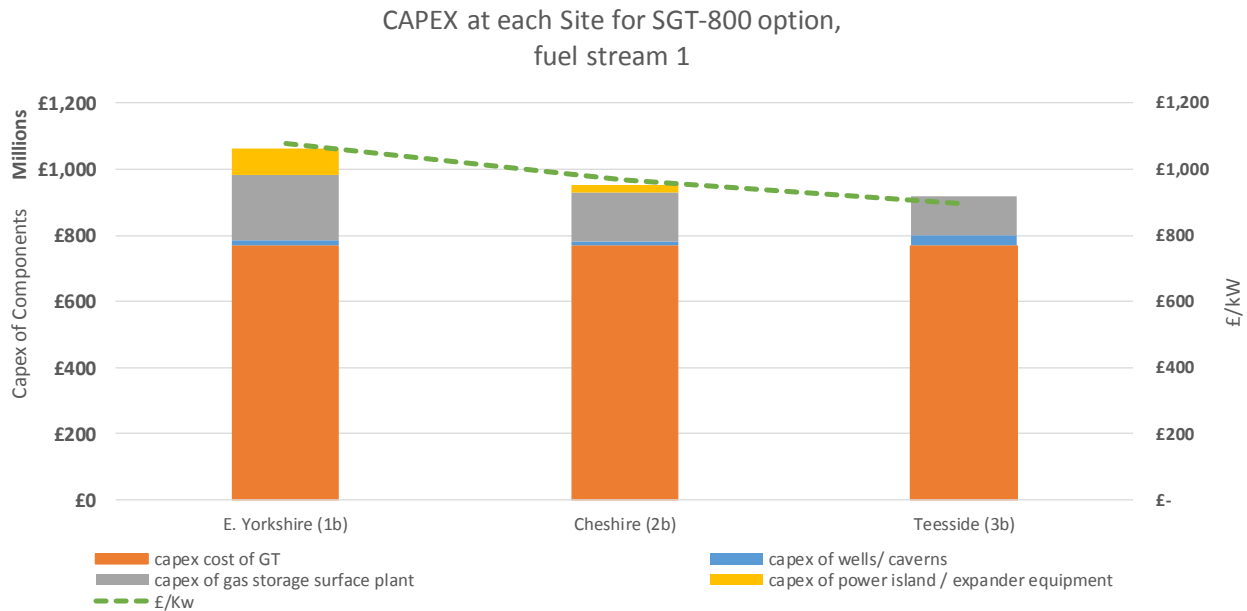


Figure 5-5: CAPEX for SGT-800, (fuel gas stream 1) in £/kW

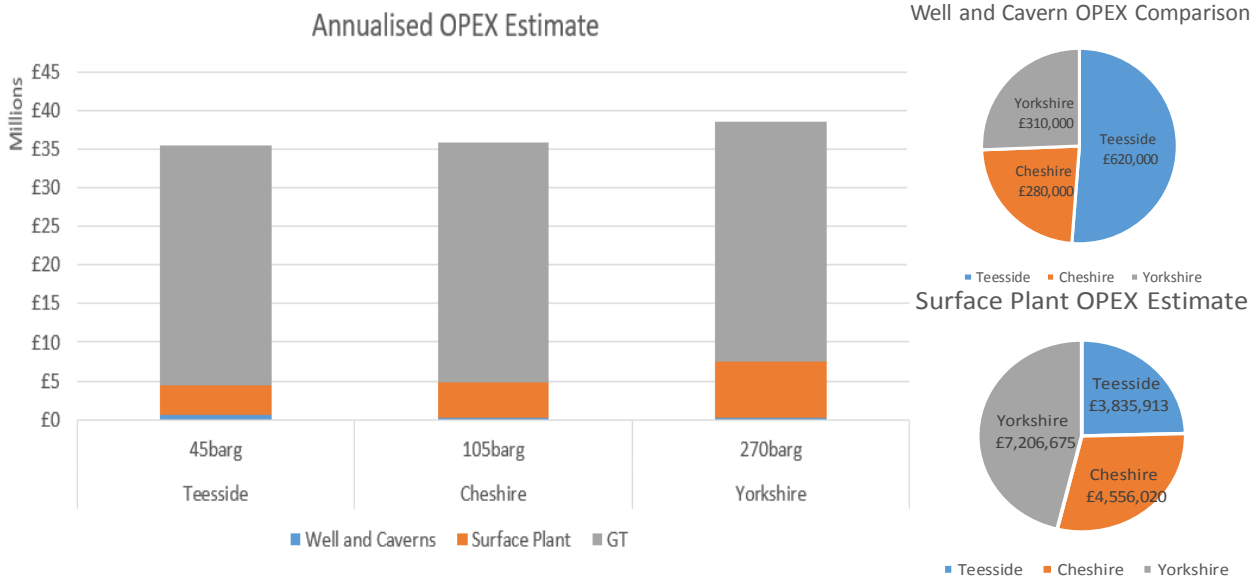


Figure 5-6: Annualised OPEX estimates for each site (AmecFw, 2012)

Conclusions

Broadly, from the CAPEX review it can be seen (Figure 5-4 and 5-5) that there is only small differences in capital required between the three locations. It has also been shown that the cavern and well completion costs are relatively modest against the GT cost, yet it should be noted that these cases consider the current H₂ capability of 25 vol% H₂ (E class) and 60 vol% (SGT-800) and so the demand on the cavern is somewhat reduced.

Looking at the more detailed findings has revealed the following:

- The cost modelling of the caverns and wells at each location shows that the East Yorkshire location would be both the most capital intensive and operational expensive option to achieve the 1GWe target.
- The Cheshire and Teesside locations would require similar levels of CAPEX to develop where the main difference between the CAPEX estimate at each site is the provision of an expansion turbine facility at the Cheshire location.
- From comparison of Figures 5-4 and 5-5, the small industrial machines, although proven for H₂ rich syngas combustion, are the highest CAPEX option due to the increased costs of installation of multiple GTs. Overall it will be difficult to justify the higher CAPEX for the SGT-800 GTs albeit this configuration of 12 x GTs can provide high levels of flexibility.

These findings are consistent with the physical limits of each site where the wells are shallower at Cheshire and Teesside. Shallower wells lead to reduced costs of drilling and a lower final operating pressure of the cavern, which then reduces the overall compression requirements.

It should be noted that the limitations of this study and the assumptions made influence the outcome of the cost modelling. Furthermore, political, societal and environmental influences and pressures have not been considered in this costing study. Therefore, conclusions are considered indicative where a site-specific assessment is necessary to develop a bespoke and fully costed solution.

5.5. Permitting and legislation

The objective of this section is to identify and assess the importance and relevance of the issues concerned with the geological uncertainty, environmental assessment, health and safety management, possible conflict between the proposed underground storage of H₂ and the existing locales, social impact studies, regulatory planning requirements and permit applications.

We have interpreted relevance to mean those issues which could theoretically have impacts of interest to regulators, and importance to mean in broad terms the possible scale of those impacts in the particular circumstances of the three sites associated with the halite bearing strata in Teesside, Cheshire and East Yorkshire.

In the following section, we describe what appear to be the key issues for each site. Since the relevant issues are generally common to all three sites they are considered first; these are then followed by an assessment of the important issues for the three individual sites.

Relevant issues

Geological uncertainty

The primary issue is the potential for H₂ fuel gas stream to escape from the storage structure, which in all three sites is expected to be a solution-mined salt cavern, and possible H₂ migration routes to sensitive receptors, including aquifers. Escape could be caused by a flaw in geological integrity of the cavern or by operational conditions that exceed its geomechanical capability. Migration routes could be natural features such as faults, man-made structures such as boreholes and mineworkings, or a combination of the two.

Environmental effects

There is a wide range of possible environmental effects of both construction and operation of underground H₂ storage facilities. The most noticeable effects are likely to be during the construction stage but, aside from permanent physical changes, they will usually be short-term. Operational effects are likely to be minor, with good management. In addition to the pollution and safety hazards posed by migrating H₂ the possible effects include loss of habitats, poor air quality (especially dust during construction), localised land and surface water contamination, landscape changes, visual impact of both temporary construction plant and permanent structures, construction noise, construction traffic movements, and damage to archaeological and cultural features.

Health and safety management

The two main issues in relation to H₂ storage are the selection of appropriate materials for well linings, pipework and the like, and, as for any surface plant, the possibility of fire and/or explosion. Material selection is crucial because, H₂ as one of the smallest molecules can readily permeate metallic structures and cause embrittlement, as well as leaking through joints and seals. Fire and explosion can affect receptors at successive distances from the plant and risk zones will need to be established; they are likely to be different from the risk zones identified for natural gas storage.

Infrastructure conflict

This appears to be most relevant in respect of traffic movements, especially at the construction stage if significant new building works are necessary. It is also possible that the siting of new or replacement plant items such as pipework, wellheads and H₂ processing facilities could cause conflict with existing plant within the current sites. Any new caverns would, of course, need to be located with appropriate consideration for cavern separating pillar widths in relation to existing caverns.

Social impact

Theoretical social impacts relate to the possible effects of a project on employment, business, local

amenities, tourism and the like. If economic effects are included then matters such as local and regional investment and security of energy supply are also relevant, although there is no clear division between social and economic impacts as these issues tend to interact.

Planning and permitting requirements

Like any new or additional developments, underground H₂ storage facilities require planning consent and various permits.

Planning consent is subject to consideration of a very wide range of criteria, including national, regional and local policies governing controls on development. Relevant national policies for this type of development call for control of night-time drilling, traffic movements, mud on roads, noise and light pollution; minimising visual intrusion and operations near to residential properties; and early consultation with the Environment Agency. The National Planning Policy Framework is intended to encourage sustainable development. Other policies relate to energy production, and in terms of need for H₂ storage it is expected that planning decisions will take account of various positive appeal outcomes for underground gas storage since 2000.

For conversion of existing caverns there will need to be a new application for Hazardous Substances Consent under the Planning (Hazardous Substances) Regulations 1992. Application is made to the Local Planning Authority. For new storage caverns, in addition, a permit is required from the HSE under the Borehole Sites and Operations Regulations 1995 and, if wastes are generated, a waste management licence from the Environment Agency (Waste Management Licensing Regulations). Combustion plant exceeding 50 MW output is required to comply with The Industrial Emissions Directive 2010/75/EU and to have a permit from the Environment Agency.

Permits usually relate to specific technical issues such as borehole drilling, hazardous substances control and waste management. All the activities considered by the proposed H₂ storage project will need planning consent and relevant permits.

East Yorkshire

Table 5-9: Permitting and Legislation Issues

Issue	Description
Geological uncertainty	<p>N-S orientated faults are present in the Atwick area in East Yorkshire and as in all such cases there is a debate about whether the fault systems act as conduits or barriers to gas movement. Faults can be envisaged as relatively open pathways but, at the depths of storage caverns (approximately 1,800 m in this instance), fault gouge has a lower permeability than the adjacent rocks and tends to act as a barrier. Nevertheless, it is common to adopt a cautious approach to cavern siting, typically by leaving a buffer zone of at least three times the maximum proposed cavern radius between caverns and major faults.</p> <p>Density data for all the strata above the Carnallitic Marl is required for geomechanical modelling of the East Yorkshire caverns. In addition, there is some uncertainty about the thickness of the Fordon Evaporite itself and this might need to be resolved if new caverns are proposed.</p>
Environmental effects	<p>The scope of environmental assessment for gas storage in East Yorkshire was set out in the section of the Environmental Impacts of the Non-Technical Summary of the Whitehill gas storage project (Environmental Resources Management, 2011). Further attention relating specifically to H₂ storage might be required in respect of air quality; the impact of any new buildings and pipelines on visual amenity, ecology and archaeology; and the effects of construction noise and traffic movements. Hazard zones and/or risk contours around the site are also likely to be affected. Potential impacts relating to offshore elements of the site are not considered significant.</p>
Infrastructure conflict	<p>Traffic conflict is unlikely to be important at this site.</p>
Social impact	<p>There could a minor, positive impact in terms of possible additional employment but this is unlikely to be an important factor.</p>
Planning requirements	<p>Several previous proposals for underground gas storage facilities in this area have been found to accord with relevant regional and local plan policies and other material considerations, resulting in their approval.</p>

Teesside

Table 5-10: Permitting and Legislation Issues

Issue	Description
Geological uncertainty	<p>Although the Boulby Halite is deeper on the Wilton (southern) side of the Tees, at 650 m as opposed to 340 m on the northern side, it is affected by what is described as a friable fault zone. However, this has not prevented gas storage in existing salt caverns at Wilton. A buffer zone of at least three times the typical cavern radius is likely to be required between any new cavern and a major fault. No uncertainties regarding the mechanical capability of the salt at Wilton have been flagged.</p>
Environmental effects	<p>The most recent available information about environmental factors likely to be of interest to regulators is from a 2009 planning application for a gas well on a small site to the east of the Wilton plant area (Egdon, 2009). It is very site-specific in terms of habitats, visual impacts, traffic movements and so on and therefore gives little indication of the factors relevant to the Wilton site. However, from the industrial nature of Wilton and such information as is included in the documents, there appear to be few if any environmental constraints on further development of storage in this location.</p>
Infrastructure conflict	<p>Existing internal infrastructure (i.e. within the Wilton site) is sufficiently complex that some structural conflicts could arise in the conversion of caverns to H₂ storage or in the construction of new caverns. At the surface or near-surface new access roads, pipe runs and the like would need to be compatible with existing plant, and below ground any new caverns would need to be carefully located to maintain pillars of adequate width between caverns.</p> <p>The Wilton site is surrounded on three sides by major roads (mostly duelled) so there is unlikely to be significant traffic conflict provided appropriate access points are used. In the 2009 planning consent (Egdon, 2009) there were no special requirements for traffic management.</p>
Social impact	<p>This is unlikely to be an important factor in H₂ storage given the existing nature of the site.</p>
Planning requirements	<p>The original gas production wells at the adjacent site were permitted in 2003 following a planning inquiry at which the Inspector found that the construction and operation of the wells would have no significant adverse impact on the nearby Kirkleatham business park. The 2009 application was approved by the local planning authority (Egdon, 2009).</p> <p>It is not clear whether proposals for H₂ storage would raise any specific planning issues but it appears unlikely. Regional and local planning policies generally encourage further development at Wilton, especially in the energy, recycling and chemical industries. The criteria against which applications will be judged are set out in the 2009 planning support statement (Egdon, 2009).</p>

Cheshire

Table 5-11: Permitting and Legislation Issues

Issue	Description
Geological uncertainty	<p>The stratigraphy and structure of the Cheshire salt field are well known from recent and historical salt mining (both conventional and solution) and from investigations for gas storage schemes. The storage horizon is the 290m thick Northwich Halite, which provides extensive opportunities for cavern construction, despite the presence of a 10m claystone band, the ‘Thirty Foot’ Marl. Some caverns have been successfully constructed through this band. There is little significant faulting other than the major King Street Fault, which forms the western boundary of the Holford-Byley section of the salt field (in which the Stublach and the Holford cavern storage sites are located), and is sufficiently distant to be of no significance. Previous uncertainty about the presence of a wet rock-head in the locality is assumed to have been resolved by the ongoing development of the Stublach caverns.</p>
Environmental effects	<p>Potential concerns at the Stublach planning stage about loss of habitats (temporary and permanent), noise, dust, sensitive archaeological sites, traffic, and landscape and visual effects are assumed to have been resolved and should not be significant in respect of underground H₂ storage.</p>
Infrastructure conflict	<p>Any conflict is most likely to be in relation to traffic movements (where several major motorways and the HS2 rail route are in close proximity), but there is no suggestion of expected conflict in the Design and Access Statement for the Stublach development (Zyda Law, 2016).</p>
Social impact	<p>This is expected to be positive but minor, relating to some custom for local suppliers and additional employment, with no effect on the socio-economic baseline</p>
Planning requirements	<p>The conclusion to the 2015 Policy Statement for the Stublach development states (Zyda Law, 2015), “The Applicant believes that the Project is in full accord with adopted and emerging national and local planning and energy policies, and that other material considerations, including security of energy supply, weigh in favour of the Project.” The approval of the project suggests that, in principle, the local planning authority concurred, but public attitudes to H₂ storage might influence a future decision.</p>





5.6. Conservative estimate of the total storage resource in the three areas under consideration

The determination of the total storage resource in the Teesside, Cheshire and East Yorkshire areas is a complex issue where there are multiple factors which could impact the suitability of one location from another. These include:

- Quality of salt – Inherently salt quality and composition varies from one location to another. Prior to leaching caverns, boreholes are drilled and salt samples taken to allow identification of impurity content and proper planning of the leaching process etc.
- Salt depth – Salt depth varies across the formation where it is necessary to ensure there is sufficient depth to allow an economically viable cavern volume with enough remaining salt depth in the roof to ensure cavern integrity is achieved.
- Faults and folds – Faults in the geological setting can create leak paths to surface therefore proximity to faults and other geological features need to be considered.
- Pillar width – Caverns must be sufficiently separated to ensure that they do not impact any adjacent caverns.
- Surface facilities & infrastructure – There are restrictions on developing salt caverns in close proximity to populated areas, industry, roads, buried services etc.
- Areas of natural beauty / protected areas – Areas such as the Yorkshire dales have been assumed as not viable for development.

Typically, the development of a new storage location is subject to an intensive feasibility study, reviewing these points and assessing the likely success of the cavern storage facility. It is however not credible to undertake such a study over the entire onshore salt mass therefore a high level study has been conducted to better understand the potential resource that could be available.

For simplicity, it has been assumed that salt conditions around existing underground storage facilities have a high probability of offering good salt conditions for new caverns. Furthermore locations in areas of high population or areas of natural beauty have been discounted due to unlikely support from community or Environment Agency. Areas which are not located near existing underground storage facilities or are not in the discounted regions, are effectively unknowns therefore it has been conservatively assumed that although there may be sufficient space for cavern development the potential for successful storage is low. Figures 5-7 and 5-8 present heat maps of the locations at Teesside, East Yorkshire and Cheshire where the following key has been used based on the criteria specified above.

- | | |
|---|--|
|  | Existing underground storage locations – Area around existing facilities with proven salt properties for storage |
|  | Areas in proximity to existing underground storage locations – Although not proven assumed to have high probability of satisfactory salt conditions. |
|  | Unknown areas where there is assumed to be a low probability of satisfactory salt conditions for storage. |
|  | Areas where storage not considered due to surface limitations (e.g. Yorkshire dales, densely populated areas) |

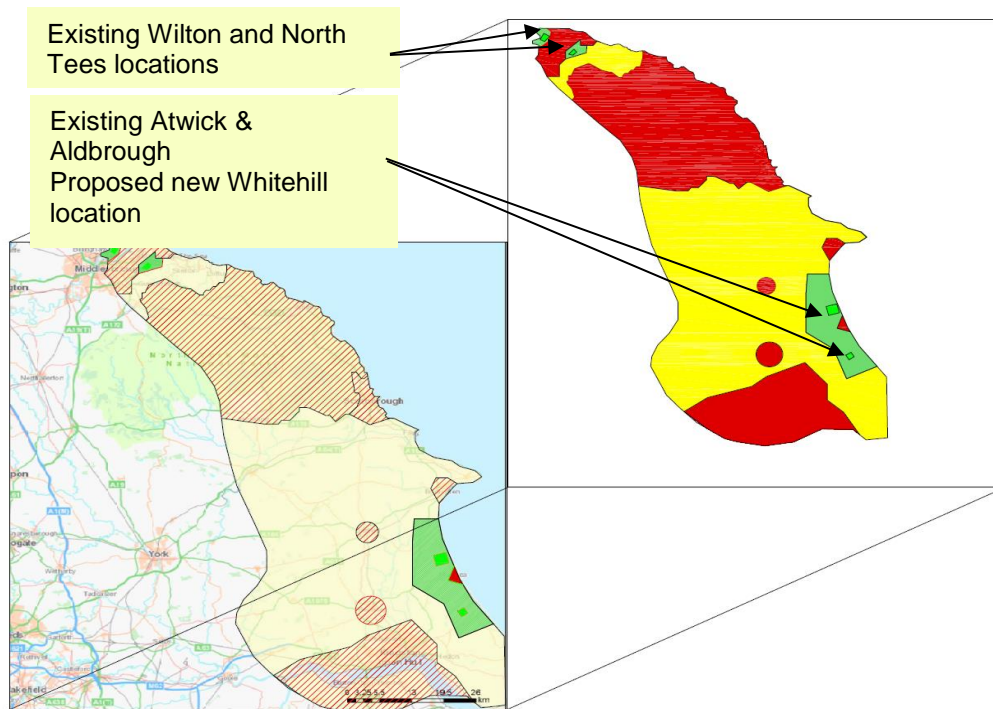


Figure 5-7: East Yorkshire and Teesside salt coverage and estimated heat map of usable salt area (map excerpt from BGS GeoIndex Onshore)

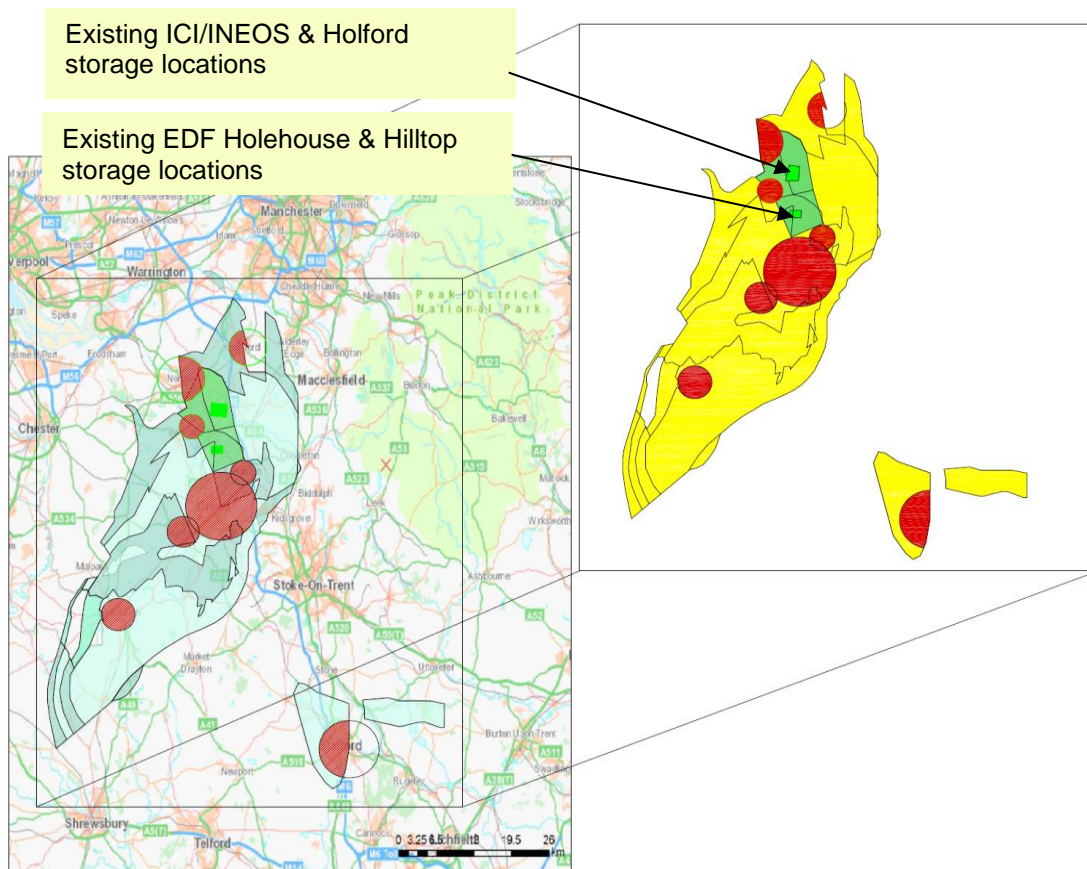


Figure 5-8: Cheshire salt coverage and estimated heat map of usable salt area (map excerpt from BGS GeoIndex Onshore)

Based on the heat maps provided in Figures 5-7 and 5-8 the total area of each category has been estimated. These areas have then been factored against the percentage area available for storage (assuming the total area is limited due to existing cavern proximity, roads, services etc.) and the probability that the salt in that area will be suitable for storage (to account for potential poor salt conditions/depth etc.). the remaining area has then been compared against the maximum cross sectional area of the representative caverns for each location to determine the total number of caverns that could be installed. This number has then been multiplied by the representative cavern volume to determine the potential storage resource available at each location. The following section presents the outcome of the assessment for each location.

East Yorkshire

Table 5-12 summarises the assessment made on the East Yorkshire area identified in Figure 5-7. From this, there is estimated to be ~1,700,000 m³ of cavern volume in the areas identified as existing underground storage facilities. It is however noted that this does not include the existing storage volume (where available space has been factored by 10%). If the entire existing salt cavern storage capacity for natural gas in East Yorkshire were to be converted to a H₂ storage facility, the total storage volume that would be made available is expected to be approximately 4,300,000 m³.

Moreover, there is already approved plans at this location which incorporate the development of 19 new caverns, the additional storage volume is predicted to be approximately 5,700,000 m³. Table 5-12 shows ~29,000,000 m³ potentially available for ~100 new caverns in proximity to existing underground storage locations suggesting that there may be further developments possible in addition to that already planned.

Assuming that there are other locations in close proximity to the existing and planned caverns which have a reasonable chance of success and some areas outwith this that have reduced chance of success it has been calculated that there could conservatively be up to ~68,000,000 m³ of new cavern storage in East Yorkshire (~250 new caverns). This number should however be treated with caution where a significant proportion of the new volume would occur in areas of unknown condition and capability.

Table 5-12: Estimated new cavern potential in East Yorkshire

Parameter	Dimension	East Yorkshire
Total area of salt at location	km ²	2,600.0
Diameter of representative cavern	m	75.2
Area of representative cavern	km ²	0.0044
Distance between caverns (pillar width) = 3 x cavern radius*	m	113
Total cavern + pillar area	km ²	0.0278
Volume of representative caverns	m ³	275,691
Existing Underground Storage Facilities		
Estimated area used by existing underground storage facilities	km ²	7.0
Factor - Available space at existing underground storage facilities	10%	km ² 0.7
Factor - Probability that available space is suitable for hydrogen storage	25%	km ² 0.2
Estimated No. of new Caverns that could be located at existing facilities	No.	6
Estimated total available new cavern volume	m ³	1,738,021
Area in Proximity to Existing Underground Storage Facilities		
Estimated area of suitable salt in proximity to existing underground storage facilities	km ²	200.0
Factor - Available space in proximity to existing underground storage facilities	10%	km ² 20.0
Factor - Probability that available space is suitable for hydrogen storage	15%	km ² 3.0
Estimated No. of new caverns that could be located in proximity to existing facilities	No.	108
Estimated total available new cavern volume	m ³	29,794,648
Remaining Salt Area		
Estimated area of remaining available salt (yellow)	km ²	1,850.0
Factor - Available space in remaining salt area	10%	km ² 185.0
Factor - Probability that available space is suitable for hydrogen storage	2%	km ² 3.7
Estimated No. of new caverns that could be located at existing facilities	No.	133
Estimated available new cavern volume	m ³	36,746,733
Estimated Total Available Cavern Volume (m³)		68,279,402

Cheshire

Table 5-13 summarises the assessment made on the Cheshire area identified in Figure 5-8. From this, there is estimated to be ~1,500,000 m³ of cavern volume in the areas identified as existing gas storage facilities. It is however noted that this does not include the existing storage volume (considered within the 10% availability factor). If the entire existing storage capacity for natural gas of the Stublach site, were to be converted to a H₂ storage facility, the total storage volume that would be made available is expected to be approximately 3,040,000 m³.

Moreover, taking into consideration the projected storage capacity of the planned “Keuper Gas” underground storage scheme and the opportunity of developing the remaining planned storage caverns in the Stublach site, one would expect that there will be an additional 37 caverns in total, resulting in an extra storage volume of approximately 11,100,000 m³. As a benchmark this suggests that the estimated volume presented in Table 5-13 of 11,771,090 m³ is based on reasonable assumptions. When considering the estimate for the areas in proximity to the existing sites and also the low probability areas away from this it is estimated that there could be ~36,000,000 m³ of new cavern storage (~100 new caverns) in the Cheshire region. This number should however be treated with caution where a large proportion of the new volume would occur in areas of unknown condition and capability.

Table 5-13: Estimated new cavern potential in Cheshire

Parameter	Dimension	Cheshire
Total area of salt at location	km ²	1,800.0
Diameter of representative cavern	m	88.9
Area of representative cavern	km ²	0.0062
Distance between caverns (pillar width) = 3 x cavern radius*	m	133
Total cavern + pillar area	km ²	0.0388
Volume of representative caverns	m ³	304,438
Existing Underground Storage Facilities		
Estimated area used by existing underground storage facilities	km ²	8.0
Factor - Available space at existing underground storage facilities	10%	km ² 0.8
Factor - Probability that available space is suitable for hydrogen storage	25%	km ² 0.2
Estimated No. of new Caverns that could be located at existing facilities	No.	5
Estimated total available new cavern volume	m ³	1,569,479
Area in Proximity to Existing Underground Storage Facilities		
Estimated area of suitable salt in proximity to existing underground storage facilities	km ²	100.0
Factor - Available space in proximity to existing underground storage facilities	10%	km ² 10.0
Factor - Probability that available space is suitable for hydrogen storage	15%	km ² 1.5
Estimated No. of new caverns that could be located in proximity to existing facilities	No.	39
Estimated total available new cavern volume	m ³	11,771,090
Remaining Salt Area		
Estimated area of remaining available salt (yellow)	km ²	1,500.0
Factor - Available space in remaining salt area	10%	km ² 150.0
Factor - Probability that available space is suitable for hydrogen storage	2%	km ² 3.0
Estimated No. of new caverns that could be located at existing facilities	No.	77
Estimated available new cavern volume	m ³	23,542,181
Estimated Total Available Cavern Volume (m³)		36,882,750

Teesside

Table 5-14 summarises the assessment made on the Teesside area identified in Figure 5-8. From this, there is estimated to be ~480,000 m³ of new cavern volume in the areas identified as existing gas storage facilities. It is however noted that this does not include the existing storage volume (considered within the 10% availability factor). If the entire existing storage capacity for natural gas of the Wilton site, were to be converted to a H₂ storage facility, the total storage volume that would be made available is expected to be approximately 295,000 m³.

Taking in to account the wider Teesside area it is estimated that there may be up to 3,000,000 m³ of new storage potential (~50 new caverns). Again this number should be treated with caution where a large proportion of the new volume would occur in areas of unknown condition and capability.

Table 5-14: Estimated new cavern potential in Teesside

Parameter		Dimension	Teesside
Total area of salt at location		km ²	1,100.0
Diameter of representative cavern		m	77.2
Area of representative cavern		km ²	0.0047
Distance between caverns (pillar width) = 3 x cavern radius*		m	39
Total cavern + pillar area		km ²	0.0105
Volume of representative caverns		m ³	51,144
Existing Underground Storage Facilities			
Estimated area used by existing underground storage facilities		km ²	4.0
Factor - Available space at existing underground storage facilities	10%	km ²	0.4
Factor - Probability that available space is suitable for hydrogen storage	25%	km ²	0.1
Estimated No. of new Caverns that could be located at existing facilities		No.	9
Estimated total available new cavern volume		m ³	485,610
Area in Proximity to Existing Underground Storage Facilities			
Estimated area of suitable salt in proximity to existing underground storage facilities		km ²	20.0
Factor - Available space in proximity to existing underground storage facilities	10%	km ²	2.0
Factor - Probability that available space is suitable for hydrogen storage	15%	km ²	0.3
Estimated No. of new caverns that could be located in proximity to existing facilities		No.	28
Estimated total available new cavern volume		m ³	1,456,830
Remaining Salt Area			
Estimated area of remaining available salt (yellow)		km ²	110.0
Factor - Available space in remaining salt area	10%	km ²	11.0
Factor - Probability that available space is suitable for hydrogen storage	2%	km ²	0.2
Estimated No. of new caverns that could be located at existing facilities		No.	21
Estimated available new cavern volume		m ³	1,068,342
Estimated Total Available Cavern Volume (m³)			3,010,782

Conclusion

Based on the simple analysis undertaken it is clear that, even when conservatively assuming only a small percentage of the available salt mass in the UK is suitable for storage, there is potential for a significant number of new caverns to be developed. As highlighted above these figures should be treated with caution where the successful deployment of underground storage is reliant on many factors where this crude assessment should be considered only as a mechanism to frame the discussion.

ATKINS

Chapter 6: Low Carbon Case



6. Defining the scenario to achieve, low carbon, high hydrogen combustion

6.1. Outlining the baseline case for a high hydrogen CCGT

Chapter 2 discusses the technology requirements and limitations to burning high H₂ ratios in modern GTs. Specifically, the technical limitations, performance and NO_x constraints have been reviewed in detail. However, the basis for this research was on proven, achievable H₂ combustion based on case studies with thousands of operating hours or from OEM research programmes that are near commercialisation.

Uncertainty remains between what is currently offered (60 vol% for SGT-800) and what could be achievable by 2030. A future low carbon case would aim to deliver very high H₂ combustion, without a significant compromise to plant performance, safety or emissions. Much of the research supporting high H₂ combustion (>80 vol%) is either in the early concept stage, sensitive information that is confidential to OEMs or demonstration projects with limited operational hours.

Since the 2000s, high H₂ combustion in GTs has been researched and developed through IGCC projects in novel industries such as Carbon Capture, Utilisation and Storage (CCUS). For example, the US Department of Energy (DOE) was set to fund several projects such as FutureGen, Hydrogen Energy California (HECA), and the Texas Clean Energy Project (TCEP⁵). These projects proposed to use “F” and “H” class GTs. Although few of the projects have yet been realised due to funding issues, several of the developments have already started and simply need further funding to improve the GT performance on H₂ rich fuel gas streams.

This chapter seeks to explore the early development research to identify a hypothetical case where high H₂, above 80 vol%, may be achievable. The GT modifications needed to achieve this will be discussed, along with the potential advances that may be seen in this technology. In addition, the likely turbine configuration with control mechanisms (e.g. steam/ N₂ dilution) will be explored along with the resulting impacts on plant performance and capital costs presented.

A Chapter Roadmap outlining the content covered in this section is given in Figure 6-1:

⁵ The TCEP project was the last project the DOE terminated funding for in 2016. Since then the development of GT combustion flexibility with H₂ rich fuel gas streams has been paused until further commercial incentive is provided. The TCEP proposed to use a Siemens SGT6-8000H, 60Hz GT in 1+1 configuration to generate up to 405 MWe (gross), which would employ blending of the H₂ rich syngas with natural gas and further dilute it with N₂ for cooling.

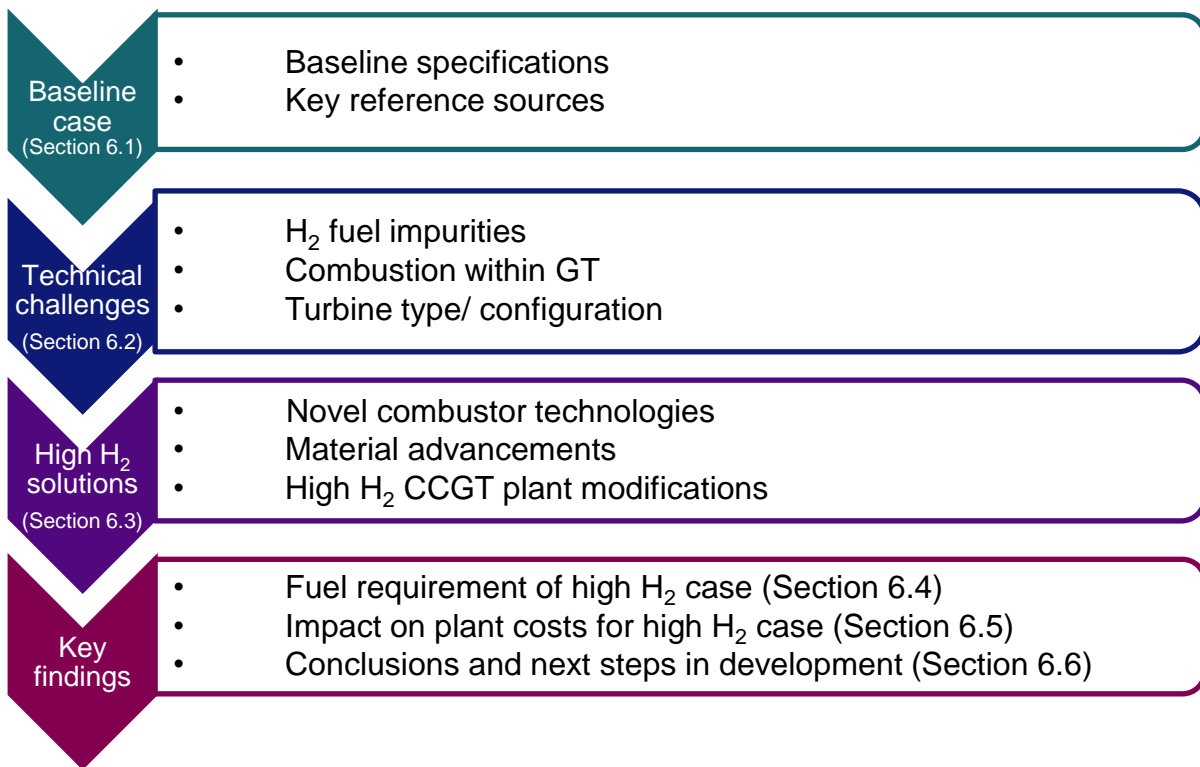


Figure 6-1: Chapter Roadmap

Baseline specifications

Based on the research completed as part of this task it is possible to define baseline specifications for what would be expected of the future, low carbon, high H₂ case. These specifications help frame this chapter and focus the review on the topics perceived as being most credible for a future, 2030+ high H₂ scenario.

Table 6-1: Indicative baseline assumptions

Specification	Value / range targeted
Turbine type	E, F class are of most interest for 2030, but developments in the H-class are expected in the longer-term. Burner design optimised for gases comprising of high H ₂ content and ensuring stable combustion. DLE or diffusion combustion may be considered as possible options dependent on the future development of burner technologies.
Turbine configuration	CCGT favoured to achieve higher lifecycle efficiencies
Power generation cycle	Scenario 3, two peaks of 5 hours duration @ 90% load.
Power loss/ gain through combusting high H ₂ from rated power	-10% overall plant loss (MW) against natural gas (NG) comparison.
Future efficiency improvement expected by 2030	+1.5% GT gross LHV gain, as indicated from Appendix F.1, where future GT capability and performance improvements are discussed.
Clean, low carbon credentials	No dependence on natural gas assumed; which includes the need for start-up or blending to control combustion stability. GT technology would

Specification	Value / range targeted
	therefore require future advances to achieve this.
Allowable emissions	NO _x emissions assumed acceptable for high H ₂ case. It is considered that a future plant would be designed as NO _x compliant within EU limits. A high H ₂ case under current technology may exceed statutory limits, yet the NO _x limits in this regard has not been a driving constraint to the research undertaken.

These baseline specifications have been based on engineering judgement, yet should be considered indicative only. They have been informed through the following sources:

- Conclusions reached from Chapter 2
- Discussion and agreement with the ETI
- Outcomes of the OEM discussions as part of Chapter 2.
- Review of early concept and R&D research papers

Key reference sources

Relevant key references relating to high H₂ combustion technologies have been researched to support the outcomes of this chapter. These included the most relevant research papers issued in the last 5 years from OEMs, academic papers and technical papers on R&D testing outcomes.

Table 6-2 below presents the most relevant references used to support this chapter.

Table 6-2: Research papers supporting high H₂ combustion

Title	Author	Description
Development and Testing of a Low NO _x Hydrogen Combustion System for Heavy-Duty Gas Turbines	(York, 2013)	Combustor Technology
Investigation of a Pure Hydrogen Fuelled Gas Turbine Burner	(Cappalletti, 2017)	Combustor Technology
Study on Optimizing the Dry Low NO _x Micromix Hydrogen	(Funke, 2016)	Combustor Technology
Performance of Multiple-Injection Dry Low-NO _x Combustors on Hydrogen-Rich Syngas Fuel in an IGCC Pilot Plant	(Asai, 2015)	Combustor Technology
Using Hydrogen as Gas Turbine Fuel: Premixed Versus Diffusive Flame Combustors	(Gazzani, 2014)	Combustor Technology
Development of Advanced Material for Future Gas Turbine Application	(Alvin, 2015)	Materials
Concept of Hydrogen Fired Gas Turbine Cycle with Exhaust Gas Recirculation	(Ditaranto, 2015)	EGR
Low Single Digit NO _x Emissions Catalytic Combustor for Advanced Hydrogen Turbines for Clean Coal Power Systems	(Alavandi, 2012)	Pre-Combustion Catalyst

6.2. Technical challenges to achieve high hydrogen

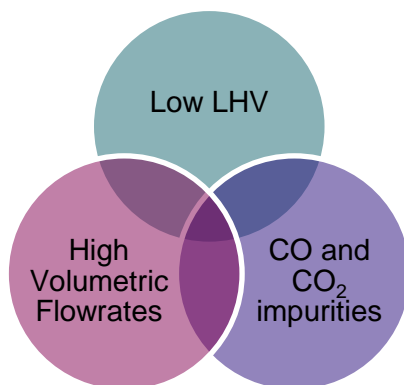
To achieve a high H₂ (> 80vol%) combustion by 2030 there are several technical challenges to overcome. These can be grouped in the following categories:



Figure 6-2: Technical challenges

H₂ fuel impurities

Typically, when H₂ is discussed as a fuel gas stream it is known to be high calorific, clean and readily available. For the wider ETI study, H₂ production through biomass gasification or auto thermal reforming (ATR) was considered. Other methods exist including steam methane reforming, methanol cracking or the separation of H₂O into O₂ and H₂ through electrolysis (ideally using renewable electricity). The biomass gasification H₂ source was selected based on delivering a balance of high H₂ purity, high feedstock rate and low relative production cost (AmecFw, 2012). However, with this fuel gas stream, the key technical challenges are identified in Figure 6-3 below:



- I. **Low LHV;** Delivering a rich H₂ feedstock with high LHV is technically challenging.
- II. **CO and CO₂ content;** These 'impurities' (and others that may be present) affect the energy content, but also the low carbon credentials of a future project and are complex and costly to remove completely.
- III. **High volumetric flowrates required;** The production source must balance the ability to deliver high volumes of rich H₂ fuel against production costs.

Figure 6-3: Technical challenges in fuel source

Fuel steam 1 (89 mol% H₂ content with 4.4 mol% CO₂, 1.5 mol% CO content), from gasification is discussed in Section 1.3. and despite a high molecular H₂ content, by mass the H₂ content is 32 wt% (see Figure 6-4). The impurities of CO and CO₂ are expected at high feedstock flowrates, and despite their small mol% contribution, as is seen in Figure 6-4, they reduce the LHV of the fuel significantly. Purer 100 mol% H₂ production could be achieved through steam methane reforming (SMR), but the cost and lifecycle energy impact would need to be assessed against the GT technology used. For instance, SMR would not be preferred if N₂ dilution is needed in the GT to control combustion (AmecFw, 2012) as N₂ production is not available as a by-product of the process through SMR, as it is with ATR.

Fuel gas stream 1 was selected as the H₂ production source for the high H₂, low carbon case. For a 2030 scenario, fuel concentrations of more than 89 mol% H₂ are considered extremely challenging. Fuel gas stream 1, also allows a comparison of the fuel requirements derived from earlier phases of this project (see Section 2.5).

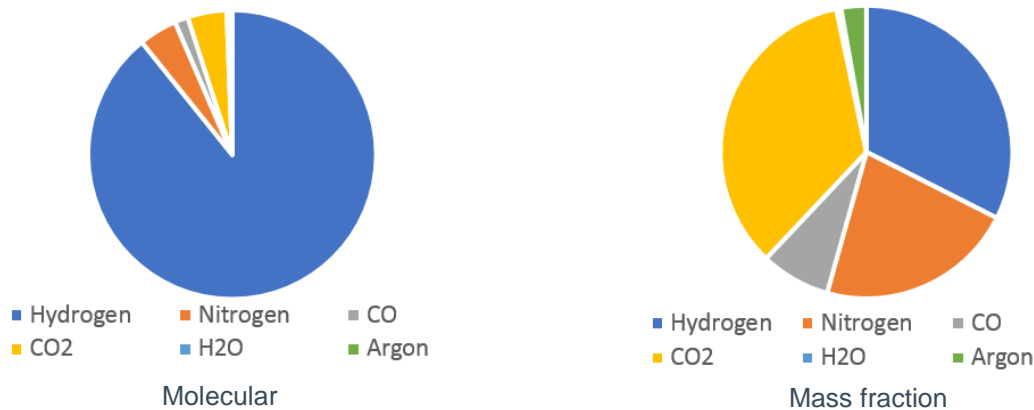


Figure 6-4: Molecular (mol%) and mass fraction (wt%) differences, fuel gas stream 1

Fuel gas stream 1 is a relatively 'skinny fuel' to that of natural gas or much purer H₂ fuel gas streams. This is particularly significant for two reasons.

1. It means the LHV content is relatively low at ~39.7 MJ/kg when compared to NG at 46 MJ/kg and pure 100 mol% H₂ at ~120 MJ/kg.
2. Although the mass flow rates to fuel a 1GW GT arrangement may be similar for H₂ or natural gas, the volumetric flowrates to achieve a 1 GW output for pure H₂ is significantly different (due to the molecular size of H₂).

Even small improvements in the purity of the H₂ source would improve the LHV of the fuel and potentially reduce required flowrates. Furthermore, carbon content in fuel gas stream 1 cannot be stripped out easily post combustion, so to maintain the low carbon credentials of a future project, the fuel should be optimised as part of the gasification and carbon capture process.

Combustion within GT

To achieve 89 mol% H₂ combustion, technical advances in the GT design would be needed. These advances would look to overcome the main technical issues which arise when H₂ volumes exceed the current GT capability (e.g. 60 vol% H₂ with the SGT-800). The technical issues that are discussed in several of the research papers can be summarised in the following categories:

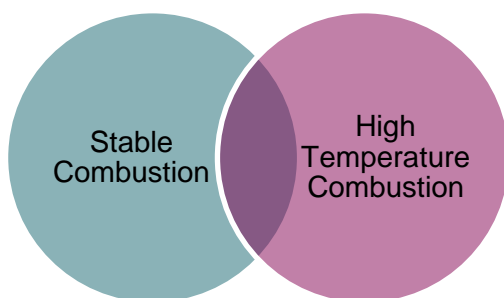


Figure 6-5: Technical challenges in combustion

- I. Stable combustion**, H₂ is highly volatile and can give rise to self-ignition particularly in premix burners, termed 'flashbacks'. Additionally, 'flame outs' or general flame instability can occur due to the wider flammability range of H₂ compared to natural gas.
- II. High temperature combustion**, H₂ burns hotter in the turbine inlet temperature (TIT) zone. Diluents in the form of steam or N₂ may be needed to lower the combustion temperature.

These technical hurdles, while possible to mitigate and control, may result in a knock-on effect on the following key performance metrics.

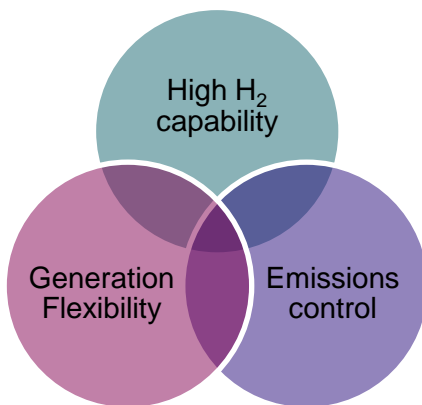
- **Increased Inspection Frequency** – High Flame temperature may incur a shortening of Operational intervals between maintenance periods,

- **Higher OPEX;** Increased inspection frequency may also affect the required maintenance regimes and parts replacement and impact on the cost of long-term service agreements (LTSA).
- **Increase in NO_x emissions;** Thermal generated NO_x increases as a direct result of the increased flame temperatures with high H₂ fuels. Advanced premix burners are yet to be available to reduce NO_x whilst maintaining high thermal efficiency. A balance is required between NO_x emissions, lower TIT and performance, high TIT and therefore higher NO_x emissions.
- **Performance characteristics;** The technical challenges and controls used can affect overall plant efficiency and power output (MW).

Turbine type / configuration

The capability of diffusion and DLE type combustors on high H₂ mixes has been discussed in Chapter 2.

Historically, H₂ fuelled IGCC's have been diffusion combustors and therefore the technology saw a wave of development during the carbon capture and storage (CCS) surge in the 1990s and into the early 2000s. Initial development of the original diffusion-type combustors saw a move to wet combustors through the addition of water or steam in the combustion zone to restrict the amounts of NO_x produced. Newer diffusion combustors use excess air and steam as advanced cooling technology which, among other things reduces NO_x emissions, but with a significant performance drop expected. More recently, with the effective halt of the UK CCS Commercialisation Programme (Damian Carrington, 2015), and limited worldwide programmes supporting CCS, the development of IGCC plant and diffusion combustion has slowed significantly. Indeed, there are very few diffusion burners capable of high H₂ in current operation and OEMs do not offer diffusion turbines as part of their conventional product range. The technical challenges associated with the GT type and configuration are given below:



- I. **High H₂ capability,** Diffusion or DLE turbine type and capability by 2030 to combust more than 80 vol% H₂.
- II. **Generation flexibility,** The CCGT configuration and associated HRSG limits the plants ability to achieve fast start/ramp up response periods. High H₂ fuel ratios are also complex to operate at varying GT loads.
- III. **Impact on Emissions;** Development work is being progressed in line with EU emissions limits, so the NO_x limits remain a key constraint.

Figure 6-6: Technical challenges in GT type / configuration

Diffusion or DLE type

Diffusion combustors can offer very high, stable H₂ combustion, 90%+, however with the penalty of unacceptable NO_x emissions. The NO_x emissions can be as high as 300-350 mg/Nm³ for smaller machines, increasing significantly for the larger turbine classes. SCR technology can go some way to remove NO_x, but is typically used to shave emissions to meet limits, rather than a total solution. The increased need for water, steam or N₂ dilution with diffusion combustion can add to project design complexity, material selection, design life and costs. Reliance on a dilution fuel gas stream, in practice, impacts plant availability, as any downtime or servicing required may impact generation (e.g. the need

for a water treatment plant).

In recent years, with the development of larger, higher efficiency natural gas turbines, technology developers have favoured the DLE designs, with cleaner low NO_x burners. For modern DLE machines a GT would require significant modifications to return to a diffusion like mode for a high H₂ fuel gas stream, like fuel gas stream 1. It is more likely that a bespoke H₂ turbine design would be the preferred choice.

The literature review undertaken for this study has shown clear research pathway towards the development of advanced DLE GT technology. In recent years a range of injectors and combustor technologies have been developed to help improve H₂ combustion while reducing temperatures and emissions. For this reason, it is considered most credible that DLE combustor technology will be the focus of development to achieve high H₂ combustion (<50 mg/Nm³ NO_x content).

Generation flexibility

Due to the flame instability of H₂, GTs using high H₂ fuel are inherently suited to base load/ steady load operation rather than rapid block loading/ load change for a peak demand matching application; where multiple starts are required. The OEMs will need to develop advanced designs of burners to cater for these rapid and flexible loading requirements.

As market demand changes, OEMs face increasing development challenges to meet both plant flexibility and performance metrics. For instance, CCGT generation will impact plant flexibility as there will be a knock-on ramp up/ down effect on the HRSG. However, bypass stacks can mitigate slow HRSG start up times (as discussed in Section 2.2). In general, multiple smaller machines would be more suited to high H₂ fuel and plant flexibility as they have benefited from increased testing and are typically designed for more challenging operational conditions. Conversely, larger class machines, like the H-class were designed to meet optimum performance or NO_x limits (<10 ppm NO_x) and have far less ability to step up or down in load fast. It is likely in the longer term that current small machine plant flexibility would be offered by the larger framed machines through OEM technology developments.

Environmental emissions; NO_x control

While NO_x emissions has not been identified as a constraint in this chapter, the ability to control NO_x emissions from the plant will be crucial in gaining planning permission for the peak demand matching plant. For natural gas the current EU limits are 25 ppm NO_x (see Section 2.1) although this limit is expected to tighten in the future. It is unclear if a GT combusting H₂ would have a higher allowable EU NO_x threshold in balance to its carbon reducing credentials.

The selection of turbine combustor types (diffusion or DLE) is of particular importance in respect of NO_x control. To control NO_x within a DLE GT the following control measures can be used:

- Post Combustion technology (Selective Catalytic Recovery (discussed in Chapter 2))
- Pre-combustion technology (e.g. H₂ fired GT with exhaust gas recovery (Ditaranto, 2015))
- Novel combustor technology aimed at NO_x reduction (see 6.3.)

6.3. Technologies with potential for high H₂ combustion.

To achieve high H₂ combustion over 60 vol% (current capability of DLE SGT-800), novel combustor technology is needed in both the DLE and diffusion combustor types. In addition to this there are several other mitigation technologies which could be deployed. These technologies are summarised in Table 6-3 where the technical challenges they seek to overcome are also identified:

Table 6-3: Technical Challenges and possible mitigations

Mitigations / Technical challenges	Diluents; like air, N ₂ , water and steam	3D printing, reduction of turbulent flow zones	Novel combustor tech.	Exhaust gas recirculation	Material advancements	Emissions; SCR capture	Ramp Down capability	GT configuration/IGV control	Maintenance regimes	Multiple smaller machines
Stable combustion	✓	✓	✓	✓					✓	
High temperature combustion	✓		✓		✓	✓			✓	
Generation flexibility			✓			✓	✓	✓	✓	✓

Novel combustor technologies

To achieve high H₂ combustion of H₂ fuel gas streams, like fuel gas stream 1, it is likely that advanced/novel combustor technologies would be adopted in the future, which are more suited to H₂ and therefore offer greater performance. The aim is an injection scheme for the H₂ fuel that is both intrinsically flashback-safe and that provides efficient mixing. Many of these technologies have focused on the challenge of reducing NO_x emissions when combusting high H₂ ratios. It is likely that development in this sector will continue to progress under this constraint.

Based on R&D and scientific papers in the last five years, the following combustor technologies (in Table 6-4) have been shown to be promising technologies for the future:

Table 6-4: Novel combustor technology summary

Innovation	Turbine type	Tech type	Max % H ₂	Main aim	Reference
Multitube fuel nozzle	Premixed	Combustor Tech	100%	100% H ₂ combustion/ Reduce NO _x	(York, 2013)
Axial swirler injection system with a cross-fuel injector	Premixed	Combustor Tech	100%	100% H ₂ combustion/ Reduce NO _x	(Cappalletti, 2017)
DLE micromix combustor	Premixed	Combustor Tech	Not available	Reduce NO _x / allow stable H combustion	(Funke, 2016)
Multi injection burner	Premixed	Combustor Tech	40%-65%	Reduce NO _x	(Asai, 2015)
Rich Catalytic H injector	Applied to premix or diffusion	Catalyst Addition	75%	Reduce NO _x / Improve efficiency	(Alavandi, 2012)

Table 6-4 summarises the combustor technology advancements in the past five years, where the technology is predominately premixed / DLE ready. High H₂ ratios have been quoted for these novel combustors / injectors, yet often the technology is still at the early testing and development phase.

Several key improvement areas are common across novel combustor technology, with the main aims as follow:

- **Separation of ignited flames** in the combustion chamber through injector nozzle spacing
- **Reduction of flame size** by utilising an increased number of smaller injectors
- **Rapid mixing** of fuel / air before entering the combustion zone.

A summary of the most relevant novel combustor types researched, is given below:

Multitube fuel nozzle: Jet-in-crossflow mixing is utilised with a new injector concept, which has now been incorporated into a full-scale, multi-nozzle combustor can. This has an energy conversion rate of more than 10 MW, at F-class conditions. This system has accumulated over 100 hours of testing.

The multitube mixer concept was successfully employed in a full-can combustion system logging more than 90% of H₂ (York, 2013).

An **axial swirler injection system with a cross-fuel injector** is designed to prevent any high turbulence regions (that can lead to flashback) while offering a low NO_x solution (Cappalletti, 2017). The fuel lances which are used to inject the fuel are free to move in the axial direction to alter the delivery point of the fuel and the mixing level.

An **advanced DLE micromix** H₂ application includes high-energy injectors that are arranged in ring structures that distribute and guide H₂ and air. This injection system leads to H₂ micro-flamelets (rather than large scale flames) which are stable and clearly separated from each other reducing the residence time of the H₂-air mixture (giving less time for auto-ignition to occur) and preventing the formation of hot spots, resulting in a more stable fuel with reduced NO_x formation (Funke, 2016).

MHPS multiple-injection burner: High temperature, NO_x generating regions are eliminated through rapid mixing of fuel and air over a short distance before entering the combustion chamber. Flame lifting is also utilised, where the H₂ flame is held stably at a point away from the burner preventing the occurrence of flashback into the burner. Having multiple-injection burners allows control of combustion and emissions. The fuel distribution ratio can be altered across the inner and outer burners to either increase combustion stability or reduce NO_x emissions (but not both) (Asai, 2015).

Rich Catalytic H Injector; Reduces NO_x emissions by rapidly mixing air with a catalysed fuel / air mixture before final combustion and in doing so, reduces reactivity and emissions. The system has been quoted to achieve as low as 1 ppm NO_x with CO below 10 ppm (Alavandi, 2012).

Material Advancements

Material advancements and coating protection continues to be an area of focus for OEMs and researchers alike, as it has the potential to offer significant performance improvements to GTs. High turbine inlet temperatures (TIT) require that turbine transition pieces, blades and vanes are protected against corrosion/oxidation using specialist thermal barrier coatings. Improvements in coatings may be required to prolong component life due to the intensity of the H₂ flame.

Typically, metal alloys are used in GTs with TIT >1300-1400°C. In TIT ranges above this, at 1400-1600°C, Oxide coated, silicon carbide based ceramics can be used. Future TIT aspirations are to achieve 1600-1700°C with advanced cooling configurations through surface or skin cooling (Alvin, 2015). It is also noted that, with increased water vapour present, degradation of the coated material is accelerated. This is particularly relevant for diffusion machines. Material advancements therefore continues to be an area of more generalised GT development and not specific to the high H₂ case. It should also be noted that, as previously discussed, high TIT can improve performance, yet forms a

direct relationship with high unwanted NO_x emissions and this must be mitigated in line with any allowable increase in TIT range.

High H₂ CCGT plant modifications

- The research undertaken has suggested advances in the high H₂ market will be with DLE machines, therefore no dilution will be required (as required for diffusion turbines). However, additional plant modifications, which may also affect the plant footprint would still be required, as follows:
- The air combustion ratio may require modification to control combustion; e.g. changes needed to the air compressor or air bleed off to control GT fuel flow.
- It is expected that SCR technology would be needed to meet emissions limits in the short term. Using SCR technology may increase the overall footprint of the plant by 1.5x.
- Safety measures and statutory requirements for combusting high H₂ fuels may lead to additional equipment, sensors and plant upgrades such as:
 - Material selection upgrade;
 - H₂ pipeline and compressors valves, seals and glands;
 - Electrical intrinsically safe certification;
 - Plant exclusion areas.
- The high volumetric flowrates required may mean added design considerations are needed to the compressor and surface plant design.

6.4. Fuel requirement of high H₂ case,

A review of the fuel requirement for a high H₂ case (using fuel gas stream 1, 89 mol%) was undertaken using 2 x (2+1) E-class turbines as a base case. This E-class machine was used for comparison of the fuel requirement only. It is possible that several alternate GTs could offer a high H₂ (>80 vol%) capability by 2030, but also that a bespoke H₂ ready turbine could appear on the market. The fuel requirement for the E-class GTs was benchmarked against the GTPRO software for a natural gas case. A summary of the key assumptions used to determine the fuel requirement is given below:

Table 6-5: High H₂ case fuel requirement example

Key Finding:	Description:
42/58% gasifier / cavern demand split	This assumes a diurnal fill/empty cycle, whereby if a longer term seasonal basis is needed this would be achieved by reducing the time generated and thereby increasing injection period.
Gasifier = constant supply	There is limited flexibility in the H ₂ production source, so flexibility needs to be absorbed by the cavern, and GT operation
~788 MW, plant net output @ 90% load (plant net output, @ 100% load, 875 MW)	The GT would deliver circa 534 MW @ average of 90% load, with the ST delivering remaining ~254 MW (based on SGT-2000E machines), includes -10% overall plant reduction in MW, and 1.5%+ GT efficiency improvement from the baseline requirements, Table 6-1.

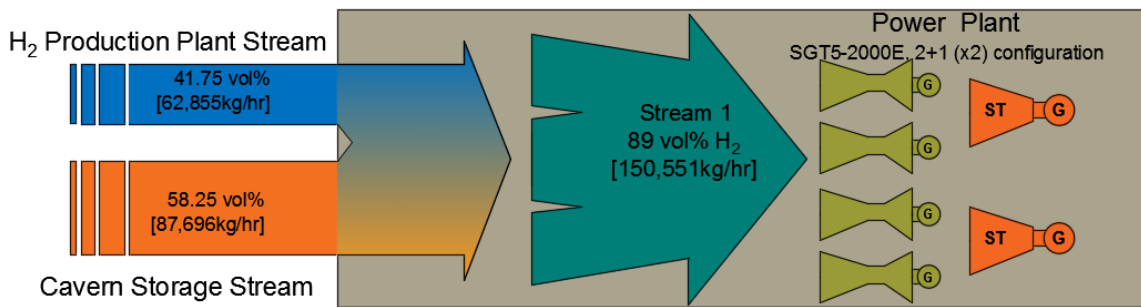


Figure 6-7: Fuel requirement high H₂ case

The methodology for the fuel requirement study is outlined in Appendix F1.2, where several key findings resulted from this work, presented below:

- Two or more caverns are needed to meet the extraction flowrate required when the cavern is at minimum pressure (based on Cheshire case 30 barg). Multiple caverns also improve the seasonal profiling by smoothing individual cavern extraction/injection demands.
- The GT demand defines the sizing of the gasifier, which in turn sets the boundaries for the injection/extraction balance in a 24 hour cycle; where a proportion of the GT fuel requirement is met directly from the H₂ production source. In order to increase the flexibility and volumes achievable as part of the injection/extraction cycle the gasifier sizing may be increased. This however means the oversized gasifier would not run at 100% load at all times. This would place less demand on the cavern and could mean the full potential of the cavern is not realised.
- Using a conventional well completion constrains injection / extraction flowrates (where a 30 m/s max erosional velocity is assumed). However, an increased tubing bore may be possible to suit the design requirements for a high H₂, fast cycling plant.
- The high H₂ case requires higher volumetric injection and extraction flowrates. For example, the total extraction that would be required from two Cheshire caverns is 354,471 Nm³/hr. This compares against a natural gas case of 116,617 Nm³/hr total. The high required volumetric flowrates may mean added design complexity in the turbine flowrate capacity.

6.5. Impact on plant costs for high H₂ case

Following discussions with the OEMs it is anticipated that currently, for a high H₂ case, the GT plant CAPEX costs would be expected to increase by nominally 10% compared against a GT fired with natural gas. This is shown in Figure 6-8, where the GT cost is shown to be the majority portion of the overall CAPEX (as discussed in Chapter 5). The GT CAPEX may increase further with the added development cost to achieve a high (> 80 vol%) H₂ case by 2030.

In addition, Table 6-6 presents indicative cost factors that contribute to the overall cost increase for a high H₂ case. For the areas of plant requiring modifications or upgrades, the cost factors indicate the increase in CAPEX expected.

Table 6-6: Cost factors for high H₂ case

Factors contributing to CAPEX	Cost factor (*values indicative only), increase against NG plant relative CAPEX:
GT modifications; novel combustor, potentially upgraded materials, smooth coatings to reduce turbulence, additional control mechanisms (excludes design and development work to achieve advanced H ₂ GT)	+10%
CAPEX of power island / expander equipment; includes compressor design optimisation to achieve high flowrates	+25%
Surface plant modifications, pipework, seals and materials	+25%
Wells and caverns CAPEX	+ 10%
Safety considerations; electrical safety, exclusion zones, monitoring and HSE	+ 5%
Relative increase of plant CAPEX, against a comparable natural gas project	~10.5%
SCR – If selected as main NO _x reduction technology, Range is dependent on the thermal NO _x emissions from the advanced H ₂ GT.	+10 to 20% (additional on total Capex, incl. ~10%+ for plant mods)

*The cost factors in table 6-6 are considered indicative only base on industry experience and should not be taken as definitive.

The indicative cost increase for a high H₂ plant has been presented in Figure 6-8 against the CAPEX expected for each plant and subsurface area. The comparative case has been averaged across the three site options from the CAPEX breakdown given in Section 5.4. As the provision of an expansion turbine is only applicable to East Yorkshire and Cheshire, the larger expansion turbine, for East Yorkshire has been compared. For the GT costs, the comparison is against the SGT-2000E, 187MW GT in a 2 x (2+1) arrangement.

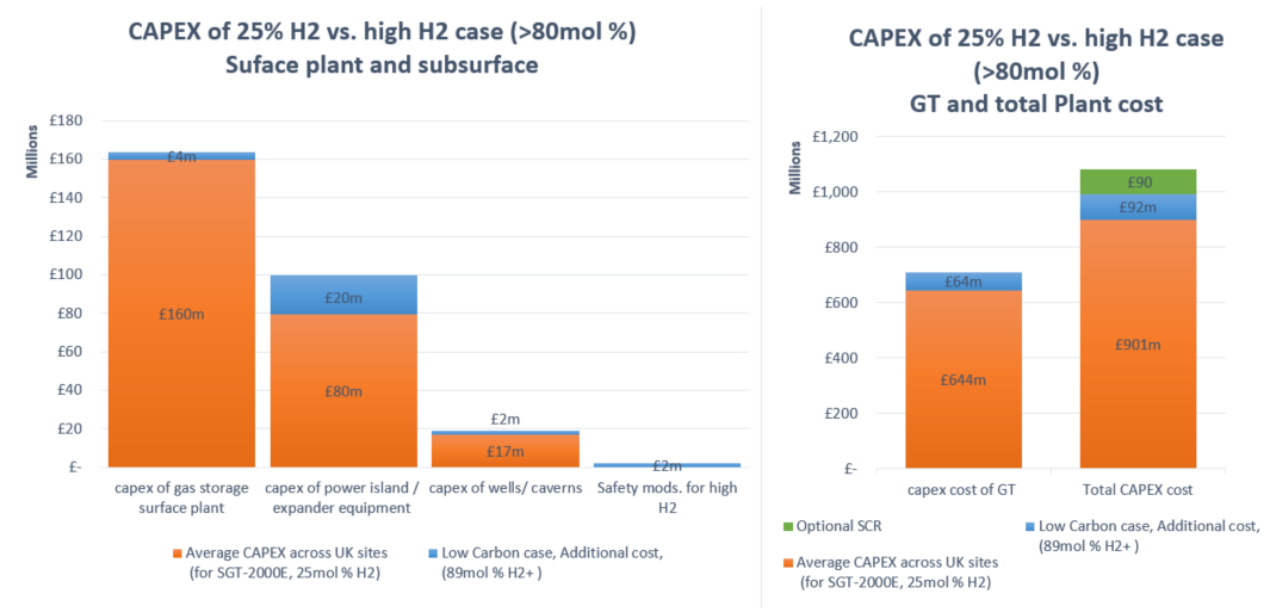


Figure 6-8: Fuel requirement high H₂ case

The total CAPEX increase expected for the high H₂ case against the comparative case is ~£92m, or around ~10% increase to total CAPEX. The optional SCR case for the reduction of NO_x can be seen in green, where the added cost of ~£90m is around 10% of the total CAPEX of the comparison case (£901m).

To achieve a high H₂ case, several mitigations may also be needed to overcome the current technical challenges of stable combustion, high temperature combustion and generation flexibility. Table 6-7 provides an indication of the potential impact of implementing these design changes to the CAPEX / OPEX.

Table 6-7: Cost factors for high H₂ case

Mitigations / Capex/Opex weighting*	Diluents; like air, N ₂ , water and steam	3D printing, reduction of turbulent flow zones	Novel combustor tech.	Exhaust gas recirculation	Material advancements	Emissions; SCR capture	Ramp Down capability	GT configuration/ IGV control	Maintenance regimes	Multiple smaller machines
Increase of Capex	Med	Med	High	Med	Med	High	Med	Low	Med	High
Increase of Opex	High	Low	Low	Low	Low	High	Low	Med	Med	Low

*The Capex/Opex weightings are indicative only, but provide a weighting (Low, Medium, High) of the Capex/Opex that may be required to introduce the mitigation technology. The spend is relative to implementing the technology (e.g. development work, infrastructure modifications or increases in operational fuel/water/power consumption). The mitigations are referenced to Section 6.3 where they are mapped against reducing the three common technical challenges when combusting high H₂ fuel (Stable combustion, high temp combustion and generation flexibility).

6.6. Conclusions and next steps in development

In this chapter, a detailed review of the available research in the field of high H₂ combustion was undertaken. From the review undertaken it is apparent that there is a significant volume of research available and this is supported by some ongoing development work in technologies required to support high H₂ combustion (e.g. novel combustors).

The technical challenges to combust a high H₂ case (more than 80 vol% H₂) are well documented and can be summarised as:

- Fuel impurities; where the LHV of the fuel gas stream can be lower than expected, and impurities add to the carbon impact. Also, given the unique properties of H₂, high volumetric flows are required.
- Combustion in the GT; with high TIT temperatures and flame instability limiting the H₂ capability.
- GT type / configuration; GTs capable of high H₂ combustion, while offering generation flexibility and low environmental emissions is a difficult balance.


While 100% H₂ would be extremely challenging by 2030, with the flame instabilities and flashback risk of H₂, a 100% H₂ in the longer term, towards 2040, is increasingly seen as a possibility. It is possible that a future high H₂ case would involve bespoke H₂ ready turbine designs to mitigate many of the technical barriers to the current capability of DLE and diffusion GTs alike.

Current projects like the Kawasaki 1MW project in Kobe (initial feedstock 20% H₂ in natural gas) paves the way for a future 100% H₂ scenario in Japan by 2040 (Agency for natural resources and energy, 2014). This is driven by an increased market in transportation (fuel cell cars / HGV), manufacturing and the introduction of H₂ power generation on a large scale. This type of long-term road mapping for H₂ is required to aid investor confidence and encourage a strong pipeline of development.

In the UK, OEMs have supported recent full-scale testing of the small framed GTs. This has proven up to 60 vol% H₂ is capable, and OEMs are developing roadmaps for high H₂ combustion. Under the Climate change act, the UK will aim to decarbonise its heat network on a large scale through the 2030s. It is likely that step changes will be needed in the energy sector to achieve this, and H₂ generation and storage, with continued development, can offer a clean, low carbon solution.

ATKINS

**Chapter 7:
Limitations of Cavern
Performance,
Cheshire case study**



7. Limits of Cavern Performance; Cheshire case study

Chapters two to five in this report explored the integration of cavern storage into a H₂ based power generation cycle. These chapters focused on current technology capability and demonstrated constraints and limitations to such an integration. However, the ability of the cavern to store H₂ in the volumes or flow rates required to meet the total demand profile requires further investigation. The aim of this chapter is therefore to further investigate the potential limitations of the cavern when some of the key limiting assumptions (e.g. demand profile) are removed.

To best achieve this, a series of sensitivity studies were undertaken on one of the identified representative cavern sites. The Cheshire site has arbitrarily been chosen as it is a dry storage facility which allows cavern behaviour to be more easily understood (i.e. linked to P_{max} and P_{min} gas pressure only), although the results are considered to provide conclusions which are representative to all sites.

7.1. Introduction

As identified in Chapter 4, the overall impact of daily injection/production cycles and the maximum flow through the maximum number of wells has proven to have a limited impact on the cavern integrity. Even under the most onerous H₂ fuel demand considered, the modelled cavern remained geomechanically stable. This implied that there was potential to extend the cavern modelling, to develop an enhanced operating regime to test the cavern capability and gain a deeper understanding of the flexibility of the cavern to provide a compliant, low carbon storage solution. The aim of the extended cavern modelling was therefore:

- I. To “stress” the representative Cheshire cavern by challenging its integrity limits through an increase of its daily operational capacity (Section 7.3)
- II. To superimpose seasonal cycles onto the current daily cycle such that the overall cavern pressures shift between minimum acceptable pressure (P_{min}) and the maximum allowable operating pressure (P_{max}) (Section 7.4).

Taking into consideration that the intention was to subject the cavern to challenging operating conditions, a decision was taken to verify the capability of the thermodynamic modelling of H₂ against available published results (as discussed in Appendix G). Consequently, this chapter comprises the investigation of the representative Cheshire cavern capability to operate at the extremes of its integrity limits, and when subject to a seasonal cycle in addition to the existing daily cycle.

7.2. Acceptable limiting condition for thermal-loading of storage caverns

Prior to undertaking a complex and time consuming coupled thermal-geomechanical assessment it was first thought prudent to identify whether a thermal-loading limiting condition exists. Such a limiting condition would reduce the number of iterations needed for identifying extreme operational scenarios that would not challenge the integrity of the investigated representative Cheshire cavern.

To understand the acceptable limits for cavern loading, a research task was undertaken to establish credible temperature constraints that the cavern could tolerate during periods of high extraction and thus cooling of the cavern walls.

In situ geomechanical investigations, concerning the design of gas storage caverns carried out in Northwich Halite (Potts et al, 1978) identified that:

- Dilation of salt at the surface of cavern’s walls, resulting from the development of tensile

stresses, occurs when the cavern temperature is over 14°C below the ambient geothermal temperature.

- As a consequence of the viscoplastic behaviour of salt, the identified dilation zone is eradicated when the loading conditions are reversed. This mechanical response of the salt is also recognised by the British Standard for underground gas storage in solution-mined salt caverns (British Standards Institution, 2016).

More recently, coupled thermo-dynamic analysis of a gas storage cavern in Northwich Halite (Pellizzaro et al, 2011), identified that stresses become tensile close to the cavern wall when the salt is cooled below 14°C, while the ambient geothermal gradient corresponds to 27°C.

Consequently, prior to utilising the ultimate limit cavern pressure criterion (defined by the minimum acceptable pressure, P_{min} and the maximum allowable operating pressure, P_{max}) it is recommended that an additional limiting condition should be considered, concerning the thermal loading of a salt cavern, based on a maximum allowable temperature difference criterion.

In particular, it is suggested that for a salt cavern which is subjected to a demanding pressure loading history, that cycles between P_{max} and P_{min} , the minimum average temperature in the cavern should not be lower than 14°C below the average geothermal gradient that characterises the salt formation which surrounds the cavern.

Taking into consideration that the average temperature around the Cheshire caverns, related to the geothermal gradient, is 25.2°C; the suggested temperature limit is expected to be $25.2 - 14 = 11.2^\circ\text{C}$.

However, as determined by Pellizzaro et al (2011), although the development of cavern temperatures below the proposed temperature limit may potentially induce “primary” cracking very close to the cavern surface, this thermal loading is not likely to lead to spalling since the cavern is surrounded by highly compressive zones inhibiting a generalised collapse.

7.3. Stress the Cheshire representative cavern to theoretical limits.

The approach employed during the investigations that challenged the integrity limits of the cavern, started by executing a series of trial and error analyses based on the initial cavern cycling conditions established on the baseline GT specification. Employing the understanding gained from the trial and error analyses, the investigations continued by modelling both long term (i.e. of the order of months) and short term (i.e. single day) cycles to gain a better understanding on how a cavern reacts to particular loading challenges. The first step was to identify the flow rates corresponding to pressures within the maximum and minimum allowable internal cavern pressures. Note that small variance in the flow rates is expected in time due to changes of the hydrogen density caused by the cavern pressure fluctuation. Finally, short shut-in periods were introduced after a change in the operation mode (injection to extraction and vice versa) to allow for surface equipment operations.

Preliminary analyses of cyclic loading

The preliminary analyses started by modelling the loading of the cavern over a 7 day period, shown in Figure 7-1 and Table 7-1, where the negative sign in the flowrate data signifies H₂ extraction. The starting pressure drop per day was estimated through industry operating guidance, where a maximum ΔP of 20 bar/day is often relied upon. For a two well per cavern basis this would result in a ~3.5 day emptying period and ~3 day fill period at max allowable flowrates (limited by erosional velocity of 30 m/s and standard well bore (8.835” ID) as specified in Section 3.2).

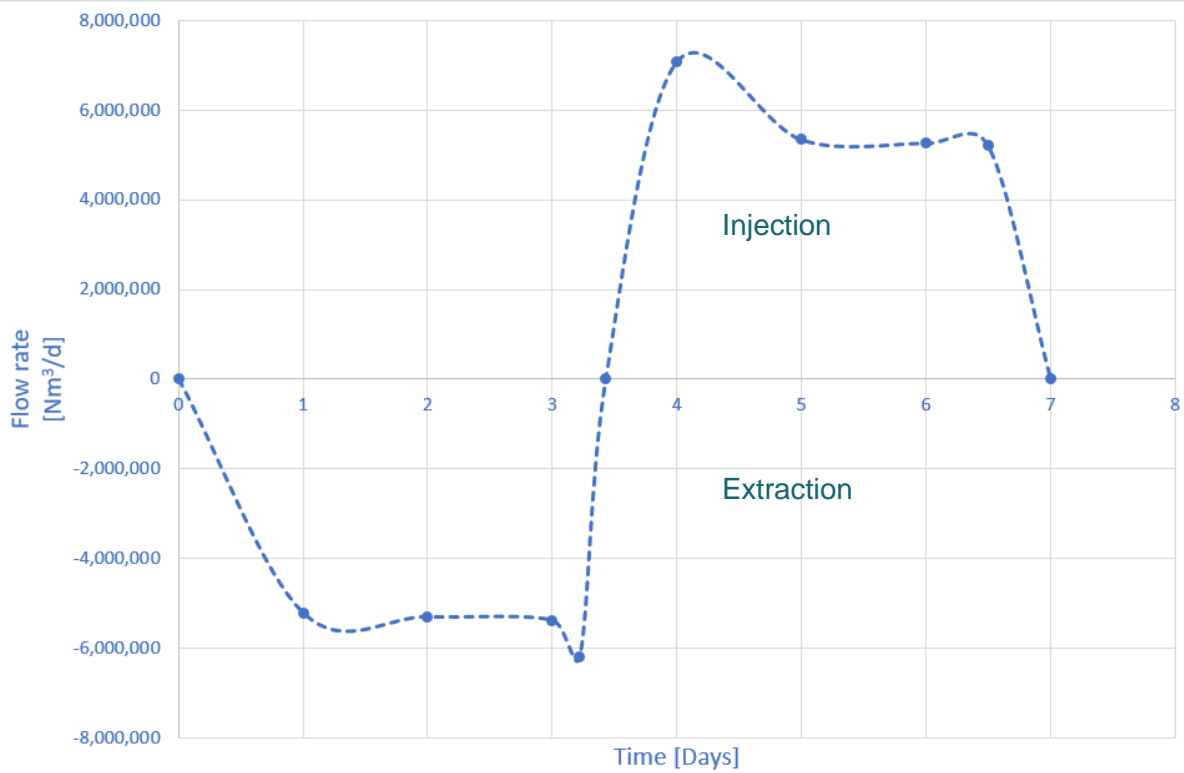


Figure 7-1: Trial and error analyses averaged flowrates, Run 1

Table 7-1: Initial cyclic loading conditions, Run 1

Day	Time [hours]	Time [days]	Flowrate [Nm³/hr]	Flowrate [Nm³/d]
1	24	1.000	-217,598.7	-5,222,369.3
2	24	1.000	-221,033.1	-5,304,794.1
3	24	1.000	-224,256.0	-5,382,144.4
4	5.27	0.219	-257,615.0	-6,182,760.8
	5.00	0.208	0	0.00
	13.73	0.572	295,509.3	7,092,224.1
5	24	1.000	222,674.1	5,344,177.8
6	24	1.000	219,339.3	5,264,143.9
7	12	0.500	216,717.4	5,201,218.2
	12	0.500	0	0.00

The result of this initial modelling, found that the specified $P_{max} = 95$ barg and $P_{min} = 30$ barg pressure limits were exceeded therefore a more iterative process would be required.

Further analysis by varying flowrates:

Four additional modelling runs were executed, where the results of the preceding modelling runs were used to refine the next :

- **Run 2a**; where the modelling started by injecting H₂ for 1 day with a flow rate of 5.3 million Nm³/d followed by a shut-in lasting for half day. After that, the modelling reverted to the normal cycles specified by the initial scenario shown in Table 7-1.
- **Run 2b**; where the modelling started by injecting H₂ for 1 day with a flow rate of 2.7 million Nm³/d followed by a shut-in lasting for half day. After that the modelling continued by employing the cycles specified in Table 7-1 with flow rates reduced to 50% of the initial scenario.
- **Run 2c**; with no initial shut in period, and thereafter follows Run 2b, with flow rates to 50% of the initial.
- **Run 2d**; with no initial shut in period, but where the modelling employed the cycles specified in Table 7-1, with flow rates reduced to 75% of the initial scenario.

The initial scenario and the additional modelling runs corresponding to Runs 2a to 2d are shown in Figure 7-2 and Table 7-2, where the graphs on Figure 7-3 show the initial cavern pressure after the cavern creation stage followed by the outcome of the respective pressure cycles. In the pressure diagrams the upper and lower pressure limits (corresponding to the specified P_{max} and P_{min}) have also been added to identify the effect that the modelled cycles had on the development of the cavern pressure.

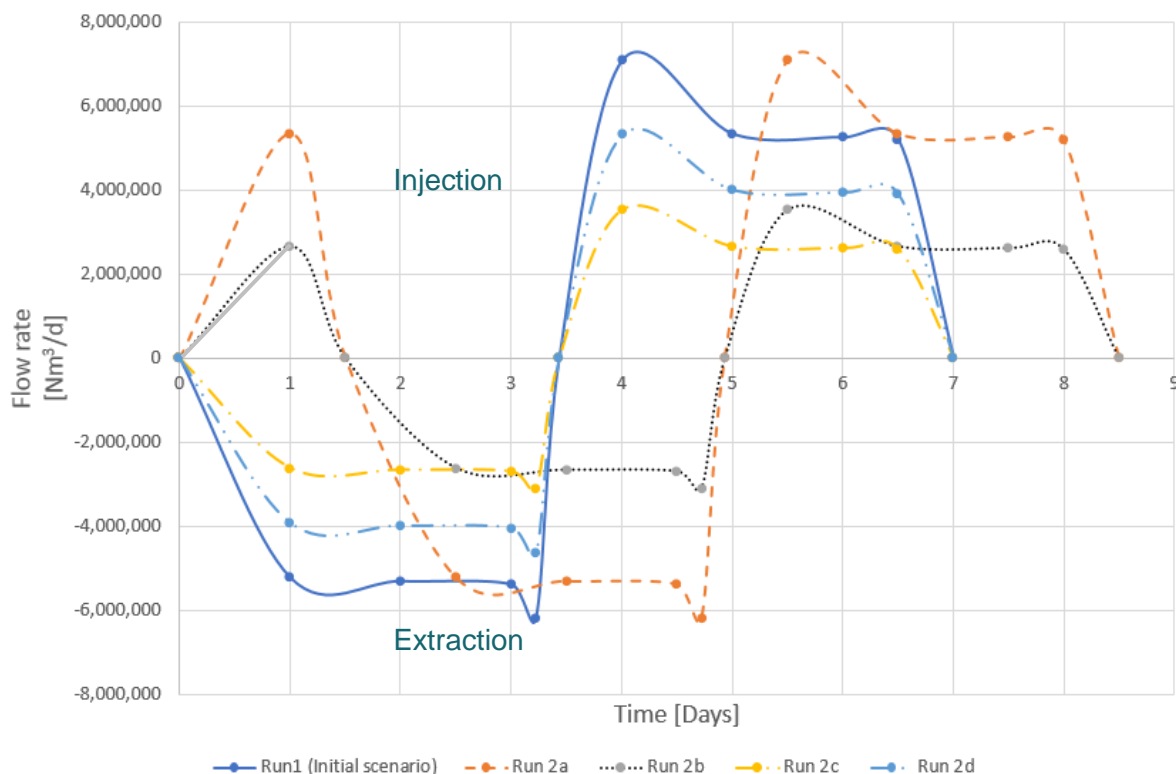


Figure 7-2: Trial and error analyses averaged flowrates, Runs 1, & 2a-2d

Table 7-2: Trial and error analyses, Runs 1, & 2a-2d

Initial scenario, Run1		Run 2a		Run 2b		Run 2c		Run 2d	
Time days	Flowrate [Nm3/d]	Time days	Flowrate [Nm3/d]	Time days	Flowrate [Nm3/d]	Time days	Flowrate [Nm3/d]	Time days	Flowrate [Nm3/d]
1	-5222369.3	1	5344177.8	1	2672088.9	1	-2611184.7	1	-3916777.0
1	-5304794.1	0.5	0	0.5	0	1	-2652397.1	1	-3978595.60
1	-5382144.4	1	-5222369.3	1	-2611184.7	1	-2691072.2	1	-4036608.3
0.22	-6182760.8	1	-5304794.1	1	-2652397.1	0.22	-3091380.4	0.22	-4637070.6
0.21	0	1	-5382144.4	1	-2691072.2	0.21	0	0.21	0
0.57	7092224.1	0.22	-6182760.8	0.22	-3091380.4	0.57	3546112.0	0.57	5319168.1
1	5344177.8	0.21	0	0.21	0	1	2672088.9	1	4008133.4
1	5264143.9	0.57	7092224.1	0.57	3546112.0	1	2632072.0	1	3948107.9
0.5	5201218.2	1	5344177.8	1	2672088.9	0.5	2600609.1		3900913.6
0.5	0	1	5264143.9	1	2632072.0	0.5	0	0.5	0
		0.5	5201218.2	0.5	2600609.1				
		0.5	0	0.5	0				

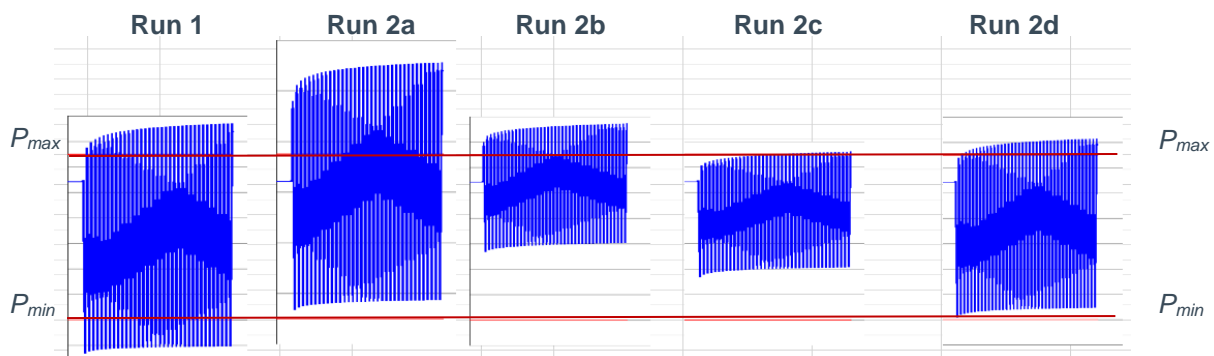


Figure 7-3: Modelling runs (Run 1, & 2a-d) against P_{max} and P_{min} limits

Assessment of the results shown in Table 7-2 indicated that there was a need to reduce the applied flow rates further to avoid exceeding the specified pressure limits. This was achieved by running two additional scenarios (Runs 2e and 2f), where:

- **Run 2e;** the modelling employed flow rates reduced to 65% of the initial scenario, and
- **Run 2f;** the modelling started by injecting H_2 for 1 day with a flow rate of 1.6 million Nm^3/d followed by a shut-in lasting for half day. After that, the modelling continued by employing flow rates reduced to 65% of the initial scenario.

The scenarios corresponding to Runs 2e and 2f are shown in Figure 7-4 and Table 7-3, where the graphs showing the outcome of the respective pressure cycles have also been presented below the table.

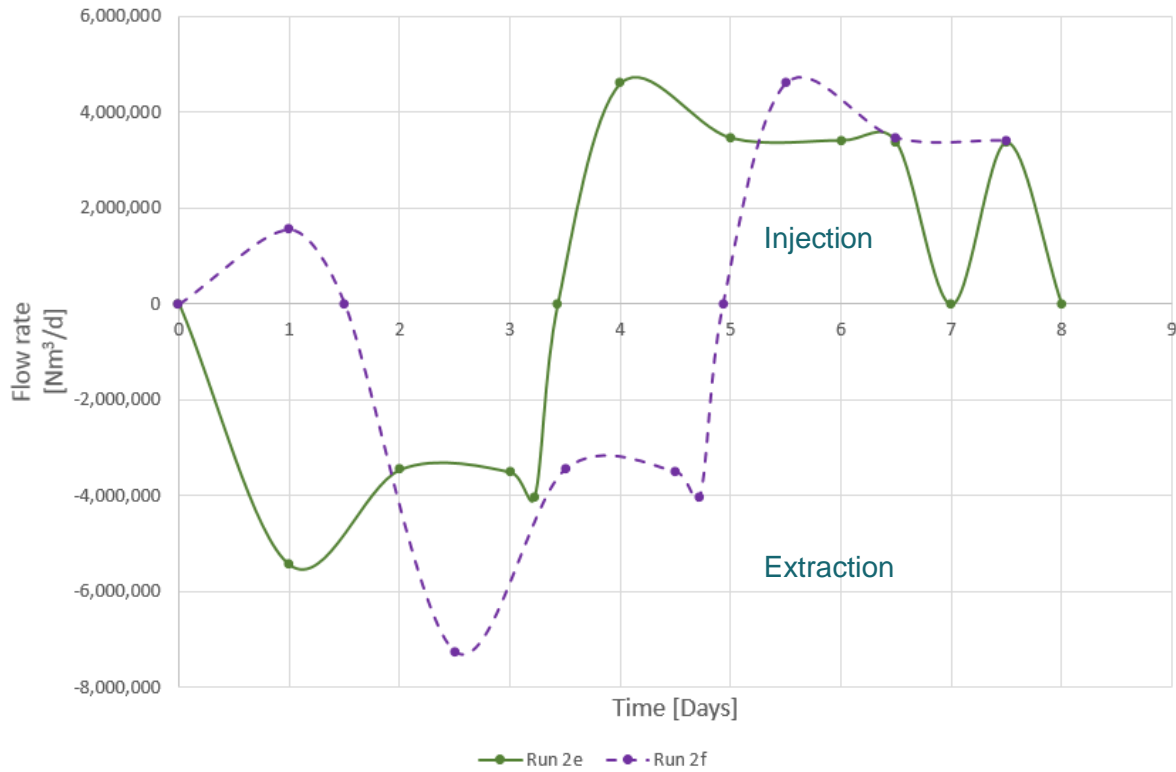


Figure 7-4: Additional trial and error analyses averaged flowrates, Runs 2e & 2f

Table 7-3: Further trial and error analyses, Runs 2e & 2f

Run 2e		Run 2f	
Time [days]	Flowrate [Nm³/d]	Time [days]	Flowrate [Nm³/d]
1	-5431264.1	1	1553654.9
1	-3448116.2	0.5	0
1	-3498393.9	1	-7259093.4
0.22	-4018794.5	1	-3448116.2
0.21	0	1	-3498393.9
0.57	4609945.7	0.22	-4018794.5
1	3473715.6	0.21	0
1	3421693.5	0.57	4609945.7
0.5	3380791.8	1	3473715.6
0.5	0	1	3421693.5
		0.5	3380791.8
		0.5	0

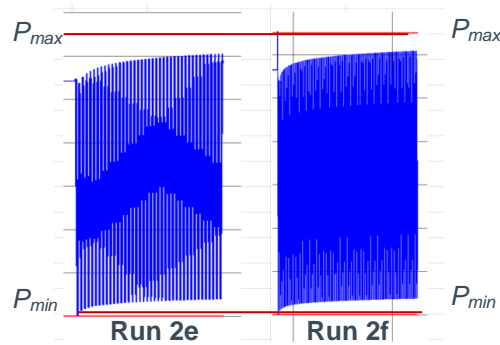


Figure 7-5: Modelling runs (2e & 2f) against P_{max} and P_{min} limits

Both runs (2e and 2f) satisfied the specified pressure limits. However, as shown in Figure 7-6, the corresponding cavern temperature results were characterised by temperatures well below the 11.2°C limit.

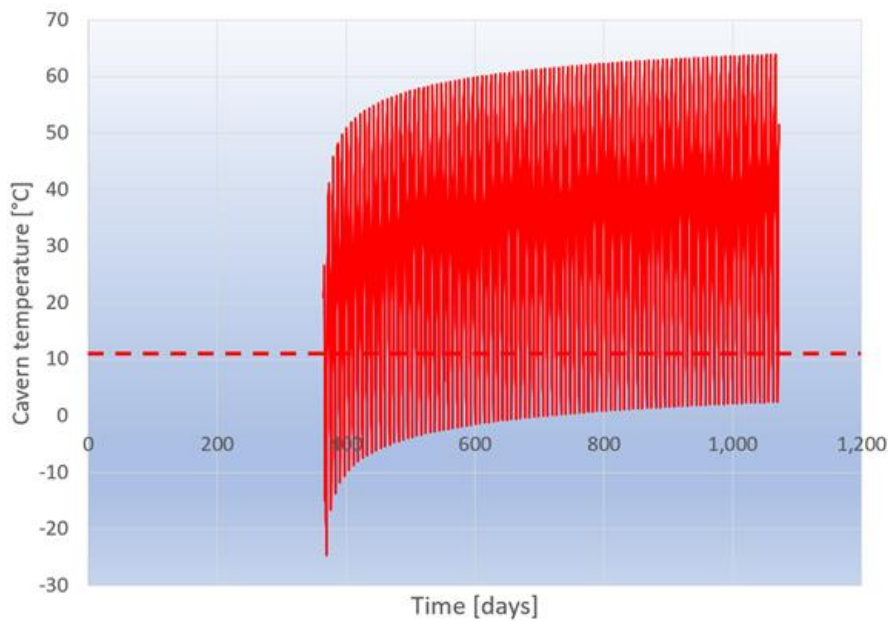


Figure 7-6: Cavern temperature cycles resulting from the execution of Run 2f

Impact of demand scenarios over prolonged period

Runs 1 and 2a - 2f indicated the flowrate limits the cavern could tolerate over a short period, with cavern pressure fluctuating from P_{max} and P_{min} , but the scenarios failed to comply with the minimum allowable temperature limit identified for the cavern (11.2°C). Therefore, investigations continued by modelling additional thermodynamic runs where for the total cycle time step was varied with empty/fill cycles with steps that last months, rather than days, to understand the minimum period that the cavern could continually extract from P_{max} to P_{min} and comply with the 11.2°C T_{min} limit.

To implement the above, a series of thermodynamic simulations were carried out for a range of H₂ daily extraction rates (ranging between 25,000 Nm³/d and 200,000 Nm³/d) with each extraction rate having a duration of 50, 80 and 100 days. The temperature and pressure results of this analysis were found to have almost linear trends and are shown respectively in Figure 7-7, Figure 7-8 and Figure 7-9. Using the results shown in these figures, it was possible to determine the cavern pressures that correspond to the intersect of temperature limit with the temperature that develops as a function of the applied flow rate.

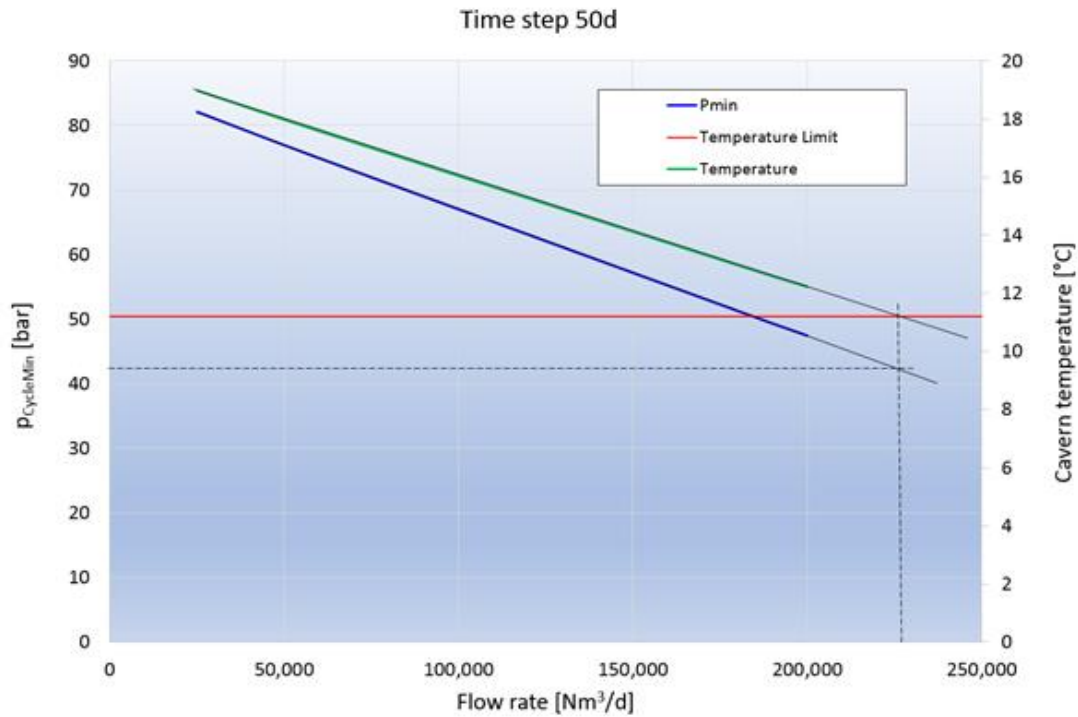


Figure 7-7: Development of temp. & pressure as a function of net H₂ flow rate per day for 50 days

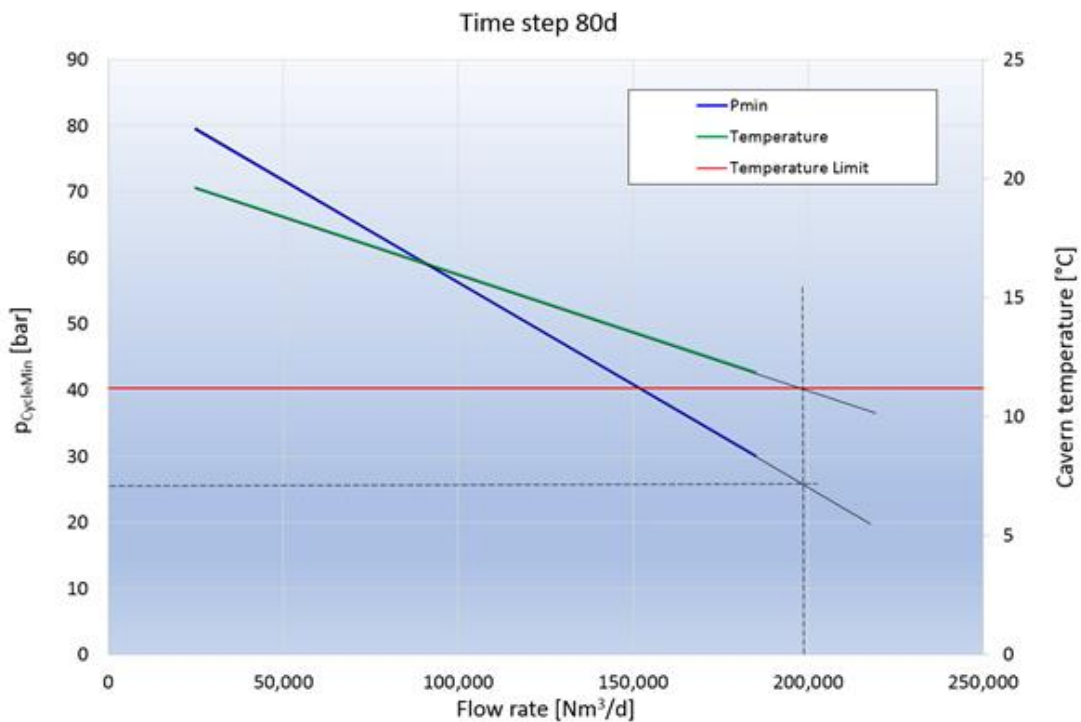


Figure 7-8: Development of temp. & pressure as a function of net H₂ flow rate per day for 80 days

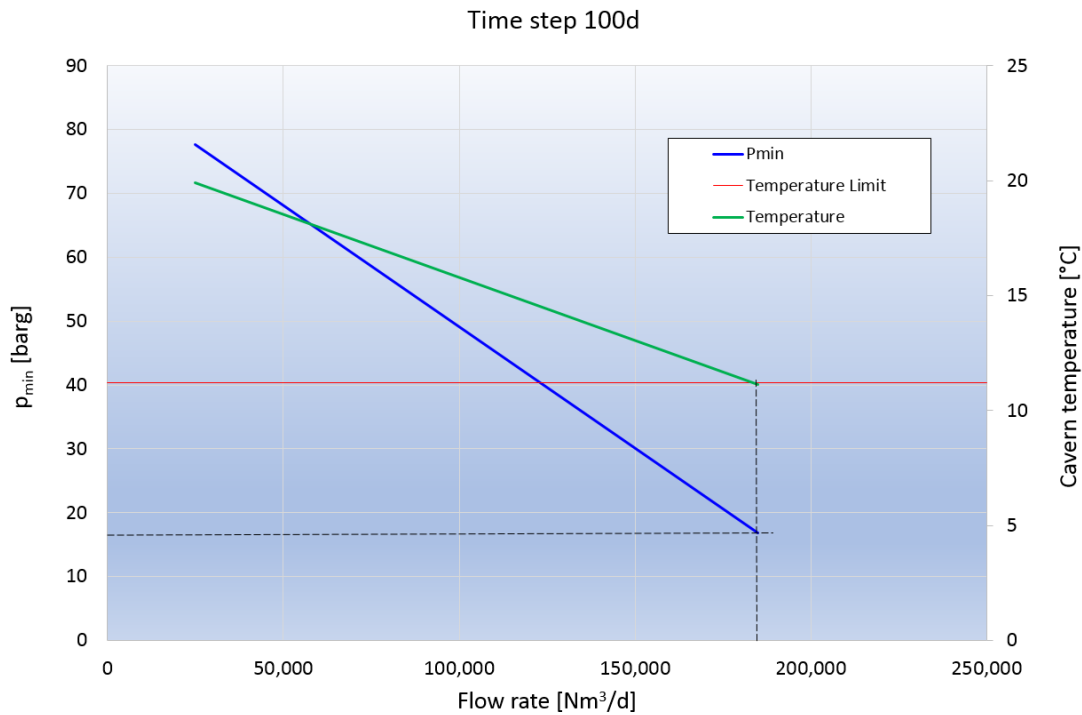


Figure 7-9: Development of temp. & pressure as a function of net H₂ flow rate per day for 100 days

Figures 7-7 to 7-9 indicate that a 100 day extraction period with flowrates more than ~150,000 Nm³/d would empty the cavern below the P_{min} , and so is unacceptable. The 80 day period, with extraction of 185,000 Nm³/day is tolerable from a temperature constraint perspective. The 50day period can offer higher flowrates daily, but again may not fully utilise the cavern inventory with a P_{min} reached of about ~45 barg before the T_{min} limit is exceeded.

The evolution of the cavern pressure that satisfies the temperature limit as a function of the applied flow rate (as derived from Figure 7-7, Figure 7-8 and Figure 7-9) is shown in Figure 7-10. This shows that a flowrate which corresponds in the reduction of cavern pressure to a P_{min} of 30 barg, over a 70 day period or less would result in the cavern remaining above the minimum temperature of 11.2°C.

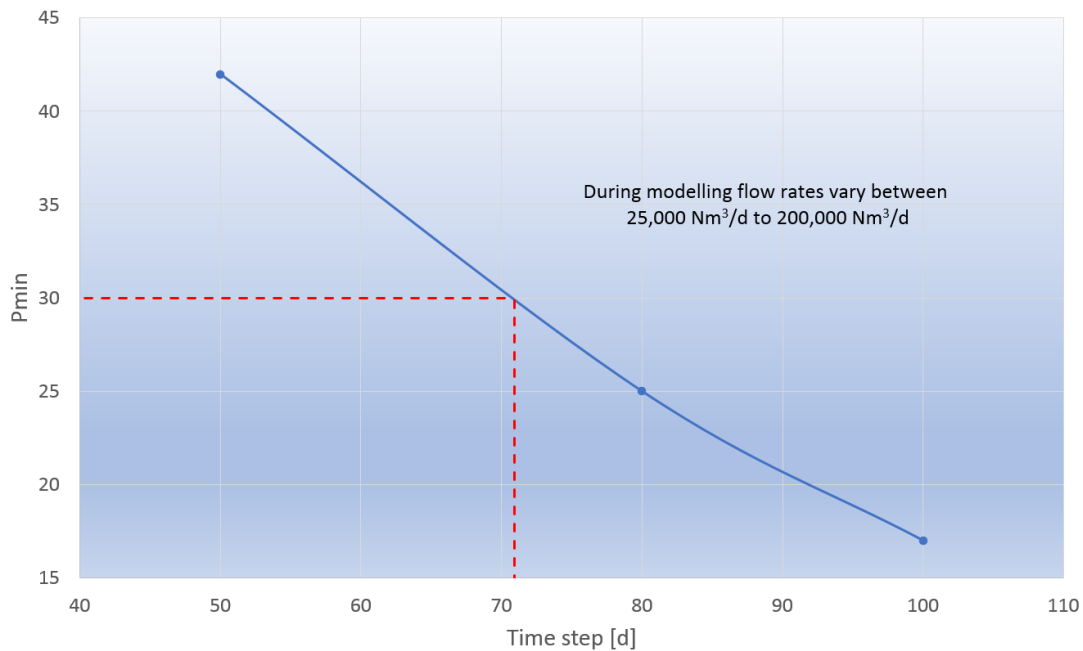


Figure 7-10: Cavern pressure that satisfies the temp. limit as a function of the applied flow rate

The results presented in Figure 7-10 provide some insight into cavern behaviour relating to extraction to P_{min} only. The results do not consider the potential impact of cavern history and injection flowrates, which may help to mitigate the temperature effects. To better understand this, two further modelling runs were executed based on the 50 and 80 day results over a 5 year period, namely:

- **Run 3a**; cyclic loading where each cycle lasted for 1.6 months (50 days emptying followed by 50 days filling) and the flow was built gradually from 90,000 Nm³/d to 296,000 Nm³/d,
- **Run 3b**; cyclic loading where each cycle lasted for 2.7 months (80 days emptying followed by 80 days filling) and the flow was built gradually from 62,500 Nm³/d to 185,000 Nm³/d.

During these additional runs, as an added measure to ease the initial high flowrates, the applied H₂ flowrates were gradually increased (over a period of 6 months) so that the corresponding pressure and temperature changes in the cavern could be kept within the limits.

The results of the pressure and temperature cycles for the 50 days and 80 days runs are shown in Figure 7-11 and Figure 7-12 respectively. Evidently the 80 days step simulation satisfies both the pressure and temperature limitations, but the 50 days step scenario results in temperatures below the 11.2°C limit.

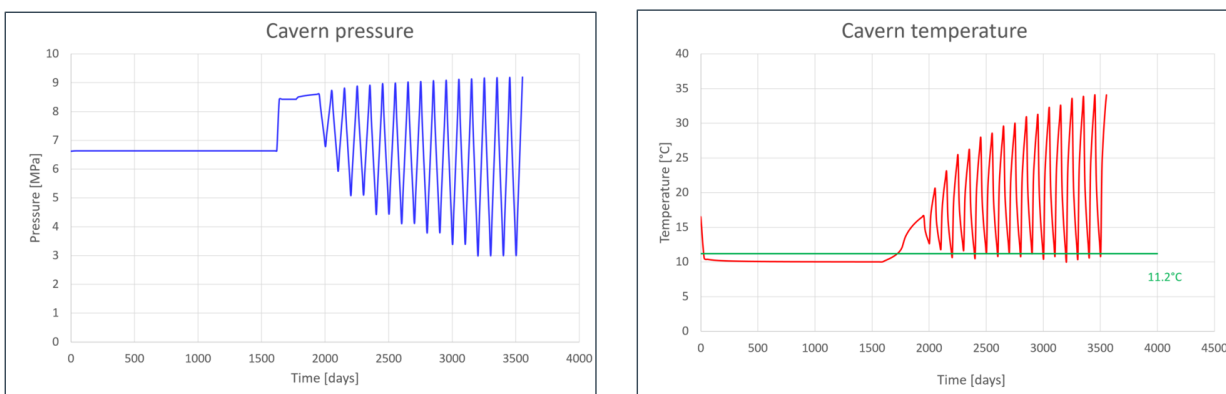


Figure 7-11: Results of the thermodynamic analysis when employing cyclic loading that incorporates 50 days steps

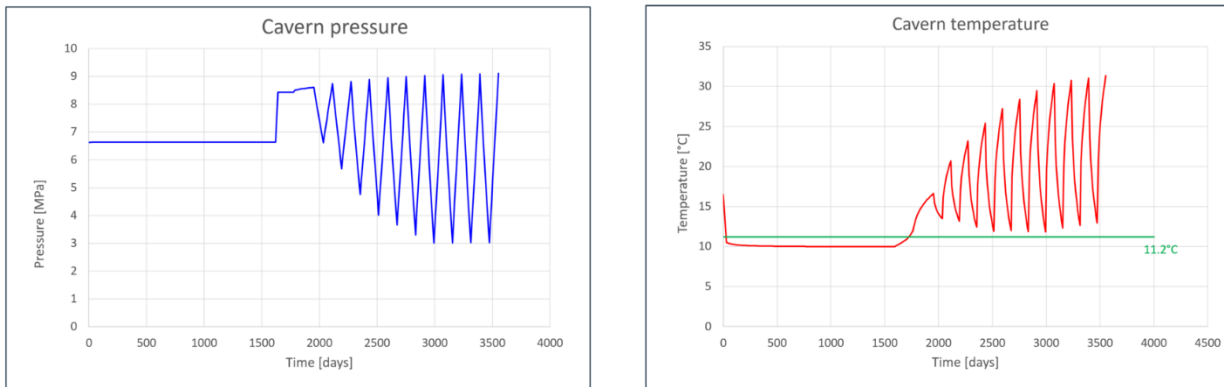


Figure 7-12: Results of the thermodynamic analysis when employing cyclic loading that incorporates 80 days steps

The consequence of these low temperatures for the 50 days step scenario, are shown in the results of the coupled thermo-mechanical analysis (using the FLAC software package) where it is evident that tensile stresses are developed at the cavern walls (see Figure 7-13 and Figure 7-14). By examining Figure 7-13 closely one can identify localised light red areas indicating temperatures below 12°C at the walls of the cavern. It is at those areas that tensile stresses due to temperature and pressure reduction are evident (Figure 7-14).

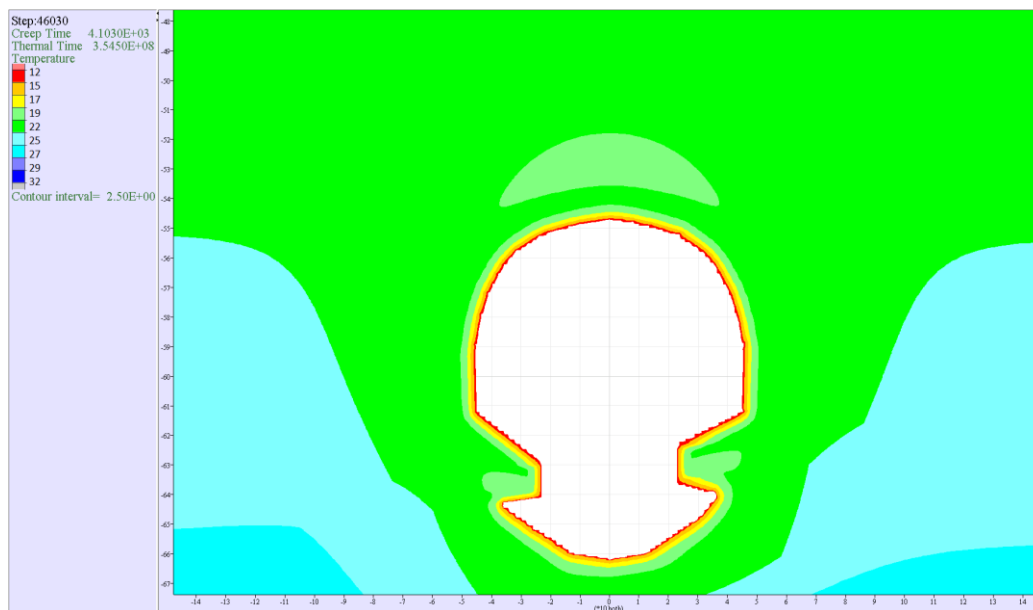


Figure 7-13: Temperature distribution results when employing 50 days steps cyclic loading

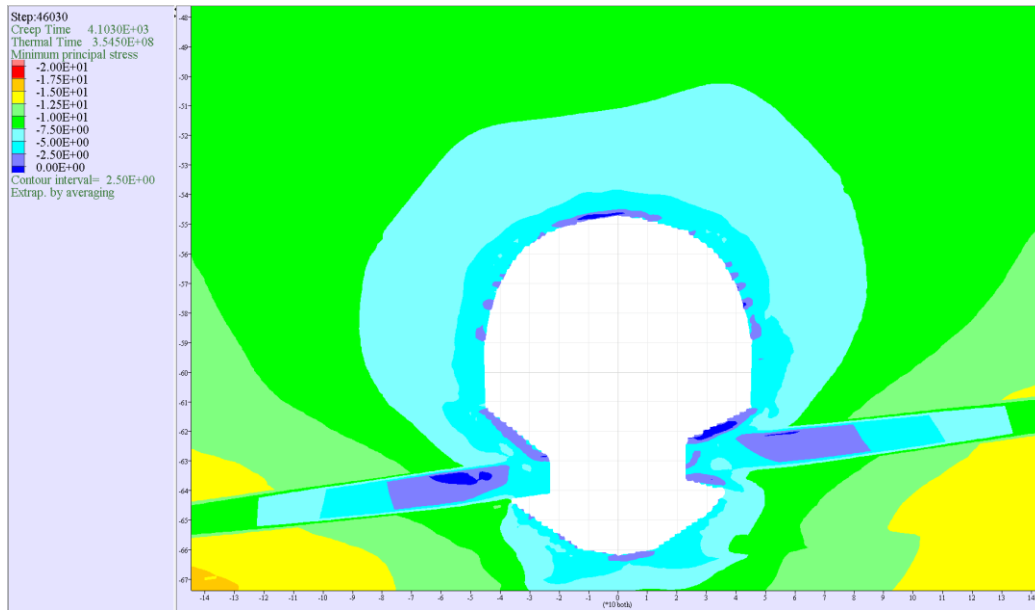


Figure 7-14: Minimum principal stress distribution results when employing 50 days steps cyclic loading

Consolidating key findings, by applying high extraction flow rates over single day

In addition to modelling the thermodynamic response of a cavern when subjected to cycles with steps that last months, further investigations were carried out for a cavern that is subjected to a single cycle which lasts a day. During these simulations, the H₂ flow rates varied between 1.5 million Nm³/d and 3.0 million Nm³/d and the effect of applied flow rates on the pressure and temperature is shown respectively in Figure 7-15 and Figure 7-16. Evidently, when a cavern is subjected to a single cycle that lasts a day, the maximum acceptable flow rate should be approximately 1.6 million Nm³/d.

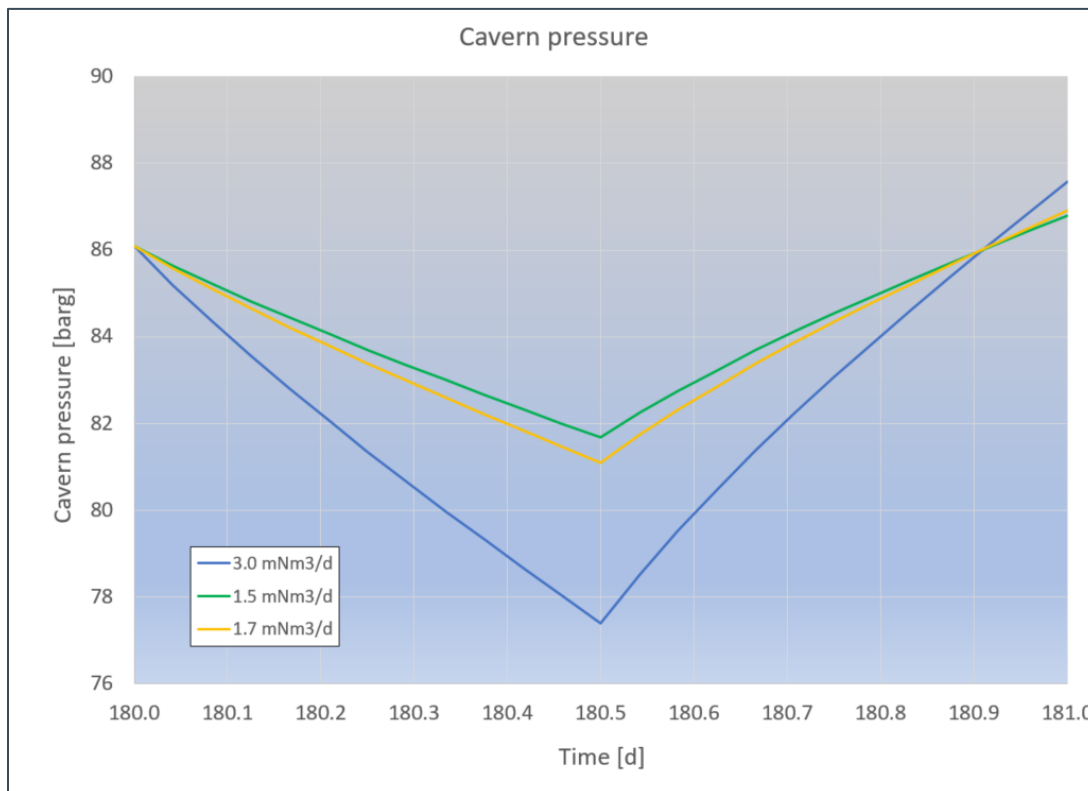


Figure 7-15: Single daily cycle, cavern pressure for a range of flow rates

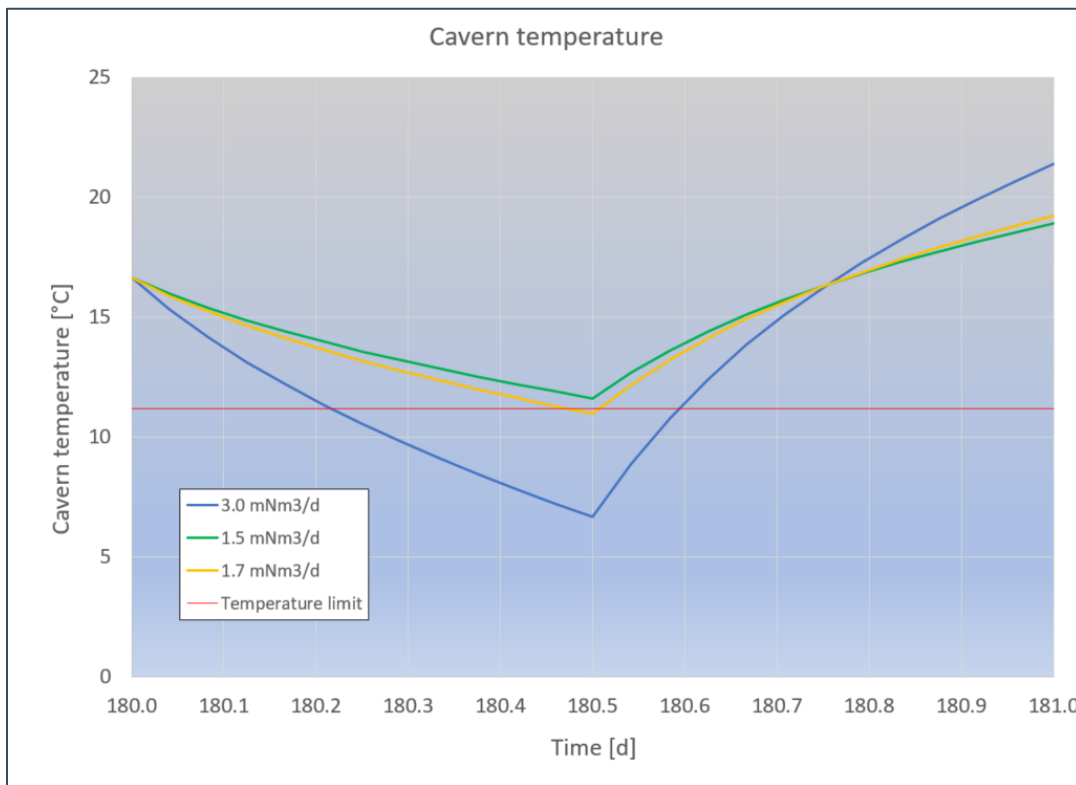


Figure 7-16: Single daily cycle, cavern temperature for a range of flow rates

Maximising the differential pressure of fast daily cycles

Further to these analyses, the response of a cavern to fast daily pressure cycles as the difference between P_{max} and P_{min} increases, was investigated over 5 years. During these loading scenarios, the employed cyclic conditions resulted in a minimum pressure of 62 barg and maximum pressure that was raised (in each run) to 70 barg, 72 barg and finally 83 barg. The minimum temperature observed throughout the modelled operations was 0.25°C with a maximum 47.43°C.

The results of the final run are shown in Figure 7-17 and 7-18 respectively for the pressure history and the temperature history. The pressure change of this run is approximately 21 bar/day due to the flow rates used, which coincidentally aligns this case with the original modelling assumption, where an industry assumed pressure change of 20bar/day was used.

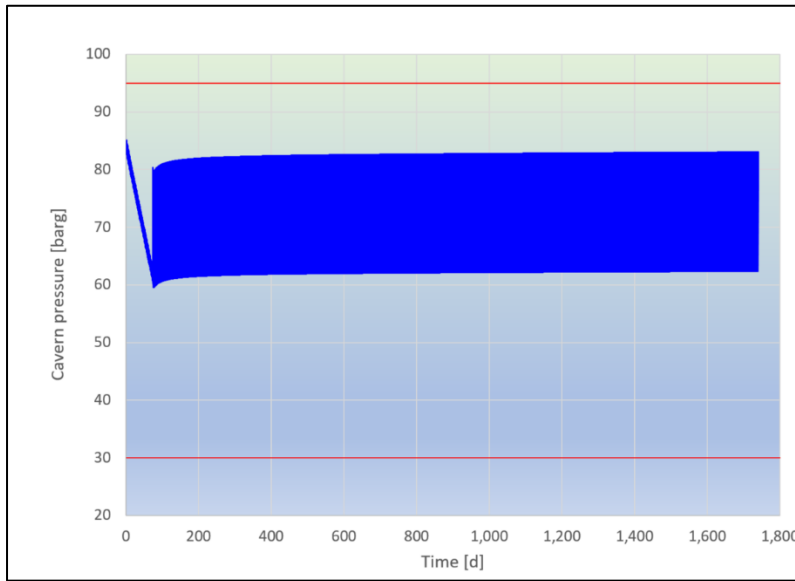


Figure 7-17: Development of cavern pressure between 62 barg and 83 barg

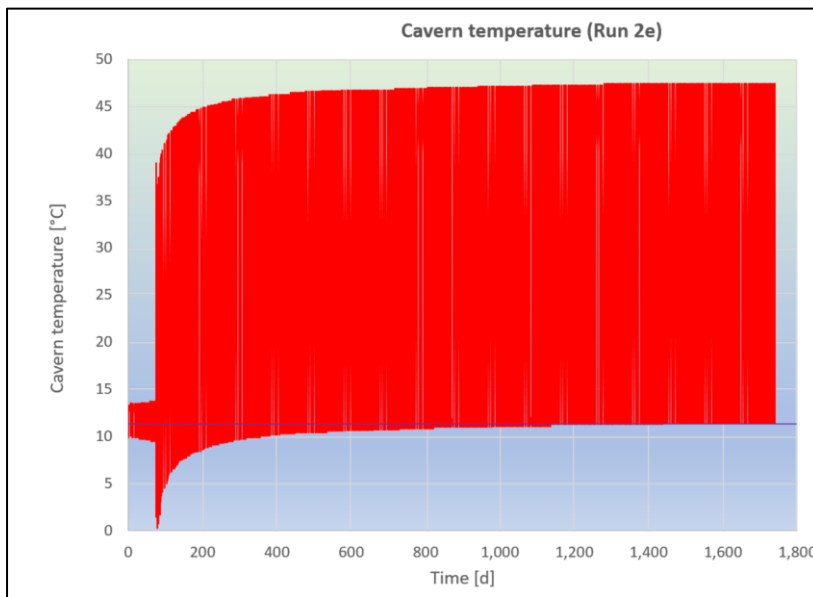


Figure 7-18: Cavern temperature history when pressure cycles between 62 barg and 83 barg

FLAC stress analysis on breach of 11.2C temp limit constraint

To investigate the relatively low temperatures shown in Figure 7-18 a coupled thermo-mechanical analysis (using the FLAC software package) was carried out to investigate whether tensile stresses are developing at the cavern walls. The minimum cavern stresses after one year of operations can be seen on Figure 7-19. Little difference can be seen in the minimum stress regime at other points in time.

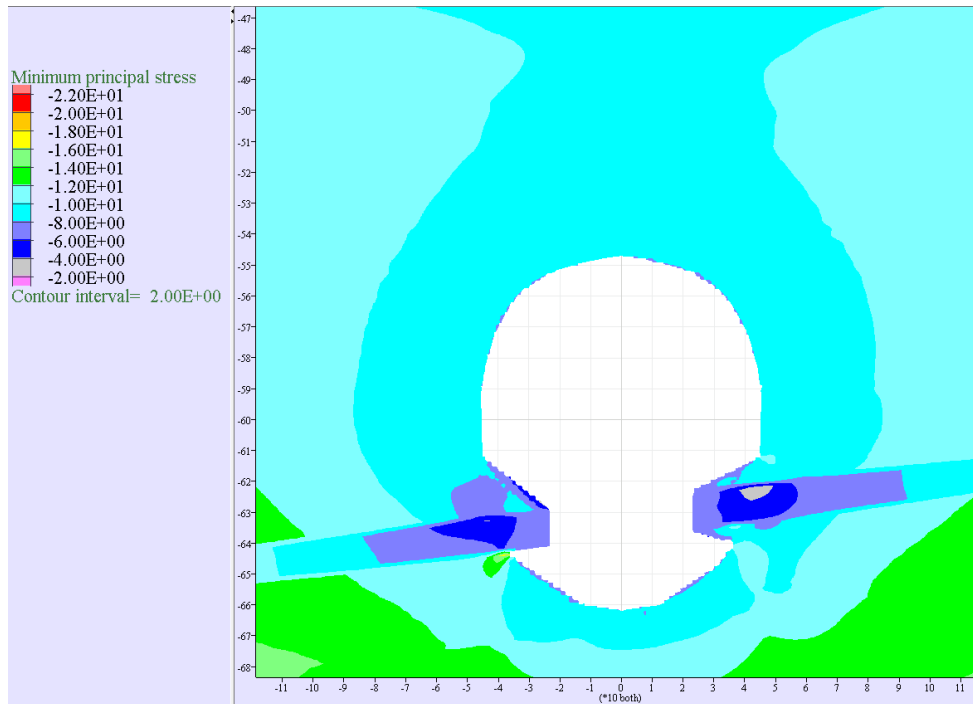


Figure 7-19: Min. principal stress distribution (in MPa) for daily cyclic loading between 62 barg and 83 barg

A key finding realised from this is that despite the fact that the cavern temperature is well below the temperature limit of 11.2°C (as shown in Figure 7-18) during the first 400 days, the distribution of the minimum principal stress (i.e. the least compressive stress component) around the cavern remains firmly in the compressive regime. It also indicates that due to the fast cycling nature, while the difference between P_{max} and P_{min} was kept constant, no tensile stresses develop at the walls of the cavern.

It is noted that the SCTS program (which has been used in this work), like most of the available software packages used in the thermodynamic computations of storage caverns, such as DeMeTher (Louvet et al, 2017), SiTherGaz (Pellizzario et al, 2011), KavPool (ESK, 2017); simulates the cavern using a single bulk cavern temperature and a single bulk cavern pressure.

As a result, the stratification of the pressure gradient is ignored (i.e. the fact that gas pressure will always be lower near the cavern roof is not considered) and the intense temperature changes that occur at the end of the production tube near the cavern roof are smoothed over by inferring a uniformity in the temperature distribution.

These two simplifications inevitably result in an underestimation of the stress concentrations that develop in the roof of the H₂ storage cavern, as the cavern is subjected to the continuous withdrawal/injection cycles. Note that the extreme low temperatures found 100 days after the commencing of operations are not considered representative of the cavern behaviour and can be avoided by minor modifications of the operational cycles.

Moreover, the geomechanical software packages that calculate the mechanical and thermal stresses, be it:

- Finite difference programs such as the program FLAC used in this work (Itasca, 2011b), or
- Finite element programs such as the program ComSol (Louvet et al, 2017)

cannot incorporate the effect of fatigue on the strength of salt. Consequently, the employed coupled thermo-mechanical modelling process is unable to incorporate a cavern loading scenario whereby the integrity of a salt cavern may be compromised if the fatigue limit of salt is exceeded. However, it is interesting to note that laboratory cyclic testing of salt specimens has shown that it may take 50 years of storage operation (assuming one pressure cycle a day) to result in an accelerated dilatant volumetric strain that could signify a potential material failure (Arnold et al, 2011).

7.4. Seasonal profile; analysis of seasonal plus diurnal loading cycles.

Having gained an understanding of the thermodynamic response of a cavern, when subjected to a range of cyclic loading scenarios, the investigations proceeded further by modelling scenarios comprising daily cycles superimposed on existing seasonal cycle, to identify how caverns behave when subjected to challenging loading conditions.

Chapter 4 has reviewed storing H₂ in salt caverns. The H₂ storage for this was analysed under a daily cycle, where the difference between P_{max} and P_{min} was kept constant. The results of this have shown that the cavern options at each location can achieve this for a fuel gas stream 1, scenario 3 case (where two 5-hour peaks are met each day and 14 hours injection). However, the fluctuations in UK gas demand introduces a challenge that H₂ would need to meet if it is to support decarbonisation on scale. Additionally, if H₂ is sourced from fossil fuels or blended with NG as a fuel gas stream, then the extraction from the cavern would track this national demand. The cavern demand could therefore face an extremely turbulent demand profile as it looks to optimise feed stock market pricing (arbitrage of energy) with generation to meet a peak demand matching electrical application.

To investigate this further a national gas demand profile from 2016 was used to interpret the changes in cavern pressure expected (National Grid, 2017). The national grid website was used to obtain UK gas demand summary reports across a one-year period. A graph of the annual UK gas demand between October 2016 and October 2017 is shown in Figure 7-20:

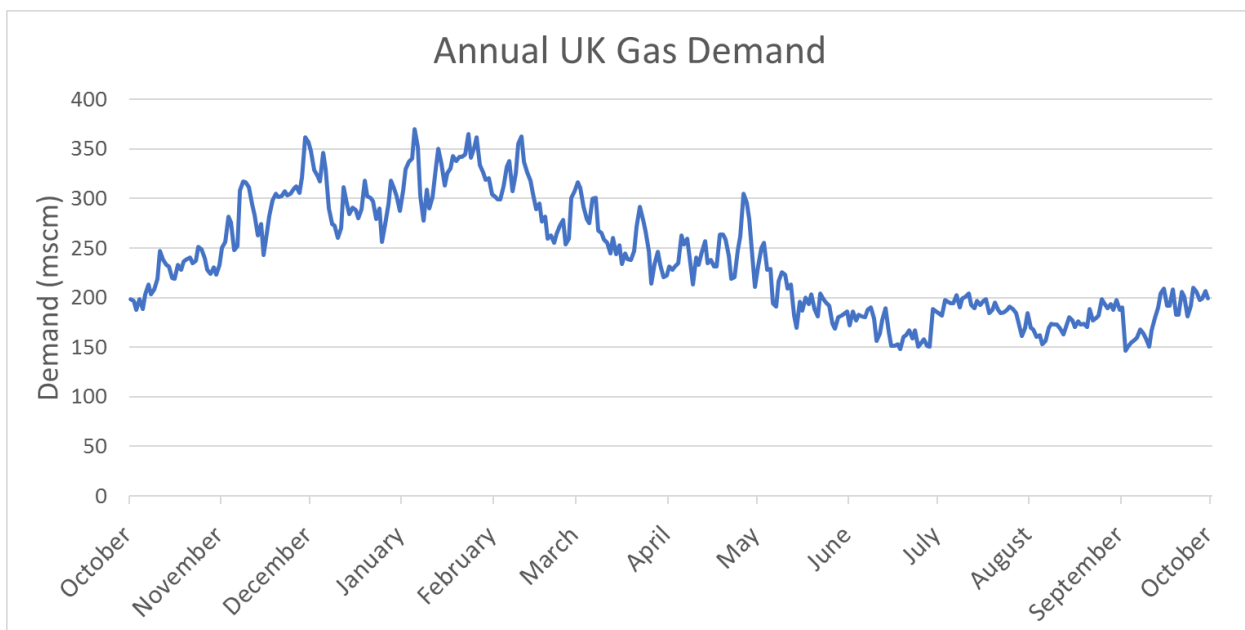


Figure 7-20: National Grid 2016 gas demand UK

From Figure 7-20, demand is highest over the cold winter period, where injection would be minimal to the cavern. Conversely, during the summer months, gas storage sites will typically inject to fill the caverns. The strain placed on the national grid over winter months highlights the importance of storage facilities. Fluctuations in seasonal gas prices also means there is opportunity to sell gas at elevated prices over a short period.

Matching hydrogen cavern storage requirements to seasonal demand

To match the seasonal demand profile the following methodology was undertaken:

- The assumed cavern parameters were taken for the Cheshire idealised profile where the cavern operating pressures are between 30 bar and 95 bar.
- The gasifier/ cavern supply split to the GT was assumed to be the same as that used by the fuel requirement study (Table 6-5).
- The H₂ production rate was assumed to be constant, either to the GT during operation or to the cavern during injection cycles.
- The generation profile was based around an average profile of Scenario 3 (as defined in Chapter 1, Figure 1-4, two 5 hour extraction cycles and two 7 hour injection cycles), yet in some instances a shortened duration of generation would be expected to reduce the cavern emptying rate on that particular day.
- Initially a two cavern basis was used, but later runs were completed with up to 5 caverns to verify the impact on the cavern.
- For the cavern to provide useful storage capacity, it was assumed that the storage of gas, and therefore buying of fuel, would need to precede that of the peak demand periods. As such, a two month lead time was assumed (identified in Figure 7-18 compared to Figure 7-17). This lead time is in line with the typical operating conditions of gas storage sites, where the gas inventory is aimed to be at full capacity before the high demand winter months. This allows the storage site to have long periods of gas extraction and to buy cheaper fuel during periods of low gas demand.

The demand cycle data was processed to develop an input format for SCTS which would allow the cavern to operate between P_{max} and P_{min} while also following the same seasonal trend. This is presented in Figure 7-21.

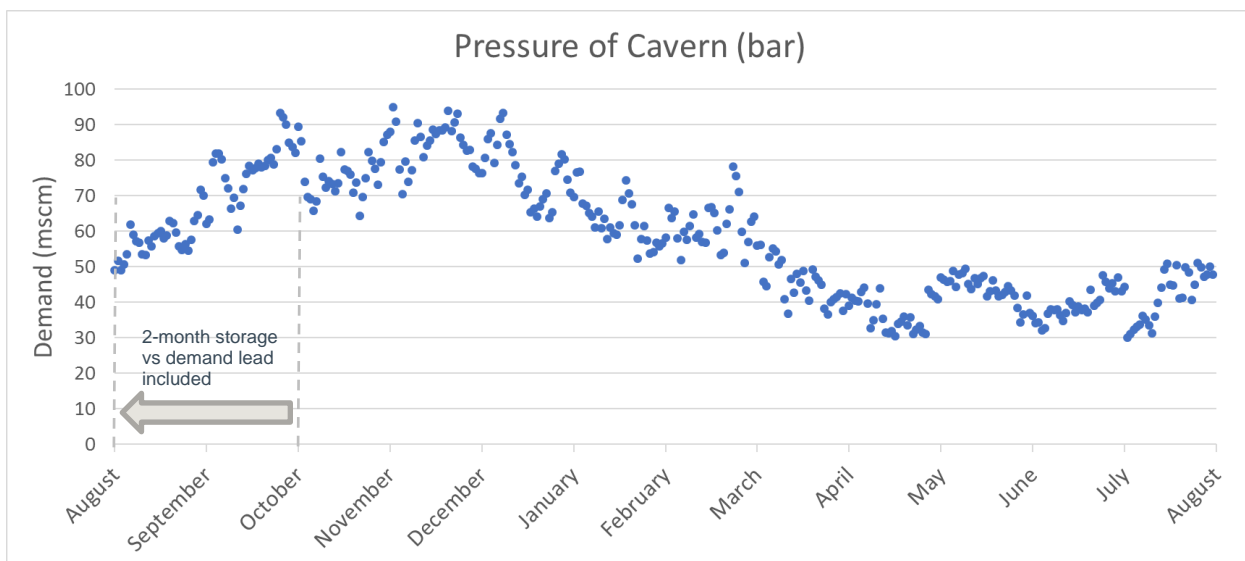


Figure 7-21: Initial cavern seasonal cycle

For consistency, the diurnal cycle superimposed onto the seasonal cycle remains Scenario 3. To enable the seasonal cycle to be realised, the diurnal cycle was modified to allow either a decrease or reduction in overall cavern volume per day. This was achieved by varying the injection total volume and where necessary reducing the generation time period to allow a higher net cavern filling on that particular day.

An example of the initial profile is shown in Figure 7-22 where these were used as the basis of the modelling.

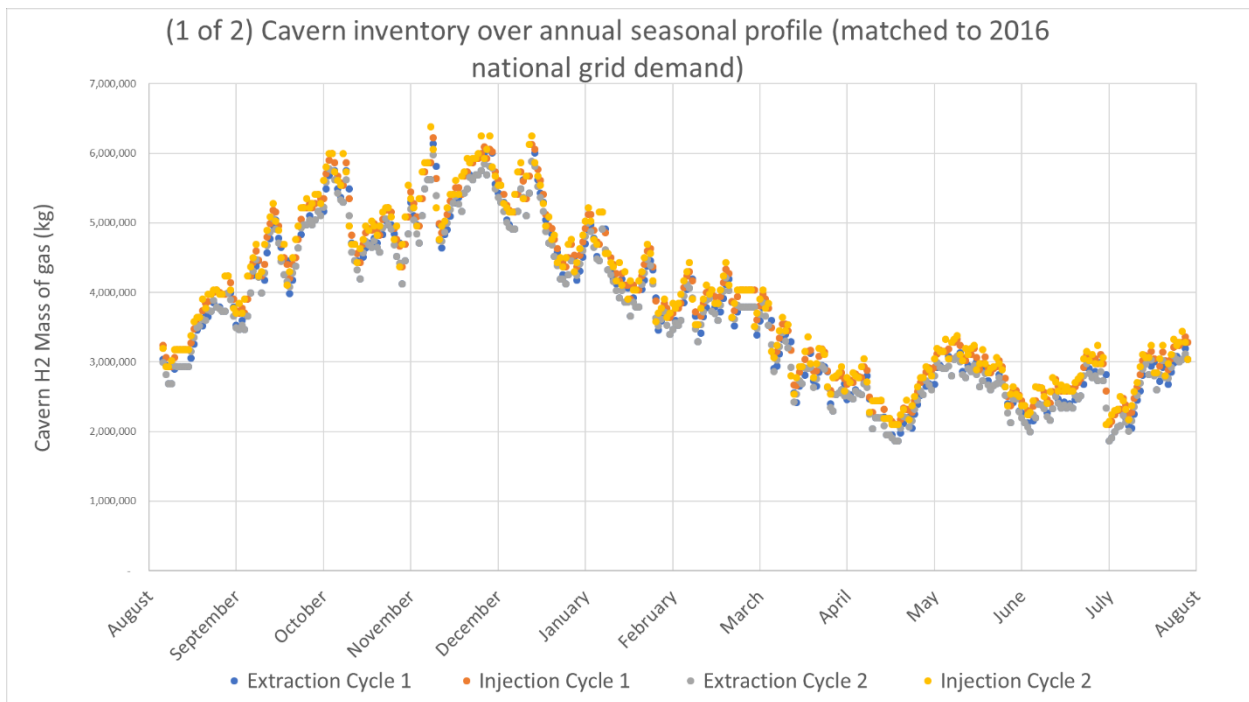


Figure 7-22: Interpreted cavern demand from national profile

The following assumptions were used to determine the required injection / extraction flowrates:

- The daily UK gas demand was plotted across a period of one year (Figure 7-20).
- The working pressures of the cavern were aligned with the demand profile; matching a P_{max} of 95 bar (cavern full) with the highest demand day and a P_{min} of 30 bar pressure (cavern empty) for the lowest demand day.
- Interpolation was then used to assign a pressure to each day based on the UK gas demand on the associated day.
- The fuel requirement for an individual cavern was estimated using the methodology outlined in Appendix F.1.2. This estimation used the LHV of fuel gas stream 1 and the expected power output from a 2x (2+1) SGT-2000E arrangement. The total fuel extracted from a cavern could then be calculated, which remained broadly consistent throughout the seasonal profiling.
- The required change in cavern inventory and injection / extraction across each day to meet the daily pressure profile could then be calculated.
- In some cases, the daily changes in gas demand were extreme and it was necessary to remove outliers to smooth the profile to within cavern and well capabilities.
- The cavern was modelled to undergo one full empty and filling cycle across the year, where the gas inventory at the year start and year end would be the same.

Results of seasonal modelling (for diurnal, Scenario 3 case) to maximise cavern use:

The combined seasonal plus diurnal loading analysis started by executing four scenarios based on the initial cycle presented in Figure 7-22 (corresponding to Runs 1, 2, 3 and 4) whereby, in order to satisfy the baseline GT specifications, the number of the required caverns were adjusted accordingly. It is noted that the following runs were undertaken as part of an iterative process where the behaviour of the cavern was better understood at the end of each run and the input conditions adjusted to improve the overall results:

Table 7-4: Seasonal modelling runs maintaining Scenario 3 daily

Modelling run	Number of caverns	Individual Cavern extraction (average)	Commentary (changes to last run)
Run 1,	2	48,720.09 (kg/hr) / 196,928.41 (Nm ³ /hr)	Initial seasonal model based on worksheet interpreting the demand profile of national demand to individual cavern.
Run 2,	3	32,480.06 (kg/hr) / 131,285.61 (Nm ³ /hr)	Offset start date to be near cavern full case to coincide with end of brine phase, 3x cavern basis has been used to reduce extraction / injection demands, Mass balancing over the year has been achieved by increasing all injection phases by a small factor to help temperature profiling, Areas of extreme and repeated extraction have been smoothed,
Run 3,	5	19,488.04 (kg/hr) / 78,771.36 (Nm ³ /hr)	5 cavern basis used in an attempt to reduce periods of high extraction and injection to reduce temperature effects.
Run 4,	3	32,480.06 (kg/hr) / 131,285.61 (Nm ³ /hr)	Return to 3 cavern basis, as 5 cavern not optimised solution when individual peaks smoothed out. Using the P _{max} , P _{min} boundaries the cavern inventory was refined to fit within estimates at the input data stage (prior to modelling results)

The results of these four runs are included in the Appendix G in the form of time diagrams per cavern, showing the H₂ flow rate, the cavern inventory, the cavern pressure and the cavern temperature. Examination of the results shown in Appendix G indicate that only the cyclic loading corresponding to Run 4 satisfied the restrictions imposed by the P_{max} and P_{min} limits (see Figure G2-14 reproduced here for convenience as Figure 7-23). However, as shown in Figure G2-15 (re-plotted here for convenience as Figure 7-24), in the initial stages of Run 4 several temperature dips were below the temperature limit of 11.2°C. Nevertheless, this is understood to be a temporary effect that occurs during the early part of the temperature history of the cavern, which is characterised by an average gradual increase of 0.033 °C/day.

Comparison of Figures 7-23 and 7-24 indicates that as H₂ is injected, the H₂ in the cavern is compressed and the cavern pressure increases leading to an increase in the cavern temperature. When the H₂ in the cavern is withdrawn and the pressure in the cavern is reduced, the resulting adiabatic expansion leads to a decrease in the cavern temperature. The salt mass that surrounds the cavern acts as a constant temperature heat source or heat sink, depending on whether the cavern H₂ temperature is higher or lower than the respective geothermal temperature.

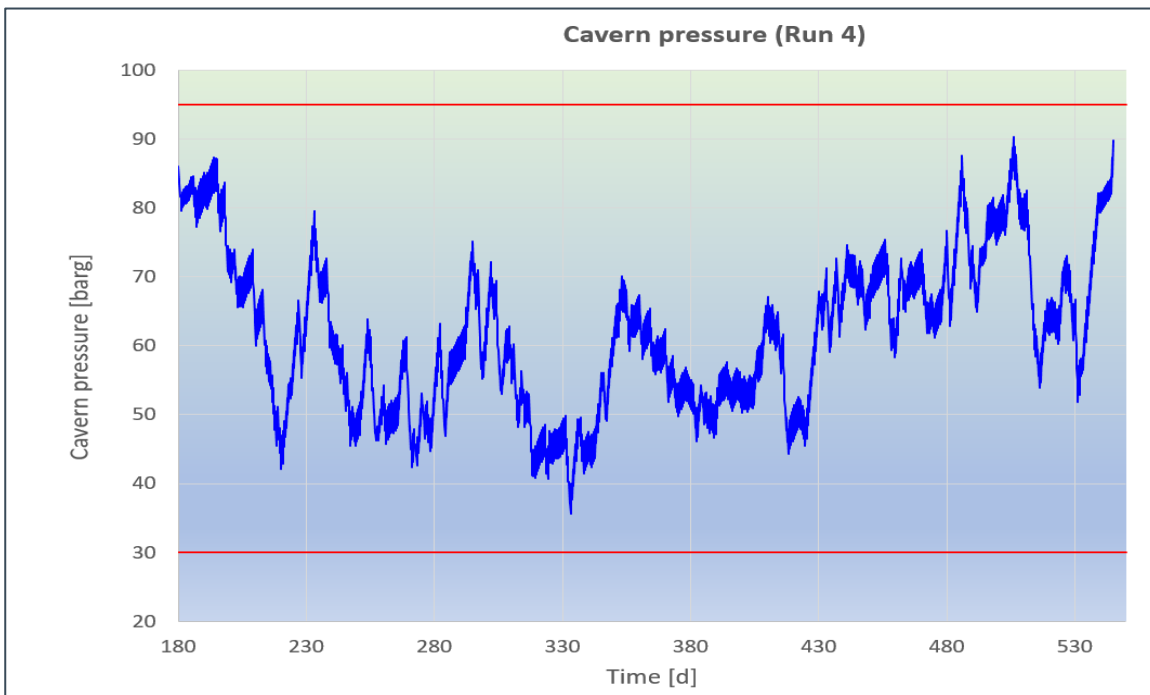


Figure 7-23: Pressure profile of individual cavern, Run 4

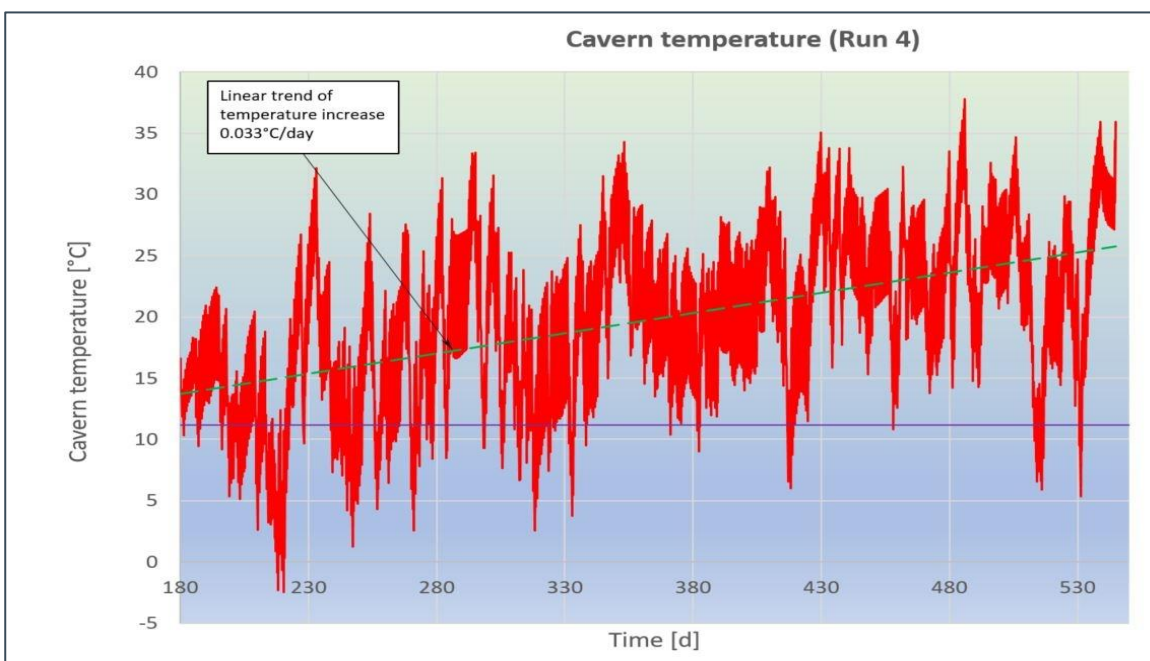


Figure 7-24: Temperature profile of individual cavern, Run 4

7.5. Conclusions/ Discussion

The analyses undertaken for this chapter have revealed that when a cavern is subjected to slow rate loading cycles (characterised by steps of the order of months) then, if the temperature in the cavern is lowered below the temperature limit of 11.2°C, tensile stresses are expected to develop at the walls of the cavern.

On the other hand, if when a cavern is subjected to fast daily loading cycles then, even if the temperature in the cavern is lowered below the temperature limit of 11.2°C, no tensile stresses develop at the walls of the cavern.

Consequently, although no tensile stresses developed in the cavern walls when the temperature limit of 11.2°C was exceeded during the daily fast loading cycles, one should not assume that the respective long-term integrity of the cavern is safeguarded.

Through completion of this stage of the study the following key findings were realised, giving a unique insight into the response of the cavern to challenging injection / extraction swings as the cavern would look to match the UK demand requirement:

- The modelled H₂ storage with 3x cavern (6 wells) at the Cheshire site is sufficient to meet the daily injection / extraction spikes required as set out by the UK national gas demand trend. Clearly, the caverns would only provide a proportion of the total UK supply, and the 1 GWe system could be scaled as required, based on this conceptual 3 cavern system.
- The salt caverns in this case study provides capacity to deliver 1 GWe consistently across the year, while also benefiting from being able to meet short term demand spikes and equally troughs in raw fuel pricing for the production of H₂. A more detailed economic analysis on this would assist in developing the initial investment case for this novel concept.
- Multiple caverns reduce the hourly injection / extraction flow rates experienced by the cavern and well production tubing. Yet, it is the net cavern balance at the end of a 24 hour period that has the largest effect over a prolonged period. For this reason, high isolated cases of injection / extraction may be tolerable if in the following days the demand profile is relaxed.
- The cumulative effect of extraction over multiple days caused significant cooling of the cavern.
- The cumulative effect of injection over multiple days causes significant warming of the cavern.
- A thermal store effect is exhibited in the cavern if the cavern is gradually warmed in its initial (approx. 6 month) phase following de-brining. This can lessen the temperature effect of high initial extraction rates, which would cause rapid cooling (below tolerable).

It is noted that, a seasonal cycle (with a superimposed diurnal generation cycle), which does not exceed cavern limitations of P_{min} , P_{max} , and T_{min} , has not been determined within this case study. However, the constraints which impact these limits have been investigated and are now understood. As such, there is a clear theoretical foundation on which to base the realisation of a H₂ peak demand matching project.

In addition, it is clear that the prediction of the thermodynamic response of a H₂ storage cavern is intimately linked to the loading history associated to the storage operations that have taken place in the past. In other words, it is not acceptable to model in isolation a prescribed stand-alone storage operation scenario related to a specific pressure history without incorporating the preceeding storage events. The effect of any imposed loading conditions is affected by what has happened before to the storage cavern. To this end, when modelling a peak demand scenario a wider, more long term view is important when assessing the cavern's thermodynamic response.

ATKINS

Chapter 8: Study Conclusions



8. Study Conclusions

The use of salt caverns for H₂ storage has been proven through several commercial projects worldwide. However, the combination of storage with power generation represents a new opportunity for energy storage, where it could be used to offset the intermittent supply provided by renewable energy sources, such as wind and solar. Specifically, the ability of caverns to accept the type of fluctuating power demand cycle defined within this document had not been considered previously. The focus of this report was to establish the capability of salt caverns to store a H₂ rich fuel source under a challenging fast 'churn' generation cycle. Specifically, the objectives were defined as follows:

- Consolidate the ETI understanding of cavern flexibility, to support ETI system level modelling activities, for up to 100% H₂ and H₂ / methane mixtures, with a focus on flexibility and cost.
- Characterise key constraints and their causes when operating fast churn storage at selected sites, including those caused by integration with the H₂ supply and the GTs.
- Identify a range of GT / CCGT offerings which match cavern capability or market needs.
- Provide insight on cavern capability and limitations on duty.
- To provide high level estimates for a complete plant solution, with greater CAPEX and OPEX certainty, in line with AACE5 level (-50% +100%).

Fundamentally this study has fulfilled each of these objectives where it has shown that salt caverns can provide the level of storage required to support H₂ peak demand power generation, without integrity issues. It has also identified that the technology required to develop such a facility is at a relatively early stage where further developments and investment is required to realise its low carbon credentials. Each of these aspects and objectives are discussed in more detail below.

The study was split into three sequential tasks, looking at the capability of current technology, the future capability and a case study example focusing on a Cheshire site solution. These can be summarised as follows:

- I. The **current capability** of H₂ storage based on best existing technology and idealised caverns at the selected sites. This work comprised of the following areas of work:
 - a) Daily power demand profiles were defined, from which the H₂ fuel flow rate was estimated for the selected fuel streams.
 - b) Considering a range of credible GTs, the high H₂ capable machines were down selected to two types of machine to match the market demand for H₂.
 - c) The fuel gas streams were assessed against surface plant and well requirements, where constraints were identified and well design optimised for fuel delivery.
 - d) Using the defined flow rates and demand profile, representative salt caverns at three key locations in the UK (East Yorkshire, Cheshire and Teesside) have been modelled to determine their capability to operate and any limitations on duty explored.
 - e) Based on the information gathered through the process, CAPEX and OPEX high level estimates were prepared, in line with AACE5 level (-50% +100%).
- II. A **future, 2030 low carbon case** was defined to investigate the impact of a high H₂ scenario by 2030 on the GT and surface infrastructure. This work comprised of the following areas of work:
 - a) Additional research in high H₂ combustion was reviewed, including research papers issued in the last 5 years from OEMs, academic papers and technical papers on R&D testing outcomes.

- b) The challenges to achieve high H₂ were discussed with OEMs and key technical challenges reviewed.
 - c) Solutions and mitigations to the technical challenges faced through high H₂ were presented and an indicative CAPEX given relative to a natural gas plant; to allow comparison to earlier CAPEX estimates.
- III. The results of task I, which focused on current GT capability, did not fully stretch the cavern capability to its limits. Additional work was therefore commissioned to investigate the **theoretical cavern limits** in more detail. This was accomplished through a series of sensitivities on a Cheshire case study where variations to the diurnal cycle were explored, under a seasonal profile, where longer periods of extraction and injection would test the cavern to its capable limits.

8.1. Current capability

The following key findings were reached:

- Salt caverns can deliver the necessary storage requirements of a H₂ storage power project without issue, for an intermittent 1 GWe design basis.
- The salt cavern volume requirements differ across locations, where multiple caverns are required (using current technology) in the Teesside salt field (wet storage mode), yet only a single cavern is required at either East Yorkshire or Cheshire.
- It was identified that fast cycling is best achieved through a two well design, where the flow rates associated with a single well were considered to result in significant pressure and temperature drops, adversely affecting the cavern.
- Broadly, from the CAPEX review there are only small differences in capital required between the three locations, where East Yorkshire is most capital intensive (circa £1060M). It has also been shown that the cavern and well completion costs are relatively modest against the GT cost (e.g. 4 x “E” class GTs has CAPEX cost of ~£644M).
- The two GTs down selected as most suited for this study were:
 - “E” class type (150 MW to 180 MW) in CCGT as two blocks of 2+1, 25 vol% capable H₂
 - Smaller industrial machine (50 MW) in CCGT, as either four blocks 3+1 or two blocks of 6+1, 60 vol% capable.

The current capability review considered daily balancing of the cavern through equal injection and extraction volumes. From a structural and thermodynamic perspective, under this operation, this does not result in significant issues to the caverns at any of the salt fields considered. As the difference between P_{max} and P_{min} was kept constant, this operation case did not fully utilise the available cavern inventory but did allow a fast churn approach to deliver 1 GWe.

On the power generation side, to generate 1 GWe with a 100 vol% H₂ fuel gas stream remains to be proven without future developments beyond GT current capability. Given current technology, the largest H₂ vol% that has been considered is 60 vol%, where in all cases, natural gas blending is needed to ensure efficient operation of the GT, while maintaining emissions and performance limits. This clearly blurs the low carbon, flexible generation aspiration of the project and so is a development hurdle yet to be overcome.

The outcome of this assessment is presented graphically in Figures 8-2 and 8-3, where the fuel requirement case for the current technology offering is presented.

8.2. Future low carbon case

Uncertainty remains between what is currently offered (60 vol% for SGT-800) and what could be achievable by 2030. The future low carbon case focused on delivering very high H₂ combustion, without

a significant compromise to plant performance, safety or emissions. Much of the research supporting high H₂ combustion (>80 vol% H₂) is either in the early concept stage, sensitive information that is confidential to OEMs or demonstration projects with limited operational hours. However, the technical challenges to combust a high H₂ case (> 80 vol% H₂) are well documented and can be summarised as:

- Fuel impurities; where the LHV of the fuel gas stream can be lower than expected, and impurities add to the carbon impact. Also, given the unique properties of H₂, high volumetric flows are required (relative to natural gas).
- Combustion in the GT; with high TIT temperatures and flame instability limiting the H₂ capability.
- GT type / configuration; GTs capable of high H₂ combustion, while offering generation flexibility and low environmental emissions is a difficult balance.

While 100% H₂ would be extremely challenging by 2030, with the flame instabilities and flashback risk of H₂, a 100% H₂ in the longer term, towards 2040, is increasingly seen as a possibility. It is possible that a future high H₂ case would involve bespoke H₂ ready turbine designs to mitigate many of the technical barriers to the current capability of DLE and diffusion GTs alike. The total CAPEX increase expected for the high H₂ case against the comparative NG case is around ~10% increase to total CAPEX.

In the UK, OEMs have supported recent full-scale testing of the small framed GTs. This has proven up to 60 vol% H₂ is capable, and OEMs are developing roadmaps for high H₂ combustion. The fuel requirement case for a high H₂ case that could combust all of fuel gas stream 1 to meet the 1 GWe requirement is given in Figure 8-1:

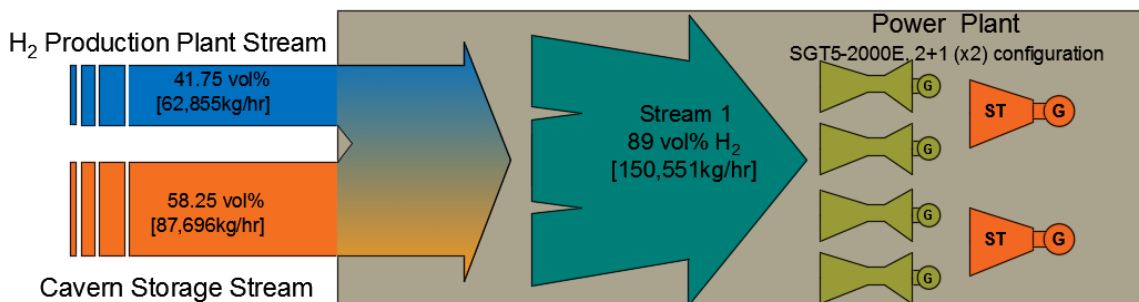


Figure 8-1: Fuel requirement high H₂ case

8.3. Theoretical cavern limits

Cavern behaviour was investigated when subjected to both a seasonal cycle and an existing daily cycle to understand the theoretical cavern capability and limitations. From this, the following key findings were reached:

- The minimum average temperature in the cavern should not be lower than 14°C below the average geothermal gradient (Pellizzaro et al, 2011). This equates to T_{min} of 11.2 °C at the Cheshire caverns.
 - This is assumed for a salt cavern which is subjected to a demanding pressure loading history, that cycles between P_{max} and P_{min} ,
 - Tensile stresses are expected to develop at the walls of the cavern, if the temperature in the cavern drops below T_{min} , where slow extraction / injection cycles have taken place.
 - For fast loading cycles, even if temperature in the cavern is lowered below T_{min} , no tensile stresses develop at the walls of the cavern (with caution due to software limitations).
- Seasonal cycles may require the cavern to be operated in one mode (e.g. injection or

- extraction) over prolonged periods of time. In contrast, daily profiles may require multi-mode use throughout 24 hours and result in either a net decrease or increase of cavern H₂ volume.
- A diurnal cycle with a net volume change of zero over a 24 hour period (i.e. extraction equates to injection) has limited impact on cavern integrity.
 - For seasonal cycles, net changes to cavern volume can adversely impact cavern integrity if these occur over prolonged periods of time.
 - Where, T_{min} is typically exceeded during intense extraction operations (e.g. several days continual extraction at max flowrate).
- Based on the Cheshire assessment, the acceptable H₂ flow rate into and out of the cavern is in the order of 1.6 million Nm³/day
 - Assumes nominal cavern temp of ~25.2°C pre-debrining due to the geothermal gradient).
 - Assumes cavern is emptied under continual extraction to P_{min} (80 days) then filled back to P_{max} (80 days),
 - Cavern behaviour is inherently linked to the loading history that has taken place in the past. As such, it is not possible to prescribe stand-alone specific operations that will result in specific pressure and temperature conditions. Every imposed loading condition is radically affected to what has happened to the cavern before.

8.4. Future areas of study

The key objectives (outlined in Chapter 1) for this study have been satisfied, however suggested areas of interest to develop this work further, are included below:

- This study has focused on representative caverns derived from those that already exist in each region. Typically, these are gas storage caverns, serving a different function to caverns which would be required for a power generation application. Nevertheless, any 'practical' H₂ system would use a newly developed cavern that will entail the design and construction of new wells and appropriate well completions. Consequently, it is possible to develop a specific cavern design for power generation scenarios which would result in an optimised cost for development. This would be recommended to be completed on a site-specific basis.
- The salt caverns in this case study provides capacity to deliver 1 GWe consistently across the year, while also benefiting from being able to meet short term demand spikes and equally troughs in raw fuel pricing of H₂. A more detailed economic analysis on this would assist in developing the initial investment case for this novel concept. This should include social impacts that relate to the possible effects of a project on employment, business, local amenities, tourism etc. The social considerations and the public acceptance of such a H₂ plant will be increasingly important to achieve planning for a novel plant of this kind.
- A purer H₂ source fuel gas stream could be considered to boost the technical capability of the project. This could be achieved through steam methane reforming (SMR) option (as outlined by AmecFw 2012). This may additionally offer improved low carbon credentials.
- With support from OEMs and cavern operators a conceptual road-mapping of H₂ implementation in the UK would be beneficial in steering investment groups and lobbying government support for such a project.

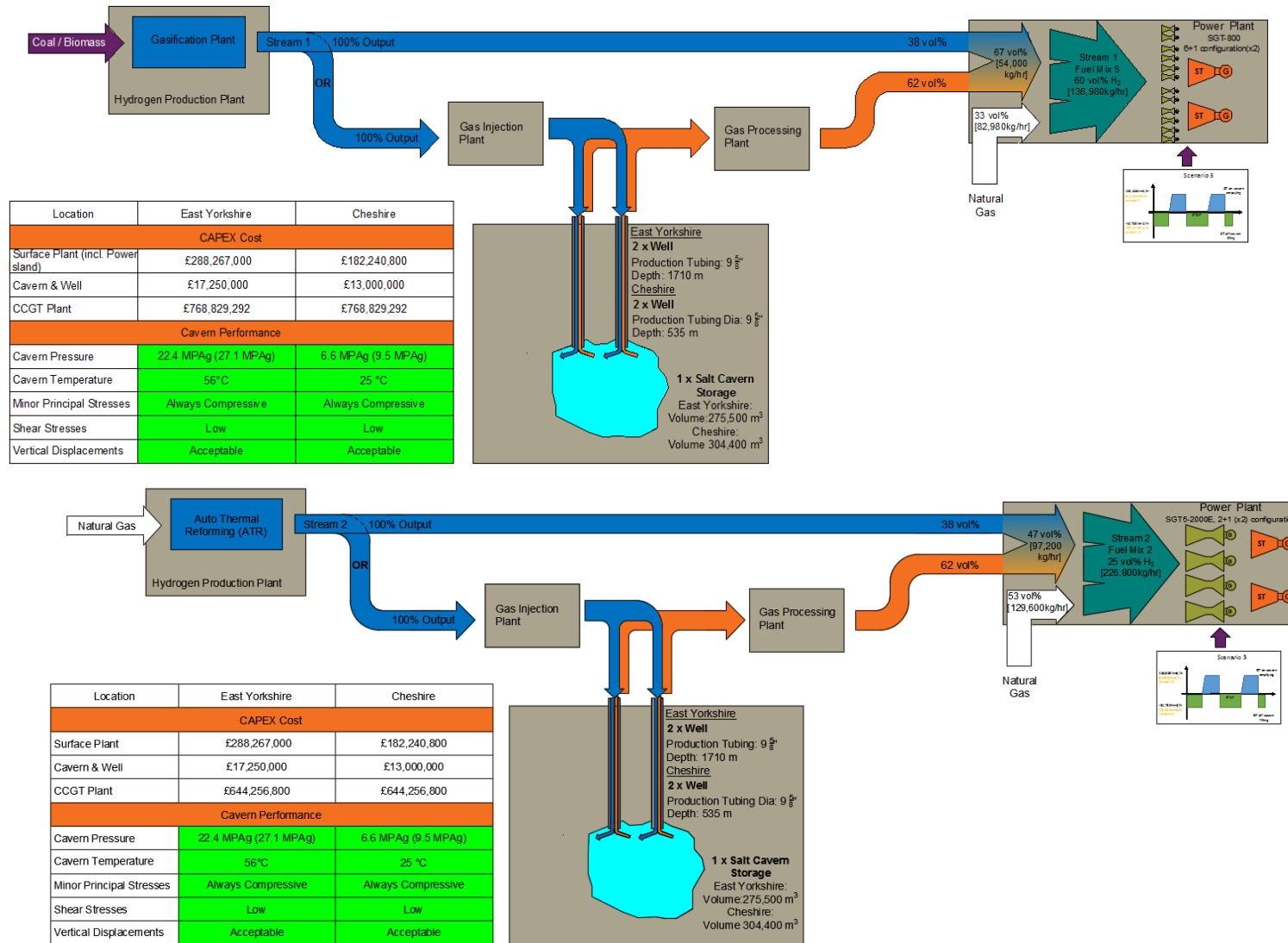


Figure 8-2: East Yorkshire & Cheshire summary, current capability

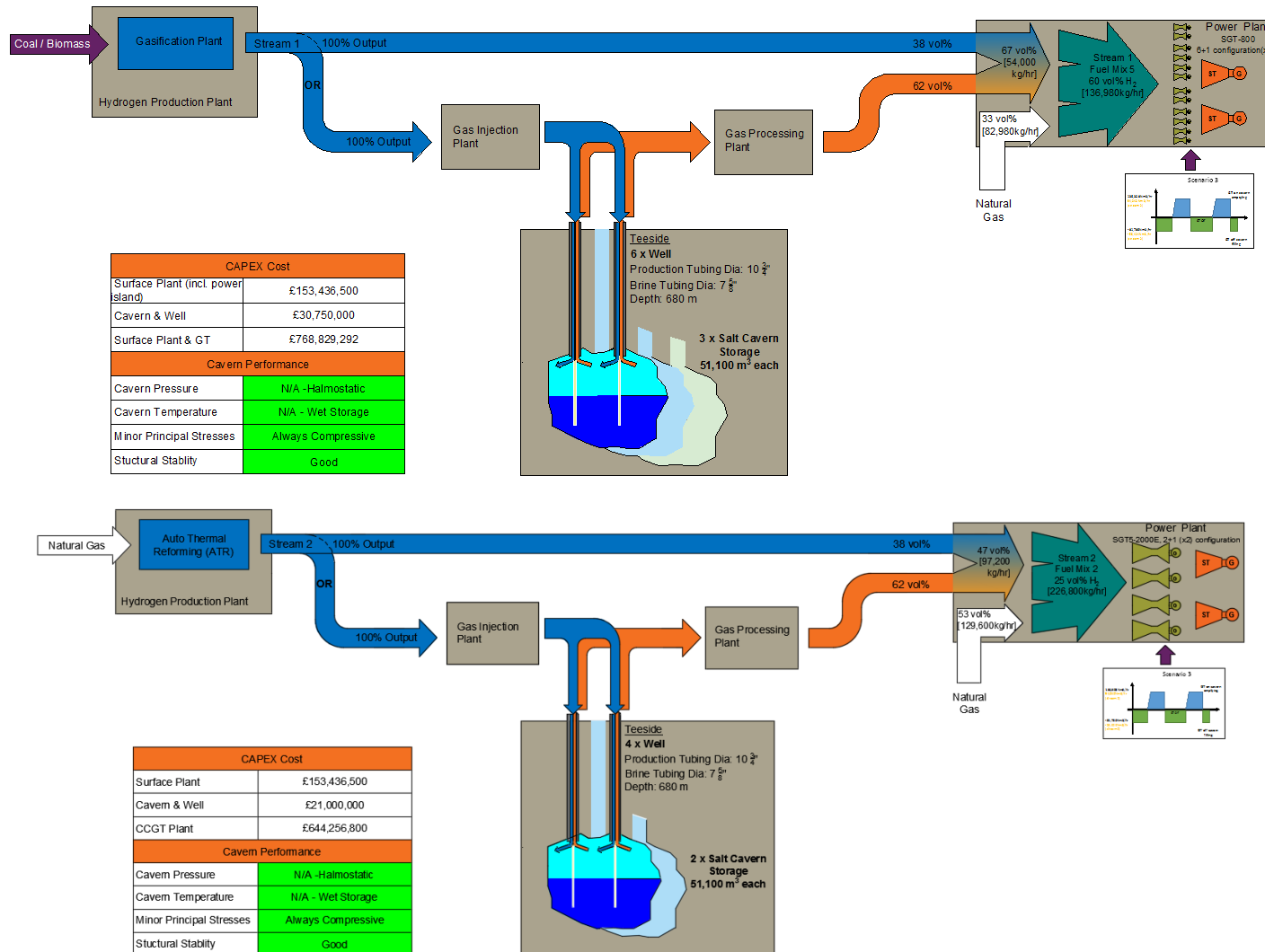


Figure 8-3: Teesside Summary, current capability

ATKINS

Chapter 9: References



9. References

Agency for Natural Resources and Energy, 2014. Summary of the Strategic Road Map for Hydrogen and Fuel Cells (provisional translation). [Online] Available at: http://www.meti.go.jp/english/press/2014/pdf/0624_04a.pdf [Accessed 28 11 2017].

Alavandi, E. B., 2012. Low Single Digit NO_x Emissions Catalytic Combustor for Advanced Hydrogen Turbines for Clean Coal Power Systems, s.l.: s.n.

Allen, D.J., Brewerton, L.J., Coley, L.M., Gibbs, B.R., Lewis, M.A., Wagstaff, S.J. & Williams, A.T. 1997. The Physical Properties of Major Aquifers in England and Wales. British Geological Survey Technical Report WD/97/34, Environment Agency Research and Development Publication 8.

Alvin, M., 2015. Development of Advanced Material for Future Gas Turbine Application , s.l.: s.n.

AmecFw, 2012. Hydrogen Storage and Flexible Turbine Systems, s.l.: ETI.

Arnold, R.D., DeVries, K.L., Nieland, J.D. & Tiruneh, H. 2011. Cyclic fatigue effects on the mechanical properties of salt, Solution Mining Research Institute; Proc. tech. conf., Galveston, Texas, USA, 17-20 April 2011: 51-64.

Asai, T. D. S. K. M. Y. N., 2015. Performance of Multiple-Injection DLN Combustors on Hydrogen-Rich Syngas Fuel in an IGCC Pilot Plant, s.l.: Mitsubishi Hitachi Power Ltd.

Brenchley, P.J. & Rawson, P.F. 2006. The Geology of England and Wales. 2nd Edition. Geological Society London, London.

British Geological Society - Geindex Onshore Maps Available at: <http://mapapps2.bgs.ac.uk/geindex/home.html>

British Geological Survey. 1986. Geothermal Energy - the Potential in the United Kingdom, R.A. Downing & D.A. Gray (eds), Natural Environment Research Council, HMSO, London.

British Standards Institution. 2016. BS EN 1918-3: 2016, Gas infrastructure - Underground gas storage, Part 3: Functional recommendations for storage in solution-mined salt caverns.

Cappalletti, A., 2017 . Investigation of a Pure Hydrogen Fueled Gas Turbine Burner, s.l.: s.n.

Chiesa, P, Lozza, G. & Mazzocchi L. Using H₂ as GT Fuel. ASME. J. Eng. GTs Power. 2005; 127(1):73-80. doi:10.1115/1.1787513.

Cooper, A. H. 2002. Halite Karst Geohazards (Natural and Man-Made) in the United Kingdom. Environmental Geology, 42, 505–512.

Damian Carrington, 2015. UK Cancels Pioneering £1bn Carbon Capture and Storage Competition. Guardian, p. 2.

Ditaranto, M., 2015. Concept of Hydrogen Fired Gas Turbine Cycle with Exhaust Gas Recirculation: Assessment of Combustion & Emissions, s.l.: Norwegian University of Science and Tech.

ETI 2016. Review of GTs and their Ability to use H₂-Containing Fuel Gas. Prepared by John Davison on behalf of the Energy Technologies Institute (ETI). Report number: CC1011/D1.

ETI, Dennis Gammer, 2015. The Role of Hydrogen in a Clean Responsive Power System, s.l.: ETI.

ESK GmbH. 2017. Kavpool, A thermodynamic simulator for optimising and maximising cavern performance, Available at: <https://www.innogy.com/web/cms/en/3783424/esk-at-a-glance/software-products/software-kavpool/>.

European Parliament, 2001. Directive 2001/80/EC of the European Parliament and of the Council of 23 October 2001 on the Limitation of Emissions of Certain Pollutants into the Air from Large Combustion

Plants, s.l.: s.n.

Evans, D.J. 2008. An Appraisal of Underground Gas Storage Technologies and Incidents, for the Development of Risk Assessment Methodology. Prepared by the British Geological Survey for the Health and Safety Executive. Report number: RR605.

Evans, D.J. & Holloway, S. 2009. A Review of Onshore UK Salt Deposits and their Potential for Underground Gas Storage. In D. J. Evans & R. A. Chadwick (eds) *Underground Gas Storage: Worldwide Experiences and Future Development in the UK and Europe*. The Geological Society, London, Special Publications. 313: 39-80.

Evans, D.J. & Kirk, K.L. 2013. An Overview of Underground Hydrogen Storage Potential of the UK Onshore and Offshore UKCS areas. British Geological Survey Internal Report. Reported number: CR/13/040.

Funke, H., 2016. Study on Optimising the DLN micromix Hydrogen Combustion Principle for Industrial Gas Turbine, s.l.: Aachen University.

Gazzani, M., Chiesa, P., Martelli, E., Sigali Stefano, & Brunetti, I. 2014. Using Hydrogen as Gas Turbine Fuel: Premixed Versus Diffusive Flame Combustors. *Journal of Engineering for Gas Turbines and Power*.

Hadj-Hassen, F. 2009. Geomechanical Characterization of the Claystone and Salt Core Samples, Hilltop, a Report of the Centre de Geosciences, Ecole des Mines, February 2009.

Horseman, S.T. & Passaris E.K.S. 1981. Creep Tests for Storage Cavity Closure Prediction. In H. R. Hardy, Jr. & M. Langer (eds), *First Conference on the Mechanical Behavior of Salt*; Proc. The Pennsylvania State University, 9-11 November 1981: 257-264. Clausthal-Zellerfeld: Trans Tech Publications.

Hounslow, M.W. & Ruffell, A.H. 2006. Triassic: Seasonal Rivers, Dusty Deserts and Saline Lakes. In Barker, R.D. & Tellam, J.H. (eds) *The Geology of England and Wales*. 2nd Edition: Geological Society London, pp. 295-324.

ISRM 1983. International Society for Rock Mechanics Suggested Method for Determining the Strength of Rock Materials in Triaxial Compression, Revised Version, *Int. J. Rock Mech. & Geomech. Abstr.*, 20(6): 283-290.

Itasca Consulting Group Inc. 2011a. *Fast Lagrangian Analysis of Continua, Constitutive Models*, Version 7.0, User's Manual, Minneapolis, Minnesota, USA.

Itasca Consulting Group Inc. 2011b. *Fast Lagrangian Analysis of Continua, Thermal Analysis*, Version 7.0, User's Manual, Minneapolis, Minnesota, USA.

Johnson, H., Warrington, G. & Stoker, S.J. 1994. Permian and Triassic of the Southern North Sea. In Knox, R.W.O'B. & Cordey, W.G. (eds) *Lithostratigraphic nomenclature of the UK North Sea*. British Geological Survey and UK Offshore Operators Association, pp 141.

Knott, I. & Haynes, P.D.M. 1991. Geological Assessment of the Zechstein Salt in East Yorkshire for Underground Gas Storage Sites. British Gas Exploration & Production Limited, Development Geology & Geophysics Department for British Gas Limited, Design Standards Department, Construction.

Kreith, F. & Black, W. Z. 1980. *Basic Heat Transfer*, 1st ed., Harper & Row, Publishers, New York, NY.

Louvet, F., Charnavel, Y. & Hevin, G. 2017. Thermodynamic studies of hydrogen storage in salt caverns, Solution Mining Research Institute; Proc. tech. conf., Albuquerque, New Mexico, 23-26 April 2017: 337-352.

Michael Welch, J. K., 2016. Siemens GT Capability on H₂ Fuels Discussion [Interview] (7 Dec 2016).

National Grid 2015. Gas Transportation Transmission Planning Code. [Online] Available at:

<http://www2.nationalgrid.com/UK/> [Accessed October 2016].

Nieland, J. D. 2004. Salt Cavern Thermal Simulator, Version 2.0, User's manual, RSI-1760, Prepared by RESPEC, Rapid City, SD, for Gas Technology Institute, Chicago, IL.

Nieland, J.D. 2008. Salt Cavern Thermodynamics - Comparison Between H₂, Natural Gas, and Air Storage, Solution Mining Research Institute; Proc. tech. conf., Galveston, Texas, 13-14 October 2008.

Oliver, P. 1982. Salt Cavity Simulation: Mathematical theory, Report no. LRST488, British Gas, London Research Station, February 1982.

Ozbek, H & Phillips, S.L. 1980. Thermal Conductivity of Aqueous NaCl Solutions from 20 to 330°C, J. Chem. Eng. Data, 1980, 25 (3): 263-267.

Passaris, E., Jessop, M. & Slingsby J. 2015. Verification of the Salt Creep Parameters Using Data from the Echometric Surveys of Aldbrough Gas Storage Caverns in the UK, Solution Mining Research Institute; Proc. tech. conf., Rochester, New York, 27-28 April 2015: 324-336.

Pellizzaro, C., Bergeret, G., Leadbetter, A. & Charnavel, Y. 2011. Thermo-Mechanical Behavior of Stublach Gas Storage Caverns, Solution Mining Research Institute; Proc. tech. conf., York, UK, 3-4 October 2011: 161-178.

Pokar, M., West, L.J. & Odling, N.E. 2006. Petrophysical Characterisation of the Sherwood Sandstone from East Yorkshire. In Barker, R.D. & Tellam, J.H. (eds) Fluid Flow and Solute Movement in Sandstones: The Onshore UK Permo-Triassic Red Bed Sequence. Geological Society London Special Publication 263, pp103-118.

Potts, E.L.J., Thompson, T.W., Passaris, E.K.S. & Horseman, S.T. 1978. An investigation into underground gas storage in brine well cavities. In A. H. Coogan & L. Hauber (eds), 5th International Symposium on Salt; Proc., Hamburg: 105-123. Cleveland: Northern Ohio Geological Society Inc.

Ramalingam, A. & Arumugam, S. 2012. Experimental Study on Specific Heat of Hot Brine for Salt Gradient Solar Pond Application, International Journal of ChemTech Research, July-Sept 2012, 4(3): 956-961.

RESPEC 2008. Mechanical Properties Testing of Salt from Scottish and Southern Energy-Statoil Natural Gas Storage Project, England Topical Report no. RSI-1996 by RESPEC for PB Energy Storage Services, Inc., July 2008.

Rocscience 2017.RS2, Rock and soil 2-Dimensional Analysis Program, [Online] Available at: <http://www.rocscience.com>. [Accessed 31 May 2017].

Siemens 2014. Siemens EconoFlex SGT-800. Prepared by Nilsson, L.-I., Jöcker, M., and Björkman, M. on Behalf of Siemens. [Online] Available at: <http://pennwell.sds06.websds.net/2014/cologne/pge/papers/T3S4O50-paper.pdf>.

Smith, D.B. 1989. The Late Permian Paleogeography of North-East England. Proceedings of the Yorkshire Geological Society. 47(4), 285-312.

Snedecor, G.W. & Cochran, W.G. 1989. *Statistical Methods*, Eighth Edition, Iowa State University Press.

Thompson, T.W. 1973. A Feasibility Study into the Use of Brine Cavities for Underground Gas Storage, PhD thesis, Volume II, University of Newcastle upon Tyne, October 1973.

Vermeer, P.A., & de Borst R. 1984. Non-Associated Plasticity for Soils, Concrete and Rock, Heron, 29(3): 1-64.

Woodcock, N. & Strachan, R. 2000. *Geological History of Britain and Ireland*. Blackwell, Oxford.

York, 2013. Development and Testing of a Low NO_x Hydrogen Combustion System for Heavy-Duty Gas Turbines, s.l.: s.n.

ATKINS

Appendices



Christopher McMichael

Atkins Ltd.
8 Mallard Way
Strathclyde Business Park
Bellshill
North Lanarkshire
ML4 3BF

Phone: +44 (0)141 220 2360
Email: christopher.mcmichael@atkinsglobal.com

